Technische Universität München
TUM School of Engineering and Design

Prosumers in District Heating and Cooling: Design of a Simulation and Experiment Environment for Testing Control Strategies

Daniel J. Zinsmeister, M.Sc.

Vollständiger Abdruck der von der TUM School of Engineering and Design
der Technischen Universität München zur Erlangung des akademischen Grades eines

Doktors der Ingenieurwissenschaften (Dr.-Ing.)

genehmigten Dissertation.

Vorsitz:

Prof. Dr. Thomas Hamacher

Prüfende der Dissertation

1. Prof. Dr. Ulrich Wagner
2. Prof. Dr. Christoph Goebel
3. Prof. Carlos Ugalde-Loo

Die Dissertation wurde am 18.12.2023 bei der Technischen Universität München eingereicht und durch die TUM School of Engineering and Design am 09.04.2024 angenommen.

Abstract

Efficient decarbonization of the heating and cooling sector necessitates the sector coupling of energy systems at both end-user and district aggregation levels. The concept of prosumers within district heating and cooling grids presents an untapped potential for sector coupling to enhance efficiency and aid decarbonization efforts. Prosumers are participants who interact bi-directionally with the energy grid. However, integrating prosumers introduces several technical challenges, such as ensuring reliability, maintaining network stability, and managing intermittent energy sources. This dissertation addresses these challenges by developing and implementing a novel simulation and experiment research environment.

A key aspect of the thesis involves designing, constructing, and commissioning the district heating and cooling research infrastructure of the Center for Combined Smart Energy Systems (CoSES) laboratory at the Technical University of Munich. The laboratory comprises five interconnected prosumers within an adaptable district heating and cooling network. It combines commercial components with Power Hardware in the Loop emulation, enabling realistic and reproducible experimental investigations.

A new simulation library, programmed as a digital twin of the CoSES laboratory, is central to developing innovative control systems. This library provides accurate building energy system models, focusing on precisely representing commercial components. These models are available as open-access resources and enable the software-independent development of control approaches and energy management systems. The digital twin design of the library facilitates the subsequent testing and refining of promising control concepts in the CoSES laboratory.

Experimental and simulation results indicate that integrating prosumers in district heating and cooling networks can reduce heating costs. Intelligent control concepts must facilitate this integration to account for the mutual influence of prosumers and temperature constraints.

These insights led to the developing of a novel thermal energy storage model for model predictive control. This one-dimensional stratified storage model accounts for the internal temperature distribution. Internal and external heat exchanges are formulated with quadratic or simpler constraints to ensure high accuracy with low computational demand. Experimental validation and a case study demonstrate the model's advantages compared to existing approaches. Moreover, including temperature information in this model makes it an ideal tool for calculating setpoints for prosumers in district heating and cooling networks.

This dissertation advances the technical understanding of prosumers in district heating and cooling networks. The research laboratory established within the scope of this thesis facilitates further research in the development and comprehensive analysis of energy management systems and sector coupling measures at both end-user and district levels.

Zusammenfassung

Die kosteneffiziente Dekarbonisierung des Wärme- und Kältesektors erfordert die Nutzung von Sektorkopplung und Synergien unterschiedlicher Erzeuger, sowohl auf individueller als auch auf Quartiersebene. Für Wärme- und Kältenetze bieten Prosumer ungenutztes Potenzial für Sektorkopplung, Effizienzsteigerung und die Unterstützung von Dekarbonisierungsmaßnahmen. Prosumer sind Teilnehmer, die Wärme oder Kälte sowohl einspeisen als auch beziehen. Die Integration von Prosumern bringt jedoch einige technische Herausforderungen mit sich, wie die Gewährleistung der Zuverlässigkeit, die Aufrechterhaltung der Netzstabilität und die Regelung fluktuierender Energiequellen. Die vorliegende Dissertation befasst sich mit diesen Herausforderungen durch die Entwicklung und Implementierung einer neuartigen Simulations- und Experimentierumgebung.

Ein wesentlicher Aspekt dieser Arbeit ist die Planung, der Bau und die Inbetriebnahme der Wärme- und Kälte-Forschungsinfrastruktur des Center for Combined Smart Energy Systems (CoSES) Labors an der Technischen Universität München. Das Labor besteht aus fünf miteinander verbundenen Prosumern innerhalb eines veränderbaren Wärme- und Kältenetzes. Es kombiniert kommerzielle Komponenten mit einer Power Hardware in the Loop-Emulation, was realistische und reproduzierbare experimentelle Untersuchungen ermöglicht.

Eine neu entwickelte Simulationsbibliothek ermöglicht die Entwicklung innovativer Regelungssysteme und ist als digitaler Zwilling des CoSES-Labors aufgebaut. Die Bibliothek bietet präzise Modelle von Gebäudeenergiesystemen mit einem Schwerpunkt auf die genaue Darstellung kommerzieller Komponenten. Diese Modelle sind frei zugänglich und dienen zur softwareunabhängigen Entwicklung von Regelungsansätzen und Energiemanagementsystemen. Der Aufbau als digitaler Zwilling erleichtert die anschließende Erprobung und Optimierung von vielversprechenden Systemen im CoSES Labor.

Experimentelle und simulative Ergebnisse zeigen, dass die Prosumer-Integration in Wärme- und Kältenetze die Heizkosten senken kann. Diese Integration erfordert jedoch intelligente Regelungskonzepte, welche Temperaturbeschränkungen und die gegenseitige Beeinflussung von Prosumern berücksichtigen.

Diese Erkenntnisse führten zur Entwicklung eines neuartigen Wärmespeichermodells für die modellprädiktive Steuerung. Dieses eindimensionale, geschichtete Speichermodell bildet die interne Temperaturverteilung ab. Interner und externer Wärmeaustausch werden dabei mit quadratischen oder einfacheren Gleichungen formuliert, um hohe Genauigkeit bei geringem Rechenaufwand zu gewährleisten. Durch experimentelle Validierung und ein Praxisbeispiel werden die Vorteile des Modells im Vergleich zu bestehenden Ansätzen gezeigt. Darüber hinaus eignet sich dieses Modell durch die Einbeziehung von Temperaturinformationen für die Bestimmung von Sollwerten für Prosumer in Wärme- und Kältenetzen.

Diese Dissertation erweitert das technische Verständnis von Prosumern in Wärme- und Kältenetzen. Über diesen spezifischen Fokus hinaus ermöglicht die Forschungsumgebung weitere Untersuchungen, wie die Entwicklung und umfassende Analyse von Energiemanagementsystemen und Sektorkopplungsmaßnahmen auf individueller und Quartiersebene.

Acknowledgements

This document marks the highlight of a journey that began when I decided to return to university to pursue a passion that I knew would bring me joy. I have found enduring happiness and fulfillment in this work environment, and I want to thank an extensive list of people.

My time as a doctoral candidate has been supported by numerous people to whom I express my deepest thanks. My supervisor, Professor Dr. Ulrich Wagner, and my mentor, Dr. Peter Tzscheutschler; the leaders of the CoSES group, Dr. Franz Christange and Dr. Vedran Perić; and Professor Dr. Thomas Hamacher and Professor Dr. Christoph Goebel, who facilitated a smooth transition from EWK to EMT. They entrusted me with the freedom to design and build the CoSES laboratory, provided me with the opportunity to pursue my PhD, and guided me into new research fields, shaping my development as a scientist and tutor.

My gratitude extends to colleagues from TUM and beyond, with whom I collaborated, shared knowledge, and engaged in insightful discussions. These interactions have provided valuable feedback, significantly enhancing my personal and scientific skills and fostering close friendships.

I extend a special thanks to my CoSES companions. We transformed an empty basement into a thriving workspace, overcoming software and hardware challenges with curses, creativity, and determination. I am also grateful to the students who contributed to constructing and programming the laboratory, handling last-minute changes, and repairing any leaking connections.

Finally, I cannot overlook the unwavering support of my family and Anne in pursuing my academic ambitions and their understanding and patience, even during constant energy-related discussions.

Thank you all for helping me stay focused on what truly matters and offering perspective during this incredible journey.

Contents

List of Figures

Abbreviations

.dll	Dynamic Link Library	32
3WV	3-Way Valve	32
4GDH	4th Generation District Heating	2
5GDHC	5th Generation District Heating and Cooling	2
ASHP	Air Source Heat Pump	10
BHP	Booster Heat Pump	2
BHPTS	Booster Heat Pump Transfer Station	3
CHP	Combined Heat and Power Units	31
COP	Coefficient of Performance	9
CoSES	Center for Combined Smart Energy Systems	4
DC	District Cooling	2
DER	Distributed Energy Resources	1
DH	District Heating	1
DHC	District Heating and Cooling	1
DHW	Domestic Hot Water	2
EMS	Energy Management System	5
EV	Electric Vehicles	31
FMU	Functional Mock-Up Units	48
GIS	Geographic Information System	9
GSHP	Ground Source Heat Pumps	10
HiL	Hardware in the Loop	9
HP	Heat Pumps	1
IO	Input/Output	9
MILP	Mixed Integer Linear Programming	11
MINLP	Mixed Integer Non Linear Programming	11
MPC	Model Predictive Control	5
MSL	Modelica Standard Library	57

Chapter 1

Introduction

Decarbonizing heating and cooling systems is a necessary and significant transformation of the energy sector, which is needed to address the urgent challenge of climate change. Residential and commercial structures are still heavily dependent on fossil fuels and account for roughly a quarter of global final energy consumption [1]. In Germany, the urgency of transitioning towards sustainable energy usage in heating is underlined by two recent laws. The first law mandates a phased increase in renewable energy usage within individual heating systems, aiming for a carbon-neutral heating sector by 2045 (Novelle des Gebäudeenergiegesetzes, [2]). Complementing this, the second law requires municipalities to perform thorough evaluations and develop strategic plans to decarbonize their heating infrastructure (Gesetz für die Wärmeplanung und zur Dekarbonisierung der Wärmenetze, [3]). This includes the establishment of minimum renewable energy quotas within District Heating (DH) grids.

Despite the political will, the path to decarbonizing the heating and cooling sector is complex and poses social and technical challenges. Central to this transition are District Heating and Cooling (DHC) grids [4] and Heat Pumps (HP)s [5, 6], which must be coupled intelligently with the electric sector to use synergies and thus reduce the overall costs for energy.

This sector coupling at the district level will lead to a smart energy system, which is defined as 'an approach in which smart electricity, thermal and gas grids are combined with storage technologies and coordinated to identify synergies between them to achieve an optimal solution for each sector as well as for the overall energy system' [7]. Such coupling is crucial for decarbonizing the energy landscape and managing the variability introduced by the increasing presence of renewable Distributed Energy Resources (DER)s [8].

District heating and cooling grids

The first DH grids were introduced in the USA in the 1880s and used steam as the heat carrier. Today, such systems are outdated as high steam temperatures lead to substantial losses and inefficient heat generation [4].

To evolve from these historic DH grids to clean, efficient, secure, and smart future DHC grids, several aspects are important, as outlined by Oxenaar et al. [9]. These aspects include prioritizing production, distribution, and consumption efficiency and utilizing the significant potential of unavoidable waste heat sources. Another element involves developing viable business models and ensuring end-user protection, as DHC grids are monopolistic structures. This is essential for the economic feasibility and acceptance of DHC grids and the affordability of heat. Furthermore,

coupling the DHC grids with the electricity sector is crucial, enabling decarbonization through power-to-heat technologies and providing the electric system with much-needed flexibility and storage capacity.

These considerations align with the evolution of DH grids, which can be categorized into different generations, as depicted in Figure 1.1. The grids have progressively advanced to the 4th Generation District Heating (4GDH), characterized by reduced temperatures that align closely with consumer needs [4]. The diminished grid temperatures have reduced grid losses and enabled the inclusion of additional sustainable heat sources and waste heat. Both effects enhance the energy efficiency of the DHC grid.

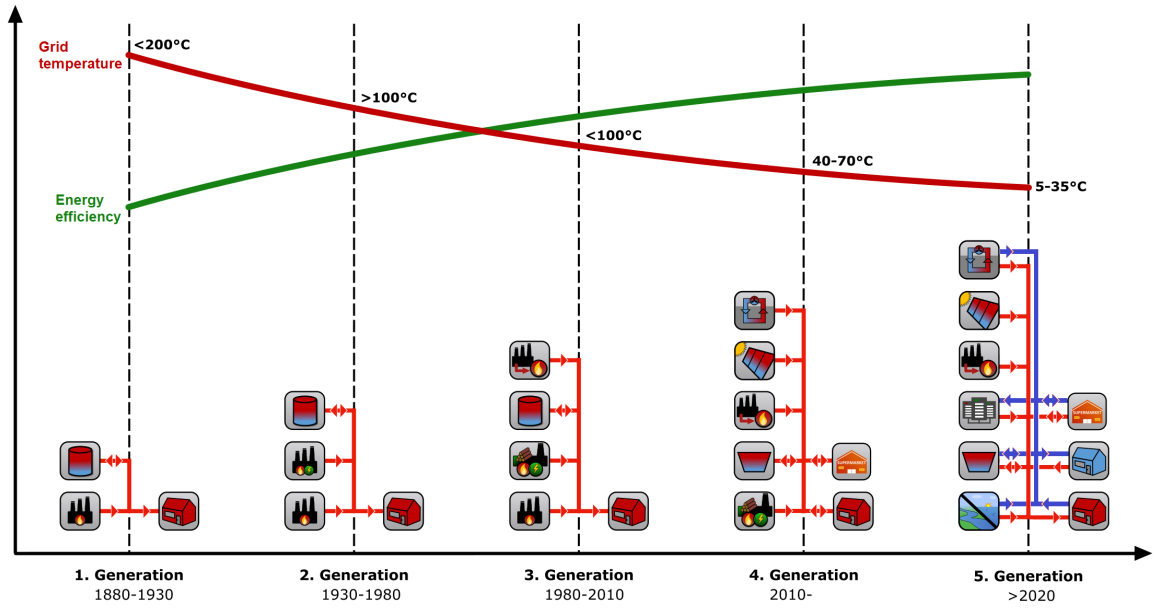

Figure 1.1: The evolution of DHC grids (adapted from [4] and [10]).

The introduction of the 5th Generation District Heating and Cooling (5GDHC) represents a paradigm shift by integrating DH and District Cooling (DC) within one grid. Operating at temperatures near ambient levels, this generation substantially reduces grid losses [11] and facilitates the integration of low-temperature heat sources previously not viable for direct heating [12]. Another key aspect is energy sharing between heating and cooling, as waste cold from heating can be used for cooling and vice versa. Reviews indicate that this co-occurrence is crucial for minimizing operational costs [12, 13, 14]. Due to the low-temperature difference between the hot and cold pipes, 5GDHC systems often exhibit higher pumping energy consumption compared to 4GDH. The low grid temperature requires a water-water HP at the transfer station to reach the desired temperature for heating and Domestic Hot Water (DHW) in the buildings, termed Booster Heat Pump (BHP).

Comparative studies between 4GDH and 5GDHC show varying results. Some studies suggest that 5GDHC can lead to significantly lower energy usage and costs compared to 4GDH, individual HPs, or condensing boilers [11, 15, 16, 17]. However, other research indicates that the performance of 5GDHC may be inferior to 4GDH, particularly in scenarios with high or exclusive heating demands [18, 19]. Another study points out that only a few locations have a sufficient overlap of heating and cooling demand to make 5GDHC viable [20]. Long- and

short-term Thermal Energy Storages (TES) systems can thus play a crucial role in balancing potential mismatches between heating and cooling demands, thereby enhancing the profitability and efficiency of 5GDHC grids [12]. Given these unique requirements of 5GDHC, the previous objective of universally upgrading older generation DH grids to the latest generation is no longer universally applicable. Therefore, some researchers view 5GDHC as a complementary technology coexisting in parallel to 4GDH rather than a direct progression, as it does not follow a 'natural evolutionary path' compared to earlier DH generations [21].

This evolution of DHC grids is essential for their decarbonization. Several review papers highlight further instrumental elements in DHC research to accelerate this process [22, 23, 24]. These elements encompass further sector coupling to integrate the DHC grid into the smart energy system; reducing temperatures in current DH grids to evolve them into 4GDH grids and enable the integration of more renewable energy sources; and the integration of decentralized sources and prosumers.

Prosumer in district heating and cooling grids

Prosumers in DHC grids can extract and inject thermal energy from or into the grid and are of particular interest for this thesis. An example of a DHC grid with prosumers is illustrated in Figure 1.2. Their integration into 4GDH networks offer an opportunity to boost system efficiency and operational economy and can be used for alleviating bottlenecks within DH systems [25]. Such bottlenecks typically occur in pipes experiencing excessively high flow rates.

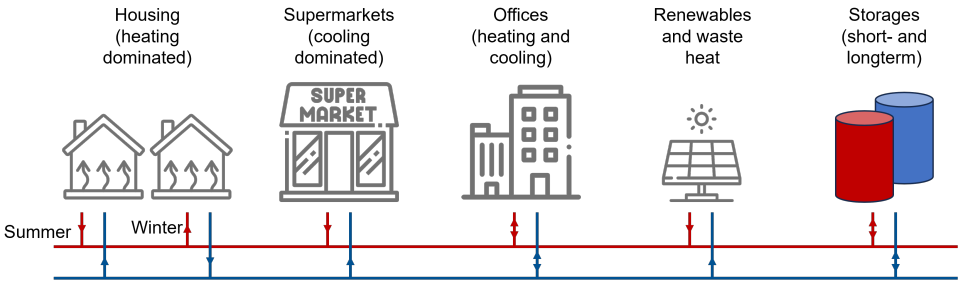

Figure 1.2: DHC grid with different prosumers.

Prosumers in heating networks benefit from utilizing synergies between temporally variable load and generation profiles and through the intelligent use of different types of generators. Implementing prosumers can lead to additional heat savings, mainly due to shorter distances required for heat transport and reduced thermal losses in the grid [26]. A comprehensive analysis of the excess heat generated by prosumers indicates substantial potential, especially when low-temperature heat is efficiently harnessed using HPs [27].

In the context of 5GDHC, prosumers occur naturally and play a crucial role by utilizing waste cold from heat extraction for cooling purposes, and vice versa. This exchange enhances the system's overall efficiency, especially when heating and cooling demands within the DHC grid are balanced. In this system, the Booster Heat Pump Transfer Station (BHPTS) consists of a BHP, a heat exchanger, and often an additional TES.

1.1 Research focus

This dissertation focuses on developing realistic operation strategies for the widespread deployment of prosumers in DHC grids. Therefore, a simulation environment is required to replicate complex prosumer behaviors within buildings and observe their impacts on the DHC network under various conditions. An experimental environment can further help to bridge the gap by testing promising controllers with commercial equipment and validating the simulation library. The research environment should replicate the thermal and electric systems within buildings to analyze new control strategies, the sector coupling potential, and the impact on the DHC and the electric grid in a close-to-reality setting.

A central research objective of this thesis is establishing the Center for Combined Smart Energy Systems (CoSES) laboratory at the Technical University of Munich (TUM), which incorporates five prosumers within a DHC grid. The author of this dissertation was responsible for the design, installation, and commissioning of the thermal side of the CoSES laboratory. Figure 1.3 offers a view of this laboratory, which was officially opened in 2019 [28]. The design of the laboratory combined with the need for a realistic simulation environment leads to the first Research Question (RQ):

RQ 1: How can the integration of prosumers in the district heating and cooling grids be analyzed and validated, through simulations and experiments?

Figure 1.3: View of the CoSES laboratory (photography by Stefan Hobmaier / TUM).

During the design phase of the CoSES laboratory, the setup of prosumers in 4GDH grids was examined in detail. Key components include one or multiple heat generators for decentralized heat production, a TES for decoupling heat production and demand, and a bidirectional heat transfer station for exchanging heat with the DH network. The heat consumption usually consists of heating and DHW consumption with different temperature requirements. While determining the optimal laboratory design, the second RQ was developed:

RQ 2: How can the components of prosumers in district heating grids be optimally arranged to maximize system efficiency?

After completion of the laboratory, the interaction of prosumers within a DH grid was explored through different experiments. In these experiments, a basic Model Predictive Control (MPC)-based Energy Management System (EMS) generated the setpoints [29, 30]. The results showed that prosumers can mostly fulfill the power setpoints for heat consumption or DH feed-in but often fall short of meeting temperature setpoints. A critical issue with these EMSs is their omission of the temperature influence to linearize the optimization problem. While this approach is common and reduces the computational effort, it is often inadequate for energy systems involving heat. To overcome this limitation, the final RQ is posed:

RQ 3: How can a model predictive control-based energy management system be formulated to include temperature information while maintaining a low computational burden?

1.2 Thesis structure

The thesis is based on six publications, which can be grouped into three chapters. Each chapter answers one of the RQs. Figure 1.4 presents the thesis structure and the papers' allocation to the RQs. The papers included in this thesis are as follows:

Publication 1: D. Zinsmeister, T. Licklederer, F. Christange, P. Tzscheutschler, and V. S. Perić. *A comparison of prosumer system configurations in district heating networks.* Energy Reports, 2021.

Publication 2: D. Zinsmeister, T. Licklederer, S. Adldinger, F. Christange, P. Tzscheutschler, T. Hamacher, and V. S. Perić. *A prosumer-based sector-coupled district heating and cooling laboratory architecture.* Smart Energy, 2023.

Publication 3: D. Zinsmeister, and V. S. Perić. *Implementation of a Digital Twin of the CoSES District Heating Prosumer Laboratory.* Energy Proceedings, 2022.

Publication 4: O. Angelidis, D. Zinsmeister, A. Ioannou, D. Friedrich, A. Thomson, G. Falcone. *5th Generation District Heating and Cooling Modelica Models for Prosumer Interaction Analysis.* Modelica Conference, 2023.

Publication 5: D. Zinsmeister, Ulrich Ludolfinger, V. S. Perić, and C. Goebel. *A benchmarking framework for energy management systems with commercial hardware models.* Energy and Buildings, 2024.

Publication 6: D. Zinsmeister, P. Tzscheutschler, V. S. Perić, and C. Goebel. *Stratified Thermal Energy Storage Model with Constant Layer Volume for Predictive Control - Formulation, Comparison, and Empirical Validation.* Renewable Energy, 2023.

Chapter 2 presents the background to the RQs and relevant DHC research trends. Since the results of RQ 2 are required for the design of the CoSES laboratory, this topic is addressed first in Chapter 3, where Publication 1 analyzes the optimal arrangement of the components within prosumers in 4GDH using a simulation study.

Chapter 4 delves into the experiment and simulation infrastructure, answering RQ 1. The CoSES laboratory is introduced in Publication 2, detailing its hardware and software structure.

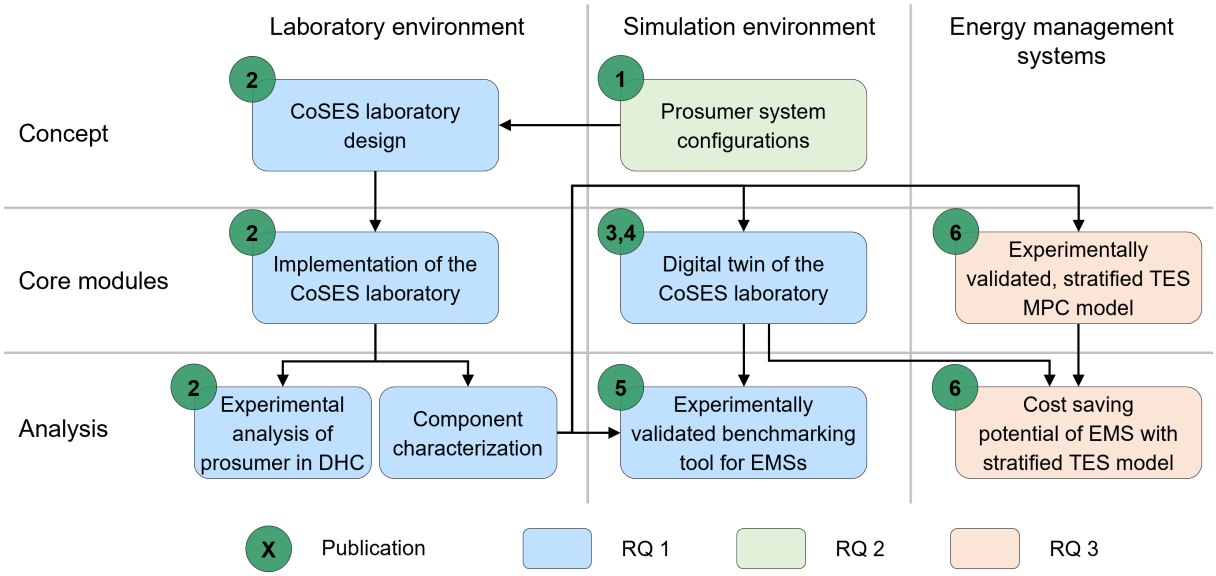

Figure 1.4: Structure of the dissertation.

The laboratory enables in-depth analyses of thermal systems at both the building and network levels. Publication 3 introduces the experimentally validated CoSES Prosumer House Model (ProHMo) simulation library. This library serves as a digital twin of the building energy systems in the laboratory. The simulation library is enhanced in Publication 4 by incorporating models for DHC grids, which allows the design and evaluation of control strategies for prosumers in 5GDHC grids. The detailed building energy system models are further used in Publication 5 and serve as an open-access benchmarking tool for EMSs. This simplifies the training and comparison of different EMSs.

The last RQ is addressed in Publication 6, which provides a stratified TES model for MPC-based EMSs. This model integrates temperature information within the TES, enabling the EMS to account for temperature constraints. Concluding the dissertation, Chapter 6 summarizes the key findings, situates them in a larger context, and makes recommendations for the future use of the presented research infrastructure.

Chapter 2

Background

This chapter addresses the current state of the art related to the topics encompassed in the RQs. Since the research infrastructure extends beyond analyzing prosumers, the chapter also explores relevant research trends that can be examined within this scope.

2.1 Prosumer system configurations within the building

The following section is extended from Publication 1 [31]. Current research on 4GDH network prosumers tends to concentrate on network behavior, often reducing the building's role to a simple power consumer or producer. The three viable feed-in configurations for prosumers into the DH grid are illustrated in Figure 2.1: return to supply (a), return to return (b), and supply to supply (c). The prevalent method in studies is the return-to-supply configuration due to its advantage in maintaining a low return temperature in the DH grid, which is crucial for efficient grid operation. This method also aligns with the prosumer's efficiency by minimizing the return temperature within the building but requires larger pumps to overcome the pressure difference between supply and return lines.

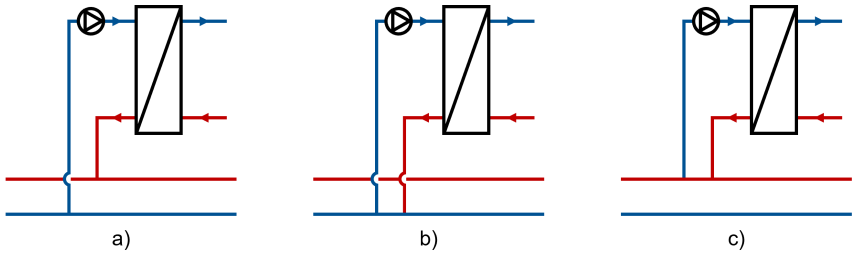

Figure 2.1: Prosumer feed-in configuration concepts.

To fully understand prosumer behavior, the building-side components must also be considered. Prosumers typically consist of one or multiple heat generators, a TES, the bidirectional heat transfer station, and the consumption of heat or cold.

Pipiciello et al. [32] introduce and characterize a bidirectional substation prototype, which can be connected to a generic prosumer system. This prototype is further used to assess prosumer potential and test new control strategies with a validated simulation model of the substation [33]. Rosemann et al. [34] explore a Solar Thermal (ST)-based prosumer substation, presenting

the concept and implementation of an experimental setup and its control system. Lamaison et al. [35] conduct a comprehensive study of bidirectional substations, examining factors like the placement of the hydraulic separation between network and building, and the balance between local consumption, total energy feed-in, and different control strategies. They conclude that configurations with dedicated heat exchangers for DHW, heating, and ST are most efficient and validate this by subsequent experiments [36]. Paulus et al. [37] assess the impact of nine distinct hydraulic schemes for substations, focusing on a return-to-return feed-in model.

While many studies focus on generic prosumer systems or ST as the sole heat generation method for DH prosumers, generator types vary, each with unique integration requirements. ST systems, for instance, require antifreeze measures in Germany for winter protection, leading to a separate circuit from the central heating network. Other heat generators have unique operational requirements for optimal efficiency, including different integration into the heating system. Additionally, TESs are generally not considered in the prosumer operation strategies despite being essential for maximizing system flexibility through decoupling heat production and consumption.

2.2 Simulation environment

A close-to-reality analysis of individual heating solutions and prosumers in DHC grids requires a simulation library that precisely replicates the behavior of commercial equipment, including their internal controls. This library should encompass models of various types of heat generators, TESs, and bidirectional heat transfer stations for 4GDH and 5GDHC. It should further integrate the coupling to the electricity sector, include realistic control unit interfaces, and be openly accessible for broader use. While there are many libraries for building energy systems and DHC grids, not all meet these criteria.

Modelica is an object-oriented simulation language ideal for these cyber-physical multi-energy systems [38]. It is a preferred choice for handling acausal connections, making it suitable for analyzing bidirectional DHC grids. Abugabbara et al. [39] evaluated various Modelica-based tools, particularly for building and energy simulations in DHC systems.

Prominent open-access Modelica libraries for energy systems include the IBPSA library [40] and its derivatives: Buildings [41], AixLib [42], BuildingSystems [43], and IDEAS [44]. The IBPSA library is a comprehensive tool for building and district energy systems, adhering to modeling best practices in this field. It encompasses many models, including heating and cooling systems, high and reduced-order building models, and various energy storage types such as water and ice tanks, boreholes and bore fields, phase-change materials, and batteries. The library can model heat transfer between rooms and the outside and multizone airflow, including natural ventilation and contaminant transport. The electrical system includes alternating and direct current systems with two- and three-phase options that allow balanced and unbalanced configurations.

The Buildings library is widely used for DHC system simulations. This library encompasses models for 5GDHC, such as detailed heat transfer stations and central HPs. It has facilitated research on agent-based control in 5GDHC [45], the dynamics of prosumers in a single-pipe 5GDHC networks [46], or the development of topology analysis tools [47]. Additionally, the inclusion of DC models in the Buildings library has enabled real-world assessments of energy

conservation strategies [48]. The AixLib library, in combination with Geographic Information System (GIS) data, is used to automatically create and streamline comprehensive, large-scale DHC grid models [49]. It is further used to evaluate the efficiency and performance of a low temperature, bidirectional DHC grid with 15 decentral prosumers with HPs and chillers [50].

Two notable but not open-access Modelica-based libraries are GreenCity [51, 52] and the library developed by Abugabbara et al. [53]. The GreenCity library is a commercial tool for SimulationX and is tailored for planning and optimizing building and neighborhood energy systems. It features detailed models for building heat consumption. The library by Abugabbara et al. is specifically designed for 5GDHC grids, offering comprehensive simulation analysis capabilities, but the limited accessibility restricts its use to a broader audience.

Besides Modelica, IDA ICE [54] and TRNSYS [55] are often used for DHC grid modeling. A calibrated simulation model in IDA ICE has uncovered design flaws in a 5GDHC grid in the Suurstoffi area [56]. Another IDA ICE model facilitates detailed simulations of 5GDHC grids, incorporating bidirectional flow and time series data for a sophisticated calculation of the Coefficient of Performance (COP) [57]. A case study highlights this model's value in the conceptual design and optimization of DHC networks [58]. Additionally, an IDA ICE model facilitates simulations of a bidirectional DHC network, improving the understanding of operational dynamics [59].

A TRNSYS model with detailed component modeling forms the basis for a thermoeconomic study comparing 4GDH and 5GDHC networks [19]. A hybrid environment combining the Modelica Buildings library with TRNSYS has further proved effective for comprehensively evaluating 5GDHC systems. It assesses the feasibility and energy savings of various demand scenarios, network configurations, seasonal storage options, and heat sources [60, 61].

2.3 Experiment environment

To bridge the gap between research and practical implementation, findings from simulation studies can be further analyzed in experiments. These experimental environments are essential for transforming theoretical research into practical applications, preparing costly field tests, and parameterizing and validating simulation models. To study the behavior and potential of prosumers in DHC grids thoroughly, testbeds should emulate the building and network behavior accurately. Numerous experimental testbeds exist that are tailored to explore distinct aspects from individual building energy systems and specific components of DHC grids to analyzing the DHC grid as a whole.

Testbeds for energy systems often utilize the Power Hardware in the Loop (PHIL) principle, which originated from electric grid simulation and is illustrated in Figure 2.2. This approach enhances Hardware in the Loop (HiL) simulations, which are used to test Input/Output (IO) signal exchange with an embedded system. PHIL by contrast emulates actual power flows in a testbed using devices such as power amplifiers or heat exchangers. In such configurations, parts of the system are simulated, e.g., a building's heat consumption. The real-time simulator produces setpoints for the power emulator, which then interacts with the device under test, e.g., a heat generator. Sensors capture the actual behavior and feed this data into the simulation model, thus influencing the system's future state and having a closed loop between hardware and simulation.

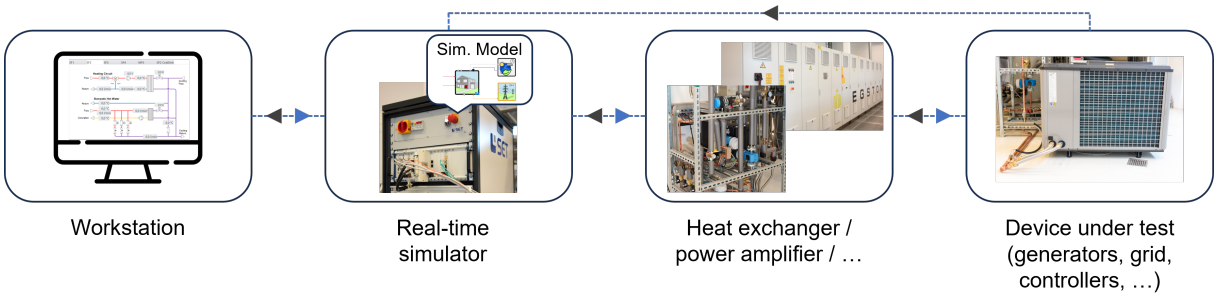

Figure 2.2: PHIL configuration.

Component testbeds

PHIL laboratories can be used to analyze the interplay between circulation pumps and the hydronic network. They enable the study of dynamic behaviors to refine control strategies [62]. By integrating real hardware with network emulators and actual pipes that replicate the hydraulic resistance of a system, PHIL setups can effectively simulate the pressure loss and flow rates, offering insights into the building's thermal dynamics [63]. These studies highlight the critical role of combining individual controls with hydronic balancing to enhance system performance.

Other laboratories are designed to delve into the dynamics of thermal energy systems in buildings, integrating components like Ground Source Heat Pumps (GSHP)s, TESs, and PHIL emulation for various temperature sources and loads [64, 65]. Such laboratories can be used for dynamic testing and detailed exergetic and exergoeconomic studies [66]. A similar experimental testbed integrated an Air Source Heat Pump (ASHP) into its design [67]. However, their testbed design with the outdoor installation of the ASHP introduces unwanted variability, as the uncontrollable air inlet conditions challenge the reproducibility and comparability of experimental results.

Focusing on DHC grid components, several laboratories investigate substation designs and control strategies of bidirectional substations, analyzing the real-world interaction between the grid and the building side [68, 69] or the behavior of ST based prosumers with a real DH grid [36]. Others study decentralized ST heat feed-in, exploring technical challenges, various hydraulic designs, and substation controls [34, 70, 71].

District heating and cooling laboratories

Numerous laboratories analyze the DHC grid and the dynamics of interaction between prosumers or consumers. Chung et al. [72] review laboratories that analyze decentral feed-in from ST collectors, proposing a laboratory design that facilitates the interplay between ST systems and the DH grid. The following paragraphs focus on laboratories that offer a broader scope and allow a more comprehensive analysis of DHC grid and prosumer interaction.

The Austrian Institute of Technology provides laboratories to validate smart applications in DHC networks. One focus are DH substations under remote control by the network operator to enhance system performance [73]. Their DigitalEnergyTestbed provides an interconnected analysis of heat and power systems and enables the digital integration of hardware and software components with a high level of interoperability [74]. They further provide the Lablink infras-

tructure, pioneering a seamless component integration within and across laboratories [75]. It introduces a communication protocol tailored to the needs of Co- or PHIL simulation systems in modern laboratories.

EURAC Research's Energy Exchange Lab features a versatile small-scale DHC network that facilitates the study of both conventional and low-temperature networks, covering various heat sources [76]. The laboratory allows testing and refining of bidirectional heat transfer stations, including their hydraulic configurations and control strategies [32]. Moreover, the laboratory's detailed characterization data can calibrate and validate models of 5GDHC transfer stations, enhancing their accuracy and reliability [77].

The District Lab of Fraunhofer IEE is an innovative testbed for the testing and advancing of low-temperature DHC systems [78]. This laboratory integrates a modular DHC grid, and a pipe test bench designed for mechanical assessments. Similarly, the NODES laboratory replicates a low-temperature DHC grid at the laboratory scale, motivated by the increasing implementation of ambient temperature DHC grids in Switzerland [79]. It features a versatile infrastructure that supports investigations into two grid options: grids with an active source and central circulation pump paired with passive, valve-controlled prosumers; or girds with a passive source and active prosumers equipped with their own circulation pumps.

2.4 Temperature information in energy management systems

Research in real-time MPC-based EMSs emphasizes the delicate balance between model accuracy and computational effort [80, 81]. Several EMS methodologies are employed in DHC systems, which are reviewed by Vandermeulen et al. [82] who highlight how the flexibility of TESs and the thermal inertia of buildings and network water can be exploited.

Despite multiple advancements, a common shortfall of many approaches is their tendency to neglect the temperature information. This missing temperature information significantly influences the usability of heat and the system's efficiency. For instance, the same amount of heat at $20\,°C$ during a shower is too cold and thus less valuable than the same power at $35\,°C$.

District heating and cooling grid models

Centralized optimization methods for DHC systems possess comprehensive information about the entire grid. This allows them to define all setpoints, encompassing central and decentralized generation, consumption, and TESs. Optimization models that include temperature behavior typically involve Mixed Integer Linear Programming (MILP) or Mixed Integer Non Linear Programming (MINLP) approaches. Short-term MILP models can optimize supply temperature by considering elements like thermal inertia and temporal temperature propagation delays of the grid [83, 84], and can be used to ensure that grid temperatures remain within contractual or desired levels [85]. MINLP optimization is often used for more complex modeling behaviors like nodal flow and pressure loss [86, 87]. Decomposing MINLP problems into two levels by combining a genetic algorithm with a MILP solver can enhance resolution speeds [88]. This can also increase the likelihood of finding globally optimal solutions for intricate DHC optimization models.

Beyond DHC grids and individual building energy systems, energy hubs offer integrated control of diverse energy flows within multi-energy systems [89, 90]. However, current energy

hub models often inadequately represent heating system behavior, particularly in accurately modeling varying temperature levels [91].

Thermal energy storage models

Within building energy systems, the TES is a crucial component where efficiency maximization depends on effective stratification [92], which has to be modelled accurately in MPC-based EMSs to outperform rule-based controls [93]. Tarragona et al. [94] provide a comprehensive review of EMSs with TESs, however a common limitation in EMS models is the linearization of TESs, neglecting the temperature profile. The following aspect on modeling TESs in EMSs extends from Publication 6 [95].

To model the temperature zones in TES, a simple method involves using a composite system of several TESs, each representing a different temperature range [96, 97, 98, 99, 100, 101]. While this approach captures zones of different temperatures, it fails to consider the interaction between different temperature layers. A more nuanced method is discretizing the TES into multiple layers with fixed volume and variable temperatures. Yet, models are often simplified in this approach by considering temperature variation only for discharging processes and ignoring the temperature dependency during the charging process and heat generator efficiencies to maintain linearity[102, 103].

Another modeling approach involves layers with constant temperatures and variable volumes, arranged in ascending temperature order [104]. Changes in layer volume occur due to heat supply or extraction. This model requires integer variables to indicate the specific layer involved in water extraction, significantly increasing the computational demands. Using MINLP models for a detailed TES description adds additional computational burdens, but a partial optimization framework can mitigate this while maintaining or enhancing solution quality [105].

2.5 CoSES research environment: Relevant research trends in district heating and cooling

The following sections will explore research trends that can be analyzed with the simulation and experimental environment outlined in this dissertation. Key trends include the integration of DHC grids into the smart energy system, the reduction of grid temperatures to transition current grids towards 4GDH systems, and the challenges associated with integrating prosumers into DHC grids.

2.5.1 Control strategies for smart energy systems

Intelligent control strategies are essential for smart energy systems and are usually implemented using central or decentralized approaches. There are multiple centralized approaches to optimize DHC grids in smart energy systems, as discussed in Section 2.4. However, they can be computationally demanding or challenging to implement due to difficulties like diverse ownership structures. Local energy markets and decentralized control approaches may offer advantages for these challenges.

The concept of local energy markets has extended from electrical systems [106] to incorporate DHC grids and the broader scope of smart energy systems. These markets are emerging as platforms for integrated energy trading, enhancing the efficiency of energy distribution and system

optimization. The adaptation of local energy markets to DHC networks requires network-aware trading mechanisms that are sensitive to pressure and temperature restrictions of DHC grids [107]. These market mechanisms are designed to facilitate energy transactions and ensure optimal coordination between heat and power systems within the constraints of current market regulations. The introduction of community-based markets promotes this integration, allowing a more cohesive and cooperative energy exchange [108, 109]. Exploring pricing mechanisms in these markets is critical for understanding how financial incentives and pricing can impact consumer behavior and energy distribution strategies [110]. The development of peer-to-peer multi-energy trading also marks a significant move towards decentralized thermo-electric systems, empowering consumers with greater control and resilience in their energy choices [111].

Decentralized control is another approach to managing the increasing complexity and diversity of multi-energy networks. A promising method in this context employs a two-stage robust optimization model. This model is designed to simplify the scheduling process in uncertain conditions. Enhanced by Fourier-Motzkin elimination and a dual decomposition algorithm, it significantly improves computational efficiency while preserving solution optimality, thus obviating the need for a central coordination center [112]. Another example of decentralized control involves optimizing the temperature setpoints of the DHC grid through agent-based control. This method supports the modular integration of a diverse range of sources and consumers, leading to a system that is both flexible and scalable [45]. Additionally, decentralized EMSs can manage multi-owner structures, effectively accommodating a mix of cooperative and non-cooperative stakeholders. Systems employing iterative algorithms can align the individual optimization efforts of local EMSs with the broader network objectives, ensuring a cohesive and efficient overall strategy [113]. However, one challenge in implementing decentralized approaches is the increased communication effort. This might lead to the risk of not finding the optimal solution in time, especially with iterative methods.

2.5.2 Temperature reduction in district heating grids

A defining feature of evolving DH grid generations is the reduced supply and return temperature, where the minimum temperature requirements of consumers often limit the supply temperature. Lowering the return temperature brings additional advantages, such as reduced volume flow due to a larger temperature difference between supply and return and more efficient heat generation.

Supply temperature reduction

Reducing the supply temperature in DH networks is a straightforward and effective strategy to reduce grid temperatures, but can result in operational challenges. These challenges include inadequate heat exchanger capacity for the necessary heat transfer, or increased volume flows to compensate for the lower temperatures. Recent research has focused on assessing the potential for temperature reduction in existing DH substations with simulation models [114], as well as exploring cost-effective measures like refining control strategies and decreasing supply temperatures [68].

Building-side measures

Building-side interventions are another option to lower DH grid temperatures. A common issue is the demand for high supply temperatures by a few key radiators to ensure occupant

comfort. Identifying and upgrading these critical radiators can significantly reduce the need for high supply temperatures, leading to more efficient heating operations [115]. Addressing faults in building heating systems, such as improperly designed heat exchangers, unregulated open bypasses, absent check valves in heating distributors, or lack of hydraulic balancing, can also reduce return temperatures [116]. Though initial costs may be high, the growing adoption of large-scale HPs shifts the cost-benefit analysis towards these interventions. Retrofitting buildings is another avenue to decrease grid temperatures, but only substantial retrofitting efforts tend to have a noticeable effect on grid temperatures [117].

Domestic hot water preparation

Preparing DHW presents another challenge in lowering temperatures in DH grids. This is primarily due to the need for high supply temperatures to prevent legionella proliferation and the low-temperature difference during periods of minimal DHW demand or to compensate for circulation losses. Circulation in DHW systems refers to continuously moving hot water through the piping system. The goal is to ensure that water does not cool down in the pipes during periods with no consumption so that the minimum temperature level at the consumer is always maintained.

One practical approach in multi-apartment buildings is deploying decentralized substations in each unit. The reduced volume within the DHW systems results in a high rate of water turnover in these systems, which can inhibit legionella at relatively lower temperatures [118]. This method can reduce temperature and heat consumption, especially when an auxiliary HP is integrated to offset circulation losses [119].

Centralized DHW preparation commonly considers three configurations: using an external heat exchanger; connecting an external heat exchanger to a TES; or employing an internal heat exchanger within a TES. Among these, the configuration involving an external heat exchanger connected to a TES yields the lowest return temperatures in the DH grid by taking advantage of the stratification within the TES [120].

Incorporating a dedicated heat source for DHW preparation can be advantageous, especially when low-temperature DH grids fail to meet DHW requirements. Systems that use HPs for this purpose have demonstrated their potential in significantly reducing grid return temperatures while offering reasonable payback periods [121]. Electric heating rods present an alternative solution, notable for their lower initial investment and space requirements. When coupled with a heat exchanger and a small TES at the consumer side, the size of the required electric heating rod can be effectively reduced, and the initial surge in electrical demand at the start of DHW consumption mitigated [122].

Cascaded district heating grids

If the required temperature level of consumers differs strongly, cascaded grids can improve efficiency. These DH grids use the return line of the primary, high-temperature DH grid to provide low-temperature heat to subsystems. Integrating buildings or zones with low-temperature heating demands into existing DH networks offers technical and economic benefits, including reduced heat losses, lower pumping power demands, and improved heat generation efficiency [123].

Optimal conditions for such integration usually involve low load fluctuations and combining buildings with high-temperature heating needs with those requiring lower temperatures

[124, 125]. In Estonia, studies on the technical and economic feasibility of incorporating low-temperature DH grids into existing systems have underscored the effectiveness of a three-pipe cascading solution, showing a promising return on investment [126]. Further research into these cascaded grids has identified the connection point of the low-temperature grid as a critical factor [127]. If temperatures or volume flows are too low, additional heat from the high-temperature supply pipe may be required, which must already be considered during the planning stage.

Improved control strategies

Effective control of DH systems presents a viable strategy for temperature reduction, with measures applicable at both building and grid levels. One straightforward yet effective method involves optimizing the heating control curves in building management systems. Particularly during partial load conditions, such optimizations can result in notable temperature reductions [128]. Similarly, optimizing the internal flow control of buildings contributes to decreased grid return temperatures [129].

The average return temperature of the grid and peak loads can effectively be reduced by lowering the grid supply temperature to align as closely with customer requirements as possible and utilizing the inherent thermal capacity of the grid for temporary heat storage [130]. Implementing a control logic that includes setpoints for the return temperature, such as through a weighted Proportional-Integral-Derivative (PID) approach, is another effective method [131].

As previously discussed, DHW preparation often poses a challenge for maintaining lower grid temperatures, which can be addressed with improved control approaches. A multi-mode charging method aligned with the cyclical demand of DHW can significantly lower the grid's return temperature [120]. A similar approach directly links the quantity of water drawn from the DH grid to ongoing consumption volumes [132]. This strategy leads to a notable decrease in return temperature and substantially reduces the total volume of water drawn from the grid.

5th generation district heating and cooling

5GDHC grids have by design grid temperatures near-ambient level and allow complete independence between grid and consumer supply temperatures. Due to the inherently low temperatures in these grids, they cannot provide heat directly but require BHPTSs. The most cost-effective method for cold extraction typically involves maintaining the grid temperature low enough to allow for direct cooling retrieval using the heat exchanger of the BHPTS [84]. When the cooling demand requires temperatures lower than that, either a reversible BHP or an additional chiller can reach the desired temperature.

2.5.3 Technical challenges of prosumer integration

Integrating prosumers into DHC networks introduces unique technical challenges distinct from managing passive consumers or central feed-in units. Advanced control strategies are essential in these settings to maintain stable grid supply temperatures, ensure efficient pump operations, and avoid mutual interference [29, 133]. The control systems must also be capable of managing differential pressure fluctuations between supply and return lines to optimize the system's performance [134]. In a related dissertation, Thomas Lickleder delves into the technical implementation and operational aspects of prosumers in DH systems from a network perspective [135].

A simple control approach involves implementing separate control loops for regulating pressure and temperature. This can be done with a two-step control strategy that first focuses on building control, ensuring that the supply temperature is above the DH feed-in temperature [136]. The second step involves maintaining the supply temperature in the DH system where the pump generates the adequate pressure-head to overcome the network's differential pressure. A similar strategy employs a cascaded closed loop controller, which consists of an inner loop targeting the differential pressure in the grid and an outer loop controlling the network supply temperature [34]. However, this method may encounter challenges due to pump-to-pump interactions in systems with numerous prosumers [137].

Addressing these pump-to-pump interactions is crucial due to the rapid pressure propagation within the grid that can lead to unstable pump control, particularly in grids with varying-sized prosumers [138, 139]. In this context, networks with fewer prosumers tend to have fewer hydraulic instabilities and control complexities [12]. A potential solution is a weighted PID control approach, which uses two actuators with three setpoints: the transferred heat power and the heat exchanger outlet temperature on the grid and house side [131]. This method effectively reduces the rigid coupling between prosumers, thus mitigating issues like pump blocking. A similar concept for heat exchangers simultaneously controls heat flow and outlet temperatures using a feed-forward controller [140]. One limitation of this controller operation is the assumption of knowing the temperature difference on the prosumer system's side.

A different approach integrates a passive balancing unit and decentralized pumps for both feed-in and extraction [141]. These pumps are controlled to maintain grid temperature setpoints. This method relaxes the control problem by utilizing the thermal inertia of the transfer station along with the passive balancing unit, enabling stable grid operation, as shown in an experimental study.

As illustrated in this section, the landscape of DHC is evolving rapidly, with advancements in 4GDH and 5GDHC systems paving the way for more efficient, sustainable, and adaptable energy networks. The trends highlighted here reflect a dynamic field poised for significant transformation from integrating prosumers and strategically managing temperature and pressure in DHC grids to exploring innovative control methods and balancing heating and cooling demands. The subsequent chapters of this dissertation present a simulation and experiment environment specifically designed to further explore and analyze these trends. This infrastructure aims to bridge the gap between theoretical insights and practical applications, contributing to a deeper understanding and effective implementation of these advanced concepts.

Chapter 3

Optimal arrangement of the heating system for prosumers

Prosumer systems in DH grids comprise heat generators, heat consumers, TES, and a bidirectional heat transfer station, which allows for various arrangements. Looking at common modern heating systems with heat generator, TES, and heat consumer already shows two parallel arrangement options, each with distinct advantages and disadvantages. These systems can be categorized into 4-pipe and 2-pipe systems [142], as illustrated in Figure 3.1.

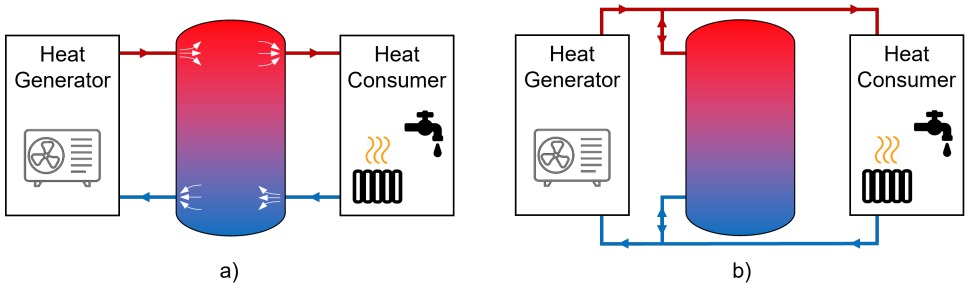

Figure 3.1: TES integration into the heating system: a) 4-pipe system vs. b) 2-pipe system

The **4-pipe system** completely separates the flow from the heat generator and the consumer, where each has its dedicated port on the TES. A challenge with this system is potential mixing due to high volume flows, especially if internal flows oppose each other, as in the example in Figure 3.1 [143]. This can be mitigated using baffle plates and strategic port positioning.

By contrast, the **2-pipe system** uses a single inlet and outlet connected to heat generation and consumption. The flow through the TES is determined by the difference between the generation's output and the consumption's intake. A limitation is that the heat generator and consumer flow are not fully decoupled, leading to potential mutual influence on volume flows, such as an unintended flow when pumps are off. This can be prevented using an electric ball valve.

Both systems present their unique advantages and challenges. The selection between them largely depends on specific demands of the heating setup, such as the type of heat generator. More possibilities arise when considering combinations with serial options. Integrating the bidirectional heat transfer station in prosumer-based systems further expands the range of possible

configurations. The connection to the DH network imposes the additional requirement to ensure low network temperatures.

Incorporating prosumers also offers new strategies to lower the supply temperature below the minimum DHW temperature requirements. One approach uses decentralized heat generators to elevate the supply temperature to necessary levels. Alternatively, implementing variable grid temperatures allows the grid to operate at high temperatures for DHW only at specific times and the TES storing high-temperature heat for later use.

The multitude of factors complicates the identification of an ideal component arrangement for prosumer systems in DH grids. Therefore, the following publication analyzes the optimal component arrangement. A simulation study with models in SimulationX allows the analysis of the feed-in potential, efficiency, and the network's return temperature. Different heat generator types and grid supply temperature levels are examined to comprehensively evaluate various possibilities. Additionally, the study considers how the primary mode of prosumers — either extracting from or feeding into the DH grid — influences the determination of the optimal system configuration.

A comparison of prosumer system configurations in district heating networks

Authors Daniel Zinsmeister, Thomas Lickleder er, Franz Christange, Peter Tzscheutschler, Vedran S. Perić

Publication medium Energy Reports, Volume 7

Digital object identifier https://doi.org/10.1016/j .egyr.2021.08.085

Author contributions

Daniel Zinsmeister:	Conceptualization, Methodology, Software, Investigation, Visualization, Writing – original draft, review & editing.
Thomas Lickleder er:	Conceptualization, Writing – original draft, review & editing.
Franz Christange:	Conceptualization, Writing - review.
Peter Tzscheutschler:	Conceptualization, Writing - review, Supervision, Project administration, Funding acquisition.
Vedran S. Perić:	Conceptualization, Writing - review, Supervision, Project administration, Funding acquisition.

Available online at www.sciencedirect.com
ScienceDirect
Energy Reports 7 (2021) 430–439
www.elsevier.com/locate/egyr

17th International Symposium on District Heating and Cooling, DHC2021, 6–9 September 2021, Nottingham, United Kingdom

A comparison of prosumer system configurations in district heating networks

Daniel Zinsmeister[a,*], Thomas Licklederer[a], Franz Christange[b], Peter Tzscheutschler[a], Vedran S. Perić[a]

[a] *Technical University of Munich, 80333 Munich, Germany*
[b] *Triowatt GmbH, 83071 Stephanskirchen, Germany*

Received 4 August 2021; accepted 7 August 2021

Abstract

Prosumer-based district heating networks attract an increasing interest in energy research. There are numerous publications addressing the prosumer integration into district heating networks with a focus on grid side operation. However, the operation of the prosumer side has not been extensively investigated in the literature where bidirectional heat transfer stations, heat generators, consumption and storages can be connected in different ways. These different connections have different influences on the district heating network operation that require deeper analysis and understanding.

This paper evaluates the influence of using different prosumer side system configurations as well as their suitability for prosumer-based district heating networks. Beginning with the characteristics of possible prosumer side configurations this paper evaluates the applicability of these configurations according to the number of components and operational flexibility. Subsequently, the most promising subset of the evaluated configurations are simulated in realistic scenarios using SimulationX® software and its Green City toolbox to gain detailed insight into their operation and efficiency. The simulated configurations are analyzed with respect to exportable excess heat, grid temperatures and the overall efficiency of the heat supply. The configurations are studied in various scenarios that differ in heat generation type (heat pump, solar thermal collectors or combustion device) and the necessary supply temperatures on the prosumer and grid side.

In conclusion, this paper provides a decision guidance to select the most suitable prosumer side configuration for a desired district heating network and consumption temperatures.

Peer-review under responsibility of the scientific committee of the 17th International Symposium on District Heating and Cooling, DHC2021, 2021.

Keywords: District heating; Prosumer; Decentralized feed-in; Heat system configurations

1. Introduction

In order to reach the climate change goals of the Paris agreement, all energy sectors have to reduce their emissions drastically, including the heating sector. Within the heating sector, district heating and cooling grids

* Corresponding author.
E-mail address: zinsmeister@tum.de (D. Zinsmeister).

https://doi.org/10.1016/j.egyr.2021.08.085

Peer-review under responsibility of the scientific committee of the 17th International Symposium on District Heating and Cooling, DHC2021, 2021.

Nomenclature

3WV	3-way valve
CG	Combustion-based heat generators
DH	Bidirectional district heating station
DHW	Domestic hot water
HC	Heating consumption
HG	Heat generation
HP	Heat pump
LTDH	Low temperature district heating
ST	Solar thermal collectors
TS	Thermal storage
ULTDH	Ultra low temperature district heating

are one promising aspect to reduce emissions [1]. District heating grids were introduced in the 19th century and have evolved since then from high temperature steam grids to modern, low temperature systems, increasing their efficiency step by step [2].

One possibility to further reduce the CO2 emissions of district heating system is to integrate prosumers. Prosumers are market participants, who can produce and consume energy. In district heating grids, prosumers can feed excess heat into the district heating grid, or extract heat from the grid, if it is more economic for them [3]. The excess heat ideally comes from low emission heat generators, such as solar thermal collectors, heat pumps or combined heat and power units. The integration of prosumers or a decentralized heat supply can also reduce heat losses due to lower transport distances [4]. The potential of prosumer based district heating stations is high especially in areas with mixed building stocks [5].

Decentralized feed-in to the district heating grid results in several effects, not considered in standard district heating grids. The decentralized feed-in can lead to a local drop of the supply temperature and a locally increased flow velocity [3]. Also, the flow direction within the district heating grid can change due to different feed-in points, resulting in a supply frontier in which there is no flow and thus the temperature drops, leading to stronger thermal stress of the pipes [6]. This might require a transformation of today's district heating networks into smart district heating networks [3].

The integration of heat from prosumers demand a new approach for the district heating substation, especially since different heat sources often require individual concepts. For the utilization of low temperature waste heat, a heat pump can be used in the heat transfer station to raise the low temperature level of waste heat to the necessary heat network temperature [7]. Decentralized heat pumps can also be used directly to substitute existing heat generators in heat networks [8]. Another possibility for the use of heat pumps in the transfer station are so-called booster heat pumps. This offers the possibility of using very low heat network temperatures. If heating and cooling are used simultaneously, the waste heat or cold of the heat pumps can also be used very effectively by means of intelligent control [9,10]. Several other publications discussed the integration of solar thermal collectors into prosumer-based district heating systems. On the grid side, the three possible feed-in types are 'return to flow', 'return to return' and 'flow to flow', of which 'return to flow' is the option, chosen as the best by Mangold et al. [11]. Rosemann et al. shows a control algorithm for a prosumer substation with solar thermal collectors, where the consumption side connects both the collectors and the district heating grid [12]. Another approach is presented by Lamaison et al. and Paulus et al. where the district heating substation works as hydraulic switch, connecting the consumer, the solar thermal collectors and the district heating grid [13,14].

The above referenced publication made good progress with the prosumer district heating connection, however their common assumption was a system without a storage. Nevertheless, can the introduction of a storage be beneficial for heat prosumers because of the increased flexibility, especially for small scale district heating grids. When using a storage, the number of possible combinations rises dramatically.

The influence of the house side of heat prosumers has not been studied to the best of our knowledge. Therefore, this paper investigates which combination is best suited for different heat prosumers. First, the different components

heat generators (HGs), heating consumption (HC), the district heating substation (DH) and the thermal storage (TS) are characterized. Based on this characterization, various configurations are defined for a scenario analysis. This scenario analysis simulates configurations with the different HG types heat pump (HP), combustion-based heat generator (CG) and solar thermal collectors (ST). The results are used to rate the configurations and offer a guidance to select the most suitable prosumer side configuration.

2. Prosumer system components

In this chapter, the different prosumer system components are described and possible restrictions for the usage in a prosumer system are highlighted.

2.1. Heat demand

The heat demand consists of HC and domestic hot water (DHW) consumption.

HC can be classified into two temperature levels: Radiator panel heating, where the supply and return temperature is 60 °C and 45 °C respectively and surface heating, where the temperature is 40 °C and 30 °C respectively. The supply temperature of the HC is controlled by a mixing station to provide a constant temperature for the heating system. The flow rate is controlled by a thermostat.

In order to decouple the DHW demand from the heat production, the DHW consumption is directly linked to the TS. To prevent problems with legionella, the temperature of the DHW reservoir is restricted, e.g. the German standard requires DHW to be heated to 60 °C or higher for DHW systems with a total content of more than 3 l [15].

2.2. Thermal storage

The integration of several TS tanks was excluded since heat systems normally only have one TS and to keep the number of variants manageable. The TS can have several connections at different heights. This improves the temperature layering within the TS, so that for example water layers with high temperature are at the top separated from colder water layers and thus preventing exergy losses by the mixing of hot and cold water. The temperature layering can be maintained very well during operation if loading and unloading is done correctly [16]. The temperature of the TS can be measured at different height levels.

In order to fulfill the hygienic requirements, the DHW circuit and TS are separated with an internal or external heat exchanger. Fig. 1 shows the two possible DHW integrations.

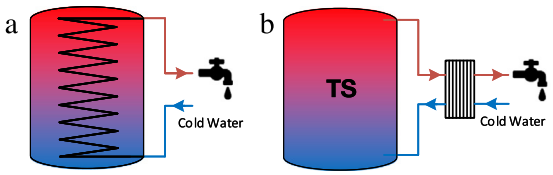

Fig. 1. DHW storage integration (a) with external heat exchanger, (b) with internal heat exchanger.

2.3. District heating substation

The focus of this paper are district heating systems with low supply temperatures, which Østergaard et al. classified as low-temperature district heating (LTDH) with supply temperature range between 50 °C and 65 °C and ultra low temperature district heating (ULTDH) with a supply temperature range between 30 to 50 °C [17].

These temperature ranges define possible configurations. LTDH are able to provide a temperature level that fulfills DHW demands and can thus be combined with high and low temperature HC and/or directly to the TS. ULTDH in contrast cannot provide heat fulfilling DHW demands and requires an additional HG.

2.4. Heat generators

For the comparison of prosumer system configurations, HGs are divided into three subgroups:

- HP, which have a constant temperature difference between supply and return temperature;
- volatile ST and
- CG with a controllable supply temperature.

Heat pumps:

With rising supply temperatures, the efficiency of HPs decreases. For this reason, the internal control of standard HPs does not allow influencing the supply temperature directly, but runs at a constant temperature difference between supply and return temperature to maximize the efficiency. In order to reach high supply temperatures, e.g. for DHW, the return temperature has to increase accordingly. This can be done best by using the layering of the TS and extracting the return water from a higher, warmer storage level.

When connecting the HP to the TS, two 3-way valves (3WV) are used to switch between low and high temperature operation. Fig. 2 shows a common configuration without the connection to DH according [18].

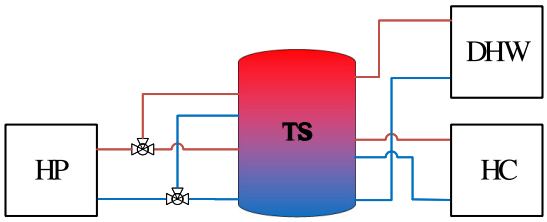

Fig. 2. Common HP integration.

Due to the bad efficiency of HPs at high temperature, only low temperature HC is considered.

Solar thermal collectors:

In contrast to other HG units, ST is a volatile HG, which means, it cannot be used as a single heat source. In order to prevent ST from freezing during winter, antifreeze is added. This requires ST to be in a separate circuit, where the heat is transferred with a heat exchanger, normally done in small heating systems with an internal heat exchanger within the TS.

Combustion-based heat generators:

The supply temperature of CG, like condensing boilers or combined heat and power, can normally be controlled directly and has little influence on the efficiency of the heat generation. The efficiency of a CG is mostly dependent on the return temperature and rises due to the condensing effect, if the return temperature is lower.

3. Prosumer system combinations

The possible prosumer system combinations can be divided into three categories:

- Parallel combinations, where all elements are connected to the TS;
- Serial combinations, where three elements are connected in series;
- Mixed combinations, where parallel and serial features are realized.

An overview and preliminary characterization of 14 possible combinations is published separately [19]. Fig. 3 shows the 9 combinations that were chosen for further investigation. The other combinations were excluded due to high estimated exergy losses, too little flexibility or because they are not usable in prosumer-based district heating grids.

The combinations can be evaluated by the following criteria:

- Costs, related to the number of necessary components like pumps and valves or if special components have to be used.
- Operational flexibility, defined by the flexibility to switch between heat extraction and feed-in and the flexibility of controlling the feed-in temperature and power.

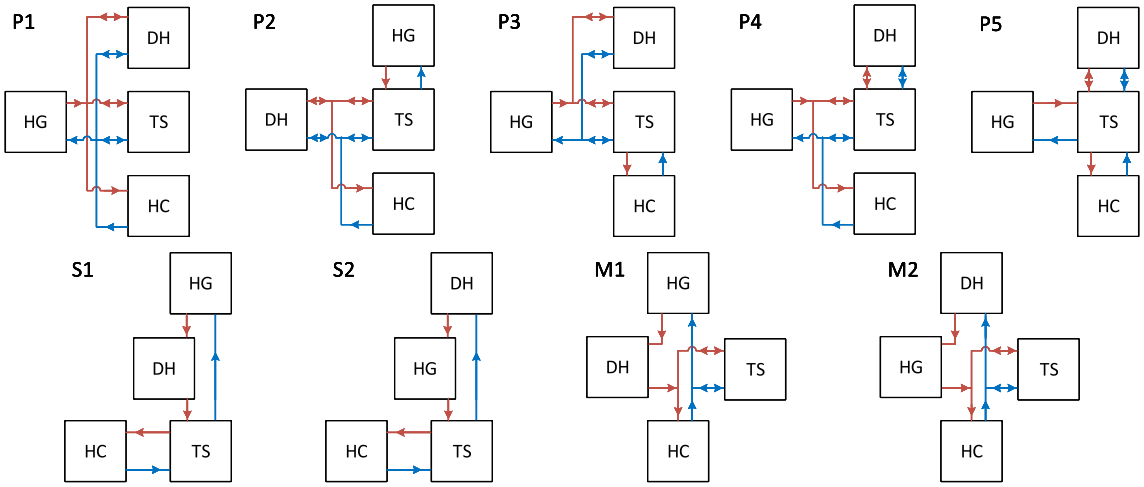

Fig. 3. Parallel combinations (P1 to P5), serial combinations (S1 and S2) and mixed combinations (M1 and M2).

4. Scenario analysis

The combinations presented in the previous chapter are evaluated using a scenario analysis to identify the configuration best suited for different heat prosumers. For this purpose, the configurations are simulated for the different cases ‘extraction’, ‘no grid’ and ‘feed-in’.

4.1. Simulation model

In order to assess the performance of different prosumer side configurations, they are simulated using the SimulationX® software. SimulationX is based on the modeling language Modelica. The integrated Green City library provides a wide range of component models of state-of-the-art energy supply systems, including detailed models of thermal components [20]. Most elements of the Green City library are accessible, thus making it possible to customize individual simulation blocks. Pipe losses and insulation are neglected for the model as these are specific to individual constructions and the paper aims at deriving general conclusions on the investigated configurations.

For the simulation, existing TS and HC models where used. The three different HG models were derived and the control strategy of Section 4.2 was implemented. The DH simulation block was split into a DH-feed-in block and a DH-extract block. Fig. 4 presents the framework of one prosumer system configuration.

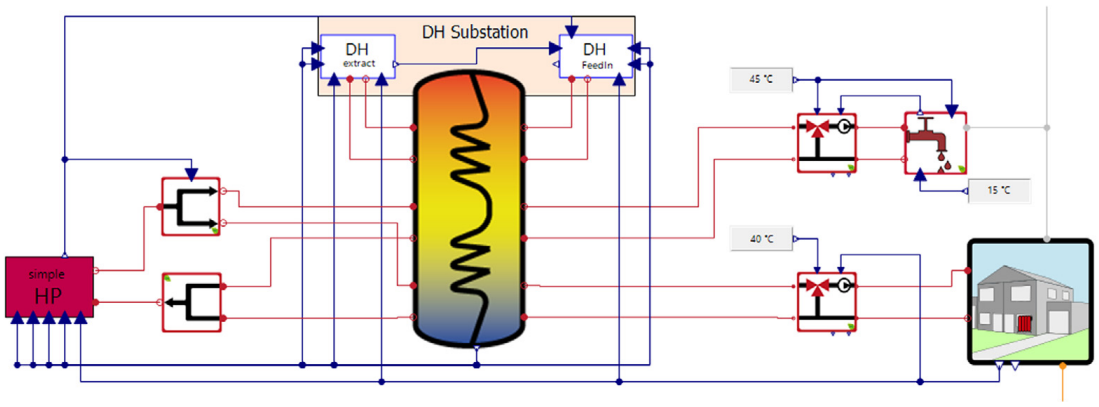

Fig. 4. Model of a prosumer with a HP and the configuration P5.

4.2. Control strategy

The control strategy of the DH was based on the strategy of Rosemann et al. [12], where the volume flow of the pump on the prosumer side operates with a constant flow rate. The flow rate on the grid side is controlled to reach the supply temperature on the prosumer side when extracting heat and to reach the supply temperature of the grid side when feeding in. When classifying the feed-in potential, the control strategy tries to feed in as much heat as possible.

The criteria for feed-in or extraction are:

- Feed-In:
  Switched on: $T_{storage,top} > 60\ °C + \Delta T$ and $T_{storage,middle} > 40\ °C + \Delta T$
  Switched off: $T_{storage,top} < 60\ °C$ or $T_{storage,middle} < 40\ °C$
- Extraction:
  Switched on: $T_{Storage,top} < 55\ °C$ or $T_{Storage,middle} < 40\ °C$
  Switched off: $T_{Storage,bottom} > 55\ °C/40\ °C$

Information about the control strategy of HG is difficult to assess, since most manufacturers do not share their individual control strategy. For this reason, a relatively simple control strategy is chosen, which only considers the temperature of the TS at different layers, which to our knowledge represents a common control philosophy for HGs, as for example implemented at [21]. Since the purpose of the scenario analysis is to determine the potential of the different configurations independent of the control strategy, a simple and similar control strategy between the different HG types is beneficial. The control strategies are implemented as follows

Heat pump (HP):

- Switched on with $T_{sup,high}$ when $T_{Storage,top,HPin} < 60\ °C$, switch off when $T_{Storage,top,HPout} > 60\ °C$
- Switched on with $T_{sup,low}$ when $T_{Storage,middle} < 40\ °C$, switch off when $T_{Storage,bottom} > 40\ °C$
- If the switch on conditions for $T_{sup,low}$ and $T_{sup,high}$ are true, $T_{sup,high}$ is produced.
- The volume flow is controlled to have a temperature difference of 10K between T_{sup} and T_{ret}.

Combustion-based heat generator (CG):

- Switched on when $T_{Storage,top} < 60\ °C$ or $T_{Storage,middle} < 40\ °C$, switch off when $T_{Storage,bottom} > 60°$
- The volume flow is controlled to have a constant supply temperature of 70 °C.

Solar thermal collectors (ST):

- The ST pump is switched on, when the collector temperature is bigger than the TS inlet temperature.
- The volume flow is controlled to reach the specified supply temperature or switched off, if the TS reaches its maximum temperature.
- The supply temperature is defined as $T_{sup} = 60\ °C$ if the TS inlet temperature is lower than 60 °C to provide water for DHW as efficient as possible. When the inlet temperature is above 60 °C, T_{sup} is changed to 80 °C to further charge the TS.

In order to reduce losses during summer, when no heating, but only DHW is required, the TS is only charged at the top half.

4.3. Scenario cases

The scenarios are simulated for a whole year. The HC is defined by a five-person household with different temperature levels: 40/30 °C (HC low) and 60/45 °C (HC high) according to 2.1. The DHW consumption is used according to the model of Jordan et al. [22]. The TS has a volume of 750 l and an internal heat exchanger for DHW and ST, if used.

The HG are sized to cover the load of the building:

- HP: 10 kW at $T_{sup} = 40\ °C$
- CG: 10 kW
- ST: flat plate collector with 12 m^2 collector surface

As described in 2.3, two different temperature levels where assumed for the DH grid. ULTDH with a supply temperature of 45 °C and LTDH with a supply temperature of 65°.

In order to classify each configuration, the scenarios are run in three different operation phases:

- No Grid:
  In this case, the heat is provided solely by the HG and is neither fed into the grid nor extracted from it in order to determine the efficiency of the configuration.
- Feed-In:
  For the case of feed-in, the potential of the configurations to provide heat to the grid will be assessed. In order to make a preselection for further holistic studies, we only examine the prosumer side possibilities in this paper. Therefore, the maximum, grid-independent feed-in potential is calculated and the HG is operated as constant as possible in order to feed as much heat as possible into the grid. In reality, however, the feed-in is strongly dependent on the current grid conditions. The return temperature of the grid is assumed in this scenario constant at 45/30 °C
- Extraction:
  In the extraction scenario, the demand should be covered by the heating network. When using ULTDH, the HG can support to provide the temperature level required for DHW.
  In this scenario, the grid supply temperature is assumed constant at 65/45 °C.

4.4. Evaluation

For each operation phase, the efficiencies are evaluated. When no grid is connected, the efficiency $\eta_{no\,grid}$ is calculated based on the heat demand E_{Demand} and the fuel consumption of the HG $E_{fuel,no\,grid}$:

$$\eta_{no\,grid} = \frac{E_{Demand}}{E_{fuel,no\,grid}} \tag{1}$$

The feed-in potential is described by the total amount of energy, fed into the grid over the year $E_{feed\,in}$. The feed-in efficiency $\eta_{feed-in}$ is calculated on basis of the additional fuel amount necessary to produce $E_{feed-in}$. For the additional fuel amount, $E_{fuel,no\,grid}$ is subtracted from the fuel amount of the feed-in scenario $E_{fuel,feed-in}$:

$$\eta_{feed-in} = \frac{E_{feed-in}}{E_{fuel,feed-in} - E_{fuel,no\,grid}} \tag{2}$$

When extracting heat from the grid, the return temperature should be as low as possible. Therefor the average grid return temperature $T_{ret,grid}$ is important to evaluate the configuration. Another criterion is the extraction efficiency, which can be calculated by dividing E_{Demand} by the amount of energy, extracted from the grid $E_{extraction}$ plus the fuel amount $E_{fuel,extraction}$, if necessary.

$$\eta_{extraction} = \frac{E_{Demand}}{E_{extraction} + E_{fuel,extraction}} \tag{3}$$

5. Results

All simulation results are published in more detail in [19].

Fig. 5 shows the results of all configurations using a CG. In this case, configuration P1 is in general the best choice. With this configuration the highest degree of flexibility is obtained, since the feed-in and consumption temperature level does not depend on the TS condition, but can be directly influenced. Due to low return temperature on the prosumer side and low TS losses, the efficiency for ‘no grid’ and ‘extraction’ are best and the return temperature on the grid side during ‘extraction’ is lowest. Since the ULTDH grid cannot provide heat that meets the temperature requirements of DHW, the CG must generate the necessary heat in this case as shown in Fig. 5c.

If the goal is to achieve the highest possible feed-in, configuration S1 might be interesting for the CG at a low temperature level of the HC (blue scenario). Another advantage is that fewer components are needed, which saves costs. However, the flexibility for ‘feed-in’ is limited, since this is only possible when the CG is active and the TS is sufficiently filled for the DHW demand. The high return temperature during ‘extraction’ is another disadvantage.

When using a HP, only P2, P5 and P5* are possible, since it must be connected directly to the TS. P5* is the same configuration as P5 but with an additional 3WV in the return line, so that the return flow of the DH can be

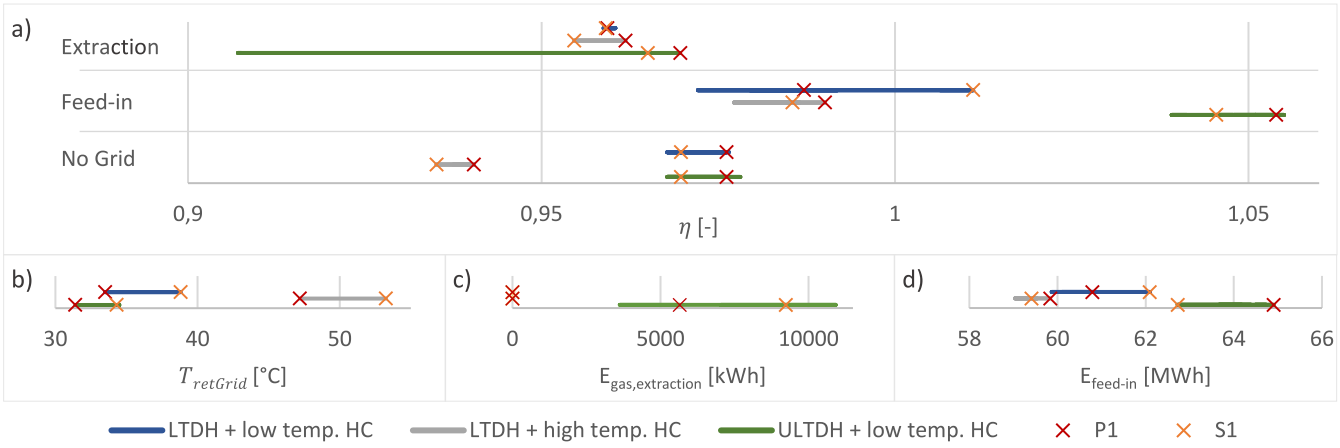

Fig. 5. Simulation results of the CG: Results lie in the range indicated by the different lines; the line color represents different scenarios; two promising configurations, P1 and S1, are marked separately. (a) shows the efficiency for the different operation phases 'extraction, 'feed-in' and 'no grid', (b) shows the averaged return temperature during 'extraction', (c) the additional gas power necessary for the CG to heat up water to DHW temperature when the grid is too cold for 'extraction' and (d) shows the maximum feed-in potential during 'feed-in'. . (For interpretation of the references to color in this figure legend, the reader is referred to the web version of this article.)

fed in at different TS heights. Fig. 6 shows the results for this generator. The efficiency for the scenario 'no grid' is the same for both configurations with an averaged efficiency (COP) of 3.83.

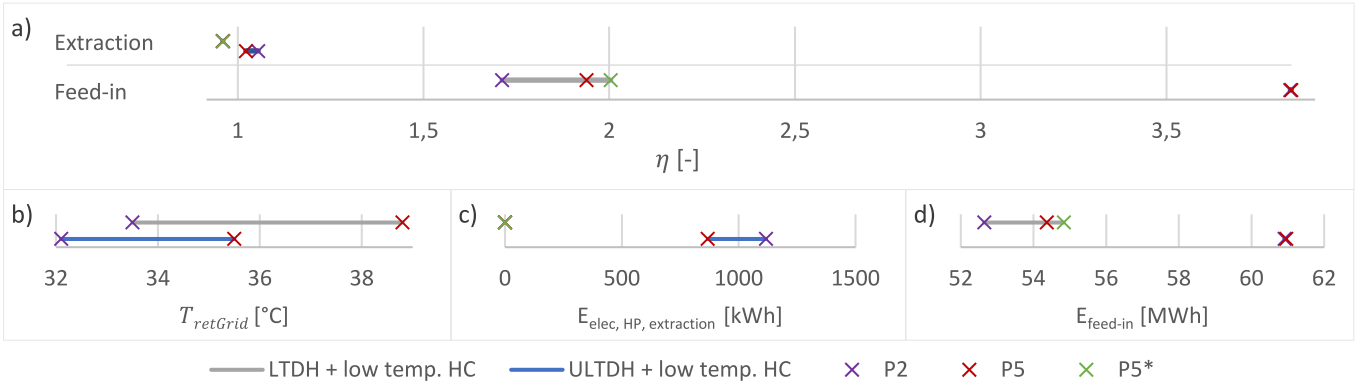

Fig. 6. Simulation results of the HP: Results lie in the range indicated by the different lines; the line color represents different scenarios; the possible configurations P2, P5 and P5* are marked separately. (a) shows the efficiency for the different operation phases 'extraction and 'feed-in', (b) shows the averaged return temperature during 'extraction', (c) the additional electric power necessary for the HP to heat up water to DHW temperature when the grid is too cold for 'extraction' and (d) shows the maximum feed-in potential during 'feed-in'. . (For interpretation of the references to color in this figure legend, the reader is referred to the web version of this article.)

The results show further that the main use case of the prosumer has to be chosen in advance in order to decide for the ideal configuration. If the prosumer extracts heat more often from the grid than it feeds in, P2 is the better choice. This configuration results in a lower return temperature on the grid side and a slightly higher efficiency. In a ULTDH grid, the HP however has to provide more additional heat to reach the DHW temperature level.

If the main purpose is to feed-in excess heat into a LTDH grid, P5/P5* is the better configuration. The efficiency, and feed-in potential is significantly higher in this case. P5* shows better results than P5, so it is advisable to use an additional 3WV. The results show that apart from increasing the efficiency due to the better layering, the feed-in criteria for switching off is exceeded less often.

For ST collectors, the simulation was done with a TS with an internal heat exchanger. This means, that only P2 and P5 are possible configurations. The results show, that both configurations show little difference in their efficiency and yield. The return temperature during extraction is, similar to the HP configuration, slightly better at P2.

Varying return temperatures on grid and house side showed for all types of HG that this shifts the results to a higher or lower level, but does not change the overall characteristics of the configurations.

Fig. 7 shows the daily feed-in potential of HP and CG and the average daily temperature over a time period of 20 days. It can be seen that the feed-in potential follows the temperature closely, since a high heat demand at low temperatures leaves only little capacity for feeding in heat. If a high feed-in potential during cold periods is required for the network, the HG should be oversized compared to dimensioning for standard operation.

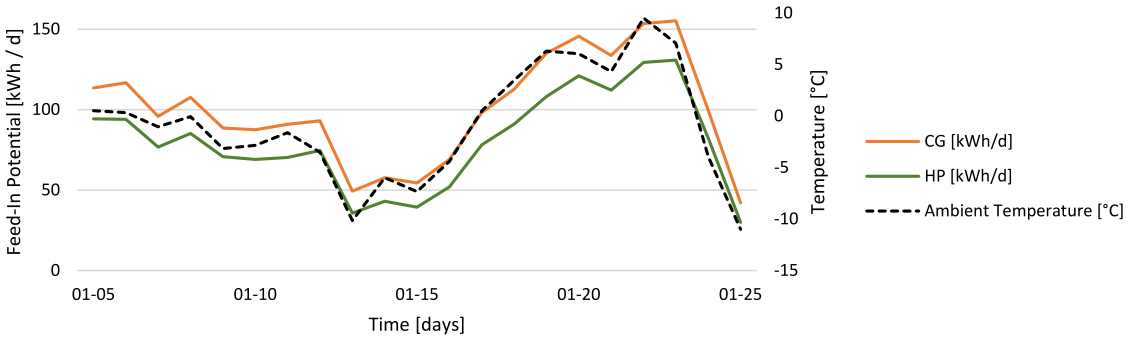

Fig. 7. Daily averaged feed-in potential of CG and HP in comparison with the ambient temperature.

6. Conclusion

The presented paper studies possible prosumer system configurations for HG, DH, TS and HC. The results provide an argumented decision guidance to select the most suitable prosumer side configuration for the desired HG, district heating network and consumption temperatures. Two configurations were identified in the scenario analysis, which in general suited best.

The configuration in which all components are directly connected to each other achieves the lowest return temperature and lowest storage losses. For a combustion-based HG, this leads to the highest efficiency due to the utilization of the condensation effect. This configuration also has the lowest return temperature on the heat grid side. This result reflects the best practice recommendations given by engineering offices and plumbers in the context of the planning of the CoSES laboratory environment at TU Munich [23]. It was recommended to use a completely parallel setup (P1). However, there are no reference papers or guidelines available on how to integrate thermal storages that would be suited to verify our results.

Since a direct connection of HP or ST with HC or DH is not possible, a different configuration must be chosen in which the HG is connected directly to the TS. At high grid temperatures, using of a 3WV between DH return flow and the inlet to the TS increases the efficiency of heat extraction from the network.

Declaration of competing interest

The authors declare that they have no known competing financial interests or personal relationships that could have appeared to influence the work reported in this paper.

Acknowledgments

This project was founded by the Federal Ministry for Economic Affairs and Energy, Germany (FKZ: 03EN3032A). The work of Vedran S. Perić was supported by Deutsche Forschungsgemeinschaft (DFG), Germany through “Optimal Operation of Integrated Low-Temperature Birdirectional Heat and Electric Grids (IntElHeat)” under project number 450821044.

References

[1] Lund H, Möller B, Mathiesen BV, Dyrelund A. The role of district heating in future renewable energy systems. Energy 2010;35(3):1381–90. http://dx.doi.org/10.1016/j.energy.2009.11.023.

[2] Lund H, Werner S, Wiltshire R, Svendsen S, Thorsen JE, Hvelplund F, et al. 4th generation district heating (4GDH). Energy 2014;68:1–11. http://dx.doi.org/10.1016/j.energy.2014.02.089.
[3] Brand L, Calvén A, Englund J, Landersjö H, Lauenburg P. Smart district heating networks – A simulation study of prosumers' impact on technical parameters in distribution networks. Appl Energy 2014;129:39–48. http://dx.doi.org/10.1016/j.apenergy.2014.04.079.
[4] Kauko H, Kvalsvik KH, Rohde D, Nord N, Utne Å. Dynamic modeling of local district heating grids with prosumers: A case study for Norway. Energy 2018;151:261–71. http://dx.doi.org/10.1016/j.energy.2018.03.033.
[5] Brange L, Englund J, Lauenburg P. Prosumers in district heating networks – A Swedish case study. Appl Energy 2016;164:492–500. http://dx.doi.org/10.1016/j.apenergy.2015.12.020.
[6] Heymann M, Rühling K, Felsmann C. Integration of solar thermal systems into district heating – DH system simulation. Energy Procedia 2017;116:394–402. http://dx.doi.org/10.1016/j.egypro.2017.05.086.
[7] Fitó J, Hodencq S, Ramousse J, Wurtz F, Stutz B, Debray F, et al. Energy- and exergy-based optimal designs of a low-temperature industrial waste heat recovery system in district heating. Energy Convers Manage 2020;211:112753. http://dx.doi.org/10.1016/j.enconman.2020.112753.
[8] Rämä M, Wahlroos M. Introduction of new decentralised renewable heat supply in an existing district heating system. Energy 2018;154:68–79. http://dx.doi.org/10.1016/j.energy.2018.03.105.
[9] Zarin Pass R, Wetter M, Piette MA. A thermodynamic analysis of a novel bidirectional district heating and cooling network. Energy 2018;144:20–30. http://dx.doi.org/10.1016/j.energy.2017.11.122.
[10] Bünning F, Wetter M, Fuchs M, Müller D. Bidirectional low temperature district energy systems with agent-based control: Performance comparison and operation optimization. Appl Energy 2018;209:502–15. http://dx.doi.org/10.1016/j.apenergy.2017.10.072.
[11] Mangold D, Schäfer K. DEZENTRAL - Dezentrale einspeisung in nah- und fernwärmesysteme unter besonderer berücksichtigung der solarthermie teilbericht des verbundpartners solites forschungsbericht zum forschungsvorhaben 03et1039c laufzeit: 2012 Bis Mai 2015, solites. 2015, http://dx.doi.org/10.2314/GBV:866742697.
[12] Rosemann T, Löser J, Rühling K. A new DH control algorithm for a combined supply and feed-in substation and testing through hardware-in-the-loop. Energy Procedia 2017;116:416–25. http://dx.doi.org/10.1016/j.egypro.2017.05.089.
[13] Lamaison N, Bavière R, Cheze D, Paulus C. A multi-criteria analysis of bidirectional solar district heating substation architecture. In: SWC 2017 ISES solar world congress: international solar energy society. Freiburg im Breisgau: International Solar Energy Society (ISES); 2018, p. 1–11. http://dx.doi.org/10.18086/swc.2017.10.02.
[14] Paulus C, Papillon P. Substations for decentralized solar district heating: Design, performance and energy cost. Energy Procedia 2014;48:1076–85. http://dx.doi.org/10.1016/j.egypro.2014.02.122.
[15] DIN. Technische regeln für trinkwasser-installationen: teil 200: Installation typ a (geschlossenes system). Planung, Bauteile, Apparate, Werkstoffe: Technische Regel des DVGW; 2012, DIN 1988-200, accessed March 5, 2021.
[16] Lipp Josef Peter. Flexible Stromerzeugung mit Mikro-KWK-Anlagen: Experimentelle Untersuchung der Möglichkeiten einer flexiblen Stromerzeugung von Mikro-KWK-Anlagen mit Hilfe einer Wärmebedarfsprognose und einem intelligenten Speichermanagementsystem.
[17] Østergaard PA, Andersen AN. Booster heat pumps and central heat pumps in district heating. Appl Energy 2016;184:1374–88. http://dx.doi.org/10.1016/j.apenergy.2016.02.144.
[18] ratiotherm GmbH & Co. KG. Planning Guide for craftsmen, planners and architects.
[19] Zinsmeister D. Possible prosumer side configurations. 2021, http://dx.doi.org/10.13140/RG.2.2.25761.12642, Unpublished.
[20] Unger R, Schwan T, Mikoleit B, Bäker B, Kehrer C, Rodemann T. Green building - modelling renewable building energy systems and electric mobility concepts using modelica. In: Proceedings of the 9th international MODELICA conference, September 3-5, 2012, Munich, Germany. Linköping University Electronic Press; 2012, p. 897–906. http://dx.doi.org/10.3384/ecp12076897.
[21] RMB Energie. Operating Manual: Combined heat and power unit neoTower® LIVING CHP 2.0, CHP 3.3, CHP 4.0.
[22] Jordan U, Vajen K. Influence of the DHW load profile on the fractional energy savings. Sol Energy 2001;69:197–208. http://dx.doi.org/10.1016/S0038-092X(00)00154-7.
[23] Peric VS, Hamacher T, Mohapatra A, Christiange F, Zinsmeister D, Tzscheutschler P, et al. CoSES laboratory for combined energy systems At TU Munich. 1–5. http://dx.doi.org/10.1109/PESGM41954.2020.9281442.

Chapter 4

Experiment and simulation infrastructure

4.1 CoSES laboratory

The CoSES smart microgrid laboratory is a state-of-the-art research facility designed to analyze five prosumers' thermal and electric behavior in detail. This unique research landscape combines real hardware, PHIL, a reconfigurable low-voltage distribution grid, as well as 4GDH and 5GDHC infrastructure. The laboratory's research infrastructure is broadly categorized into electric and thermal systems. On the electric side, the primary focus is on the power dynamics of microgrids. This includes exploring the impact and integration of DERs and sector coupling, e.g., with Electric Vehicles (EV)s and HPs. Further research areas are voltage and frequency stability and the transitions between islanded and grid-connected operations. Regarding thermal systems, the research revolves around the structure and control of individual heating concepts and future DHC networks. This encompasses integrating prosumers, reducing grid temperatures, designing advanced control strategies, and strengthening sector coupling as described in Section 2.5.

The general hardware and software requirements of the thermal system of the CoSES laboratory align with those defined by Mohapatra et al. [144] for the electric system, though less time-critical: The facility should house five prosumers that utilize commercial, state-of-the-art components when feasible and detailed PHIL emulation where direct implementation does not make sense. Environmental factors like consumption profiles and weather patterns should be controllable and replicable. The hardware setup should also be easy to reconfigure and expand to changing research demands.

The software environment should efficiently manage a variety of controllers, IO cards, and signals. It should support models irrespective of the originating program, ensuring no constraints caused by specific software capabilities. Furthermore, an open interface is required to facilitate effortless interaction, allow different communication protocols, and promote seamless integration and collaboration among researchers and across various platforms.

Laboratory hardware

Based on these requirements, the CoSES laboratory incorporates commercial components for heat production, including Combined Heat and Power Units (CHP)s, HPs, mixing stations

for temperature and volume flow regulation, thermal and electric storage systems, Photovoltaic (PV), and EV charging stations. For heat consumers and emulation of environmental conditions, the laboratory employs PHIL to include dynamic responsiveness. Unlike traditional experiments with recorded time series as setpoints, the laboratory's current state dynamically influences future setpoints. For instance, a drop in heat output results in a decline of the simulated room temperature, subsequently leading to a heightened demand, which influences the new setpoint. Moreover, PHIL experiments offer the advantage of reproducibility compared to field tests.

The laboratory's modular building design simplifies the system's complexity and offers flexibility for easy interchangeability and reconfiguration. These modules are interconnected using metal hoses, facilitating swift adjustments to the hydraulic arrangement, such as altering connections to ports situated at varying heights on the TES. Moreover, select modules are designed to allow simple switching between different configurations. With the integration of ball valves, rapid transitions between these configurations are possible without breaching the hydraulic circuit. For instance, by simply manipulating specific ball valves, the TES connection can seamlessly toggle between the 2-pipe and 4-pipe configurations as elaborated in Chapter 3, eliminating the need for module reassembly.

Laboratory control

Each building is equipped with real-time controllers and IO cards from National Instruments (NI), which are managed by NI VeriStand. This choice is motivated by multiple factors: NI provides a diverse range of real-time controllers and IO cards specifically designed for varied applications. Their robust interface ensures seamless integration between hardware and the real-time software environment, streamlining the management of controllers and signals. Furthermore, NI VeriStand supports Dynamic Link Library (.dll) model integration, making it compatible with a wide array of programs, such as SimulationX, which is used for the PHIL simulation models. A further advantage is its API compatibility with NI LabVIEW, which simplifies managing non-time-critical tasks like data logging, algorithmic communication, and debugging of NI LabVIEW-developed models. The software is modular and similar in structure to the hardware, allowing software modules to be reused in different buildings.

Specific prosumer requirements

To investigate prosumers within DHC grids, our laboratory design adheres to several specific requirements:

- *Multiple Prosumers:* Multiple prosumers in the laboratory are vital to allow an in-depth analysis of their mutual hydraulic and thermal influence and to gain knowledge of the intricate dynamics and interactions within the grid.
- *Bidirectional Transfer Stations:* Prosumers are equipped with a bidirectional transfer station enabling reversible flow. Since bidirectional pumps are unavailable, the laboratory employs two pumps and ball valves to realize bidirectional flows through the heat exchanger. An alternate approach would be combining two 3-Way Valve (3WV) with a singular pump. Both approaches are shown in Figure 4.1a). Each prosumer is equipped with a heat exchanger, and one is additionally equipped with a BHPTS for 5GDHC. Additional BHPTS can be emulated with PHIL, as described by Angelidis et al. [12].

- *Diverse Network Analysis:* The laboratory allows the investigation of various network topologies and types. This encompasses topologies such as line, ring, tree, and meshed structures. Additionally, the laboratory allows the study of network types featuring non-pressurized or pressurized supply lines, as illustrated in Figure 4.1b). One advantage of non-pressurized supply lines in prosumer-based DHC grids is the comparatively lower pressure head required for individual pumps. However, this necessitates a pump instead of a control valve for extraction from the supply line.

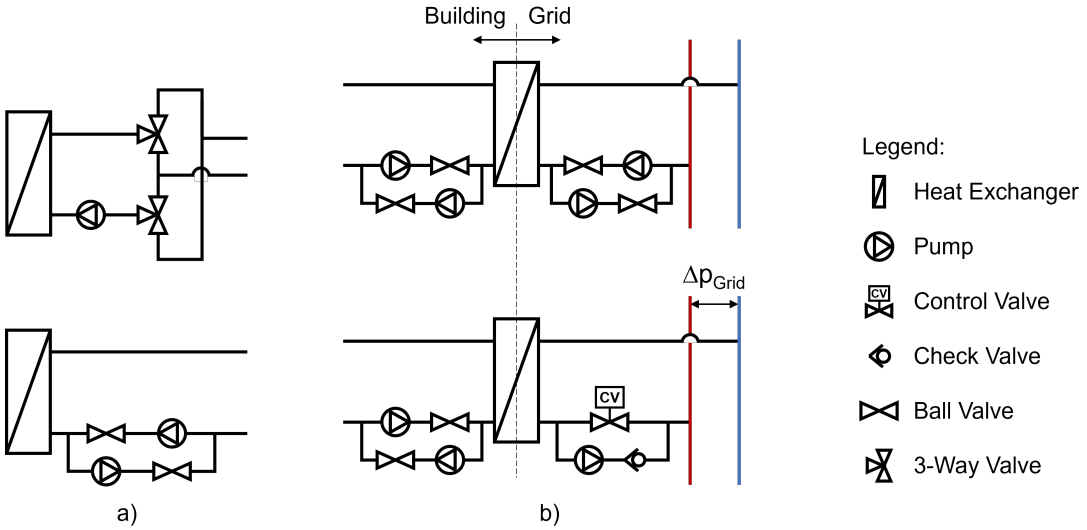

Figure 4.1: Integration of prosumers in DHC: a) illustrates potential hydraulic configurations, b) presents two types of DHC networks: non-pressurized supply line (top) vs. pressurized supply line (bottom).

The following paper describes the modules and the software concept of the CoSES laboratory and the first experimental results. The primary objective is to enhance collaboration with fellow researchers by providing them with a comprehensive understanding of the laboratory, its capabilities, and its limitations. By doing so, interested researchers can better determine if and how the CoSES laboratory might support their research activities. Furthermore, our detailed description of the hardware and software design aims to provide inspiration for researchers planning to develop a similar laboratory setup.

A prosumer-based sector-coupled district heating and cooling laboratory architecture

Authors Daniel Zinsmeister, Thomas Lickleder er, Stefan Adldinger, Franz Christange, Peter Tzscheutschler, Thomas Hamacher, Vedran S. Perić

Publication medium Smart Energy, Volume 9

Digital object identifier https://doi.org/10.1016/j .segy.2023.100095

Author contributions

Daniel Zinsmeister:	Conceptualization, Visualization, Writing – original draft, review & editing.
Thomas Lickleder er:	Conceptualization, Writing – original draft, review & editing.
Stefan Adldinger:	Writing – original draft
Franz Christange:	Conceptualization, Writing - review.
Peter Tzscheutschler	Conceptualization, Writing - review, Supervision, Project administration, Funding acquisition.
Thomas Hamacher	Conceptualization,Supervision, Funding acquisition.
Vedran S. Perić	Conceptualization, Writing - review, Supervision, Project administration, Funding acquisition.

Smart Energy 9 (2023) 100095

Contents lists available at ScienceDirect

Smart Energy

journal homepage: www.journals.elsevier.com/smart-energy

A prosumer-based sector-coupled district heating and cooling laboratory architecture

Daniel Zinsmeister [a,*], Thomas Licklederer [a], Stefan Adldinger [b], Franz Christange [c], Peter Tzscheutschler [a], Thomas Hamacher [a], Vedran S. Perić [a]

[a] Technical University of Munich, Arcisstrasse 21, Munich, 80333, Bavaria, Germany
[b] Stadtwerke Neuburg an der Donau, Heinrichsheimstrasse 2, Neuburg an der Donau, 86633, Bavaria, Germany
[c] Triowatt GmbH, Falkenstr. 12c, Stephanskirchen, 83071, Bavaria, Germany

ARTICLE INFO

Keywords:
District heating
District cooling
Decentralized feed-in
Prosumer
Sector coupling
Power-hardware-in-the-loop
Laboratory

ABSTRACT

New control strategies for thermal systems and innovative district heating and cooling grids can help to decarbonize the thermal sector. Before implementing these new concepts, they should be validated, ideally with commercial hardware but without influencing user comfort. For this reason, the laboratory at the research center for Combined Smart Energy Systems (CoSES) at the Technical University of Munich (TUM) was designed. By combining commercial hardware with Power Hardware in the Loop simulations, the laboratory enables research in a controllable, but realistic setting without affecting real users. It consists of five prosumers equipped with heat generators and thermal storages. All prosumers are linked with an adjustable district heating and cooling grid. The modular hardware and control architecture presented in this paper covers management-, automation-, field-level control and offers interfaces to external control. A case study shows that prosumer integration into flexible district heating grids can reduce overall heating costs but requires intelligent control concepts for transfer stations and heat generators. The conducted experiments emphasize the importance of validating control strategies in laboratory environments. They allow the analysis of phenomena that are difficult and impractical to model accurately with existing simulation tools. The structure and capabilities of the laboratory are presented in order to foster collaboration with other researchers.

1. Introduction

Around half of the global final energy consumption is caused by heating and cooling [1]. 46% of the heating and cooling energy is used in residential and commercial buildings, mainly for space heating and domestic hot water (DHW) [1]. Currently, most of the energy used for heating comes from fossil fuels or biomass [1] while space cooling is typically provided by electrically powered fans or air conditioners [2]. To decarbonize this sector, district heating and cooling (DHC) grids can be a key element [3–6]. In recent years, the development of DHC grids has been focused on the following key aspects:

- Grid temperatures for district heating grids are reduced to minimize transport losses and enable the integration of low temperature heat sources [7].
- DHC, electric and gas grids are combined to exploit synergies. Those synergies can increase energy flexibility needed for balancing intermittent and volatile renewable energy sources and achieve the optimal efficiency of the overall energy system [8–11].
- Formerly unused energy sources are integrated into DHC grids, by using booster heat pump transfer stations that feed excess cold into the DHC grid during heating and vice versa [9,12,13] or by integrating decentralized heat sources and prosumers analog to the electric grid [14–16].
- Control strategies are improved to reduce grid return temperatures, e.g. by motivation tariffs [17] or by integrating low temperature district heating grids into an existing district heating grids [18]. In addition, energy sources can be integrated in a more intelligent way, e.g. by introducing new market mechanisms to district heating systems [19,20] or by implementing Model Predictive Control (MPC) to improve waste heat utilization [21].

When developing and evaluating new approaches in DHC research, simulation models are often used. However, simulations do not always

* Corresponding author.
E-mail address: d.zinsmeister@tum.de (D. Zinsmeister).

https://doi.org/10.1016/j.segy.2023.100095
Received 5 December 2022; Received in revised form 27 February 2023; Accepted 27 February 2023
Available online 5 March 2023

adequately represent realistic behavior, like the dynamic behavior or the internal control of components. Laboratories are still useful to emulate commercial products, map interactions of different control layers (management, automation, field control) and to validate control strategies without influencing user comfort. The requirements for a smart energy laboratory with a focus on district heating systems are:

- a detailed emulation of prosumer behavior in smart energy systems including heat and cooling rates within the building must be possible,
- commercial equipment for heat generators and storages shall be used,
- the boundary conditions and all components must be completely controllable, independent from external influences and the environment (climate, weather etc.),
- sector coupling must be featured to enable investigations on the interaction of the thermal sector with other sectors, such as electricity or mobility.

Several laboratories for heating or DHC systems test individual components, like heat pumps [22], booster heat pump transfer stations [23] or decentral feed-in stations [24,25]. In order to test the behavior of DHC grids, other laboratories consider complete, small-scale DHC grids. The Energy Exchange Lab at Eurag Research [26] in Bozen emulates the behavior of a small low temperature district heating grid with different generators (combined heat and power, condensing boiler and solar thermal) and a configurable grid length. Heat pumps emulate prosumers that extract heat or feed it into the grid. The District LAB of Fraunhofer IEE is being built and will feature a flexible heating grid, a pipe test bench for mechanical tests and different control concepts [27]. The NODES laboratory investigates the effects of thermal cross-linking, in unidirectional, bidirectional, or meshed grid topologies. It consists of a simplified district heating grid with three consumers, a seasonal storage and a heat source [28].

Although these laboratories focus on the investigation of DHC grids, prosumers and consumers are not emulated in detail, neglecting effects within buildings. Moreover, the synergy between DHC grids and electric grids cannot be analyzed in detail in these laboratories. In order to fill this gap, the research center for Combined Smart Energy Systems (CoSES) at Technical University of Munich (TUM) was developed [29]. The CoSES laboratory enables research on innovative concepts of DHC grids and smart energy systems. It emulates five houses, one multi-family house (MF) and four single-family houses (SFs), equipped with decentralized electricity and heat generators, electric vehicle charging stations and controllable thermal and electricity loads. A configurable electric and DHC grid connects the houses. The setup allows a holistic investigation of sector coupling in the building domain and supplements the existing laboratories with its detailed emulation of prosumers and their impact on DHC and power grids.

This paper describes the architecture of the CoSES laboratory, with focus on a detailed description of the thermal subsystem. The proposed design of the laboratory can be used as an architecture template for other DHC laboratories. The goal is to present the design, capabilities and limitations of the laboratory, as well as the operation principles in order to share the experience, help in designing similar laboratories and foster collaboration and exchange with similar laboratories as well as with other research institutions and companies in this field. The laboratory is designed to test control strategies for new generation DHC grids, analyze new concepts for bidirectional heat and cold transfer, generate data to validate simulation models and quantify the sector coupling potential of different setups.

The laboratory can be used for research on 3rd and 4th generation and ambient temperature heat grids. Older generations cannot be tested as they require temperatures above 100 °C. Moreover, research on 2nd, 3rd and 4th generation cooling grids is possible. The classification into the different generations is based on Lund et al. [8] and Østergaard et al. [30].

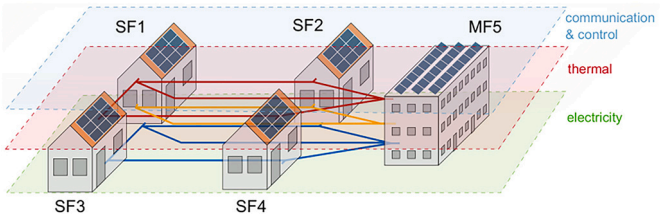

Fig. 1. Different layers of the CoSES laboratory. Five prosumers are connected by a district heating and cooling grid.

A case study is conducted with the target demonstrating how the laboratory works. The case study shows that the laboratory provides insights into DHC systems that are hard to simulate. This includes the behavior of commercial equipment. Heat generators, for example, are influenced by their internal control and external influences that can hardly be captured, while pumps and valves behave non-linearly. In addition, we were able to gain first findings on the operation of prosumer-based DHCs.

The paper is structured as follows: Chapter 2 describes the hardware components of the laboratory. The communication and control structure is presented in chapter 3. Chapter 4 shows a case study before chapter 5 discusses the strength, limitations and research potential of the laboratory. In chapter 6 the conclusions are drawn.

2. Thermal energy system

Fig. 1 shows the layout of the CoSES laboratory, which can be divided into three layers:

- The electricity layer consists of a flexible electric grid, battery storages, electric vehicle charging stations and emulates distributed generators and consumption at household level. The electric side is described in detail by Mohapatra et al. [31] and Christange [32].
- The thermal layer consists of five thermal prosumers that are connected with an adjustable DHC grid and is described in detail in the following section.
- The communication and control layer controls and monitors the experiments and is described in detail in section 3.

The laboratory consists of five houses which are connected with a DHC grid. The length of the grid between the houses can be adjusted with a DHC grid emulator according to the experiment setting (see Subsection 2.1). This module is necessary since the houses in the CoSES laboratory are located with a maximum distance of 10 meters. It emulates heat losses and the time delay of temperature changes between two houses over variable distances, as will be explained in the later subsection. The modules can also be used to add additional emulated houses into the system by mimicking the dynamics of a house through cooling or heating the water in the pipe.

The laboratory components were selected with the aim of covering as wide a range of household technologies as possible. A catalog of criteria was prepared for this purpose; among other things, all heat generators had to be controllable by an energy management system. In addition, heat generators were selected to cover a broad range of applications:

- Heat generators with a low purchase price: condensing boiler
- Conventional technology for sector coupling: combined heat and power units (CHPs)
- Renewable technology for sector coupling: Heat Pumps (HPs), with different heat sources
- Volatile renewable heat generators: solar thermal emulators

Table 1
Overview of the heat modules of each house.

	SF1	SF2	SF3	SF4	MF5
Heat Generator	CHP (2 kW_{el}, 5.2 kW_{th}) Condensing boiler (20 kW_{th}) Solar thermal (9 kW_{th})	Condensing boiler (20 kW_{th}) Air source HP (10 + 6 kW_{heat}, 9 kW_{cold}) Solar thermal (9 kW_{th})	Ground source HP (10 + 6 kW_{heat}) Solar thermal (9 kW_{th})	Stirling engine (1 kW_{el}, 6 kW_{th}) Integrated auxiliary boiler (20 kW_{th}) Integrated electric heating rod (6 kW_{th})	CHP (5 kW_{el}, 11.9 kW_{th}) CHP (18 kW_{el}, 34 kW_{th}) Condensing boiler (50 kW_{th})
Thermal Storage	800 l	785 l	1000 l	1000 l	2000 l
Domestic Hot Water	Fresh water storage (500 l)	Fresh water station	Fresh water station	Internal heat exchanger	Fresh water station
Transfer Station	Bidirectional HCTS (30 kW_{th}) bHPTS (19 kW_{heat}, 14 kW_{cold})	Bidirectional HCTS (30 kW_{th})	Bidirectional HCTS (30 kW_{th})	Bidirectional HCTS (30 kW_{th})	Bidirectional HCTS (60 kW_{th})
Thermal load emulator	30 kW_{heat}, 9 kW_{cold}	30 kW_{heat}, 9 kW_{cold}	30 kW_{heat}, 9 kW_{cold}	30 kW_{heat}	60 kW_{heat}

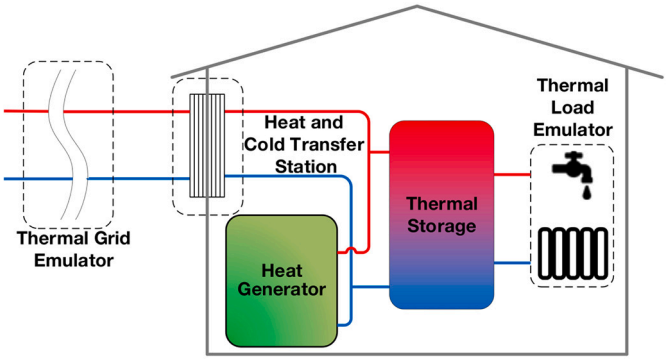

Fig. 2. General structure of the houses, the red line indicates the supply pipe, blue the return pipe.

Furthermore, thermal storage systems are used to decouple generation and demand. For this purpose, different sizes, designs and connections were selected for the storage units. Fig. 2 and Table 1 show the general structure of each house, which consist of the following elements:

- Heat and cold transfer stations (HCTS, see Subsection 2.2):
  Each house is equipped with a bidirectional HCTS. SF1 has an additional booster heat pump transfer station (bHPTS).
  The bidirectional HCTS connects the house to the DHC grid. With this module, heat or cold can be extracted from or fed into the grid. It is designed for a return-to-supply feed-in, since this is the most efficient feed-in setup [33]. Other setups, like supply-to-supply or return-to-return feed-in as described by Lamaison et al. [33] could be realized with minor modifications.
  The bHPTS can be used for both, heating and cooling. It consists of a standard heat exchanger and a booster heat pump (BHP), a water-source heat pump, using the DHC grid as the heat source. If grid temperatures are higher than the water in the heating system, a heat exchanger is used to extract heat from the grid. If grid temperatures are too low for direct usage, the BHP operates. The cold extraction operates in a similar way.
- Heat generators (see Subsection 2.3):
  In order to have realistic behavior, the laboratory uses real heat generators. Solar thermal heat generators are emulated with controllable electric heaters, to run experiments independent of outdoor weather conditions. Table 1 provides an overview of the technical specifications of the different heat generators and in which house they are installed.
- Thermal load emulators (see Subsection 2.4):
  Since no real consumers are connected in the CoSES laboratory, the heat and cold consumption is emulated. Setpoints can be provided by PHIL or from predefined data, e.g. from field test measurements.
- Thermal storages and domestic hot water (DHW) systems (see Subsection 2.5):
  Thermal storages of different sizes from 500 l to 2000 l are used in the laboratory. All storages have several inlet and outlet ports at different heights. Three storages are connected to solar thermal systems with an internal heat exchanger and the storage in SF4 is equipped with an internal electric heating rod.
  Since DHW has very high hygiene requirements as compared to the heating system, the two circuits are separated. DHW is heated by the thermal storage tank using heat exchangers.

The CoSES laboratory uses a modular system architecture, which allows easy adaptations and expansions according to specific experiment requirements.

2.1. District heating and cooling grid emulator

Fig. 3 shows the structure of one pipe of the DHC grid emulator, which heats or cools the water in the DHC grid according to the desired pipe temperature for supply or return. The pipe temperature is provided by the user or a PHIL simulation model. Check valves are used to rectify the flow in the active part of the emulator, allowing it to be used in both flow directions (①). The DHC grid emulator has two operation modes:

- If the desired pipe temperature is higher than the inlet temperature, the water is heated up by an electric heating rod (⑤).
- If the desired pipe temperature is lower than the inlet temperature, the 4-way-mixer is used to exchange hot water from the grid with cooling water (②). A control valve on the cooling water inlet is used to match the cooling water pressure to the grid pressure (③). Another control valve at the cooling water pipe controls the water flow, to ensure that the flow rates in the DHC grid, upstream and downstream of the mixer, are identical (④). The electric heating rod has a high thermal mass, which has a negative effect on the dynamic response. For this reason, a bypass is included. A 3-way mixing valve controls whether the flow goes through the bypass or the heating rods (⑥).

2.2. Heat and cold transfer station

Two different types of HCTS are installed at the CoSES laboratory, bidirectional HCTS and a bHPTS.

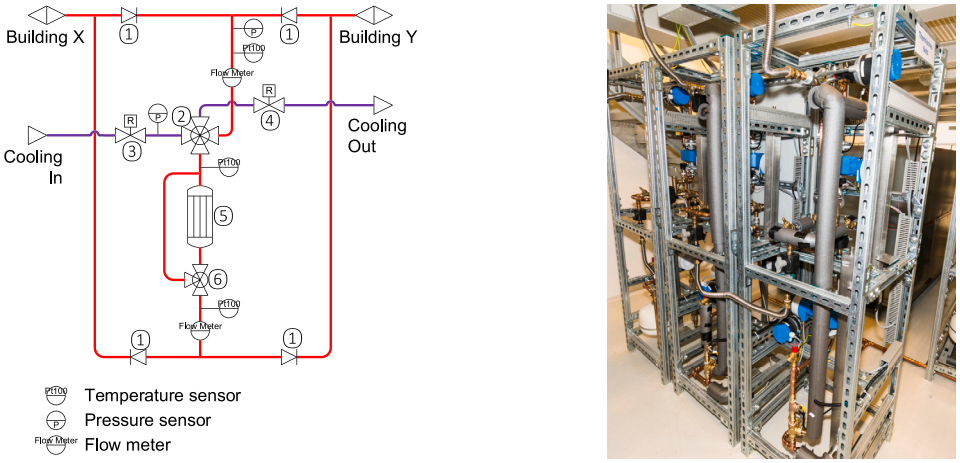

Fig. 3. District heating and cooling grid emulator: a) schematic drawing; b) setup at the CoSES laboratory.

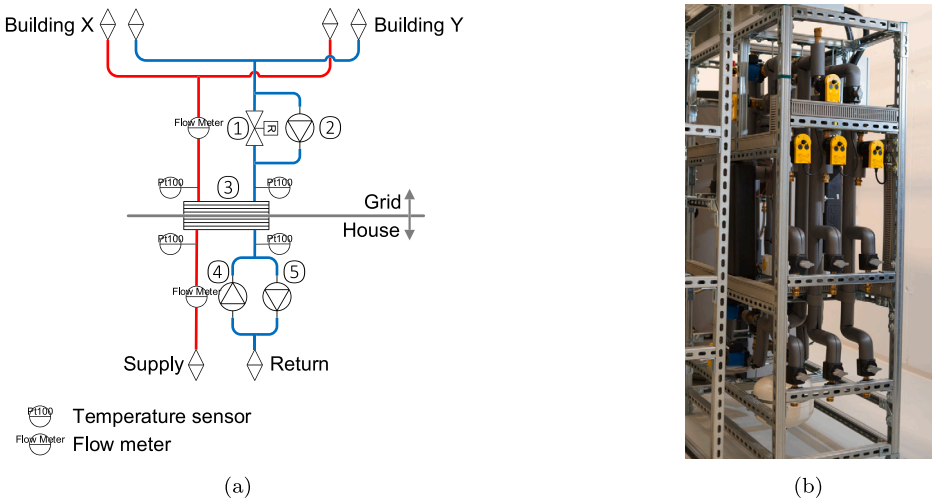

Fig. 4. Bidirectional heat and cold transfer station: a) schematic drawing; b) setup at the CoSES laboratory.

2.2.1. Bidirectional heat and cold transfer station

Each bidirectional HCTS has two circuits that can be used in a district heating grid with three different temperature levels or a DHC grid. Fig. 4 shows one circuit of the bidirectional HCTS. A heat exchanger separates the DHC grid and the house circuit (③). Due to the pressure difference between the supply pipe (red) and return pipe (blue), the water flow for heat or cold extraction from the grid can be controlled by a control valve (①), while a grid pump is required for feed-in (②). On the house side, the flow is controlled by two separate pumps (④ and ⑤).

2.2.2. Booster heat pump transfer station

In the laboratory, the bHPTS 'WP Grid HiQ F14' from Ratiotherm [34] is installed and its schematic is shown in Fig. 5. The heat exchanger (①) and the BHP (②) separate the grid from the house.

Inside the house, the flow can be channeled through the heat exchanger or the HP by the electric ball valves (④). The flow rate is controlled by the pump (⑤) and an electric heating rod is installed as an auxiliary heater (⑥).

On the grid side, the flow through the heat exchanger or BHP is controlled by another set of control valves (③). In standard configuration, water flows from the warm supply pipe to the cold return pipe for both heat and cold extraction. The pressure in the supply pipe is higher and therefore, no additional pump is needed to generate water flow for cold extraction. More efficient options for cold extraction, where the flow direction changes, can be investigated with the additional pump that generates the volume flow from the return to the supply pipe (⑦). Electric ball valves are used to include or bypass the pump (⑧).

2.3. Heat generators

The installed heat generators are connected to a higher-level energy or building management system which provides the generation setpoints. The internal structure and control of these heat generators is not modified to preserve the behavior of commercially available products.

Two different types of HPs are installed in the laboratory. An air source heat pump (ASHP) with a nominal heating/cooling rate of 10 kW/9 kW and a ground source heat pump (GSHP) for heating only with a nominal heat rate of 10 kW. Both HPs have a 6 kW electric heater as an auxiliary heater that is activated when the heat output is too low.

The commercial HPs installed in our laboratory are operated with a constant temperature difference between supply and return. This means that the supply temperature can not be specified as a setpoint to the HP, but depends on the return temperature from the thermal storage. In order to efficiently provide DHW at a high temperature and heating at a low temperature, the stratification within the thermal storage is used.

Fig. 6 shows the schematic of the HP testbed in the laboratory. Two 3-way valves (①) allow the HP to change the connection to the thermal storage and switch between the high temperature at the top and the

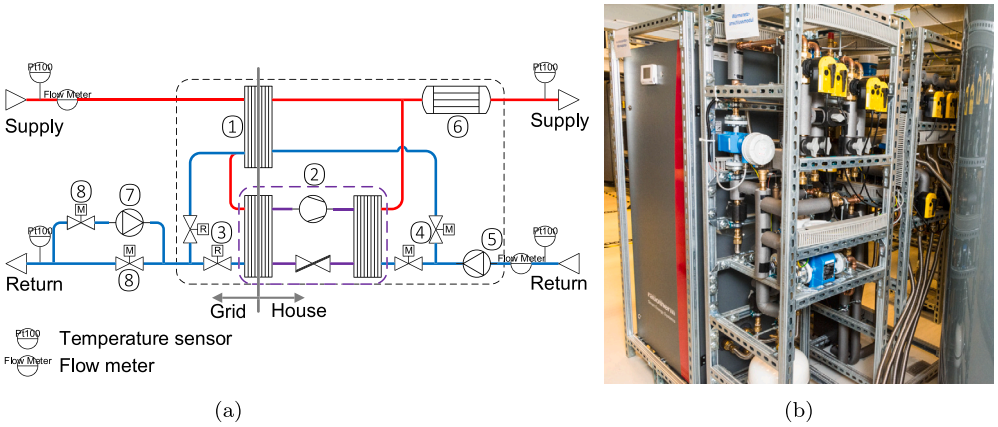

Fig. 5. Booster heat pump transfer station: a) schematic drawing; b) setup at the CoSES laboratory.

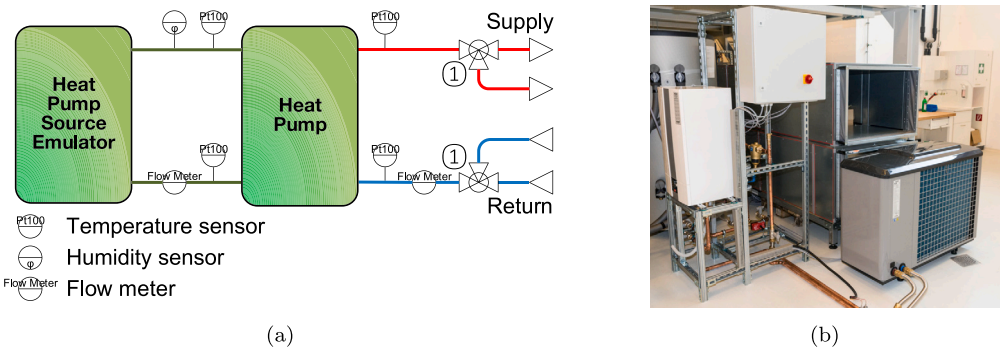

Fig. 6. Heat pump emulator: a) schematic drawing; b) setup of the air source heat pump at the CoSES laboratory.

low temperature at the bottom. The ambient heat source is provided according to experiment specifications by heating up brine for the GSHP or setting the air humidity and temperature in a heating, ventilation and air conditioning (HVAC) system for the ASHP.

The laboratory is further equipped with gas powered CHPs and condensing boilers. Four different CHPs are used, three gas engine CHPs and one Stirling CHP. Three different Wolf 'CGB' condensing boilers are installed with a thermal output of 14, 20 and 50 kW [35].

Solar thermal heat generators are emulated in the laboratory, to run experiments independent of outdoor weather conditions. The heat source is a 9 kW electric heating rod, which corresponds to a solar thermal system of up to 15 m^2. The water flow is controlled by a pump. Solar thermal systems are usually filled with brine to prevent freezing and are therefore connected to a separate circuit. They are integrated into the heating system through an internal heat exchanger in the thermal storage tanks.

2.4. Thermal load emulator

For experiments, it is necessary to emulate heat and cold consumption in detail. Therefore, thermal load emulators for heat and cold are used and controlled according to setpoints defined by the PHIL setup (see chapter 3.2) or field test data.

2.4.1. Heat consumption

The heat consumption module is constructed similar to the testbed described by El Baz et al. [22] and is shown in Fig. 7.

A commercially available mixing module is installed, which consists of a 3-way mixer (①) and a pump (②). The 3-way mixer is used to reduce the supply temperature according to the setpoint of the heating system, e.g. 40 °C for space heating. In real houses, the pump generates the pressure difference to enable the water flow in the heating system and the flow rate is controlled by thermostatic radiator valves in each room. Since those valves are not installed in the emulator, a controllable pump is used to control the volume flow according to the target flow rate. The consumed heat is extracted by a heat exchanger (③). A control valve in the cooling circuit controls the cooling water flow, to reach the target return temperature in the heating circuit (④).

The DHW circuit uses three solenoid valves to emulate the opening and closing of different DHW consumers (⑤). The flow rate through the solenoid valves is set corresponding to different consumers, e.g. taps or showers, by three needle valves (⑥). The cold water flow is supplied by the cooling circuit. As prevalent in houses these days, a circulation pump is used to prevent the DHW pipe from cooling down (⑦). The resulting losses are extracted by a heat exchanger (⑧) and a control valve (⑨), the same way as in the heating circuit.

2.4.2. Cold consumption

The cold consumption is emulated with the solar thermal module. As a pump is already installed in the cold generator, the pump in the module is bypassed when used as a cold consumer. The electric heater is controlled to match the cold consumption.

2.5. Thermal storage and domestic hot water system

The thermal storage is integrated differently for each house and is equipped with 10 temperature sensors on its surface at different heights, to measure the temperature profile in the thermal storage. Fig. 8 shows the storage integration of SF2. Simulations showed that this is the most efficient configuration [36]. The ASHP is connected to four ports at different heights and the solar thermal module is connected to an internal heat exchanger. DHW is provided by a fresh water station. Ball valves (not illustrated in the figure) are connected at each port of the thermal storage, allowing a simple reconfiguration.

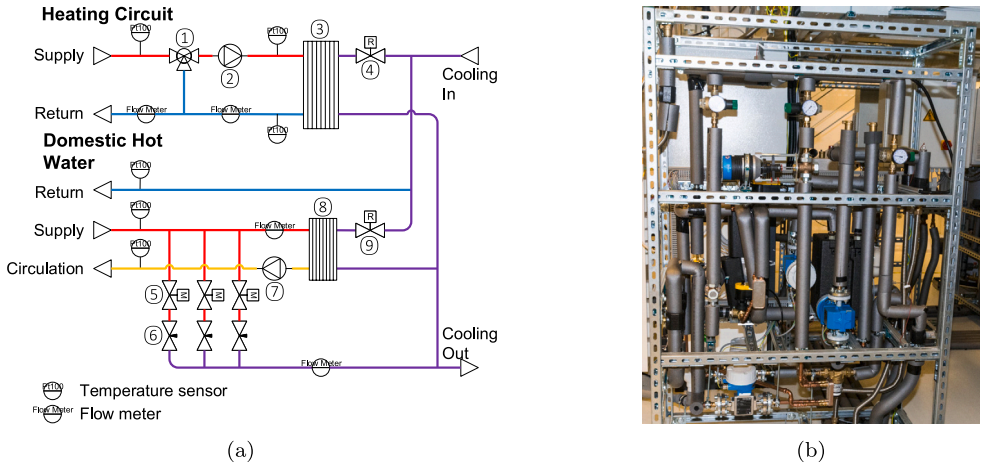

Fig. 7. Heat consumption emulator: a) schematic drawing adapted from [22]; b) setup at the CoSES laboratory.

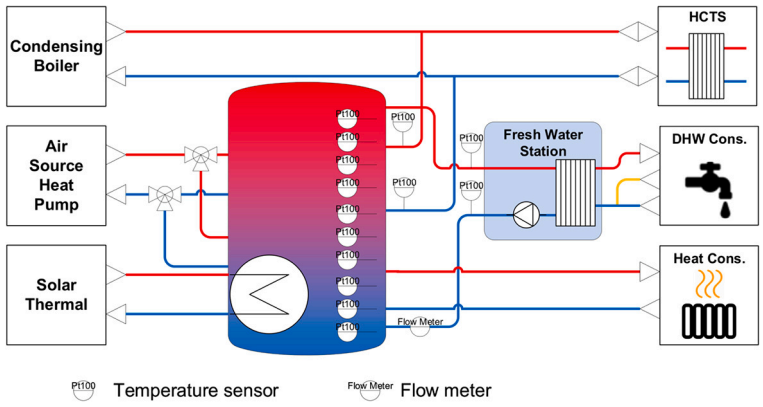

Fig. 8. Thermal storage connection of SF2.

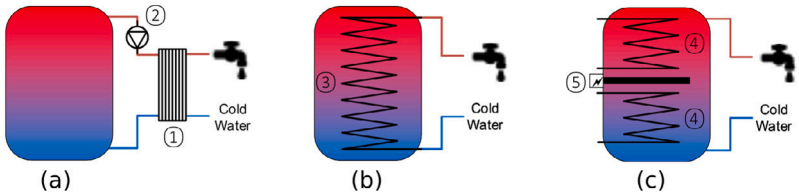

Fig. 9. Schematics of different domestic hot water installations: a) fresh water station, b) combined thermal storage and c) a separate domestic hot water storage.

At the CoSES laboratory, the DHW preparation is always connected to the thermal storage. Fig. 9 shows the three implemented options to provide DHW:

- Fig. 9.a: Fresh water station — The two circuits are separated by an external heat exchanger (①). An additional pump is necessary to pump hot water through the heat exchanger on the thermal storage side (②).
- Fig. 9.b: Combined thermal storage — An internal heat exchanger separates the heating and DHW circuit (③). In this case, no additional pump is necessary.
- Fig. 9.c: DHW storage tank — DHW is heated by one or more internal heat exchangers (④), which can be connected to the heating side or solar thermal collectors with an additional pump. An internal electrical heating rod can also be used to provide heat (⑤).

3. Monitoring and control system

The monitoring and control of the laboratory meets various requirements, such as processing more than 600 sensors and 300 actuators, a high operation frequency and real-time control. This is realized with the NI VeriStand software environment that enables easy management of real time experiments. NI VeriStand can configure input/output (IO) channels, log data, and communicate in real time with hardware [37]. It also offers the possibility to include external simulation models as dynamic link libraries (dll). These simulation models can be used for PHIL applications.

Table 2 gives an overview of the sensors for the equipment of the thermal side of the CoSES laboratory.

3.1. General control structure

In order to manage the high number of IO signals and the various hardware modules, a modular control software is developed. This allows intuitive understanding, modification and expansion of the control software. Necessary software modules are then combined for each house according to hardware specifications.

Each house is controlled by two controllers of National Instruments, an Industrial Controller (IC) for the thermal subsystem and a PXI for the electric subsystem. A compactRIO (cRIO), connected to the IC, acquires

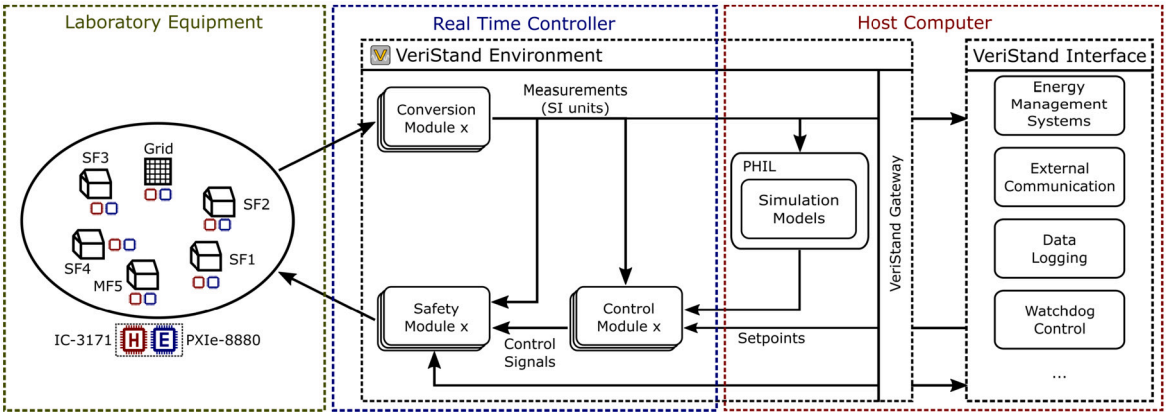

Fig. 10. Control structure of the thermal system: The laboratory equipment with its sensors and actuators exchanges information with the VeriStand environment. The VeriStand environment is divided into two parts, one running on the real time controller, the other on the host computer.

Table 2
Overview of sensors used in the CoSES laboratory.

Parameter	Sensor type	Accuracy	Source
Temperature	4-wire PT100 resistance sensors of quality class A	$\pm(0.15 + 0.002 \cdot \lvert T \rvert)$	[38]
Humidity	Combined air and humidity sensor	±2%	[39]
Water flow	Magnetic flow meter 'Proline Promag E / H 100' with different diameters	±0.5% ± 1 mm/s	[40][41]
Gas flow	Calibrated bellows gas meter GR 2.5 from WDV Molliné		[42]
Air flow	Hot film anemometer	±0.04 m/s + 2%	[43]
Voltage	LEM CV 3-1000	±0.2%	[44]
Current	LEM LF210-S/SP3	±0.2%	[45]

temperatures, counter signals (e.g. from the gas flow meter) and digital inputs, while the Remote I/O (REM IO) system measures analog input signals. Analog and digital output signals are sent from the REM IO system to the components. The execution rate of the controller of the thermal subsystem is 100 Hz. Fig. 10 shows the control structure of the thermal subsystem.

The control structure can be divided into 5 parts, 'Conversion', 'Logic', 'Control' and 'Safety' are deployed directly on the IC while the 'VeriStand Interface' runs in LabVIEW on the host PC and uses an API to interact with NI VeriStand [46]:

1. The 'Conversion' block converts raw measurement data such as 0-10 V signals, counter signals, and resistance measurements into the corresponding standard unit values. Additional values such as heat rate or state of charge can be calculated.
2. The 'Logic' block generates setpoints for the laboratory. The setpoints can come from PHIL simulation models, an energy management system, external inputs, or direct inputs from the operator.
3. The 'Control' block converts setpoints into the respective analog or digital output signals, typically using PID and bang-bang controllers.
4. The 'Safety' block checks whether signals can be implemented safely and if the communication between the host PC and the laboratory is active. If thresholds are violated or the connection is lost, a safe value, usually '0' or 'off' is passed. All safety interventions are recorded with error codes.
5. The 'VeriStand Interface' in LabVIEW is used for data logging, the integration of energy management systems and external communication. Common communication protocols enable the communication to other software or applications such as internet-of-things (IoT) as implemented by Mayer et al. [47].

3.2. Power hardware in the loop

The PHIL approach is a key concept for the design of the CoSES Laboratory. PHIL simulation systems are designed based on the hybrid configuration of simulation tools and real hardware and interface through digital and analog input/output signals [48]. This allows to simulate parts of real systems without losing critical information, which simplifies the laboratory setup. At the same time, the coupling of software and hardware can ensure that deviations from setpoints in the experiment are taken into account in the simulation through the feedback loop and thus influence the future reaction of the experiment. Furthermore by combining physical and simulated systems, environmental conditions and user behavior can be integrated into experiments. Compared to field tests, this allows PHIL experiments to be more easily adapted and better reproducible, while not compromising user comfort.

PHIL models can be easily integrated or replaced in the monitoring and control concept of the CoSES laboratory. First, a model for NI VeriStand must be created in dll format. The model must run at a constant step size that is a multiple of the execution rate of the controller or host computer. As shown in Fig. 10, the PHIL model is integrated into the NI VeriStand project, where it is connected to 'Measurements' and 'Setpoints'.

PHIL and simulation models are used for several modules that are otherwise hard to emulate in the laboratory:

- Heating and DHW system: A detailed description of the PHIL approach for this system is described below.
- Cooling system: Set values for supply temperature and volume flow are generated to keep the room temperature at its set value. The measured supply temperatures and volume flow are used to calculate the set return temperature of the cooling system. This setpoint is sent to the cold consumption emulator described in 2.4
- DHC pipes: The outlet temperature setpoint of the pipe is calculated in a simulation model based on the measured inlet temperature and flow rate. The simulation model considers losses and gains caused by the environment. The emulator described in subsection 2.1 is controlled so that the set outlet temperature is met.
- ASHP: The setpoints for air temperature and humidity are determined based on the environment conditions of the PHIL simulation. An HVAC system with an electric heating rod and steam humidifier is controlled to emulate the setpoints accordingly.
- GSHP: The set value for supply temperature of the brine is calculated in a simulation model based on the measured return temperature and flow rate. The simulation model calculates heat gains for different types of ground collectors depending on the environment. The brine is then heated up to reach the set temperature. A more detailed description of the PHIL system can be found in [22].

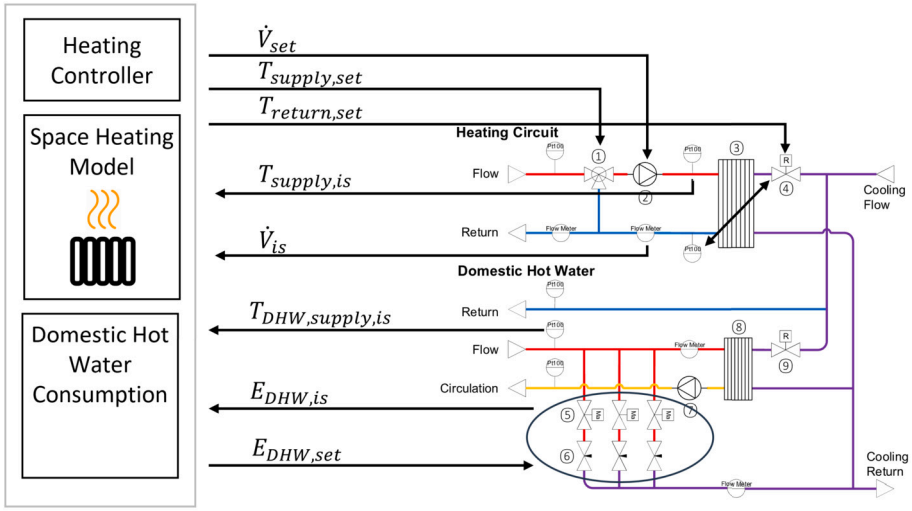

Fig. 11. PHIL setup of the CoSES laboratory. The simulation models generate setpoints for the laboratory considering inputs from laboratory measurements.

- Solar thermal modules: An electric heater emulates the behavior of solar thermal modules as described in subsection 2.3. The electric heater setpoint is calculated based on the measured return temperature and flow rate, solar thermal panel type, irradiance and ambient temperature.

As an example, Fig. 11 shows the application of the PHIL concept in the CoSES laboratory for the heat consumption emulator similar to [49]. The simulation model of the building is implemented in the Modelica-based program SimulationX. It simulates the heating controller and the heating and DHW consumption.

The heating controller defines the set water flow through the heating system ($\dot{V}_{set}$) and the supply temperature ($T_{sup,set}$) based on the current room and outdoor temperature. The setpoints are sent to the 3-way mixer and pump (① and ② in Fig. 7).

The actual flow rate ($\dot{V}_{is}$) and supply temperature ($T_{sup,is}$) are measured in the testbed and then sent to the simulation model, where the set return temperature from the heating system ($T_{ret,set}$) is calculated. The water of the heating system is cooled by a heat exchanger. The cooling water flow is controlled by a control valve (④ in Fig. 7) to follow the return temperature setpoint.

If setpoints cannot be met, e.g. because the thermal storage is too cold or the pumping power is too low, this will be considered in the simulation model and lead to a reduction of the room temperature. This reduction of the room temperature has to be compensated at a later point. Due to this feed-back loop, results are more realistic when using PHIL.

The DHW consumption model works in a similar way. The simulation model defines the set heat demand of the DHW system ($E_{DHW,set}$) based on load profiles. If the DHW supply temperature ($T_{DHW,sup,is}$) is below a chosen minimum temperature, the DHW consumption cannot be fulfilled and has to be either fulfilled at a later point and/or the results highlight those times.

4. Results

In the previous sections, we showed a detailed description of the laboratory infrastructure and the control setup. In this section, we validate the PHIL system for some selected cases to show the functionality of the laboratory. We further present a case study with three houses to demonstrate capabilities of the laboratory and provide insights into prosumers behavior in DHC systems that are difficult to accurately model in existing simulation tools.

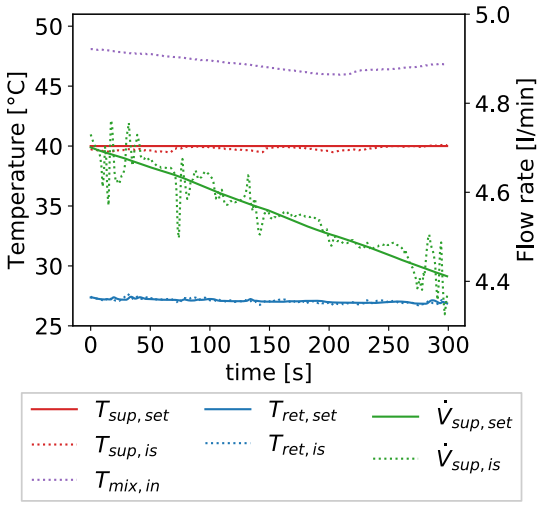

Fig. 12. Validation of the PHIL system of the heating system.

4.1. Validation of the power hardware in the loop system

The goal of this section is to demonstrate that the PHIL emulators can follow the provided setpoints similar to [49]. All controllers used for the PHIL emulators were tuned and validated by step test experiments. The results of these experiments are not included in this paper as they are trivial. We will not validate the underlying models, as they can be replaced and are ideally already validated in the simulation library.

Fig. 12 shows the validation of the PHIL emulator of the heating system as described in subsection 3.2. As can be seen, the setpoints can be followed well. The 3-way mixer (① in Fig. 7) mixes cold water from the return (T_{ret}) with the inlet water ($T_{mix,in}$) and follows the setpoint for the supply temperature (T_{sup}) well. The pump (② in Fig. 7) and the control valve (④ in Fig. 7 also follow the setpoints for the flow rate ($\dot{V}_{sup}$) and return temperature (T_{ret}) accurately.

The heat consumption for DHW is specified as an energy setpoint (E_{DHW}) instead of a setpoint of the water flow. This allows minor deviations in the water flow to be neglected as long as the drawn heat is the same after a short time period. Therefore, Fig. 13 shows the drawn heat for DHW over time. We can see that there is a small delay during strong consumption rates, but the total consumption stays the same. We can further see that the supply temperature is above the minimum domestic hot water temperature during consumption. It cools down slightly

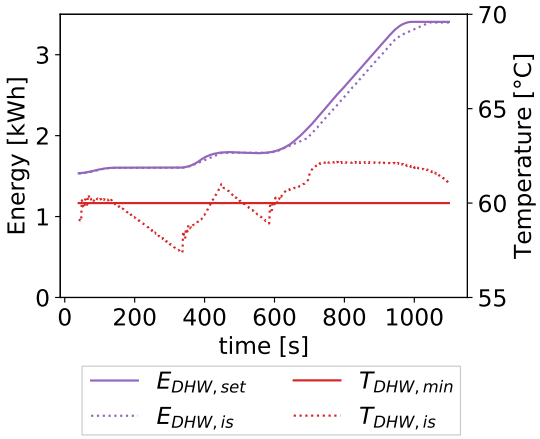

Fig. 13. Validation of the PHIL system of the DHW system.

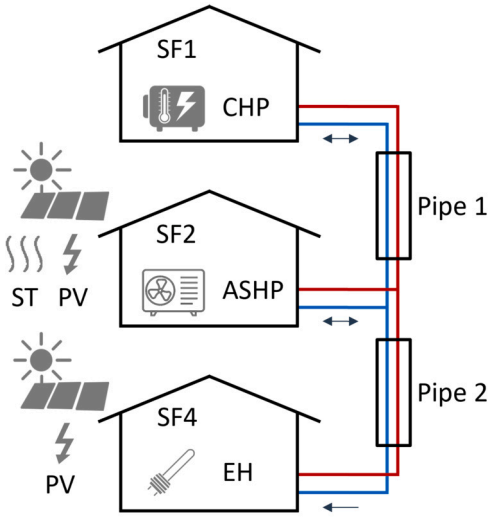

Fig. 14. Setup of the case study.

when no water is drawn. This effect can be prevented if the circulation pump is activate.

4.2. Case study with three houses

A case study analyzes the integration of prosumers in a DHC system. For this purpose, 3 houses are used, equipped according to Table 1 and as specified in Fig. 14:

- SF1 uses a radiator heating system. Heat is generated by a CHP and can be stored in an 800 l thermal storage. DHW is provided by a 500 l DHW storage, which is connected to the thermal storage and CHP.
- SF2 uses a space heating system. Heat is generated by an ASHP and solar thermal panels and can be stored in a 785 l thermal storage. DHW is provided by a fresh water station. It is further equipped with PV panels.
- SF4 uses a radiator heating system. Heat is drawn from the grid or generated with a back-up electric heating rod and can be stored in a 1000 l combined thermal storage for heating and DHW. It is equipped with PV panels that can be used to directly generate heat with the heating rod.

SF1 and SF2 are heat prosumers, meaning that they can feed-in or extract heat from the grid, while SF4 is a pure consumer.

In the first step, setpoints are generated with a MPC. A cost optimization is conducted for the 3 houses over 24 hours in 15-minute steps with the optimization tool urbs [50]. The optimization goal was to minimize the total costs for heating and electricity. The costs consist of expenses for gas (0.14 EUR/kWh) and electricity (0.32 EUR/kWh) and revenues from the sale of electricity produced by PV (0.06 EUR/kWh) and the CHP (0.16 EUR/kWh). Electricity and heat demand as well as solar radiation are provided as time series to the model. The same optimization is conducted as a benchmark without a heat grid.

The optimization results are shown in Fig. 15. The top graph shows the generated and consumed heat. The CHP operates mostly during the night, when there is no heat from solar thermal and electricity from PV. After the sun rises, heat from renewable sources becomes cheaper and dominates the production mix. At this time the thermal storage is recharged. Looking at the feed-in and extraction rates, we can see that at night, SF1 exports heat to SF4 and during the day to SF4.

The optimization showed cost savings of 30% compared to individual heating systems, mainly due to better usage of the equipment and the high individual heating costs of SF4.

In the morning and evening hours, when the PV production picks up or declines, heat is transferred to SF4 both from SF1 and SF2 in

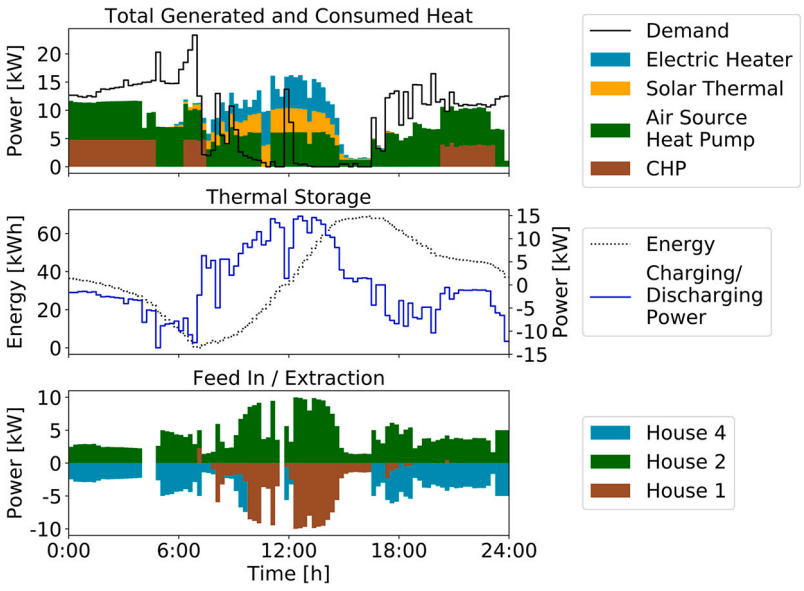

Fig. 15. Optimal heat flow between buildings.

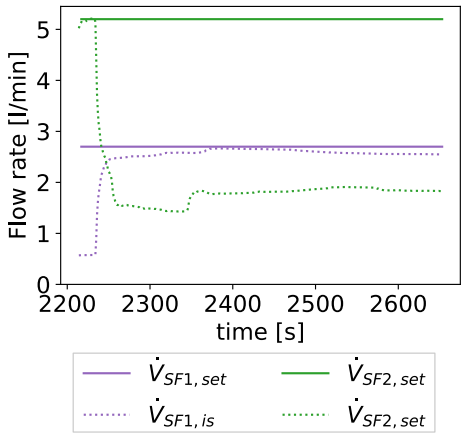

Fig. 16. Pump blocking: The pump in SF1 has to overcome a higher pressure difference and is blocked by the pump in SF1. A better control strategy could avoid this problem as demonstrated by manually reducing the power of the pump in SF2 after 2230 s.

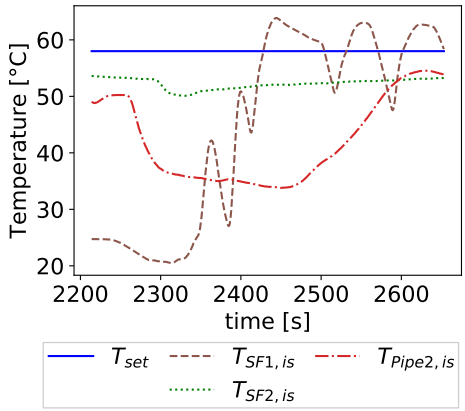

Fig. 17. Mixing of hot and cold water in district heating pipes: Pipe 1 between SF1 and SF2 cooled during the down time. When SF1 starts to feed in, the water in pipe 2 cools down at the beginning until pipe 1 is warm.

a short time period. This means that we have 2 sources at the same time. With multiple feed-in pumps, the pumps might block each other as mentioned by Licklederer et al. [51]. Fig. 16 shows this effect, when SF1 and SF2 should feed in and SF4 extracts heat. Since SF1 is further away from SF4, its pump has to overcome a higher hydraulic resistance. This results in SF2 being able to provide the required heat while SF1 provides only a small volume flow and is almost blocked. At 2250 s, the power of the pump in SF2 was manually reduced to show that a better control strategy could prevent this and result in a better distribution of the volume flow.

Another challenge arises due to the fact that there was no flow between SF1 and SF2 before SF1 starts feeding in. This means that the temperature in the pipe is at ambient temperature. Fig. 17 shows problems that can occur in this situation. When SF1 starts feeding in, cold water from pipe 1 mixes with hot water from SF2, which results in a reduction of the temperature in pipe 2. This destroys exergy and means that SF4 cannot extract heat from the grid in that time period due to too low temperatures. The delay and oscillation of the feed-in temperature of SF1 are caused by its controller, which could be further improved. One option to prevent the grid cooling would be to flush pipe 1 with hot water from SF2, before SF1 feeds in. However this has to be considered in the resource scheduling.

The case study also showed that the chosen MPC is inaccurate. It simplifies the thermohydraulic system to heat only and neglects temperature and pressure constraints. This results in two problems: The thermal storage in SF2 is fed by a HP with high volume flow and low temperature difference between supply and return, which resulted in strong mixing. Although the state of charge of the thermal storage is according to the optimization results, the outlet temperature and thus the feed-in temperature of SF2 are too low (see Fig. 17). Hou et al. [21] introduced a detailed MPC for prosumers in a DHC system with a thermal storage and waste heat from a data center. They achieved more robust results than rule-based control. They show that MPCs can be suitable to provide good control for prosumer-based DHC systems when the models are detailed enough.

Furthermore, neglecting pressure and temperature in the heat network model can lead to setpoints for the volume flow, which cannot be reached and might result in feed-in pumps blocking each other. A more accurate model of the heat network can reduce the impact of this problem.

The findings of the case study show that the laboratory is able to reproduce the behavior of district heating systems. The results further show that the laboratory is a good complement to simulation models, as it allows validation of control algorithms on real hardware and highlights phenomena that may have been neglected in simulation models. It allows researchers to test their algorithms in a real-world environment, providing another step toward implementing innovative approaches from research in practice.

5. Discussion

The focus of the thermal side of the CoSES laboratory is on a detailed study of thermal prosumer systems in DHCs as well as heating solutions for individual homes. Because of this focus, the laboratory has different strengths, limitations, and use cases, which are discussed in this chapter.

5.1. Strength

The strengths of the laboratory lie in the very detailed replication of the five prosumers by using commercial devices. In combination with PHIL, a close to reality operation of the thermal system can be emulated. The modular design allows a simple exchange of components depending on the research purpose, e.g. experimental heat transfer stations can be replaced by commercial ones to analyze and replicate the behavior of field experiments. Since most pumps and valves can be controlled by the user, novel control strategies can be tested at field level.

Another strength is the integration of the thermal and electric energy system. This allows to analyze and optimize sector coupling of thermal and electric systems, including real electrical components such as PV, batteries or electric vehicles. By measuring the experimental electric grid of the CoSES laboratory, effects of different control strategies on the electric grid can be determined.

The use of PHIL allows to emulate environmental conditions in a controlled laboratory environment without affecting user comfort, as would be the case in field tests. In addition, experiment results are independent of environmental conditions and thus reproducible.

5.2. Limitations

Several limitations of the laboratory come from its design. Due to the short distance between the buildings, a PHIL emulator for the thermal grid is used to replicate temperature losses and dynamic temperature changes. However, this setup cannot reproduce the pressure behavior in the pipes of the thermal network. The design with standard pipes limits its research to 3rd and 4th generation and ambient temperature heat grids as well as 2nd, 3rd and 4th generation cooling grids. Older generations for heat grids cannot be tested as they require temperatures above 100 °C.

The PHIL approach also has drawbacks, as it is only as good as the simulation models used for it. Ideally, these simulation models should

be validated against real data. This was the motivation of using commercial hardware as much as possible in the initial laboratory design.

Furthermore, the components of the SFs are designed for typical household size. This means that they can only feed a small amount of excess heat into the grid when the buildings are integrated as prosumers. As a result, the flow rates during feed in are low. At the same time, feeding heat into the DHC grid requires a high differential pressure. Since there are no commercially available pumps that have their ideal operating point at low flow rates and high pressure, this results in poor efficiency of the pumps used in the laboratory. However, the same problem occurs with prosumers in practice at similar small heat rates. The size of the components leads to a further limitation, as heat pumps and CHPs have little influence on the experimental electric grid.

5.3. Research potential

Since the entire system is simulated in detail and all components can be controlled, the laboratory is well suited for validating new control strategies. These include control strategies at field level, e.g. the control of pumps and control valves of bidirectional heat transfer stations as well as EMS. EMS can be tested under real conditions and in a reproducible way to identify unforeseen influences.

By characterizing components installed in the CoSES laboratory (as done for a CHP [52] and a thermal storage [53]), simulation models can be validated. This has already been done for the Modelica-based simulation library CoSES ProHMo [49] and a hybrid one dimensional multi-node model of a thermal storage [54].

The impact of sector coupling on the electric grid can be analyzed and optimized with workarounds, even though the heat generators in the CoSES laboratory are too small:

- The voltage and current profile of the heat pump or CHP is measured in detail, scaled and emulated in real time by the Egston load emulator.
- The Egston load emulator artificially creates further burdens on the grid.
- In a joint experiment with other laboratories, the voltage and current profile can be measured externally and emulated by the Egston load emulator. This can be done in real time or sequentially.

In addition, the CoSES laboratory can be used to prequalify control strategies and components prior to a field test. The laboratory includes commercial heat generators that are affected by their internal control and external influences, as well as pumps and valves that behave nonlinearly. Prequalification of control strategies can help to detect errors in advance, reducing the time required for the field tests while increasing the significance of the results. Similarly, problems that occur in reality can be reproduced and addressed in a controlled laboratory environment.

The open communication interface allows the laboratory to be combined with other facilities. The CoSES laboratory can be used by other facilities, for instance, to provide detailed information about the behavior in the building or in the electricity grid. Likewise, other facilities can provide information for experiments in the CoSES laboratory, for example about the hydraulics in the DHC grid as setpoints for the DHC grid emulator.

6. Conclusion and outlook

This paper presents the CoSES laboratory at TUM that bridges between simulation models and field tests in the evaluation and analysis of innovative DHC and smart energy systems. The detailed description of the architecture can serve as an example for the design of other DHC laboratories. It consists of five thermal and electric prosumer houses that are connected with a thermal and electric grid. The laboratory replicates dynamics and efficiencies of commercial components and their internal control, of which generic simulation models are sometimes lacking. In contrast to field tests, weather conditions and user behavior are emulated, improving reproducibility and allowing it to run independently from external influences without affecting user comfort. Due to its modular design, the configuration can be adapted to individual experiment requirements, thus enabling a wide range of experiments. The CoSES laboratory is therefore well suited for a broad spectrum of research areas:

- Commercial equipment can be characterized to generate data for the validation of simulation models. So far, data for a thermal storage [53] and a CHP [52] are published.
- Control strategies for HCTS and a bHPTS can be improved and validated with a focus the interaction of multiple sources, their pump control and effects from flexibly operating DHC grids.
- Energy management systems for individual houses or whole districts can be tested under the influence of commercial components and their internal control.
- The interaction between different control structures from high level control to field level control can be analyzed.
- The influence of the thermal side on smart energy systems and vice versa through sector coupling can be analyzed.

A case study demonstrates the functionality of the laboratory and the advantage of the PHIL approach. The case study showed that prosumer integration into flexible district heating grids can reduce overall heating costs but requires intelligent control concepts for transfer stations. Simple control concepts might lead to problems, when multiple houses feed in at the same time. It further showed that a simple MPC that neglect temperatures and pressure constraints might be too inaccurate for flexible operation of prosumer based DHC systems.

Experimental case studies are a good complement to simulation models as they replicate phenomena that are difficult to capture in generic simulation models, such as internal control strategies of commercial components, delayed and inaccurate implementation of setpoints, and the behavior of the thermohydraulic system.

The presented laboratory can contribute to further improve DHC grids, to decarbonize the heating and cooling sector and to further develop smart energy systems. Its modular structure allows the expansion of the setup for new research questions. Currently planned expansions include equipment for cooling concepts of houses and the analysis of electrolyzer/fuel cell systems for long-term storage of surplus electricity. The CoSES laboratory welcomes collaborations with other researchers and companies optimizing the thermal and electric system at the house or district level.

CRediT author statement

Daniel Zinsmeister: Conceptualization, Visualization, Writing - Original Draft and Editing. **Thomas Licklederer:** Conceptualization, Writing - Original Draft, Review and Editing. **Stefan Adldinger:** Writing - Original Draft. **Franz Christange:** Conceptualization, Writing - Review. **Peter Tzscheutschler:** Conceptualization, Writing - Review, Supervision, Project administration, Funding acquisition. **Thomas Hamacher:** Conceptualization, Supervision, Funding acquisition. **Vedran S. Perić:** Conceptualization, Writing - Review, Supervision, Project administration, Funding acquisition.

Declaration of competing interest

The authors declare that they have no known competing financial interests or personal relationships that could have appeared to influence the work reported in this paper.

Data availability

Data will be made available on request.

Acknowledgements

This project was funded by the Federal Ministry for Economic Affairs and Climate Action, Germany (FKZ: 03EN3032). The work of Vedran S. Perić was supported by Deutsche Forschungsgemeinschaft (DFG), Germany through “Optimal Operation of Integrated Low-Temperature Birdirectional Heat and Electric Grids (IntElHeat)” under project number 450821044. The construction of the CoSES laboratory was supported by Deutsche Forschungsgemeinschaft (DFG) through the project “Flexible reconfigurable microgrid laboratory” under project number 350746631.

References

[1] Ferroukh Rabia, Frankl Paolo, Abid Rana. Renewable energy policies in a time of transition: heating and cooling. https://www.irena.org/-/media/Files/IRENA/Agency/Publication/2020/Nov/IRENA_IEA_REN21_Policies_Heating_Cooling_2020.pdf, 2020.

[2] Dean Brian, Dulac John, Morgan Trevor, Remme Uwe. The future of cooling: opportunities for energy-efficient air conditioning. https://iea.blob.core.windows.net/assets/0bb45525-277f-4c9c-8d0c-9c0cb5e7d525/The_Future_of_Cooling.pdf, 2018.

[3] Kavvadias K, Jiménez Navarro JP, Thomassen G. Decarbonising the eu heating sector: integration of the power and heating sector (2019). https://doi.org/10.2760/072688. https://op.europa.eu/en/publication-detail/-/publication/208e7048-b406-11e9-9d01-01aa75ed71a1/language-en.

[4] Connolly D, Lund H, Mathiesen BV, Werner S, Möller B, Persson U, et al. Heat roadmap Europe: combining district heating with heat savings to decarbonise the eu energy system. Energy Policy 2014;65:475–89. https://doi.org/10.1016/J.ENPOL.2013.10.035.

[5] Clean energy for all europeans package. https://ec.europa.eu/energy/topics/energy-strategy/clean-energy-all-europeans_en, 2021.

[6] Lund H, Duic N, Østergaard PA, Mathiesen BV. Future district heating systems and technologies: on the role of smart energy systems and 4th generation district heating. Energy 2018;165:614–9. https://doi.org/10.1016/j.energy.2018.09.115.

[7] Lund H, Østergaard PA, Chang M, Werner S, Svendsen S, Sorknæs P, et al. The status of 4th generation district heating: research and results. Energy 2018;164:147–59. https://doi.org/10.1016/j.energy.2018.08.206.

[8] Lund H, Werner S, Wiltshire R, Svendsen S, Thorsen JE, Hvelplund F, et al. 4th generation district heating (4gdh): integrating smart thermal grids into future sustainable energy systems. Energy 2014;68:1–11. https://doi.org/10.1016/j.energy.2014.02.089.

[9] Lund H, Østergaard PA, Connolly D, Mathiesen BV. Smart energy and smart energy systems. Energy 2017;137:556–65. https://doi.org/10.1016/j.energy.2017.05.123.

[10] Edtmayer H, Nageler P, Heimrath R, Mach T, Hochenauer C. Investigation on sector coupling potentials of a 5th generation district heating and cooling network. Energy 2021;230:120836. https://doi.org/10.1016/j.energy.2021.120836.

[11] Gudmundsson O, Thorsen JE, Brand M. The role of district heating in coupling of the future renewable energy sectors. Energy Proc 2018;149:445–54. https://doi.org/10.1016/j.egypro.2018.08.209.

[12] Bünning F, Wetter M, Fuchs M, Müller D. Bidirectional low temperature district energy systems with agent-based control: performance comparison and operation optimization. Appl Energy 2018;209:502–15. https://doi.org/10.1016/j.apenergy.2017.10.072.

[13] Zarin Pass R, Wetter M, Piette MA. A thermodynamic analysis of a novel bidirectional district heating and cooling network. Energy 2018;144:20–30. https://doi.org/10.1016/j.energy.2017.11.122.

[14] Brange L, Englund J, Lauenburg P. Prosumers in district heating networks – a Swedish case study. Appl Energy 2016;164:492–500. https://doi.org/10.1016/j.apenergy.2015.12.020.

[15] Kauko H, Kvalsvik KH, Rohde D, Nord N, Utne Å. Dynamic modeling of local district heating grids with prosumers: a case study for Norway. Energy 2018;151:261–71. https://doi.org/10.1016/j.energy.2018.03.033.

[16] Rosemann T, Löser J, Rühling K. A new dh control algorithm for a combined supply and feed-in substation and testing through hardware-in-the-loop. Energy Proc 2017;116:416–25. https://doi.org/10.1016/j.egypro.2017.05.089.

[17] Lund H, Thorsen JE, Jensen SS, Madsen FP. Fourth-generation district heating and motivation tariffs. ASME Open J Eng 2022;1. https://doi.org/10.1115/1.4053420.

[18] Volkova A, Reuter S, Puschnigg S, Kauko H, Schmidt R-R, Leitner B, et al. Cascade sub-low temperature district heating networks in existing district heating systems. Smart Energy 2022;5:100064. https://doi.org/10.1016/j.segy.2022.100064.

[19] Huynh T, Schmidt F, Thiem S, Kautz M, Steinke F, Niessen S. Local energy markets for thermal-electric energy systems considering energy carrier dependency and energy storage systems. Smart Energy 2022;6:100065. https://doi.org/10.1016/j.segy.2022.100065.

[20] Frölke L, Sousa T, Pinson P. A network-aware market mechanism for decentralized district heating systems. Appl Energy 2022;306:117956. https://doi.org/10.1016/j.apenergy.2021.117956.

[21] Hou J, Li H, Nord N, Huang G. Model predictive control for a university heat prosumer with data centre waste heat and thermal energy storage. Energy 2023;267:126579. https://doi.org/10.1016/j.energy.2022.126579.

[22] El-Baz W, Tzscheutschler P, Wagner U. Experimental study and modeling of ground-source heat pumps with combi-storage in buildings. Energies 2018;11(5):1174. https://doi.org/10.3390/en11051174.

[23] Thorsen JE, Ommen T, Meesenburg W, Smith KM, Oliver EM. Energylab nordhavn (d10.1c): heat booster substation and circulation booster for domestic hot water. https://backend.orbit.dtu.dk/ws/portalfiles/portal/245670581/d10.1c_heat_boosters_for_hot_tap_water_and_heating.pdf, 2019.

[24] Heymann M, Rosemann T, Rühling K, Tietze T, Hafner B. Concept and measurement results of two decentralized solar thermal feed-in substations. Energy Proc 2018;149:363–72. https://doi.org/10.1016/j.egypro.2018.08.200.

[25] Schäfer K, Schmidt T. Experimental plant for analyzing the technical feasibility of decentralized solar heat feed-in. In: EuroSun 2018 conference proceedings; 2018.

[26] Fedrizzi R. Energy exchange lab: facility for tests on advanced district heating and cooling networks. https://webassets.eurac.edu/31538/1621456833-energyexchangelaben-2020.pdf, 2020.

[27] Kallert A, Lottis D, Shan M, Schmidt D. New experimental facility for innovative district heating systems—district lab. Energy Rep 2021;7:62–9. https://doi.org/10.1016/j.egyr.2021.09.039.

[28] Messmer C, Ackermann C, Spoerri R, Dahinden C, Afjei T, Sulzer M. Virtual test bench by linking the ‘fhnw - energy research lab’ and the ‘hslu - nodes lab’. http://hpc2017.org/wp-content/uploads/2017/05/P.2.3.4-Virtual-test-bench-by-linking-the-FHNW-Energy-Research-Lab-and-the-HSLU-NODES-Lab.pdf, 2017.

[29] Perić VS, Hamacher T, Mohapatra A, Christiange F, Zinsmeister D, Tzscheutschler P, et al. Coses laboratory for combined energy systems at TU Munich. In: 2020 IEEE power & energy society general meeting (PESGM). IEEE; 02.08.2020 - 06.08.2020. p. 1–5.

[30] Østergaard PA, Werner S, Dyrelund A, Lund H, Arabkoohsar A, Sorknæs P, et al. The four generations of district cooling - a categorization of the development in district cooling from origin to future prospect. Energy 2022;253:124098. https://doi.org/10.1016/j.energy.2022.124098.

[31] Mohapatra A, Hamacher T, Perić VS. Phil infrastructure in coses microgrid laboratory. In: 2022 IEEE PES innovative smart grid technologies conference Europe (ISGT-Europe). IEEE; 2022. p. 1–6.

[32] Christange F. The combined smart energy systems laboratory. Dissertation. Technical University of Munich; 2021. http://mediatum.ub.tum.de/?id=1540691.

[33] Lamaison N, Bavière R, Cheze D, Paulus C. A multi-criteria analysis of bidirectional solar district heating substation architecture. In: Romero M, Mugnier D, Renné D, Guthrie K, Griffiths S, editors. Proceedings of SWC2017/SHC2017, international solar energy society; 29.10.2017 - 02.11.2017. p. 1–11.

[34] District heating transfer station wp grid-hiq. https://ratiotherm-systems.com/waermepumpen/nahwaerme-waermepumpen/wp-grid-hiq/, 2022.

[35] Wall mounted gas condensing boiler cgb-2. https://www.wolf.eu/en/products/gas-heating-systems/wall-mounted-gas-condensing-boiler-cgb-2/, 2021.

[36] Zinsmeister D, Licklederer T, Christange F, Tzscheutschler P, Perić VS. A comparison of prosumer system configurations in district heating networks. Energy Rep 2021;7:430–9. https://doi.org/10.1016/j.egyr.2021.08.085.

[37] What is veristand? https://www.ni.com/en-us/shop/data-acquisition-and-control/application-software-for-data-acquisition-and-control-category/what-is-veristand.html, 2021.

[38] DKE Deutsche Kommission Elektrotechnik Elektronik Informationstechnik in DIN und VDE, Industrielle platin–widerstandsthermometer und platin–temperatursensoren.

[39] Sensorshop24. Kanalkombifühler für temperatur und feuchte (0-10v/4-20ma). https://www.sensorshop24.de/kanalkombifuehler-fuer-temperatur-und-feuchte-0-10v-4-20ma.

[40] Endress + Hauser. Technical information proline promag h 100. https://portal.endress.com/dla/5000612/9225/000/06/TI01101DEN_0717.pdf.

[41] Endress + Hauser. Technical information proline promag e 100. https://portal.endress.com/dla/5000883/5389/000/02/TI01159DEN_0317.pdf, 1.10.2021.

[42] Molliné WDV. Balgengaszähler gr. https://www.molline.de/fileadmin/content/content/Bilder/produkte_gaszaehler/Balgengaszaehler_GR/DB0300_Balgengaszaehler-GR.pdf.

[43] E+E. Sensor for very low air velocity: Ee660. https://www.epluse.com/products/air-velocity-instrumentation/air-flow-transmitters-and-probes/ee660, 2023.

[44] LEM International SA. Cv3. https://www.lem.com/en/cv-31000.

[45] LEM International SA. Lem lf210-s. https://www.lem.com/en/lf-210ssp3.

[46] National Instruments Corp. Apis in veristand. https://www.ni.com/documentation/en/veristand/latest/manual/api-veristand/, 2021.

[47] Mayer M, Mohapatra A, Perić VS. Iot integration for combined energy systems at the coses laboratory; 2021. p. 195–200.

[48] Lauss G, Faruque MO, Schoder K, Dufour C, Viehweider A, Langston J. Characteristics and design of power hardware-in-the-loop simulations for electrical power systems. IEEE Trans Ind Inform 2016;63(1):406–17. https://doi.org/10.1109/TIE.2015.2464308.

[49] Zinsmeister D, Perić VS. Implementation of a digital twin of the coses district heating prosumer laboratory. In: 14th international conference on applied energy - ICAE2022; 08.08.2022 - 11.08.2022.

[50] Dorfner Johannes, Schönleber Konrad, Dorfner Magdalena, sonercandas, froehlie, smuellr, et al. tum-ens/urbs: urbs v1.0.1. https://doi.org/10.5281/zenodo.594200, 2019.
[51] Licklederer T, Zinsmeister D, Elizarov I, Perić V, Tzscheutschler P. Characteristics and challenges in prosumer-dominated thermal networks. J Phys Conf Ser 2021;2042(1):012039. https://doi.org/10.1088/1742-6596/2042/1/012039.
[52] Zinsmeister Daniel, Licklederer Thomas. Characterization of a combined heat and power unit at the coses laboratory. https://doi.org/10.13140/RG.2.2.31035.34089/1, 2021.
[53] Zinsmeister Daniel, Licklederer Thomas. Characterization of a thermal storage at the coses laboratory. https://doi.org/10.13140/RG.2.2.13461.19687, 2022.
[54] de La Cruz-Loredo I, Zinsmeister D, Licklederer T, Ugalde-Loo CE, Morales DA, Bastida H, et al. Experimental validation of a hybrid 1-d multi-node model of a hot water thermal energy storage tank. Appl Energy 2023;332:120556. https://doi.org/10.1016/j.apenergy.2022.120556.

4.2 CoSES ProHMo simulation library

4.2.1 Digital twin of the laboratory

Before conducting experiments, new control concepts and EMSs should be tested and tuned on a realistic simulation model. This helps to identify potential problems ahead of time, thereby preventing the waste of time and resources. Numerous simulation libraries that replicate the heating systems of buildings are available. Most of these libraries are based on Modelica, a language particularly suited for analyzing multi-energy systems. Existing libraries are mainly based on generic models, which makes it difficult to replicate the behavior of commercial heat generators in the CoSES laboratory. Therefore, a new simulation library is designed and implemented as a digital twin of the CoSES laboratory.

Several requirements guided the development of this simulation library. It must allow a detailed simulation of the laboratory's equipment, including possible communication points with EMSs. A low computational load must be maintained to enable efficient simulation runs without overly taxing computational resources. Ideally, an interface to NI VeriStand should be available, permitting the direct use of models in PHIL and Software in the Loop (SiL) applications. In this context, SiL enables the emulation of experiments in the real-time environment NI VeriStand without actual equipment, while having identical input and output signals. This method aids in checking for communication errors with the experimental testbed before the actual experimentation and assists in training laboratory users.

The following paper describes the structure of the ProHMo simulation library and its experimental validation. The digital twin was developed based on the GreenCity library in SimulationX [51]. GreenCity is a simulation library designed for planning, optimizing, and evaluating district and building energy systems. It simplifies the hydraulic system by neglecting pressure restrictions and losses. This approach is suitable for systems operating under unidirectional flow conditions where the pumps are always able to maintain the required flow rate. These conditions typically apply to heating systems in buildings. GreenCity further offers detailed heat consumption and storage models, which are adapted to replicate the desired behavior. For the heat generator models, look-up tables are utilized to calculate the steady-state efficiency based on temperatures and modulation setpoints and depict the dynamic behavior. The required data is generated by characterizing commercial components of the CoSES laboratory. The obtained data is published for utilization by other scientists [145, 146].

The ProsNET simulation library for the CoSES laboratory was developed simultaneously in Dymola. It analyzes the impact of prosumers on the DHC gird and is designed to construct these models in a user-friendly manner [147]. For an integrated analysis of the behavior of prosumers within the grid, models from ProHMo can be incorporated into ProsNET as Functional Mock-Up Units (FMU)s. This integration can also be executed for other libraries not based on SimulationX.

Implementation of a Digital Twin of the CoSES District Heating Prosumer Laboratory

Authors Daniel Zinsmeister, Vedran S. Perić

Publication medium Energy Proceedings, Volume 26

Digital object identifier https://doi.org/10.46855/energy-proceedings-10153

Author contributions

Daniel Zinsmeister:	Conceptualization, Visualization, Writing – original draft, review & editing.
Vedran S. Perić:	Conceptualization, Writing - review, Supervision, Project administration, Funding acquisition.

Energy Proceedings
Vol 26, 2022
ISSN 2004-2965

Implementation of a Digital Twin of the CoSES District Heating Prosumer Laboratory#

Daniel Zinsmeister[1*], Vedran Perić [1]

1 Technical University of Munich, Arcisstraße 21, Munich, 80333, Germany

ABSTRACT

This paper presents a digital twin for the district heating prosumer laboratory at the Center for Combined Smart Energy Systems (CoSES) consisting of heat generators, thermal storages and heat consumption. It is developed using a newly created, Modelica-based simulation library named CoSES ProHMo. Existing simulation models often fail to accurately represent the behavior of commercial hardware components. Therefore, the digital twin features new, accurate heat generator models and tuned models for thermal storage units and heat consumption. The component models are parametrized using measurements from the CoSES laboratory. It can be exported and used in other programs via the Functional Mock-up Interface (FMI). This allows the digital twin to be used platform-independently to design control strategies for realistic heating systems. If desired, the control strategies can be ported to an embedded controller and further tested in the CoSES laboratory. A case study with multiple heat generators, thermal storages and a heat sink was designed to demonstrate the utility of the library. The analysis of the results shows previously unanticipated interactions between different heat generators and the internal controllers of commercial hardware. Based on these findings, the proposed digital twin library can be used by the research community to create realistic scenarios for testing novel control strategies for heating systems and prosumers in district heating grids.

Keywords: Digital Twin, Simulation, Modelica, Power Hardware in the Loop, Prosumer, District Heating

1. INTRODUCTION

Smart Energy Systems are a cost-effective way to accelerate the energy transition by combining electricity, heat, transport and gas sectors to exploit synergies between them [1]. In this context, the introduction of thermal prosumers in district heating grids can further drive sector coupling between electricity and heat by combining several buildings to a larger system with more flexibility. Thermal prosumers are houses that can extract or provide heat from/to the grid. With prosumers being integrated into district heating grids, new control concepts for buildings and grids have to be designed.

These concepts are developed using simulation models and can be further improved in laboratories with commercial hardware and under close to real-world conditions. For laboratories, Power-Hardware-in-the-Loop (PHIL) is a powerful tool to emulate elements that cannot be integrated, such as consumer behavior. In a PHIL setup, part of the system is simulated and sends setpoints to a test environment, where they are converted into a real power flow whose measurements are sent back to the simulation model. This PHIL concept is the basis of the Center for Combined Smart Energy Systems (CoSES) laboratory at the Technical University of Munich (TUM), which was designed to investigate control concepts for smart energy systems [2]. The laboratory consists of five connected houses with different generators, storages and loads on electric and heat side. Several components of the CoSES laboratory have already been characterized and can be used to validate simulation models [3, 4].

When testing new control strategies in laboratories, it is important that simulations and experiments provide comparable results. Most simulation libraries for heating systems are based on generic simulation models which allow the qualitative analysis of heating systems. However, these simulation models often fail to accurately represent the behavior of commercial hardware components. Therefore, a digital twin of the CoSES laboratory is developed based on the newly created simulation library named CoSES ProHMo to develop and tune control strategies prior to experiments. It features accurate heat generator models and tuned models for thermal storage units and heat consumption, which are parametrized using measurements from the CoSES laboratory. The main contribution of this paper is the digital twin library that

can be used by the research community to develop novel control strategies in realistic scenarios for heating systems and prosumers in district heating grids.

The remainder of this papers arranged as follows. Section 2 presents the CoSES ProHMo library as the basis of the digital twin and options to export the models to other programs. These models are used to generate dynamic PHIL setpoints for the CoSES laboratory (section 3). In section 4, a case study compares the simulation results with the results of a PHIL experiment.

2. SIMULATION MODELS

The digital twin of the CoSES laboratory should mimic the behavior of its components in detail, ideally with a short simulation time. It should further be conductive to development work where the implementer is changing strategies or parameters. This enables the development and testing of suitable control strategies.

To implement the digital twin, the CoSES ProHMo simulation library is used. It is created in Modelica, an object-oriented modelling language for cyber-physical systems [6]. The structure is shown in Fig. 1. Since the Green City library [5] already provides accurate, predefined simulation models for building energy systems, it serves as a basis for the heat consumption, thermal storages and environment. These models are adapted and parametrized to replicate the behavior of the CoSES laboratory. Heat generator models are created from scratch to accurately mimic the behavior of the commercial components in the CoSES laboratory. The CoSES ProHMo library can be exported via the Functional Mock-up Interface (FMI) to other programs or used in NI VeriStand for PHIL or Software in the Loop (SiL) experiments. It is described in the following section and published on github [7].

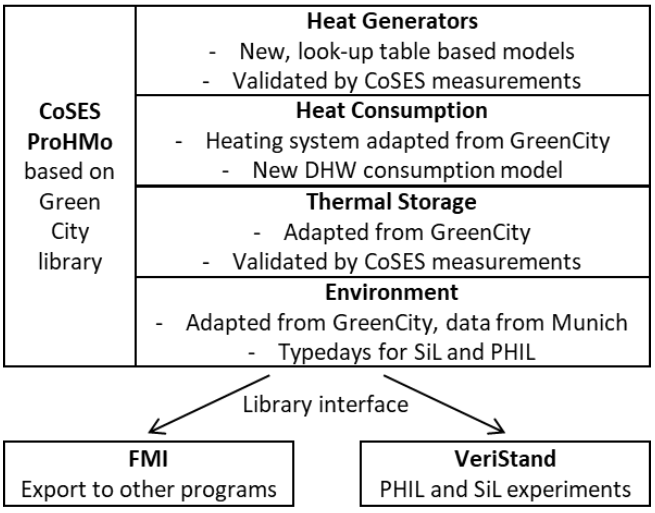

Fig. 1: Structure of the CoSES ProHMo simulation library

The models of the CoSES ProHMo library neglect pressure constraints and pressure losses within the system, which reduces the simulation time. This simplification is valid under the assumption that the system has a unidirectional flow and that pumps can provide the desired flow rate at any time, which is the case for heating systems under normal heating conditions. It replicates the behavior of the commercial components of the CoSES laboratory, including their internal control and specific behavior. Since internal control strategies vary among manufacturers, other equipment might behave differently.

2.1 Heat generators

Each house of the CoSES laboratory is equipped with one or more heat generators. Despite adjustments, generic heat generator models of various simulation libraries could not adequately replicate the behavior of the components. Generic models are good for qualitative analysis, but in this case not sufficient to represent the behavior of specific heat generators in detail. Therefore, heat generator models of the CoSES ProHMo library are based on look-up tables that provide data on dynamic behavior and efficiency. These look-up tables are derived from measurements in the CoSES laboratory. All models use Modelica Standard Library (MSL) objects and can be imported directly in other Modelica based simulation programs. The library so far consists of models of condensing boilers, air-source and ground-source heat pumps and combined heat and power units (CHPs). All models are similar in design and documented in detail in the Modelica documentation.

The behavior of the CHP is described here as an example and based on experimental characterizations [3]. It is divided into four sections as illustrated in Fig. 2:

- Start-up and cool-down process: The start-up and cool-down behavior are provided by a time dependent look-up table.
- Warm-up process: Energy required to warm up the CHP is subtracted from the steady-state efficiency and decreases linearly during the warm-up phase. The warm-up energy and time depends on the downtime.
- Steady-state: Two-dimensional look-up table provide the efficiency, which depends on the return temperature and power modulation. Load changes during steady-state are modeled with a rising or falling flank.

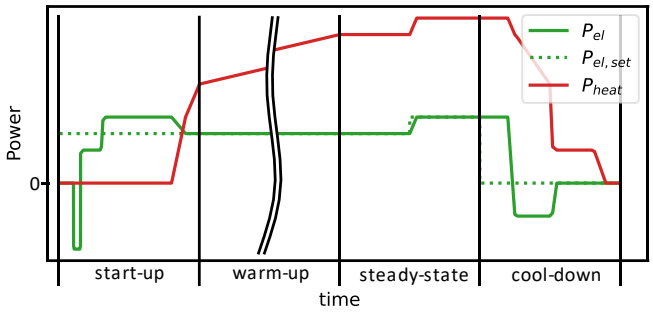

Fig. 2: Schematic of the four operation sections of the CHP

2.2 Heat consumption

The space heating system and domestic hot water (DHW) consumption constitute the heat consumption of a house. The Green City library already provides a detailed model of the consumption of space heating systems. This model was adapted in parts to better represent the desired characteristics of the heating system:

- The area specific heating power is adaptable so that the return temperature can be influenced.
- Electric consumption and presence profiles can be specified to better reflect their impact on heating consumption. Electric consumption profiles are implemented from [8].
- The set room temperature is variable, depending on presence and night time reduction settings.

For the DHW consumption, a new model was created that contains consumption profiles as a time series based on [9]. The model further checks if the DHW temperature is within the desired temperature range.

2.3 Thermal storages and heat distribution

The simulation library uses a slightly adapted version of Green City's stratified thermal storage model. It was calibrated using measurement data of the CoSES laboratory [4] and has additional inlet and outlet ports.

Depending on the type of heat generator, it is useful to position the thermal storage tank in different ways between the heat generation and consumption [10]. The different heat distribution systems are modeled and can connect the thermal storage with the heat generators, heat consumption and bidirectional district heating substation according to the requirements.

2.4 Environment Data

The Green City library includes a model for weather data from various locations. In order to integrate individual weather data and type day analysis, this model was extended. For the case study of this paper, weather data of the year 2021 in Munich was used, which is available on github [7]. For real-time simulations and PHIL experiments, type days were derived based on VDI 4655 [11].

2.5 Library interface

SimulationX and Modelica offer various ways to use simulation models in other programs. If only elements of the MSL are used, they can be used in all Modelica-based simulation programs without further adjustments, as for example in the case of the heat generators from section 2.1. To use the library outside of SimulationX, different interfaces are available to export the code, among others code export via FMI or creating .dll files for NI VeriStand.

FMI is a free standard to exchange dynamic models using a combination of XML files, binaries and C code and is supported by many tools [12]. The file can be unzipped and modified if necessary. FMI model export has the advantage that well-designed libraries can be integrated into other programs, e.g. the SimulationX based CoSES ProHMo models of this paper are used in the ProsNet library for bidirectional district heating grids in Dymola [13].

In the CoSES laboratory .dll files are used to import models into NI VeriStand for SiL and PHIL applications. When importing the digital twin in NI VeriStand for SiL tests, controllers and communication interfaces can be tested in real time prior to the experiment to find errors, saving time and money.

3. POWER HARDWARE IN THE LOOP SETUP IN THE COSES LABORATORY

PHIL combines a physical and a simulated system. It can integrate environmental conditions and user behavior in experiments that are difficult to be accounted for. The setpoints are specified by the simulation model and converted into power flows in the laboratory, whose measured values are in turn sent back to the simulation model. In addition to the more realistic representation of the environment and user behavior, the results are better reproducible since the experiments can be performed independently of ambient conditions.

The PHIL setup of the space heating system in the CoSES laboratory is shown as an example in Fig. 3. The heating controller defines the set water flow through the heating system (V_{set}) and the supply temperature ($T_{sup,set}$) based on the current room and outdoor temperature. The simulation model of the space heating system further calculates the return temperature ($T_{ret,set}$) using the measured supply temperature (T_{sup}) and water flow ($\dot{V}_{sup}$) from the testbed.

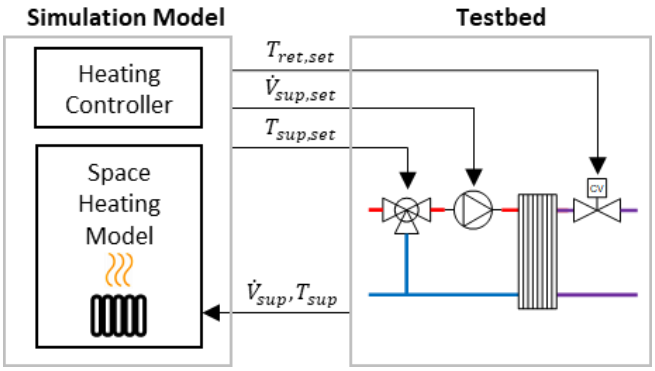

Fig. 3: Setup and data exchange of the PHIL experiment for the space heating system

The testbed consists of a commercial mixing station with a 3-way mixing valve and a pump to control the supply temperature and water flow of the heating system. If the inlet temperature into the mixing station is higher than the set supply temperature, the 3-way mixing valve injects cold water from the return pipe. The heat is extracted by a heat exchanger. A control valve on the cooling water side regulates the cooling water flow and thus the heat extraction and the return temperature of the heating system.

Other PHIL applications in the CoSES laboratory are domestic hot water consumption, solar thermal heat generators, the environment of air source and ground heat pumps and the district heating grid.

4. CASE STUDY AND RESULTS

A case study was conducted on one of the emulated houses in the CoSES laboratory to compare simulation and experimental results. Fig. 4 and Fig. 5 show the panoramic view and configuration of the testbed. It consists of a CHP unit (A) and a condensing boiler (B) with a nominal heat output of 6 and 20 kW, respectively. The condensing boiler operates at a constant water flow and temperature difference of 10 K between supply and return pipe, while the CHP produces heat at a constant supply temperature of 80 °C, adjusting the water flow depending on the return temperature. The consumption is emulated for a building with 6 inhabitants and a heated area of 300 m² (C). Two thermal storages are used for heating (D) and to provide DHW (E).

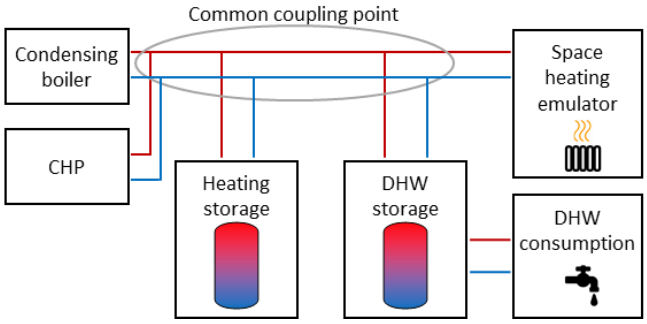

Fig. 5: Configuration of house 1 for the case study

A rule-based controller is used in this case study. The on/off conditions are:

- CHP / Condensing boiler:
  On condition: $T_{Sto,heat,top} < 65\ °C\ /\ 60\ °C$
  Off condition: $T_{Sto,heat,bottom} > 70\ °C$
- DHW storage charging
  On condition: $T_{Sto,DHW,top} < 50\ °C$ and $T_{Sto,DHW,top} < T_{Sto,heat,top}$
  Off condition: $T_{Sto,DHW,top} > 65\ °C$

4.1 Power Hardware in the Loop results

Fig. 6 shows the set and measured values of the PHIL testbed of the space heating system. The graph shows that the values, especially the return temperature, can be followed accurately.

The slow oscillation of the supply temperature and flow rate is caused by the controller of the mixing station and the missing thermal inertia of the heating system. These deviations are measured and sent to the simulation model. The same applies if the set supply temperature is higher than the inlet temperature of the mixing station or the volume flow is higher than the maximum volume flow of the pump and therefore the desired values cannot be achieved. These discrepancies

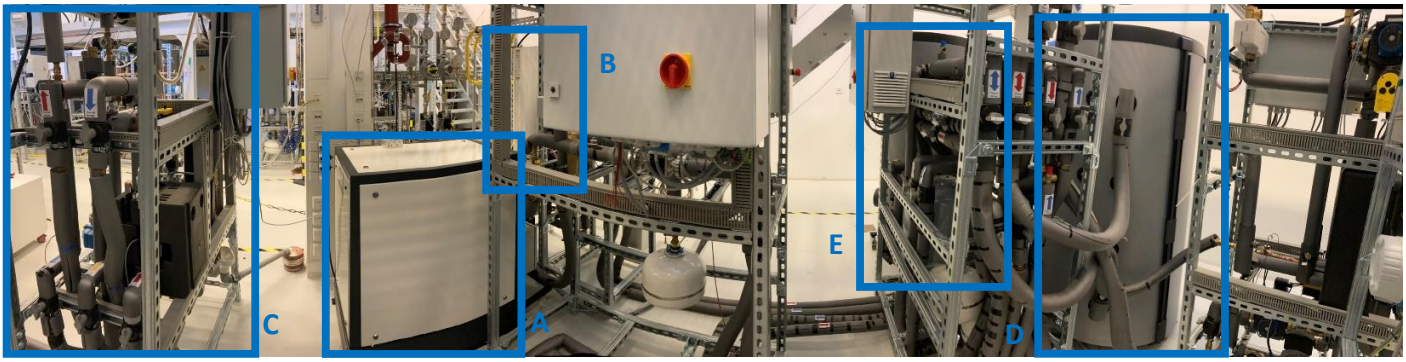

Fig. 4: Panorama picture of house 1

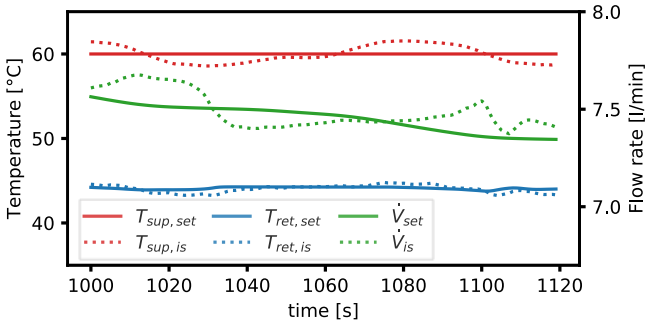

Fig. 6: Set and measured value of the PHIL testbed for space heating consumption

lead to a change in the room temperature and must be compensated for at a later time when the heating system provides the desired values again. The response to previous deviations is one of the advantages when using PHIL for the heating system.

The difference between the consumed heat of the simulation model and the PHIL testbed is $< 0.1\,\%$, which shows that the emulator works as planned.

4.2 Comparison of simulation and experimental results

Since the thermal storage is the balancing element between heat consumption and generation, it represents the behavior of the whole system very well and can be used to compare the results.

Fig. 7 shows the temperatures in the thermal storage and its state of charge (SOC) for the experiment and the simulation. The SOC and thus the energy content of the thermal storage is very accurately reproduced by the simulation model. The temperature plots of the different layers show that the temperatures in the simulation model reflect the internal temperature distribution less accurately and that the temperature stratification is less prominent in the simulation model. This is due to a too high heat exchange between the different levels, which cannot be further reduced in the simulation model due to numerical problems. However, the overall behavior is close enough to the measured values, especially at higher layers.

The inlet and outlet temperature of the thermal storage are shown in Fig. 8. During the charging process, the behavior is not exactly reproduced due to the previously mentioned discrepancy in the stratification of the thermal storage. The shape of the "temperature waves" is flatter in the simulation results, what results in a slightly different efficiency. Since the condensing boiler is active and operates at a constant temperature difference, this leads to a different inlet temperature at the top of the storage. The oscillating inlet temperature at the top is caused by the CHP and described below. During discharging, the experimental and simulation results match well.

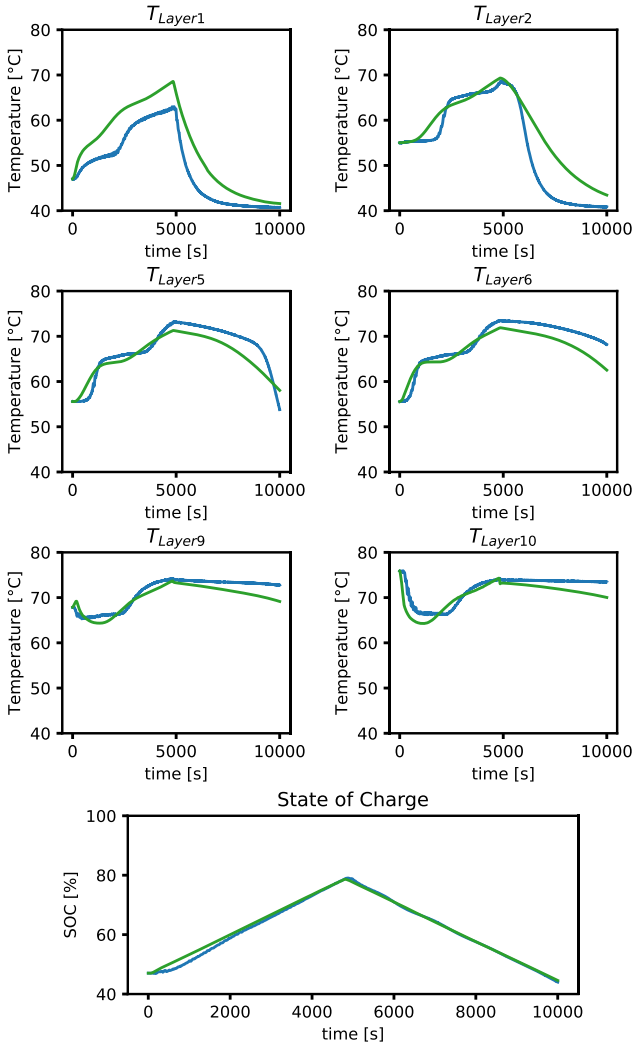

Fig. 7: Simulation (green) and experimental (blue) results during charging and discharging of the thermal storage

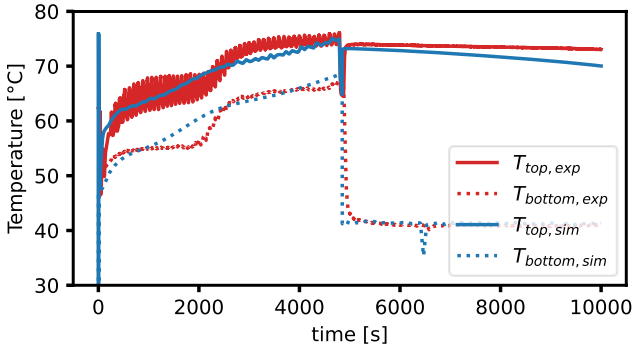

Fig. 8: Storage inlet and outlet temperatures

The different temperatures in the storage would lead to slightly different control signals and would make the comparability difficult. Therefore, the same setpoints for the heat generators are used in the simulation model as in the experiment.

If the condensing boiler and the CHP are active at the same time, the water flow through the CHP is influenced by the suction effect of the higher water flow of the

condensing boiler. The control of the pump in the CHP cannot compensate for this, resulting in too high a flow through the CHP when the pump is active. Because of this, more heat is withdrawn from the CHP than produced, which results in the pump being switched off after a while. Hence, the periodic on and off behavior of the pump shown in Fig. 9 and the fluctuating supply temperature into the thermal storage in Fig. 8. This effect was unexpected and can probably be observed often in houses with multiple heat generators. It slightly affects the overall heat generation but has no influence on the electric power generation.

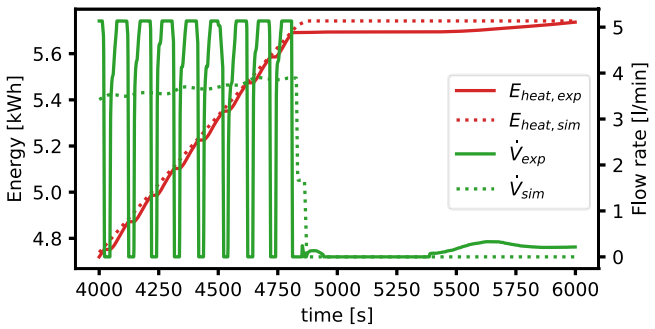

Fig. 9: Deviating flow through the CHP when affected by other components

The difference in heat generated by the condensing boiler and the CHP between simulation and experiment is $< 1\,\%$ and $5.9\,\%$, respectively. The higher deviation of the CHP is caused by an unexpected flow when it is deactivated as illustrated in Fig. 9. If this effect is ignored, the difference between simulation and experiment of the CHP is $< 1\,\%$.

The flow through the deactivated heat generator is caused by the space heating pump. Heat generators, space heating system and thermal storage are connected via a common coupling point. Therefore, part of the water flow is unintentionally drawn through the deactivated heat generators instead of being taken from the thermal storage. This is not considered in the simulation model and leads to a higher heat extraction from the CHP, because it extracts heat from its thermal inertia while being switched off. However, it also reduces the supply temperature of the space heating system once the heat generator is too cold.

This unwanted effect can be prevented by installing an automatic valve at the heat generator, which is open when it is active. Another option would be to connect the thermal storage so that it decouples heat generators and the heating system. However, this would increase the return temperature to the heat generators and thus reduce their efficiency [10].

5. CONCLUSION

This paper presents a digital twin of the CoSES laboratory to investigate prosumers in district heating systems. Existing models of heating systems in generic software often fail to accurately represent the behavior of commercial hardware components. This requires the development of specific models for an accurate analysis and control design of particular systems. Therefore, the CoSES ProHMo library was created for the digital twin, which consists of validated models of heat generator, heat consumers and thermal storages. The models can be exported and used in other programs via FMI. Researchers can use the proposed digital twin library to develop control strategies for realistic heating systems with commercial equipment. If desired, the designed control strategies can be ported to an embedded controller for commercial hardware in the PHIL testbed at the CoSES laboratory to gain further insights.

ACKNOWLEDGEMENT

The work of Daniel Zinsmeister was supported by the Federal Ministry for Economic Affairs and Energy, Germany (FKZ: 03EN3032). The work of Vedran S. Perić was supported by Deutsche Forschungsgemeinschaft (DFG), Germany (FKZ: 450821044). The construction of the CoSES laboratory was supported by Deutsche Forschungsgemeinschaft (DFG), Germany (FKZ: 350746631).

REFERENCE

[1] Lund, H., Østergaard, P.A., Connolly, D., Mathiesen, B.V. (2017). Smart energy and smart energy systems, *Energy*, Vol. 137, 556–565, doi: 10.1016/j.energy.2017.05.123.

[2] Peric, V.S., Hamacher, T., Mohapatra, A., Christiange, F., Zinsmeister, D., Tzscheutschler, P., Wagner, U., Aigner, C., Witzmann, R. (2020). CoSES Laboratory for Combined Energy Systems At TU Munich, In: *2020 IEEE Power & Energy Society General Meeting (PESGM)*, IEEE, 1–5, doi: 10.1109/PESGM41954.2020.9281442.

[3] Zinsmeister, D., Lickleder, T. *Characterization of a Combined Heat and Power Unit at the CoSES laboratory*, doi: 10.13140/RG.2.2.31035.34089/1.

[4] Zinsmeister, D., Lickleder, T. *Characterization of a Thermal Storage at the CoSES laboratory*, doi: 10.13140/RG.2.2.13461.19687.

[5] Unger, R., Schwan, T., Mikoleit, B., Bäker, B., Kehrer, C., Rodemann, T. (2012). "Green Building" - Modelling renewable building energy systems and electric mobility concepts using Modelica, In: *Proceedings of the 9th International MODELICA Conference, September 3-5, 2012, Munich, Germany*, Linköping University Electronic Press, 897–906, doi: 10.3384/ecp12076897.

[6] Modelica Association. Modelica Language, from *https://modelica.org/modelicalanguage.html*.

[7] Zinsmeister, D. CoSES thermal Prosumer House Model (ProHMo), from *https://github.com/DZinsmeister/CoSES_thermal_ProHMo.git*.
[8] Tjarko Tjaden, Joseph Bergner, Johannes Weniger, Volker Quaschning. *Repräsentative elektrische Lastprofile für Wohngebäude in Deutschland auf 1-sekündiger Datenbasis*, doi: 10.13140/RG.2.1.5112.0080/1.
[9] Jordan, U., Vajen, K. (2001). Influence Of The DHW Load Profile On The Fractional Energy Savings, *Solar Energy*, Vol. 69, 197–208, doi: 10.1016/S0038-092X(00)00154-7.
[10] Zinsmeister, D., Lickleder, T., Christange, F., Tzscheutschler, P., Perić, V.S. (2021). A comparison of prosumer system configurations in district heating networks, *Energy Reports*, Vol. 7, 430–439, doi: 10.1016/j.egyr.2021.08.085.
[11] VDI. Referenzlastprofile von Wohngebäuden für Strom, Heizung und Trinkwarmwasser sowie Referenzerzeugungsprofile für Fotovoltaikanlagen, VDI 4655, Blatt 1, accessed September 22, 2020.
[12] Functional Mock-up Interface. Functional Mock-up Interface Specification, from *https://fmi-standard.org/docs/3.0-dev/*.
[13] Elizarov, I., Lickleder, T. (2021). ProsNet – a Modelica library for prosumer-based heat networks: description and validation, *Journal of Physics: Conference Series*, Vol. 2042, No. 1, 12031, doi: 10.1088/1742-6596/2042/1/012031.

4.2.2 Library expansion for 5th generation district heating and cooling analysis

Applied research in 5GDHC, especially in areas such as the design of control concepts and nuanced analysis of prosumer interactions, has been constrained by the limited availability of detailed simulation libraries. Abugabbara et al. [53] conducted a meticulous simulation analysis, but their library is not openly accessible. Zanetti et al. [46] investigated prosumers in a single pipe 5GDHC reservoir network using the Modelica Buildings library [41]. Their approach utilizes basic BHPTS models, which only allow passive cooling with heat exchangers, limiting the scope of their analysis by excluding passive cooling functionalities.

Recognizing these limitations, several requirements for enhancing a simulation library have been established to develop control strategies for 5GDHC. Key objectives include a realistic representation of the BHPTS with integrated BHP and direct heat exchanger, the incorporation of a balancing unit to manage hydraulic and thermal discrepancies, and a detailed model of the heat network to address pump limitations and effects of bidirectional water flow.

The ProHMo library already includes simulation models of the BHPTS installed in the CoSES laboratory. It is expanded for the analysis of prosumers in 5GDHC grids, a development fostered during the collaborative research stay of Orestis Angelidis. An accurate network representation requires precise grid component models that include pressure restrictions. This is accomplished using Modelica Standard Library (MSL) components for the DHC grid. The prosumer model, which neglects pressure restrictions, and the DHC network model, which incorporates them, are interconnected using hydraulic interfaces. Input variables (e.g., volume flow, supply temperature) and output variables (e.g., desired volume flow, return temperature) are exchanged as real values in the simulation environment.

In the design process of the balancing unit, two systems are analyzed: System A, where a TES within the balancing unit is directly connected to the heat network, and System B, where the balancing unit is integrated similarly to the prosumer with a heat exchanger (see Figure 4.2). In System B, the bidirectional pump on the building side must regulate and switch quickly to balance the DHC network. By contrast, System A leverages the stratification and inertia of the TES to temporarily balance thermal disparities. In prolonged imbalance, the HP heats or cools the upper or lower parts of the TES. An added benefit of System A is the reduced pressure loss in the storage compared to the pressure loss across the heat exchanger, making it a more efficient design. Therefore, System A was pursued further in this study.

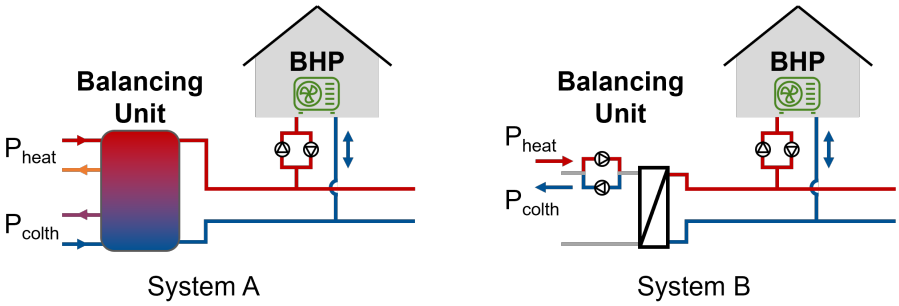

Figure 4.2: Balancing unit integration: with a TES (System A) or with a heat exchanger (System B).

A rule-based control strategy is designed for the prosumer and the balancing unit. The control aims to reduce the frequency of on/off cycles of the HPs to increase the system's overall efficiency. The pumps within the BHPTS can be controlled in two modes: maintaining a constant grid flow or sustaining a consistent grid return temperature. Both modes are compared in a subsequent submission, providing a detailed experimental analysis of their functionalities and performance impacts [141].

5th Generation District Heating and Cooling Modelica Models for Prosumer Interaction Analysis

Authors Orestis Angelidis, Daniel Zinsmeister, Anastasia Ioannou, Daniel Friedrich, Alan Thomson, Gioia Falcone

Publication medium Proceedings of the 15th International Modelica Conference 2023

Digital object identifier https://doi.org/10.3384/ecp204607

Author contributions

Orestis Angelidis:	Conceptualization, Methodology, Simulation, Visualization, Writing – original draft, review & editing.
Daniel Zinsmeister:	Conceptualization, Methodology, Simulation, Writing – review.
Anastasia Ioannou:	Conceptualization, Writing - review, Supervision.
Daniel Friedrich:	Conceptualization, Writing - review, Supervision.
Alan Thomson:	Conceptualization, Writing - review, Supervision.
Gioia Falcone:	Conceptualization, Writing - review, Supervision.

5th Generation District Heating and Cooling Modelica Models for Prosumer Interaction Analysis

Angelidis, O.[1], Zinsmeister, D.[2] , Ioannou, A.[1], Friedrich, D.[3], Thomson, A.[4], Falcone, G.[1]

[1] James Watt School of Engineering, University of Glasgow, Glasgow G12 8QQ, UK, 2072680a@student.gla.ac.uk

[2]Technical University of Munich, Arcisstrasse 21, Munich, 80333, Germany, d.zinsmeister@tum.de

[3] School of Engineering, The University of Edinburgh, Edinburgh EH9 3FB, UK, D.Friedrich@ed.ac.uk

[4] Ramboll, 240 Blackfriars Rd, London SE1 8NW, UK, Alan.Thomson@ramboll.com

Abstract

5th Generation District Heating and Cooling (5GDHC) provides a promising pathway for decarbonising the thermal sector. To quantify the synergies between heating, cooling, and electricity, complex thermofluid models are required. Modelica offers a potential solution for developing such models but despite recent research efforts, there is a lack of bespoke 5GDHC component models in literature. This paper addresses this gap by presenting a comprehensive set of Modelica models for key elements of 5GDHC systems and their interactions: prosumers, balancing units, and hydraulic interfaces. The models comprise some commercial libraries. To facilitate accessibility, Functional Mock-up Units (FMU) are generated for these models, which can be opened by any Modelica environment using Functional Mock-up Interface (FMI). Component design, relevant controls, and the applicability of Power Hardware-in-the-Loop (PHIL) setups are discussed. A theoretical use case exemplifies hardware minimisation, using only heat exchangers to investigate prosumer behaviour. The paper concludes with a discussion on the potential use of these models, opportunities for improvement, and the need for further research and experimental investigations in understanding 5GDHC systems.

Keywords: 5th Generation District Heating and Cooling, Power Hardware-in-the-Loop, Energy Systems

1 Introduction

Among the efforts to limit the impact of climate breakdown and rise of global temperature levels, the decarbonisation of thermal networks represents a crucial challenge, especially while trying to maintain security of supply and low costs (IEA 2021). A system that is attracting increasing attention is 5th Generation District Heating and Cooling (5GDHC) which offers opportunities for synergies between heating and cooling loads, low temperature waste heat utilisation and sector coupling with the electricity grid through the use of heat pumps (Gjoka, Rismanchi, and Crawford 2023). This system utilises an ambient network for meeting both heating and cooling demands with decentralised energy stations. They feature water source heat pumps, boosting the temperature for meeting heating or cooling needs and thus commonly referred to as Booster Heat Pumps (BHP), Thermal Energy Storage (TES) and hydraulic pumps. Since buildings are feeding heat/coolth into the ambient network while they are using coolth/heat, they are referred to as prosumers. The thermal and hydraulic balance is provided to the system by a balancing unit, which adds heat or coolth depending on the demand requirement of the network (Buffa et al. 2019).

However, this pumping and energy unit decentralisation leads to a bidirectional flow regime in the network when heating and cooling demands are present. This may in turn cause thermodynamic subcycles, hydraulic misbalances such as “pump hunting” depending on the topology of the network and the transient behaviour of the network medium (Angelidis et al. 2023). To capture the operational complexity of such systems, it is key to accurately model thermofluid behaviour. Detailing the hydraulic and energy flow interaction coupled with overarching controls is a challenge that fits the multi-engineering scope of the Modelica simulation language (Abugabbara 2021). Modelica allows for accurate simulation of the system dynamics including bidirectionality of flow, pressure constraints, flow characteristics and energy interactions between heating and cooling. It is recognised by the International Energy Agency as one of the key computational tools for building system modelling (Wetter and Treeck 2017). Modelica features multiple open access libraries with validated components for buildings and community heating and cooling energy systems, including the Buildings (Wetter et al. 2014) and AixLib (Mueller et al. 2016) libraries, summarised in one library under BESMod (Wüllhorst et al. 2022).

Regarding 5GDHC systems, publications have focused on describing modelling methodologies and subcomponent development, aimed mainly at studying particular elements (Blacha et al. 2019; Abugabbara, Javed, and Johansson 2022; van der Heijde et al. 2017). However, these studies have limitations. The developed models are not provided for reuse, nor include a comprehensive explanation of the interplay between control regimes and prosumer, balancing unit, and decentralised pumping station interaction. Furthermore, they have been mostly case-specific, with only some Buildings library components providing limited insights on BHP and TES interaction and overarching control. Finally, prosumer interaction, the function of the balancing unit and the effects of decentralised pumping to system performance has not been experimentally validated. This is mainly due to the large

number of units and hardware components required to study such interactions. Power Hardware-in-the-Loop (PHIL) provides a method for combining simulation tools with real hardware, interfacing through digital and analogue input/output signals, that could facilitate system-wide experiments with the use of minimal hardware. Facilitating such experiments through the provision of bespoke Modelica models for 5GDHC would be a step forward in understanding and quantifying the complex behaviour of such systems.

The aim of this paper is to present a set of comprehensive Modelica models, including experimentally validated subcomponents from the ProHMo library[1] for prosumers, hydraulic interface, and balancing unit to accurately simulate 5GDHC systems. The models have been developed to facilitate PHIL implementations, enabling experimental analyses of prosumer interactions in 5GDHC. A methodology for utilising only a heat exchanger (HEX) to replicate prosumer behaviour is presented along with a discussion on usability of the models using Functional Mock Up Interface (FMI). This feature allows the presented components to be used in any Modelica environment or in combination with Energy Management Systems (EMS) from other coding environments such as Python.

The library design is discussed in section 2, with a detailed investigation of the system components along with rule-based control strategies implemented. Section 3 includes an exemplary use case of the components for a simple 5GDHC system with two prosumers and a balancing unit. In section 4, the methodology for PHIL setups is discussed for experimental analysis of prosumer interaction or developed digital twins with minimal hardware use. Section 5 includes a discussion on strengths and limitations of the presented models along with the areas for further research. Finally, section 6 concludes with future use cases and research options.

2 Component Design

The development of the Modelica components is guided by five key guiding principles, namely usability, scalability, accuracy, flexibility & validity (Wetter and Treeck 2017). The prosumer and balancing unit models were based on equipment from the thermal Prosumer House Model (ProHMo) library (Zinsmeister and Perić 2022). The ProHMo library includes experimentally validated components from the Center for Combined Smart Energy Systems (CoSES) lab that are scalable. It is based on the Green city library from the commercial Modelica environment Simulation X (Zinsmeister and Perić 2022). The library uses a thermal only approach to simplify the models and shorten simulation time, where pressure influences are neglected. This simplification is valid for heating systems within houses (Zinsmeister and Perić 2022; Zinsmeister et al. 2023).

To model the interaction of prosumers in a district heating network with several prosumers, it is important to represent the network in detail, including pressure losses and bidirectionality of flow. For this purpose, the building models of ProHMo are coupled with hydraulic components through a communication interface submodel, referred to in this paper as hydraulic interface. The hydraulic interface serves as an accurate and comprehensive representation of the hydraulic components within the system, their behaviour and interaction. It comprises interconnected hydraulic elements (pumps, valves, sensors, pipes and elements of hydraulic resistance), facilitated by hydraulic connectors, and replicates all relevant elements encountered in real-world applications.

Furthermore, fitting control strategies are needed for all components for different grid operations. In this section, the development of bespoke components for 5GDHC is presented, allowing the setup for creating digital twins, an example of which is shown in Figure 1. In this figure, two prosumers are connected with a balancing unit through a thermal grid. The hydraulic interfaces allow for the hydraulic connection of the only thermal connector models. The prosumer and balancing unit models, as well as the hydraulic interfaces, are discussed below.

2.1 Prosumers

The prosumer model includes energy transformation units, thermal stores and demands. It can represent both Space Heating (SH) and Space Cooling (SC) demand along with Domestic Hot Water (DHW). The Modelica model is shown in Figure 2.

2.1.1 Model Description

The operation of the BHP and a Direct Cooling Heat Exchanger (HEX_{DC}) is the focal point in the prosumer component. HEX_{DC} allows for direct utilisation of the coolth from the network's cold pipe (if low enough) without upscaling it via a BHP. It has been shown that their use in 5GDHC is instrumental to the system's efficient operation (Wirtz et al. 2021). For SH and DHW, the load is to be supplied mainly from the BHP with any additional loads supplied by an auxiliary heater (electric resistance) placed within the BHP unit. For heating, the energy transformation units are connected in series with the TES which is discharged by the heat sinks. Cooling is directly supplied by the energy transformation units (HEX_{DC} or BHP) without going through the TES.

The BHP model is based on measurements of a commercial BHP found in the CoSES lab, reproducing its efficiency and dynamics. The TES model has also been experimentally validated (Zinsmeister and Perić 2022) and is represented by a one dimensional stratified model, where the TES is split into multiple layers of constant size. 10 temperature layers are used in the ProHMo library to match the number of temperature sensors in the physical unit in the lab. The maximum temperature, seen at level

[1] Available online at: https://gitlab.lrz.de/energy-management-technologies-public/coses_prohmo

DOI 10.3384/ecp204607

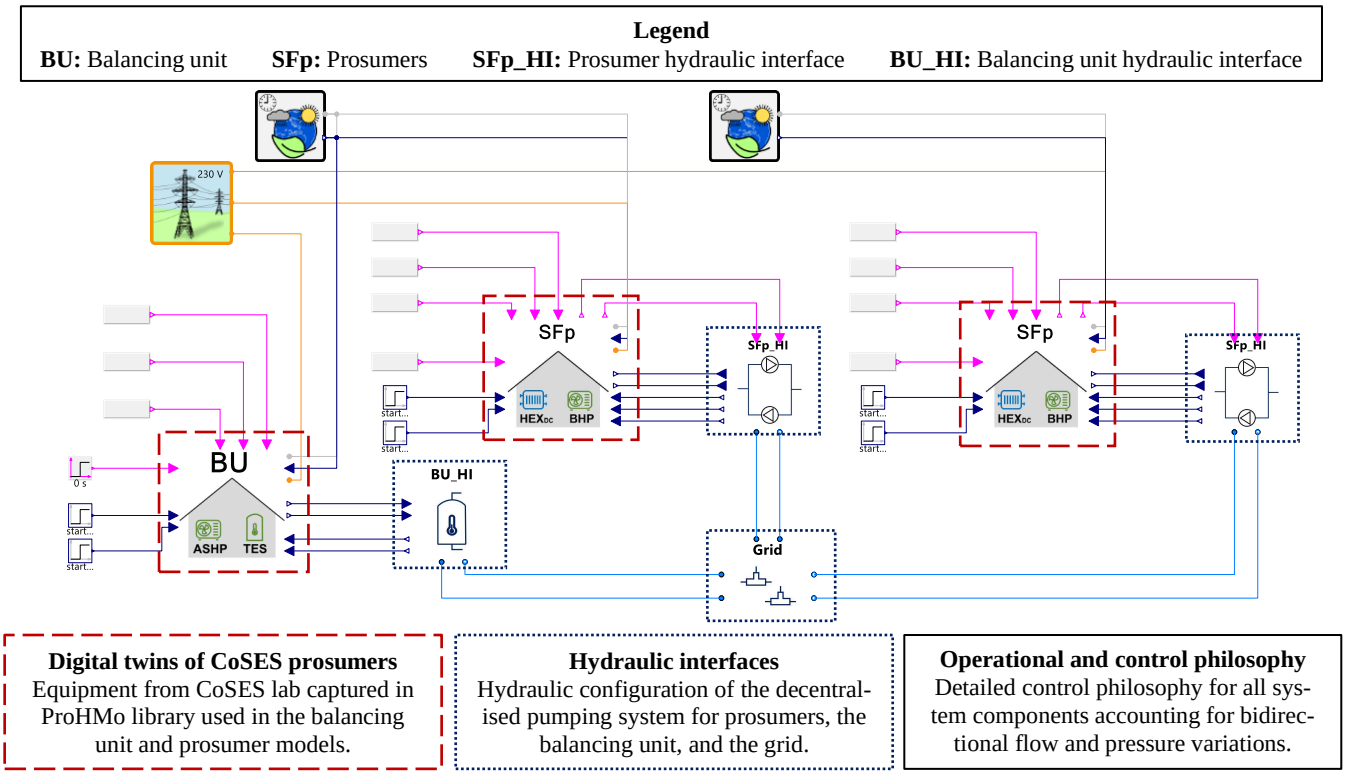

Figure 1. Library components used for 5GDHC system development.

10, is set to 60°C. This value satisfies both DHW supply and legionella avoidance requirements (Chartered Institution of Building Services Engineers (CIBSE) 2020). A hydraulic switch, namely a 3-Way Valve (3WV), can change the charging levels based on temperature in the TES. Discharching for SH is from layers 5 (Flow) and 1 (Return) since there is a low temperature heating system (underfloor heating) and layer 10 (Flow) and 1 (Return) for DHW. The discharge of the TES is modulated by a pump valve setup based on temperature and flow requirements from the heat sinks.

The SH and SC demands are captured by adapted Green City library models which allow for different number of residents, construction characteristics, building type and terminal units. The default is set to new buildings with underfloor heating/cooling systems which is most relevant for 5GDHC prosumers with heating and cooling demands (Angelidis et al. 2023). The flow and return temperature depend on the flowrate supplied by the tertiary pumps (variable flowrate pumps in the building) but are designed for 40-30°C for heating and 15-20°C for cooling. Both SH and SC are modulating around a temperature setpoint (21°C for heating and 23°C for cooling) by varying the request inlet flowrate. Similarly, DHW is modelled, requiring a temperature of 60°C and, based on the consumption, returning a cooled down water at varying flowrates. There is a heat exchanger between the end DHW consumption and the water from the TES. DHW is dependent on the number of residents and can be switched off during

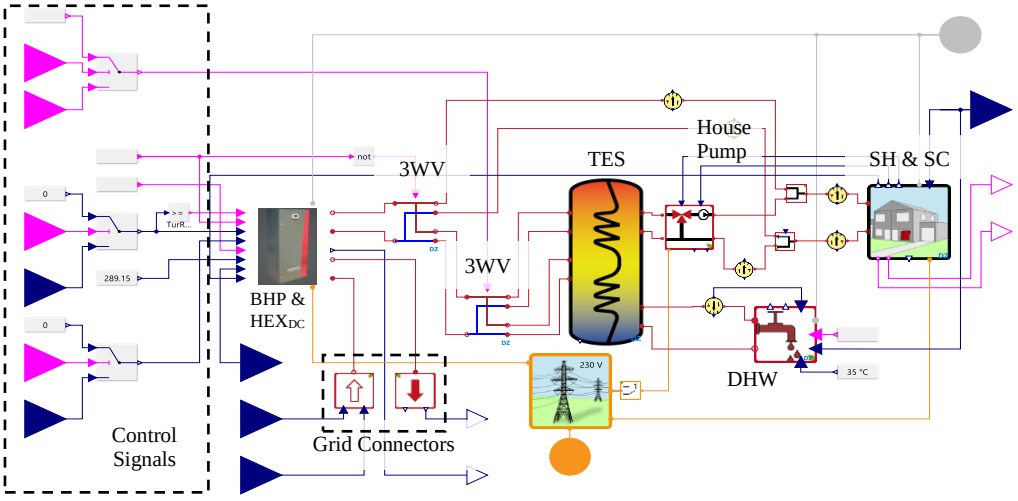

Figure 2. Prosumer Modelica Model

cooling operation (if no DHW is required during cooling periods). At each time step, there can only be heating or cooling demands with a 3WV alternating between BHP or HEX_{DC} when in cooling mode.

2.1.2 Control Strategy

The control strategy for modulating the BHP in heating mode is built around the discharging rate of the TES. The goal for the control is to keep a stratified TES, minimise the starts and stops of the BHP, keep a minimum temperature of 55°C on the TES at layer 9 and maximise system efficiency. Based on these objectives, the control uses a 3WV to charge the top or middle of the TES, with priority given to charging the top layer. To avoid on/off control with hysteresis (system lagging to the input signal), a novel control method is proposed with the modulation of the BHP as a function of the reference TES temperature layer. Equation 1 shows how the modulation factor is determined by the ratio between the actual and maximum temperature difference for the TES temperature layer against set maximum and minimum values.

$$mf = (((\max(0, \min(1, (1 - \frac{T_{reference} - T_{sup,minT}}{T_{sup,maxT} - T_{sup,minT}})))) \quad (1)$$

where mf is the modulation factor for the BHP, $T_{reference}$ is the reference temperature layer, $T_{sup,minT}$ is the minimum temperature value for the reference temperature layer and $T_{sup,maxT}$ the maximum temperature value for the layer. When the reference temperature is equal to the maximum allowed temperature, the modulation factor is zero. Conversely, when the temperature matches the minimum allowed temperature, the modulation factor is 1. To ensure the modulation factor stays within the bounds of 0 and 1, a max-min definition is applied. This approach accounts for cases that the temperature levels in the TES exceed the upper limit (e.g., on start-up).

To maintain TES stratification, the prosumer component utilizes two modulation factors: one for the top for DHW and one for the middle for SH, as shown in Figure 3. Depending on the setting of the 3WV, the respective modulating factor is used, with the reference temperature layer set to layer 7 for charging of the top of the TES and layer 4 for the middle. These layers are chosen to limit hysteresis and the impact of water inflow to/outflow from the TES.

It is seen that the higher layer modulation factor mf_h is utilising a temperature band between the start and stop temperature setpoints, $T_{StartHP,h}$ and $T_{StopHP,h}$ respectively. In a similar manner, the lower layer modulation factor mf_l is determined by a lower temperature range $T_{StartHP,l}$ and $T_{StopHP,l}$. This control strategy allows for a stratified TES, maximisation of BHP operation and abiding to top level minimum temperature requirements. An operation example for 1 day is shown in Figure 4. The difference between layer 5 and 6 occurs due to the water outflow from the TES for SH demands occurring at layer 5.

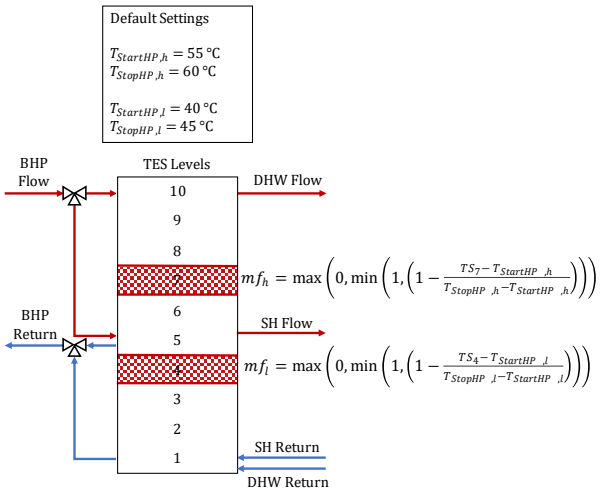

Figure 3. Schematic of control methodology for BHP.

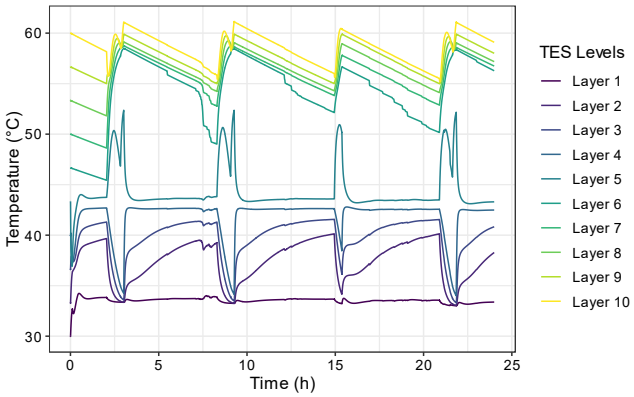

Figure 4. TES operation under modulation of the BHP

For SC, at default settings, priority is given to HEX_{DC} over the BHP (in cooling mode). The choice of switching to the use of the BHP if the room is not cooled after a designated time (defined by the user) is also provided.

Finally, a further control option has been added for the operation of the BHP. This allows for operation of the evaporator and/or the compressor under constant temperature difference or flowrate, both of which are available for commercial BHP units. Depending on the operation, the power modulation is achieved by varying the non-fixed variable within limits set by the user. The equations governing these behaviours have been modified in the models utilizing conditional functions ("if" statements) to adapt their operation accordingly. By implementing these adjustments, the BHP and grid inlets can be dynamically controlled, enabling greater flexibility in their operation. This adaptability allows for improved system performance and optimization tailored to the specific use case, with due consideration given to external factors such as flowrate and temperature differences.

2.2 Balancing unit

The balancing unit is responsible for providing thermal and hydraulic balance to the network. The Modelica

DOI
10.3384/ecp204607

model is captured in Figure 5 and described in the following sections.

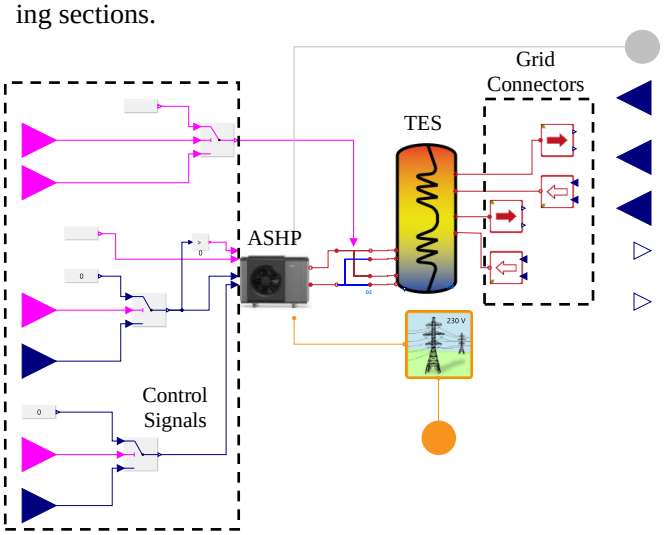

Figure 5. Balancing Unit Modelica Model

2.2.1 Model Description

An Air Source Heat Pump (ASHP) is connected in series with a TES that acts as a passive interface between the hot and cold pipes. This setup with the TES directly connected to the hot and cold pipe of the network (hot grid pipe at the top of the TES and cold grid pipe at the bottom), provides a passive hydraulic balance, critical for the operational integrity of the system featuring decentralised pumps and energy transformation units. The TES is therefore suppling heat or cold depending on the energy misbalance. The hot grid pipe is connected to the top of the TES (layer 10) while the cold pipe to the bottom (layer 1), allowing for a stratified TES with the hot pipe temperature at the top (e.g., 20°C) and the cold pipe temperature at the bottom (e.g., 15°C). Depending on the thermal balance needed by the network, the TES is cooling down (during heating balance needed) or heating up (during cooling balance needed). The ASHP needs to keep the TES temperature within the operational limits by recharging the top or bottom of the TES with heat or coolth respectively.

2.2.2 Control Strategy

To achieve this operational strategy, the ASHP is connected in series with the TES where a 3WV can change the TES charging levels based on mode of operation of the ASHP. Therefore, charging for heating uses level 9-6 for flow and return and level 2-5 for flow and return for cooling operation. This setup allows for unidirectional flow through the ASHP while keeping a stratified TES without mixing when variations between heating to cooling dominant system operation occurs. The mode of the ASHP depends on the flow direction of the grid, with cooling activated when the flow leaves the bottom of the TES, and heating when the flow leaves from the top.

The ASHP operation is following the same rule-based control for the modulation factor as the one described in equation (1). The operation of the balancing unit is captured in Figure 6, with an explanation of operation during heating and cooling dominant network operations described in the following paragraphs.

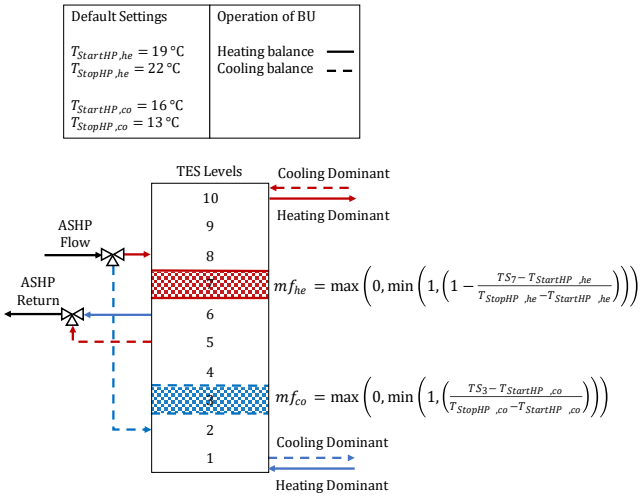

Figure 6. Balancing unit setup and connection schematic

Like the BHP heating setup, there are two modulation factors for the ASHP, in this case depending on the operation mode (heating or cooling). During heating, the flow going through the TES is from the bottom to the top with the ASHP in heating mode. The heating modulation factor mf_{he} is used which is calculated based on equation (1) with the upper and lower temperature bands being $T_{StartHP,he}$ and $T_{StopHP,he}$. For cooling, flow is reversed in the grid, with hot water coming in at the top of the TES and cold one coming out at the bottom. Therefore, the ASHP is in cooling mode, cooling down the lower half of the TES. For the modulation factor during cooling mf_{co} there is no need to subtract the ratio of the reference temperature from 1 since it directly responds to the cooling power requirements. This operation also allows for a stratified TES that can respond to dynamic changes in heating/cooling balance requirements.

2.3 Hydraulic Interface

The hydraulic interface is needed for the connection of Modelica components with thermal connectors to a system with hydraulic connectors that can capture bidirectional flow as well as pressure variations.

The hydraulic interface can avoid utilising library components that are only available in Simulation X, therefore open access Modelica standard library components are preferred. The functionality of the interface follows the methodology presented in the ProsNet library (Elizarov and Lickleder 2021), where the primary and secondary side communicate through a set of input/output signals. The key novelty in the approach developed in this paper, is the introduction of a thermal volume to represent the prosumer, considering thermal inertia and pressure variations of the system. Therefore, we can combine the benefits of utilising thermal only connectors in the prosumer and balancing unit components (low computational times

and lower complexity) without compromising the hydraulic performance of the system. At the same time, this setup allows for a clear separation between the thermal only models utilising Simulation X components that can be turned into Functional Mock-Up units (FMU) as discussed in Section 2.4. The hydraulic interfaces for the prosumer, the balancing unit, and the grid model are illustrated in Figure 7.

For the prosumer hydraulic interface unit, the key inputs and outputs from the hydraulic interface are temperature [°C] and flowrate [l/min]. Signals for the set flowrate $\dot{V}_{g,set}$ asked by the prosumer and the output temperature $T_{p,out}$ from the prosumer are sent to a volume representing the prosumer, allowing for thermal inertia to be accounted for, resulting in the temperature the grid actually sees from the prosumer, $T_{g,out}$. Depending on the instantaneous demand mode (heating or cooling), the respective pump from the interface becomes active and flow is thus changing direction respectively. We use a PI controller to

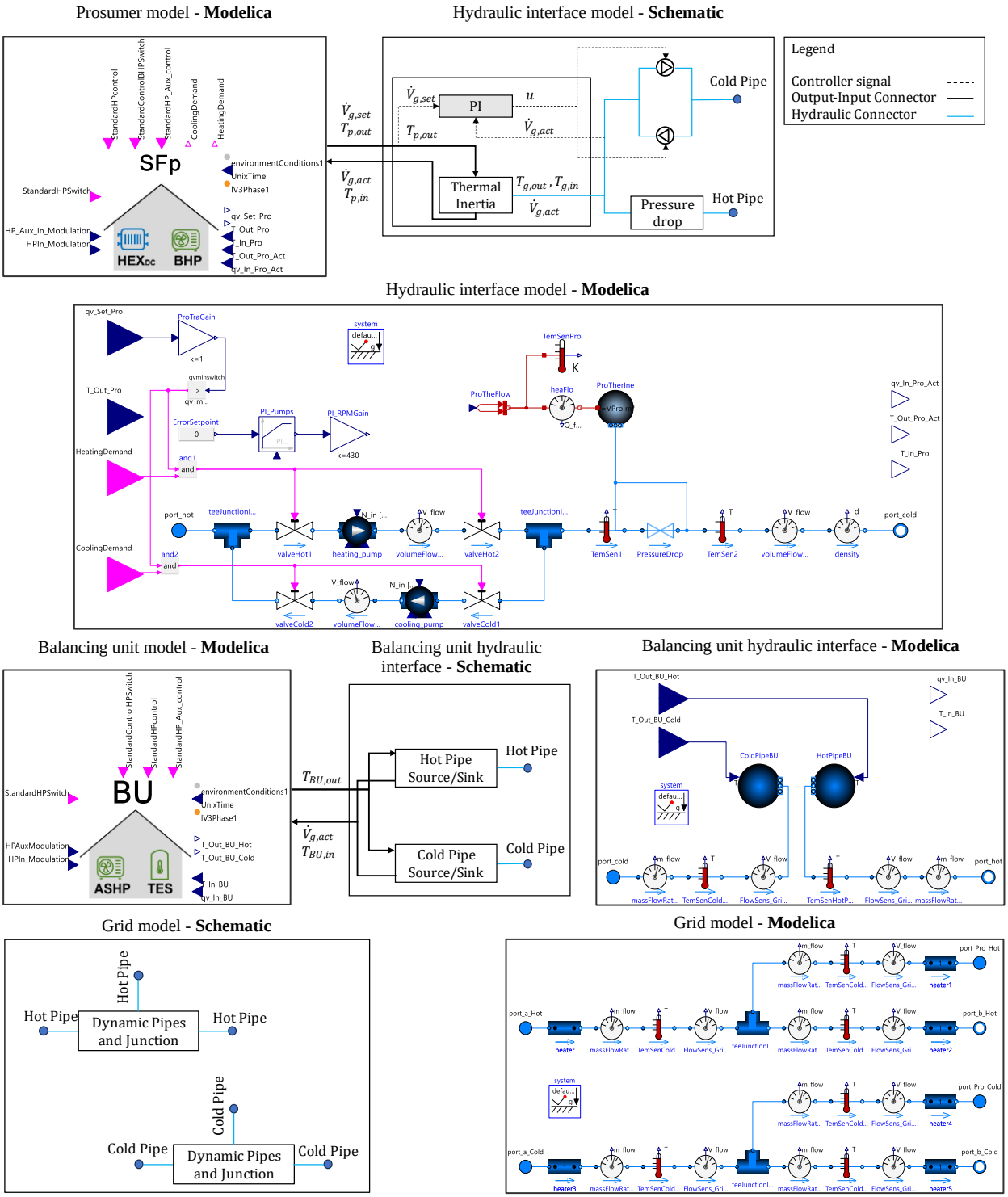

Figure 7. Hydraulic interfaces for prosumer and balancing unit as well as hydraulic model of the grid

DOI 10.3384/ecp204607

give the setpoint u to the respective pump, considering the actual $\dot{V}_{g,act}$ and set flowrate $\dot{V}_{g,set}$. Then, $\dot{V}_{g,act}$ and $T_{g,in}$ are fed back to the prosumer as inputs.

For the balancing unit's hydraulic interface, the key input is the temperature from the balancing unit. The temperature corresponds to the top or bottom of the TES, depending on the flow direction, namely the sign of $\dot{V}_{g,act}$ as described in Section 2.2.2. If $\dot{V}_{g,act}$ is positive, which means there is dominant heating demands in the grid (flow from cold to hot port), then the hot pipe volume acts as a source with $T_{BU,out}$ being equal to the temperature at the top of the TES. $T_{BU,in}$ equal to the temperature of the cold pipe flows at the bottom of the TES. The opposite happens when there is cooling dominant operation and thus a negative $\dot{V}_{g,act}$, with the cold pipe volume becoming a source and the hot pipe volume becoming a sink.

The pipe network, namely the grid model, comprises dynamic pipes, sensors and junctions to allow for the connection of the prosumers and the BU. The grid model allows for parallel connection between loads, and includes ports for both the hot and cold pipes.

2.4 FMUs of Prosumers and Balancing Unit

To further increase the usability of the model, both prosumer and balancing unit models are developed so that they can be exported to FMUs, allowing for their use through the FMI standard for application in all Modelica environments (The Modelica Association 2023). With FMUs for these components, an arbitrary size of network can be built, with varying topologies and design and operational characteristics in any Modelica environment. However, the benefits from using a FMU come at a cost of transparency and editability. The components become "black boxes" that have specific elements that can be edited, significantly limiting the flexibility of the models to change. To maximise their usability, a set of key parameters have been made editable in the FMU. These follow the ProHMo library methodology as described in (Zinsmeister and Perić 2022), and include:

- Inputs for individual control setpoints
- Weather files
- Consumption parameters
- Energy generator unit capacities
- TES dimensions

3 Exemplary Use Case

To showcase the usability of the produced models, a simple system is used. It involves a heating and cooling prosumer as well as a balancing unit connected through a grid element in parallel. This setup is the one shown in Figure 1, Section 2. A constant temperature difference is kept between the cold and the hot pipe, and the grid pipes are modulated based on variable flowrate. HEX_{DC} is used for the cooling prosumer while the BHP for the heating prosumer (connected in series to the TES).

The simulation is performed for one day, with an aim to observe the behaviour of the system and qualitatively verify its operation. Figure 8 displays key outputs, namely the temperature levels of the top and bottom layers of the BU TES, the temperature in the living zones of the prosumers as well as the temperature and flowrate values on the grid's junction.

Plot A indicates the fluctuations of the temperature levels in the TES of the balancing unit, responding to heating and cooling requirements in the grid while keeping the upper (22°C) and lower (13°C) temperature limits. The spikes observed occur during ASHP start-up, with a momentary large intake. Plot B shows that the temperatures in both prosumer's living areas are maintained at the target reference temperatures (21°C for heating and 23°C for cooling). Larger deviations are observed during cooling due to the controller setting, underfloor cooling system behavior and the house pump's flowrate capacity.

Graphs C and D present temperature levels at both the hot and cold pipes. In plots E and F, flow halts for the cooling prosumer after hour 13, causing the respective pipe temperatures to track ambient temperatures and those of the segment preceding it. During the flow interruption

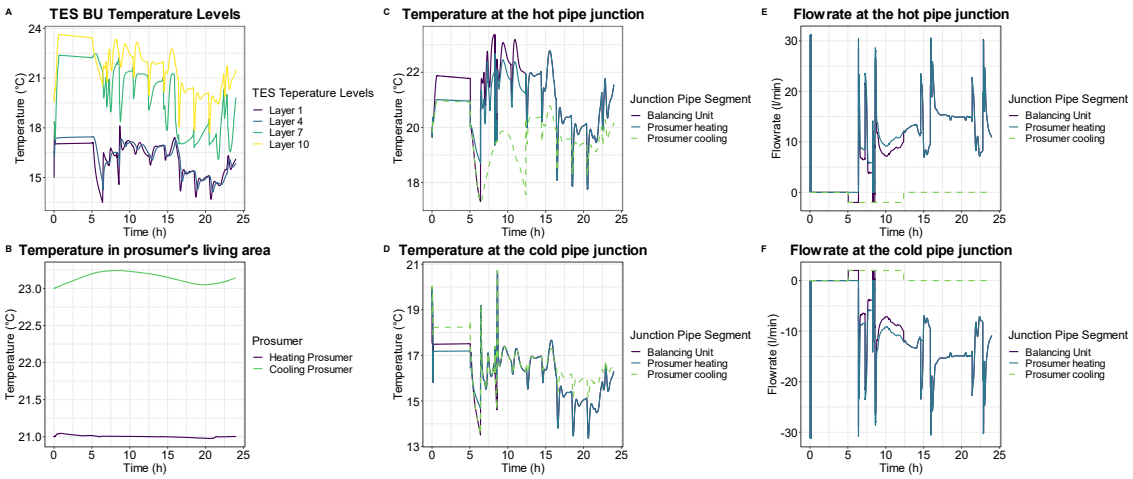

Figure 8. Exemplary case study outputs

until hour 5, the balancing unit remains idle, with the TES temperature slightly decreasing due to energy losses.

Overall, hydraulic and thermodynamic balances are kept in the system. The temperatures are maintained in the prosumer houses and bidirectionality of flow is captured. The balancing unit can operate both in heating and cooling mode ensuring that the top and bottom temperature levels are kept. It is shown that the components provide a working basis for investigations of different design cases and operation strategies. The next section describes how such designs can be validated with minimal hardware utilising PHIL approaches.

4 Power Hardware-in-the-Loop

Prosumer behaviour and interaction under different design conditions and control methodologies is one of the key gaps in research of 5GDHC systems. Experimentally validating models would require multiple BHP and buildings with both heating and cooling demand as well as the ancillary equipment (valves, pipes etc.) for developing a thermal network. To facilitate experimental validation of generated system models or the experimental assessment of prosumer interaction under varying control and design philosophies, the components are designed in such a way as to be able to utilise PHIL with minimal hardware requirements. Figure 9 illustrates how PHIL can be used for experimentally simulating a prosumer with only a HEX.

The HEX is sending metered signals to the prosumer simulation model for the flowrate and temperature present both on the primary and secondary side of the HEX. These are converted to standard unit values via a conversion module and fed to Modelica, which in turn sends back control signals. For the conversion & control modules, various software/hardware interaction methodologies are available. For example, the CoSES lab utilises Industrial Controllers for the hardware, communicating in real time with NI VeriStand for the conversion of logged data and control setpoints, as thoroughly explained in (Zinsmeister et al. 2023). Regarding hardware, other than the HEX, a heating and/or cooling unit are required to raise/drop the temperature for both the prosumer and grid side.

Prosumers' BHP and HEX_{DC} can be emulated with a PHIL setup. As mentioned in Section 2.1, the prosumer model features a BHP and HEX_{DC}, controlled in either constant flowrate or temperature difference. For the HEX_{DC} operation, based on the measured flowrate and temperature, the set return temperature of the house $T_{h,set}$ is calculated based on the heating/cooling system of the building and the building and outdoor temperature. The 3WV mixes water from the supply side to reach $T_{h,set}$. A signal is also provided for the grid pump $\dot{V}_{g,set}$, as explained in Figure 7 found in Section 2.3. For the BHP emulation, the grid pump is still operated according to the control signal $\dot{V}_{g,set}$ but the house side operates differently. The 3WV is closed, so that it doesn't mix water from the supply into the return line and the pump on the building side is operated to supply $\dot{V}_{h,set}$ to achieve the outlet temperature of the heat pump on the grid side.

Further implementations are possible that follow the same principles as the ones mentioned above. These could include multiple HEX connected in series or in parallel to study the interaction of various prosumers. In addition, the balancing unit could be connected in a similar approach to study its characteristics. Even an entire network with multiple prosumers and balancing units could be included as a simulation model on the grid side which would allow for investigating the impact of single/multiple prosumers on larger grids.

5 Discussion

This paper presents a set of models for the development of 5GDHC systems. The models have been developed with a focus on usability, scalability, accuracy, flexibility, and validity. The following sections provide some insight on strengths and limitations as well as a discussion on potential applications of the models.

5.1 Strengths

These components utilise validated models from the ProHMo library that are modular and can provide a detailed representation of component operation and building behaviour. They provide a good rule-based control allowing for BHP operation with low number of starts and stops for a longer component lifetime and a stratified TES. Start up and slew times are included as well as solutions for hysteresis. Computational time is kept low since we are using hydraulic equations only for the network, significantly reducing the complexity of the model. The models are made open access and have platform independent

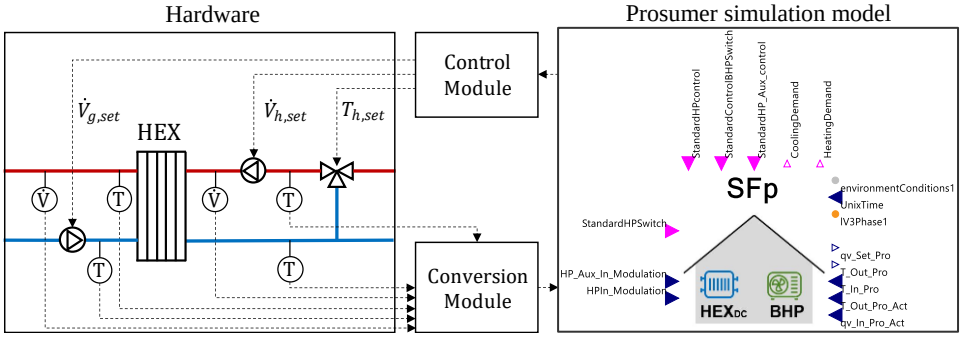

Figure 9. PHIL for a prosumer using a heat exchanger.

DOI
10.3384/ecp204607

FMUs where commercial components are used. They can be coupled with various grid models and elements such as seasonal thermal storage.

Another key benefit that is arising from these models, is the capacity for PHIL experimentations with minimal hardware to study prosumer interaction. The models can be used to emulate both building and BHP/HEX_{DC} behaviour. Different levels of detail for PHIL experiments allow a detailed analysis of grid behaviour and component interaction with low costs, space requirements and overall complexity.

5.2 Limitations

The key limitations of the components come from the use of the ProHMo library. It is built in Simulation X which is not an open access tool. This limits the capacity to freely edit the components. FMU provision has been presented as a workaround, but it does not fully open the "black box" of the component and does not allow for simple drag and drop of the individual components for use on any Modelica environment. The prosumer and balancing unit component models could be integrated into other libraries which are using open access components, while keeping the methodology of their operation intact.

The building models are focused on residential properties and may not accurately represent different consumer classes such as office blocks or retail properties. Moreover, the operational behaviors of the energy transformation components are tied to the units used in the CoSES lab, which are designed for household-scale applications. Consequently, when attempting to model much larger units or units with different technical specifications (e.g., refrigerants), the scalability and accuracy of the models may be compromised.

5.3 Potential Applications

The main benefit of this work is the provision of bespoke models and methodologies that facilitate the studying and analysis of 5GDHC systems. They can act as a basis for the creation of research cases on the impact of several parameters on the overall performance of the system. For example, they could be used to investigate different network topologies and the effect that network behaviour has on the hydraulic operation. The effect of including different consumer classes as prosumers as well as the seasonal co-occurrence of their heating/cooling demands could also be studied. The models could be used to replicate bespoke networks for industrial applications with given building schedules. Detailed operational strategies could also be investigated, identifying the effect of the hydraulic setup on the creation of thermodynamic subcycles and pump hunting phenomena. By developing relevant network and ground models, the effect of the ground type on the network performance can be studied for different insulation levels of the pipework, with a focus on the capacity for thermal losses under different network temperature regimes, insulation series and pipe materials. The impact on the number and location of balancing units as well as the introduction of passive balancing units such as seasonal energy storage (e.g., aquifers) can be quantified. The level of centralisation can also be studied, by changing the consumption parameters, allowing for a deeper investigation of the thermal zoning effect and combination of 4GDH with 4GDC and 5GDHC networks.

6 Conclusions

This paper presents a comprehensive set of Modelica models for the key components of 5GDHC, namely prosumers, balancing units, and hydraulic interfaces.

The component design and assessment, including their interconnections and control strategies, have been discussed and demonstrated through an exemplary use case. The paper has also demonstrated the applicability of PHIL setups for experimental analysis of prosumer interactions with the use of minimal hardware requirements, exemplified through a theoretical case study setup utilizing only a HEX to model a prosumer.

The presented models and methodologies provide an advancement in the understanding and analysis of 5GDHC systems. The provision of FMU models allows for their utilization in various coding environments through FMI, promoting open access as part of the ProHMo library.

Overall, this work contributes to the development of tools and methodologies for the analysis and study of 5GDHC systems, offering potential avenues for future research and application. By further refining and expanding the accessibility of the models, the understanding and adoption of 5GDHC systems can be advanced in a more open and collaborative manner.

Acknowledgments

This work was partially funded by the University of Glasgow, Energy Technology Partnership (ETP) and Ramboll under grant agreement N° ETP 189. The authors would like to thank the Ramboll Foundation for its financial support under grant agreement N° 2020-101 and Ramboll UK Energy Systems business unit for its technical support. The work of Daniel Zinsmeister was funded by the Federal Ministry for Economic Affairs and Climate Action, Germany (FKZ: 03EN3032).

Nomenclature

Abbreviation	*Meaning*
5GDHC	5th Generation District Heating and Cooling
3WV	3-Way Valve
ASHP	Air Source Heat Pump
BHP	Booster Heat Pump
DHW	Domestic Hot Water
EMS	Energy Management System
FMI	Functional Mock-Up Interface

Abbreviation	*Meaning*
FMU	Functional Mock-Up Unit
HEX	Heat Exchanger
HEX_{DC}	Direct Cooling Heat Exchanger
PHIL	Power Hardware In the Loop
SC	Space Cooling
SH	Space Heating
TES	Thermal Energy Storage

References

Abugabbara, Marwan. 2021. *Modelling and Simulation of the Fifth-Generation District Heating and Cooling*. Lunds Universitet. https://portal.research.lu.se/ws/files/98018067/MA_LicDiss.pdf.

Abugabbara, Marwan, Saqib Javed, and Dennis Johansson. 2022. "A Simulation Model for the Design and Analysis of District Systems with Simultaneous Heating and Cooling Demands." *Energy* 261 (December): 125245. https://doi.org/10.1016/j.energy.2022.125245.

Angelidis, Orestis, Anastasia Ioannou, Daniel Friedrich, Alan Thomson, and Gioia Falcone. 2023. "District Heating and Cooling Networks with Decentralised Energy Substations: Opportunities and Barriers for Holistic Energy System Decarbonisation." *Energy* 269 (April): 126740. https://doi.org/10.1016/j.energy.2023.126740.

Blacha, Tobias, Michael Mans, Peter Remmen, and Dirk Mueller. 2019. "Dynamic Simulation Of Bidirectional Low-Temperature Networks - A Case Study To Facilitate The Integration Of Renewable Energies." In , 3491–98. Rome, Italy. https://doi.org/10.26868/25222708.2019.210670.

Buffa, Simone, Marco Cozzini, Matteo D'Antoni, Marco Baratieri, and Roberto Fedrizzi. 2019. "5th Generation District Heating and Cooling Systems: A Review of Existing Cases in Europe." *Renewable and Sustainable Energy Reviews* 104 (April): 504–22. https://doi.org/10.1016/j.rser.2018.12.059.

Chartered Institution of Building Services Engineers (CIBSE). 2020. *CP1 Heat Networks: Code of Practice for the UK (2020)*. 2nd ed. London: Association for Decentralised Energy (ADE). https://www.cibse.org/knowledge/knowledge-items/detail?id=a0q3Y00000IMrmGQAT.

Elizarov, Ilya, and Thomas Lickleder. 2021. "ProsNet – a Modelica Library for Prosumer-Based Heat Networks: Description and Validation." *Journal of Physics: Conference Series* 2042 (1): 012031. https://doi.org/10.1088/1742-6596/2042/1/012031.

Gjoka, Kristian, Behzad Rismanchi, and Robert H. Crawford. 2023. "Fifth-Generation District Heating and Cooling Systems: A Review of Recent Advancements and Implementation Barriers." *Renewable and Sustainable Energy Reviews* 171 (January): 112997. https://doi.org/10.1016/j.rser.2022.112997.

Heijde, Bram van der, M. Fuchs, C. Ribas Tugores, G. Schweiger, K. Sartor, D. Basciotti, D. Müller, C. Nytsch-Geusen, M. Wetter, and L. Helsen. 2017. "Dynamic Equation-Based Thermo-Hydraulic Pipe Model for District Heating and Cooling Systems." *Energy Conversion and Management* 151 (November): 158–69. https://doi.org/10.1016/j.enconman.2017.08.072.

IEA. 2021. "Heating." Tracking Report. Paris. https://www.iea.org/reports/heating.

Mueller, Dirk, Moritz Lauster, Ana Constantin, Marcus Fuchs, and Peter Remmen. 2016. *AixLib – An Open-Source Modelica Library within the IEA-EBC Annex 60 Framework*.

The Modelica Association. 2023. "FMI 3.0 Implementers' Guide." The Modelica Association. https://modelica.github.io/fmi-guides/main/fmi-guide/#_references.

Wetter, Michael, and Christoph van Treeck. 2017. *IEA EBC Annex 60: New Generation Computing Tools for Building and Community Energy Systems*. Annex 60. Lawrence Berkeley National Laboratory and RWTH Aachen University: IEA. https://www.iea-annex60.org/downloads/iea-ebc-annex60-final-report.pdf.

Wetter, Michael, Wangda Zuo, Thierry S. Nouidui, and Xiufeng Pang. 2014. "Modelica Buildings Library." *Journal of Building Performance Simulation* 7 (4): 253–70. https://doi.org/10.1080/19401493.2013.765506.

Wirtz, Marco, Lisa Neumaier, Peter Remmen, and Dirk Müller. 2021. "Temperature Control in 5th Generation District Heating and Cooling Networks: An MILP-Based Operation Optimization." *Applied Energy* 288 (April): 116608. https://doi.org/10.1016/j.apenergy.2021.116608.

Wüllhorst, Fabian, Laura Maier, David Jansen, Larissa Kühn, Dominik Hering, and Dirk Müller. 2022. "BESMod - A Modelica Library Providing Building Energy System Modules." *Modelica Conferences*, 9–18. https://doi.org/10.3384/ECP211869.

Zinsmeister, Daniel, Thomas Lickleder, Stefan Adldinger, Franz Christange, Peter Tzscheutschler, Thomas Hamacher, and Vedran S. Perić. 2023. "A Prosumer-Based Sector-Coupled District Heating and Cooling Laboratory Architecture." *Smart Energy* 9 (February): 100095. https://doi.org/10.1016/j.segy.2023.100095.

Zinsmeister, Daniel, and Vedran Perić. 2022. "Implementation of a Digital Twin of the CoSES District Heating Prosumer Laboratory." In *Energy Proceedings*, 7. Bochum, Germany.

4.2.3 Benchmarking tool for energy management systems

While emerging control algorithms for EMSs show promise, their widespread practical adoption has yet to be realized. These new or enhanced algorithms are typically demonstrated and evaluated through individual simulations. Yet, the absence of a unified comparative framework leaves the performance of each control algorithm in specific applications and the generalizability of the benefits uncertain. Validating and comparing these controls using standardized and realistic models could significantly help to demonstrate and quantify the improvements and bridge the gap between academic research and practical implementation.

Moreover, creating and validating a simulation model is a complex task that often requires expertise in a specific simulation tool, such as Modelica. Many MPC-based EMSs tend to analyze the results using the MPC model itself, which can affect the validity due to the simplifications necessary for a fast-solving optimization model. In addition, the growing popularity of Reinforcement Learning (RL)-based EMS approaches necessitates suitable simulation models for their training. An easy-to-use benchmark model would be advantageous in this context. It could speed up the process of training and benchmarking EMSs, thus promoting an environment conducive to rapid prototyping.

For this reason, the existing CoSES ProHMo library is expanded to enable the use of its experimentally validated building models as a benchmarking and training tool for EMSs. Figure 4.3 shows some salient requirements expected from a benchmarking tool for EMS. Each building model has a backup control to ensure user comfort, which can be turned off if desired. This backup control overrides the EMS setpoints, e.g., when TES temperatures fall below predetermined limits.

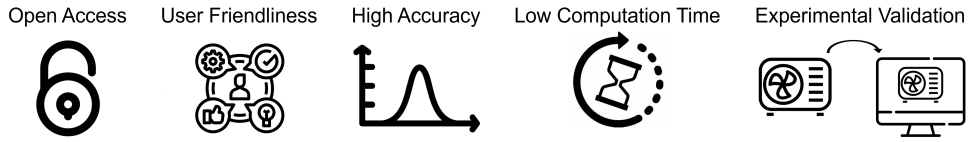

Figure 4.3: Requirements for a benchmarking tool for EMSs.

The performance of the benchmarking tool is illustrated by analyzing, tuning, and comparing a MPC- and a RL-based EMS approach. The comparison of both EMSs shows that the MPC-based EMS, equipped with perfect forecasts, achieves the lowest operational costs. Although the RL-based EMSs do not surpass the MPC-based system in performance, their independence from forecast data highlights their potential for real-world applications.

A benchmarking framework for energy management systems with commercial hardware models

Authors Daniel Zinsmeister, Ulrich Ludolfinger, Vedran S. Perić, Christoph Goebel

Publication medium Energy and Buildings, Volume 321

Digital object identifier https://doi.org/10.1016/j .enbuild.2024.114648

Author contributions

Daniel Zinsmeister:	Conceptualization, Visualization, Writing – original draft, review & editing.
Ulrich Ludolfinger:	Conceptualization, Writing - review, Supervision, Project administration, Funding acquisition.
Vedran S. Perić:	Conceptualization, Writing - review, Supervision, Project administration, Funding acquisition.
Christoph Goebel:	Conceptualization, Writing - review, Supervision, Project administration, Funding acquisition.

Energy & Buildings 321 (2024) 114648

Contents lists available at ScienceDirect

Energy & Buildings

journal homepage: www.elsevier.com/locate/enbuild

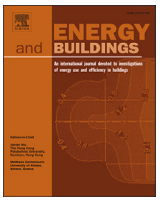

A benchmarking framework for energy management systems with commercial hardware models

Daniel Zinsmeister [a,*], Ulrich Ludolfinger [b], Vedran S. Perić [a], Christoph Goebel [a]

[a] Technical University of Munich, Arcisstrasse 21, Munich, 80333, Bavaria, Germany
[b] University of Applied Sciences Landshut, Am Lurzenhof 1, Landshut, 84036, Bavaria, Germany

ARTICLE INFO

Keywords:
Modelica
FMI
Open access
Energy management system
Model predictive control
Reinforcement learning
Experimental validation

ABSTRACT

Energy Management Systems (EMS) for buildings are pivotal in leveraging flexibility from sector coupling in future power systems. Currently, most EMS are designed and evaluated using non-standardized and incompatible simulation models built within the specific EMS development cycle. Such evaluation techniques make it difficult to compare different EMS solutions according to well-defined and universal performance indicators. Therefore, open-access benchmark models of realistic building energy systems would be beneficial for wider research community. This article introduces the ProHMo benchmarking framework which provides experimentally validated commercial heating and cooling equipment models in various building energy system configurations. The building energy system models are available as openly accessible Functional Mock-Up Units (FMU) to allow for toolchain-independent benchmarking of EMS. The framework includes a Python code template that enables easy integration with different EMS interfaces. In a case study, we show the potential of the benchmarking framework by comparing a rule-based, optimization-based, and reinforcement learning-based EMS. The results show that the optimization-based EMS with perfect foresight achieves the lowest costs. Although the reinforcement learning-based EMS performs slightly poorer, it operates independently of forecasts, which makes it attractive for practical applications. The ProHMo benchmarking framework is designed to equip researchers with a robust framework for developing, evaluating, and comparing different EMS, particularly those focused on optimization and data-driven control methods.

1. Introduction

The future of energy systems will rely significantly on renewable energy sources [1]. However, the inherent intermittency of power generation from solar and wind necessitates enhanced flexibility within energy systems to address these fluctuations. In combination with intelligent control, sector coupling emerges as a pivotal strategy in ensuring this flexibility [2]. The multi-energy systems on the district and building level can offer the desired flexibility. In this context, the utilization of Energy Management Systems (EMS) is central to harnessing the flexibility [3].

The current literature on EMS for building energy systems showcases a variety of control methods, use cases, and evaluation approaches. The EMS are primarily designed to optimize cost-effectiveness, energy efficiency, or user comfort. These systems are mostly equipped with components like Heat Pumps (HP)s, Photovoltaic (PV), Thermal Energy Storages (TES)s, and Batteries (BAT)s. Different studies introduce or compare EMS control methods like Model Predictive Control (MPC)-based optimization, Reinforcement Learning (RL), or Rule-Based (RB) control. Table 1 shows a selection of different EMS for building energy systems, their method, and how they are evaluated.

The diversity in analyzing and validating EMS strategies leads to challenges in comparing different EMS approaches, as observed by Blum et al. [13] and Drgoňa et al. [14]. Adding to this, Fischer et al. [4] raise concerns that many EMS get favorable evaluations by being benchmarked against poorly calibrated RB controllers.

Another difficulty arises in setting up simulation models to evaluate EMS [13]. It is essential to develop sophisticated simulation models that accurately reflect the complexity of building energy systems to compare EMS in a realistic environment. This requires significant effort and expertise, not only in creating models but also in ensuring the real-world utility of control outputs. A critical aspect of this process is the validation and verification of the models, which involves testing and comparison with measurements of real energy systems.

* Corresponding author.
E-mail address: d.zinsmeister@tum.de (D. Zinsmeister).

https://doi.org/10.1016/j.enbuild.2024.114648
Received 14 December 2023; Received in revised form 30 July 2024; Accepted 7 August 2024
Available online 12 August 2024

Table 1
Selective overview of EMS for building energy systems and the simulation tool they were evaluated with. ✓ indicate if the evaluation models are Open Access (OA) while the availability of the library as OA is denoted by ✓*.

Ref	Short description	Type	Evaluation model	
			Model	OA
[4]	Comparison of RB vs. MPC-based EMS for a building with common components.	RB & MPC	COLSIM	✗
[5]	Quantification of optimal control using a flexibility envelope on common building energy system components.	RB & MPC	MPC model	✗
[6]	Comparison of RB vs. nonlinear optimization for buildings with different heat and electricity generators and storages.	RB & MPC	MPC model	✗
[7]	Comparison of different optimal control objectives and parameters for a building with different heat and electricity generators and storages.	MPC	MPC model	✓
[8]	Comparisons of quadratic, nonlinear, and mixed integer nonlinear optimal control formulations and solver choices for a building with HP and variable room temperature.	MPC	*IDEAS*	✓*
[9]	EMS for heat generators and controllable thermostats, utilization the load shift potential of heating systems by providing setpoints for the room temperature.	RL	*IDEAS*	✓*
[10]	EMS that adjusts temperature setpoints to optimize user comfort while conserving energy.	RL	IESVE	✗
[11]	Comparison of RL models against the outcomes of an MPC model for a building equipped with different heat and electricity generators and storages.	RL	MPC model from [7]	✓
[12]	EMS designed for buildings equipped with PV, HP, and TES.	RL	ProHMo	✓

Considering these facts, there is a need to establish a common benchmarking framework for EMS of buildings. Such a framework should have the following properties:

- It allows realistic simulation of relevant building behavior affected by exogenous factors.
- Models are based on measurement data obtained from commercial hardware, are experimentally validated, and are computationally efficient.
- The framework is published under an open access license for reproducible EMS research.
- It calculates necessary metrics for validating and comparing different EMS control methods, such as total energy consumption and costs.
- It is user-friendly and allows for seamless development of EMS control methods to accelerate EMS research.

The framework should also include a control procedure that prevents comfort violations in the building and can overwrite setpoints. This is important for a close-to-reality analysis, as most users would not tolerate comfort violations resulting from malfunctioning EMS.

To the best of the authors' knowledge, no benchmarking framework is available that encompasses all requisite properties while incorporating crucial aspects of building energy systems. Addressing this, we introduce the ProHMo benchmark framework and simulation library, which replicates the commercial equipment in the Center for Combined Smart Energy Systems (CoSES) laboratory [15,16]. The ProHMo framework stands out for its comprehensive building energy system models, encompassing essential elements. This includes various experimentally validated component models for Heating, Ventilation, and Air Conditioning (HVAC), PV, and BAT. The HVAC components accurately replicate the dynamic behavior and internal control of commercial components, capturing intricate details often neglected in other libraries due to the complexity that requires experimental data. Moreover, key building parameters such as size, insulation, and age are included to accurately simulate heating, Domestic Hot Water (DHW), and cooling consumption.

Users have the flexibility to customize predefined building energy system models to suit their specific requirements. This involves selecting the necessary benchmark equipment, adjusting component or building parameters, and incorporating individual weather data information. The benchmarking process is versatile by providing building energy models as Functional Mock-Up Units (FMU)s, allowing different EMS approaches and programming languages. The framework includes code templates demonstrating the interface between the EMS and FMUs. This approach can be used to integrate and compare different EMS within the same framework.

The remainder of the paper is structured as follows: First, we present the state of the art in building energy system models and corresponding benchmarking frameworks (section 2). In Section 3 we introduce the ProHMo framework and the corresponding library. Then we present the experimental validation of the building model in the CoSES laboratory (section 4) and demonstrate the library for comparing different EMS control methods (section 5). In section 6 we discuss the strengths and limitations of the library and framework, before providing the conclusions in section 7.

2. State of the art

Fig. 1 provides an overview of existing simulation libraries for building energy systems as well as the corresponding extensions that enable benchmarking based on the underlying simulation libraries.

2.1. Simulation libraries

Three modeling languages are frequently used for simulating building energy systems: Modelica [17], EnergyPlus [18], and TRNSYS [19]. All three modeling languages support model export according to the Functional Mock-Up Interface (FMI) standard [20]. FMI is increasingly used in co-simulation [21] and ideal for benchmarking EMS.

Well-known open-access Modelica libraries for building energy systems include the IBPSA library [22] and its derivatives: Buildings [23], AixLib [24], BuildingSystems [25], and IDEAS [26]. The IBPSA library is a comprehensive tool for modeling building and community energy and control systems. It applies best practices in the field and offers a wide range of models. These include different HVAC systems and diverse energy storage types, such as TESs, boreholes, phase-change materials, and BATs. Buildings are modeled as detailed or reduced-order building models. The detailed building models contain information on the building envelope and model heat exchange mechanisms, such as heat transfer between rooms and the outside air and multi-zone airflow. The electrical system is modeled with two- and three-phase options for balanced or unbalanced systems. One difficulty when using IBPSA models is the lack of an internal control logic for HVAC systems, such as mechanisms to automatically shut down heat generators upon reaching maximum temperature. This may lead to unrealistic results (e.g., HPs heating water above $100\,°C$) and simulation errors when temperatures exceed the maximum limits of components.

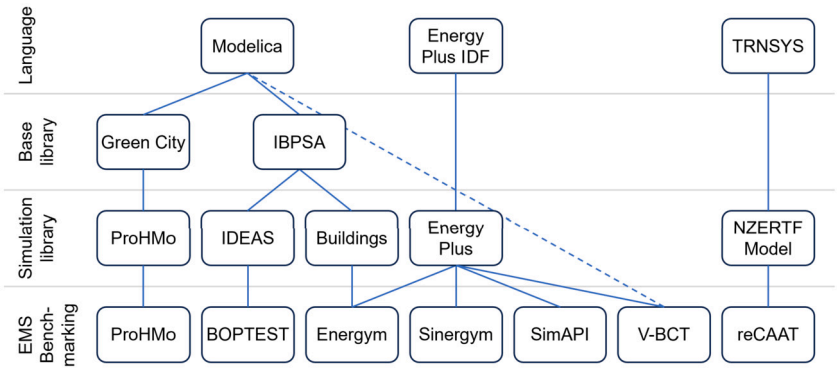

Fig. 1. Overview of frameworks to benchmark and train EMS.

Another Modelica-based simulation library for energy systems is the commercial GreenCity library [27,28]. Like IBPSA, it is tailored for planning and optimizing building and district energy systems and features detailed models for electric and thermal generation, distribution systems, storage, and consumption. GreenCity adopts a simplified approach to modeling the hydraulic system by neglecting pressure constraints and losses. This approach is viable for operating conditions with unidirectional flow, where pumps can always maintain the required flow rate. These conditions are typical for the heating system in buildings.

EnergyPlus is a comprehensive building energy simulation software including highly detailed models for heat and mass flow within the building energy systems [18]. Plugins like Honeybee [29] allow the integration of EnergyPlus into other building performance analysis tools. The software can handle complex interactions between different building energy systems and the building itself. It allows users to specify a parameter file with building parameters such as geometry, materials, and HVAC equipment and controls. These specifications, along with hourly weather data, enable EnergyPlus to simulate a building's energy performance realistically. The efficiency of the HVAC system is formulated with equations, which can be fitted to emulate commercial components, e.g., as done for different HPs [30]. It uses a fixed time step integration method with a minimum time step size of 60 seconds. This complicates modeling the dynamic behavior of commercial HVAC components, as the dynamic behavior cannot be described with simple equations and would require lower time step sizes.

TRNSYS [19] is a commercial software environment for simulating the behavior of transient systems. It is commonly used for detailed analysis and optimization of thermal and electrical energy systems. Users can create their own components or use existing, customizable component models of common equipment, such wind turbines, BAT and HVAC systems. Balke et al. [31] developed a simulation model of the Net-Zero Energy Residential Test Facility (NZERTF), a four-bedroom residential building with a simulated occupancy of four people. The simulation model includes components for HVAC, water heating, solar PV, and other equipment.

2.2. Benchmark frameworks

The increasing interest in advanced control methods for building energy systems and the need for training models for RL-based EMS led to several benchmarking frameworks. Each benchmarking framework is based on one or several simulation libraries for building energy systems.

The BOPTEST framework [13] is based on the IDEAS library [26]. It includes a baseline and backup control that can overwrite EMS setpoints if the user's comfort is violated. The containerized run-time environment facilitates rapid and repeatable deployment of building emulators representing various system configurations. Key Performance Indicator (KPI)s can be generated as a postprocessing step to compare different EMS.

Other benchmarking frameworks focus on the training and testing RL algorithms, adhering to the Gymnasium API standard. Energym [32] and Sinergym [33] include detailed building energy system models. Sinergym uses EnergyPlus models while Energym provides different simulation models based on the Buildings library [23] or EnergyPlus [18]. This allows users to select models based on their research focus. EnergyPlus offers detailed building consumption models and the Buildings library includes detailed models for the HVAC system. A unique feature of Sinergym is that randomness can be added to the weather data of different zones.

SimAPI [34] and the V-BCT framework [35] are co-simulation interfaces for building energy systems. SimAPI facilitates interaction between calibrated EnergyPlus building models and cloud-based control algorithms. V-BCT uses the open-source platform VOLTTRON [36] to integrate data, devices, and systems for testing control applications. Its capabilities are shown in a case study with an EnergyPlus model, but it also allows other modeling libraries. A special feature of the framework is that it can consider the delay of new setpoints, which may be caused by the execution time of control sequences. reCAAT [37] consists of a simulation manager that links custom control algorithms, user setpoint preferences, electricity pricing information, and weather data with a simulation model and calculates basic KPIs during postprocessing. The simulation model is based on the NZERFT TRNSYS model [31] and coupled to an external control algorithm with a custom TRNSYS type using socket communication.

Table 2 provides a comparative analysis between the ProHMo framework and the other benchmarking frameworks presented in this section. It is observed that only ProHMo and reCAAT offer a complete and close-to-reality description of building energy systems, including the DHW consumption and providing realistic component behavior. They are also the only two frameworks that comprise experimentally validated models. Regarding realistic component modeling, many popular frameworks are lacking in their representation of commercial components, such as HVAC, by neglecting their dynamic behaviors and considering only the efficiency data. The scarcity of detailed information and the variance in internal controls across different manufacturers further complicate accuracy in modeling dynamics. Extending the realism considerations, an optional backup controller to prevent consumer comfort violations is only available within ProHMo and BOPTEST among the compared frameworks. Beyond these metrics, the utility of a framework can be improved by options to customize the components, standardization of KPIs, and being made open access.

3. The ProHMo benchmarking framework

The ProHMo library was initially introduced in [38] and is accessible via the ProHMo GitLab repository.[1] It was originally designed as a digital twin of the CoSES laboratory, to examine and refine control

[1] https://gitlab.lrz.de//energy-management-technologies-public//coses_prohmo.

Table 2
Comparison of different benchmarking tools for EMS.

	DHW consumption	realistic component behavior	experimentally validated models	backup control	customizable components	standardized KPI calculation	open access
ProHMo	✓	✓	✓	✓	✓	✓	✓
BOPTEST	✗	(✓)[1]	✗	✓	✗	✓	✓
Energym	✓	(✗)[1,2]	✗	✗	(✗)[3]	(✓)[4]	✓
reCAAT	✓	✓	✓	✗	✗	✓	✗
Sinergym	✓	(✗)[5]	✗	✗	✓	✗	✓
SimAPI	✗	(✗)[5]	✗	✗	(✗)[3]	✗	✓
V-BCT	✗	(✓)[1]	✗	✗	(✗)[3]	✗	(✓)[6]

[1] no replication of dynamic behavior of commercial components.
[2] Modelica models use first-order approximations of building envelopes with constant zone temperature limits.
[3] only by changing EnergyPlus file.
[4] no KPIs for total energy consumption and costs.
[5] no information on HVAC system.
[6] github link is expired.

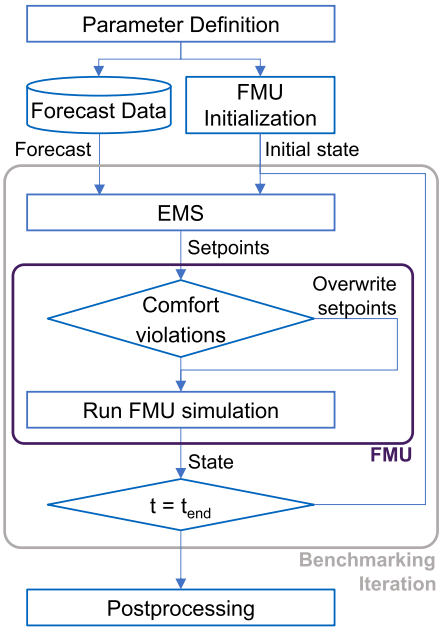

Fig. 2. Schematic representation of the communication template that interacts between EMS and FMU.

strategies before experiments. Therefore, it allows an easy transition between simulation studies and experiments. The work on the ProHMo library models has shown that accurate modeling of the dynamic behavior of commercial hardware cannot be done with generic models, which are common in simulation tools. Although the ProHMo library does not cover every commercial component comprehensively, it demonstrates a process that modelers and practitioners need to follow.

The ProHMo benchmarking framework uses building energy system models that are experimentally validated using the components of the CoSES laboratory [15,16], providing co-simulation models as open-access FMUs. To facilitate the adoption of the benchmarking framework, we offer an easy-to-use code template, available on our GitLab repository.[2] this template aims to streamline the simulation environment setup with a communication interface and postprocessing tool. The structure of the code template is shown in Fig. 2.

The first step in the benchmarking framework involves its parametrization. Users can choose from a set of existing files containing pricing, weather, and forecast data, or provide paths to their own files. Furthermore, users can define the benchmarking period, the control and prediction horizon length used by the EMS control method, and whether the backup control should be activated. To accommodate diverse user requirements and enhance flexibility, multiple model parameters can be adjusted as listed in Appendix A.1.

After defining the parameters, the framework loads forecast data and initializes the FMU. The initial state and the forecast data for the next prediction horizon are provided to the EMS, which generates setpoints sent to the FMU. If the backup control is activated and detects any comfort violations, it overwrites the setpoints of the EMS. After completing the simulation over the control period duration, the EMS receives the updated state and the forecast information for the subsequent iteration.

At the end of each simulation run, the postprocessing phase computes KPIs, such as:

- Total energy costs ($C_{op,tot}$).
- Cumulative energy consumption (E_{tot}).
- Computation duration of the EMS (t_{comp}) and simulation duration (t_{sim}).
- Number of starts (n_{starts}) and operational duration (t_{op}) of heat generators.
- Charge cycles of the BAT ($n_{BatCyle}$).
- Heating (dc_{heat}), cooling (dc_{cool}), and DHW discomfort (dc_{DHW}) metrics, which are defined in Appendix B.

These KPIs are stored in an output file with the relevant simulation results as a time series. The simulation results include the target and actual setpoints, State of Charge (SOC) of the storage units, and power demand and generation. This file enables further postprocessing and graphical representation of the results.

3.1. ProHMo simulation library

Fig. 3 displays a building energy system model of ProHMo. Users can customize the components and environment settings according to their preferences. The default parameters, detailed in Appendix A.1, correspond to the equipment used in the CoSES laboratory.

The modulation or power setpoints serve as input signals for the different components, with their specific signals and ranges detailed in Appendix A.2. When a user chooses the RB control or the backup control is active and in overwrite mode, a switch function alternates between the user-defined input signal and the RB control setpoint for the control signals.

All buildings include one or more heat generators, in this case, a Solar Thermal Panel (ST) and an Air Source Heat Pump (ASHP) with an auxiliary electric heating rod. The reversible ASHP can provide heating and cooling. In cooling mode, the distribution system bypasses the TES. During heating mode, the ASHP is connected to the TES and alternates

[2] https://gitlab.lrz.de/energy-management-technologies-public/coses_prohmo/-/tree/main/CodeExport/FMIModels.

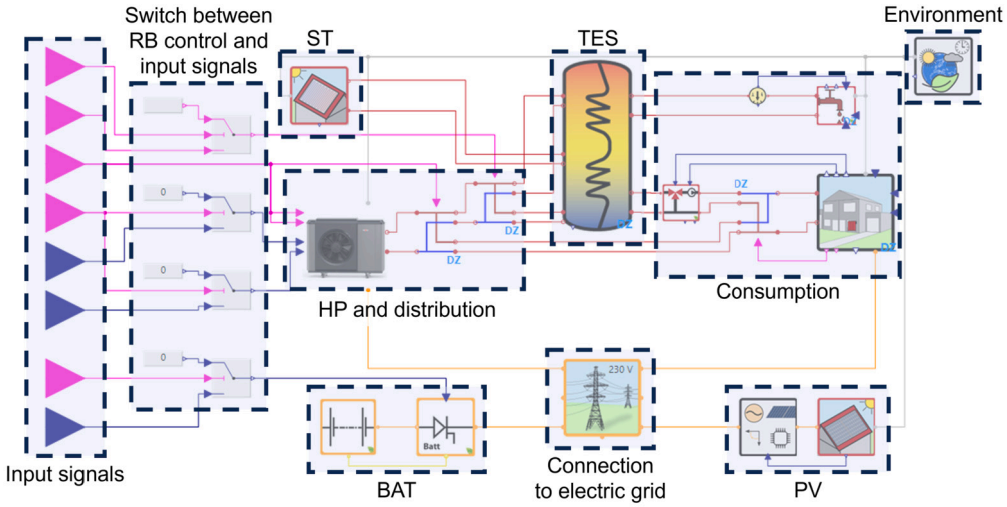

Fig. 3. Modelica model of a building energy system with different components and its input interface.

CoSES ProHMo based on Green City	**Generators** - look-up table-based models - based on measurements from CoSES **TES** - one-dimensional, layered TES model, - adapted from GreenCity - parametrized with CoSES measurements **Consumption** - building model adapted from GreenCity - DHW consumption based on DHWcalc [39] **Environment** - weather of Munich[1] - adaptable environmental files

[1] Weather data courtesy of the Meteorological Institute Munich

Fig. 4. ProHMo structure: Green marks the newly developed generator models, blue the adapted models from GreenCity. (For interpretation of the colors in the figure(s), the reader is referred to the web version of this article.)

between distributing heat to the top section DHW and the bottom section for space heating. The stratification within the TES allows the ASHP to operate at varying temperature levels, taking advantage of lower temperatures to ensure efficient operation. Electricity for the building and the ASHP can be provided by the electric grid, the PV system, or the BAT. Excess electricity is fed back into the grid or stored in the BAT.

The components of the ProHMo library can be structured as shown in Fig. 4. Several components are based on the GreenCity library [27,28], which delivers precise simulation models for generic building energy systems and a user-friendly modeling approach.

Heat generator models

The accurate capture of commercial components behavior is ensured in ProHMo through the new heat generator component library. The models are built using components from the Modelica Standard Library (MSL), allowing seamless integration into other Modelica-based simulation libraries. Their behavior is defined by lookup tables, created based on characterization measurements conducted in the CoSES laboratory. The steady-state efficiency is calculated using lookup tables and depends on the water inlet temperature, source temperature (for HPs), and modulation setpoints.

Beyond static behavior, the ProHMo models also capture dynamic behavior through lookup tables containing time-dependent data acquired from measurements in the CoSES laboratory. Moreover, the models have internal controls, such as automatic shutdown mechanisms to prevent overheating damage. Without these internal controls, the simulations would provide unrealistic results when temperature thresholds are exceeded.

Consumption models

The heat consumption is modeled using the 3-zone building model of the GreenCity library. General parameters such as total living area, year of construction, layout, and window type are incorporated using a method described by Loga et al. [40]. The model is slightly adapted to reproduce typical heating system return temperatures. The introduction of variable room temperature setpoints allows the heating system model to be used for active demand response. In addition, a DHW consumption model is implemented, which is based on stochastic demand profiles of DHWcalc [39] and checks whether the DHW temperature is above the set minimum temperature. The consumption models are also used for Power Hardware in the Loop (PHIL) experiments in the CoSES laboratory [16], allowing an easy transition between simulation and experiment.

3.2. Backup control

We provide a backup control to safeguard against comfort violations arising from incorrect or missing setpoints of the EMS. This backup system is designed as a RB control, mirroring the design of common RB control systems found in modern buildings. Therefore, it can serve as a baseline benchmark for evaluating the performance of EMS. Since this backup control can impact the performance of different EMS, users can deactivate it in the parameter definition. For example, deactivation may be necessary to train RB EMS or to evaluate the performance of EMS without any assistance.

Table 3 shows the parameters for the ASHP and the auxiliary heater. Control parameters for the other components and buildings are described in the GitLab documentation. The heat generator is activated or deactivated based on the TES temperature at different layer heights ($T_{TS,x}$, where 'x' marks the layer, 1 is the bottom layer, 10 is the top layer). To save energy, the heating criteria only apply during the heating season while DHW remains a year-round necessity.

4. Library validation

The experimental validation of the ProHMo library evaluates the accuracy of the commercial heat generation and storage components and compares them to the other simulation libraries. By analyzing the system

Table 3
Parameters of the RB control.

Device	On criteria	Off criteria
ASHP	$T_{TS,9} < T_{DHW,min}$	$T_{TS,7} > T_{DHW,min} + 5\ K$
	$T_{TS,4} < T_{heating,min}$ [1]	$T_{TS,2} > T_{heating,min} + 5\ K$ [1]
Aux. Heater	$T_{TS,9} < T_{DHW,min} - 5\ K$	$T_{TS,7} > T_{DHW,min}$
	$T_{TS,4} < T_{heating,min} - 5\ K$ [1]	$T_{TS,2} > T_{heating,min}$ [1]

[1] only during heating season.

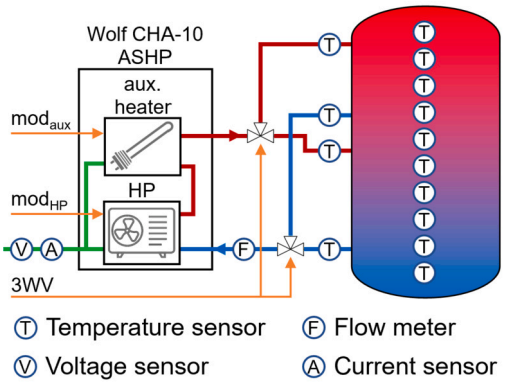

Fig. 5. Schematic representation of the experimental setup featuring the Wolf CHA 10 ASHP connected to the TES with two 3WVs that can switch between the upper and lower segments of the TES.

behavior, we gain additional insights into the interaction of the components that might not be evident when validating them separately. We present in this publication a system with an ASHP and a TES. HPs will be key in decarbonizing future building energy systems with decentral heat generation [41,42], with ASHPs being the most common type installed [42]. A TES can provide flexibility in the future energy system, allowing it to charge and discharge according to electricity prices [43,44]. The library further encompasses experimentally validated HVAC component models and systems with alternative component configurations, which are not included to prevent repetition.

4.1. Experimental setup

Fig. 5 illustrates the schematic representation of the experimental setup within the CoSES laboratory. The experiment encompasses a 10 kW Wolf CHA 10 ASHP and a 785 l Wolf BSP-800 TES. In the figure, the orange arrows show the control signals: the position of the 3-Way Valves (3WV) and the modulation of the ASHP (mod_{HP}) and auxiliary heater (mod_{aux}). The red and blue lines denote warm supply and cold return pipes respectively, while the green line signifies the electric connection. The heat exchange is measured by temperature sensors (T) positioned in the supply and return line, and volume flow meters (F). 10 temperature sensors are uniformly dispersed across the TES surface to measure its temperature distribution and located between the exterior wall and the thermal insulation. The electric power is monitored by voltage (V) and current sensors (A) on each phase. The attributes of these sensors are detailed in Appendix C. The data is measured and processed as described in [16] with a resolution of 1 second.

We use two 3WVs to connect the ASHP and the TES, which has a total height of 1.75 m. This allows the use of the stratification of the TES for heat extraction, either for DHW at the top or space heating at the bottom. The supply line is connected to ports at heights of 1.43 m and 0.63 m, while the return line extracts from ports at 1.03 m and 0.26 m.

The ASHP can provide both heating and cooling. It operates with modulating capabilities ranging from 20% to 100% of its power output (10 $kW_{heat/cold}$), with efficiency rising at reduced modulation. It is equipped with an additional 9 kW auxiliary electric heater, which can be activated in three steps if the HP power is not sufficient.

4.2. Experiment results

To capture the behavior of the ASHP and TES in diverse operational conditions, we use varying air temperatures (T_{air}) and variable setpoints for the modulation of the ASHP, auxiliary heater, and the 3WV. We divide the validation into two intervals: the first interval represents a cold environment triggering deicing and the second interval represents milder air temperatures. Given that most ASHP models from other libraries do not model cooling, we omitted this aspect for our validation. The specific setpoints and temperatures are defined before the experiment and shown in Fig. 6.

Fig. 7 illustrates the operational dynamics of the ASHP, which meets the modulation setpoints well. During start-up and whenever the 3WV switches, a brief draw of heat can be noticed that is required to flush cold water from the pipes and the system. Furthermore, the Coefficient of Performance (COP) drops with rising TES temperature, which is not mitigated by the rising air temperature at the later state of the experiment. Notably, the efficiency sharply declines when the auxiliary heater is engaged, marked by red circles on the efficiency graph. This shows the importance of a well-controlled system to prevent reduced efficiency.

ASHPs require deicing measures during prolonged low ambient temperature conditions to remove ice buildup from the ASHP's outdoor unit to maintain optimal performance and efficiency in cold conditions. The top right graph in Fig. 7 shows the electric and thermal power during this process. Typically, deicing is automated and managed by the ASHP's internal control system. The most common method employed by modern ASHPs involves temporarily reversing their operational cycle. This reversal heats the outdoor unit, melting the ice. However, it also draws heat from the heating system. Integrating a small TES is essential to mitigate any comfort issues during this process. Deicing measures can have considerable influence in cold climates, as they reduce the overall efficiency of the ASHP.

The TES behavior is presented in Fig. 8, indicating low stratification due to the low temperature difference between the ASHP's supply and return, which is set at 5 K. Significant stratification can only be achieved between the upper and lower sections of the TES when only the upper section is heated, as observed around 5:00. This can be achieved by controlling the 3WV accordingly.

The TES shows fluctuations for the layer temperatures between 0:50 and 1:10 after the high TES inlet temperature during the operation with the auxiliary heater and the subsequent cold inlet temperature during deicing. The likely cause of these unwanted fluctuations is internal currents triggered by the high-temperature difference in the inlet flow.

4.3. Model comparison

The ProHMo simulation model is compared to models from IDEAS and GreenCity. IDEAS is selected to represent the IBPSA library and because it forms the basis for the BOPTEST framework. GreenCity is chosen as the ProHMo predecessor, allowing a direct assessment of the library's improvement. The simulation models of all libraries are set up to represent the building energy system shown in Fig. 5. The TES is modeled as a stratified storage with 10 layers, where the ASHP connects to the first and fifth layers for heating and the sixth and ninth layers for DHW. Table 4 specifies key model and input parameters used for the model comparison. To ensure comparability between the experiment and simulations, the temperature information and the control setpoints for the ASHP and 3WV are the same as in the experiment, shown in Fig. 6.

Like ProHMo, the ASHP models from GreenCity and IDEAS utilize lookup tables to calculate thermal and electric power. These look-up tables are parametrized to represent the behavior of the Wolf CHA 10 ASHP. The models are further calibrated to lower overall discrepancies to the experimental results. Originally, the ASHP models from both libraries were designed for temperature setpoints, calculating the mod-

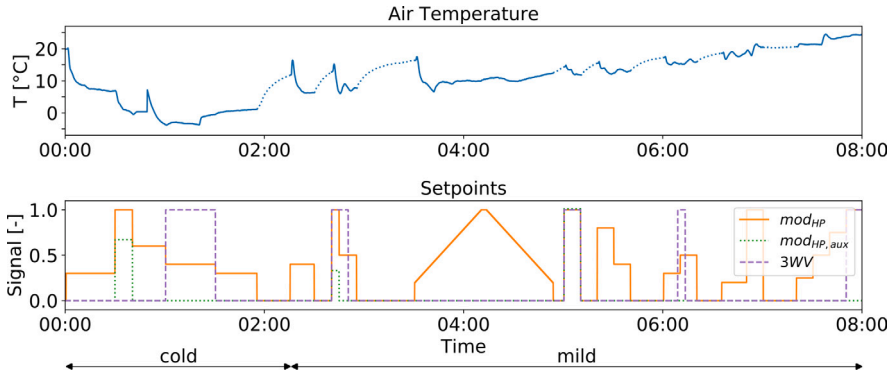

Fig. 6. The air temperature emulates a cold and mild environment. The dotted trajectory indicates periods when the ASHP is inactive, resulting in a temperature rise due to heat exchange with the environment. The control setpoints for ASHP and auxiliary heater modulation (mod_{HP}, $mod_{HP,aux}$) and 3WV are shown in the bottom diagram. The 3WV can alternate between heating the upper segment (1) and the lower segment (0).

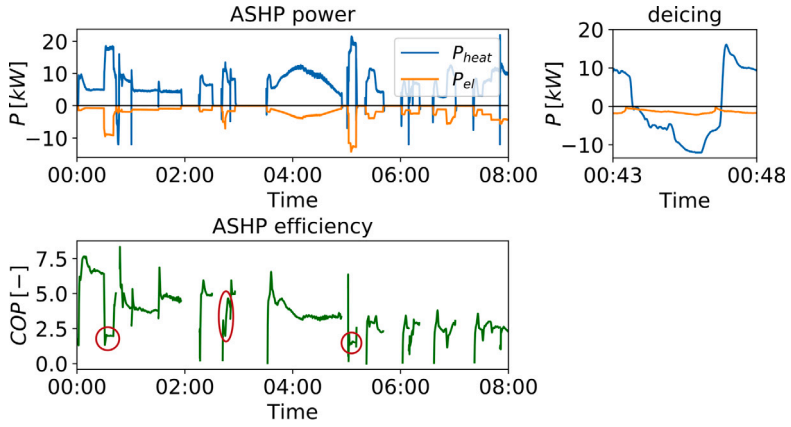

Fig. 7. Power profile and efficiency of the ASHP during the experiment. The top right graph zooms into the power profile during deicing.

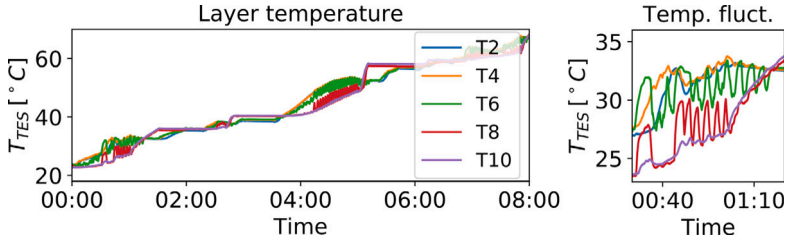

Fig. 8. Temperature distribution and SOC of the TES. The top right graph zooms into a period with high temperature fluctuation.

Table 4
Key model and input parameters.

ASHP		TES	
heat output	$P_{heat} = f(mod_{HP}{}^{1}, T_{air}, T_{ret})$	volume	$V = 785\ l$
efficiency	$COP = f(mod_{HP}{}^{1}, T_{air}, T_{ret})$	diameter	$D = 0.79\ m$
control input	mod_{HP}	number of layers	$n = 10$
	mod_{aux}	DHW connection	$n_{in} = 6, n_{out} = 9$
	$3WV$	heating connection	$n_{in} = 1, n_{out} = 5$
env. input	T_{air}		

[1] only for ProHMo and IDEAS.

ulation setpoint as a function based on the current and set temperature. However, state-of-the-art commercial HPs uses modulation setpoints, simplifying their integration into EMS. We have updated the models to accommodate power modulation setpoints directly and a fixed temperature difference between inlet and outlet water flow, keeping the original structure otherwise to conduct an unbiased comparison between the libraries. The modified models and the validation results are available online [45].

The key distinction in the IDEAS heat generator models is their absence of internal control behavior. This includes dynamic behavior during start-up, steady state, and deicing, as well as shutdown mechanisms when maximum temperatures are reached. In contrast, the GreenCity heat generators model dynamics as proportional transmission behavior with 1st order delay, including shutdown mechanisms. However, they do not account for varying efficiency during part-load operations.

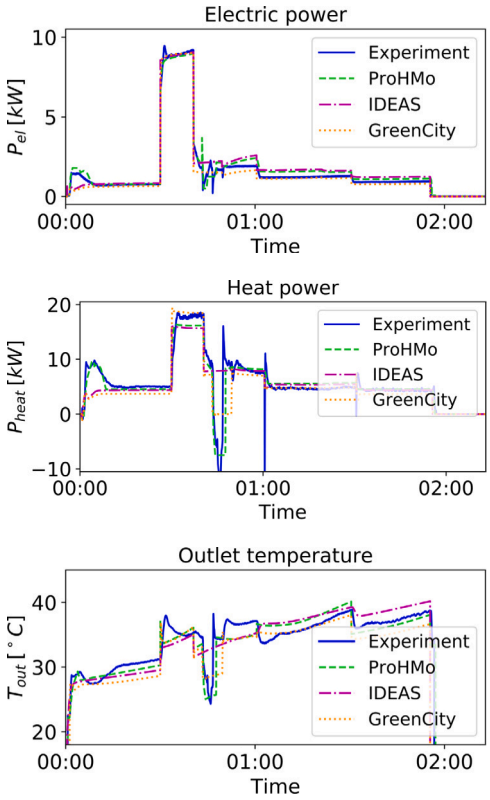

Fig. 9. Comparison of experimental measurements and simulation results of the electric power consumption (top), heat output (middle) and outlet temperature (bottom) of the ASHP for the cold environment.

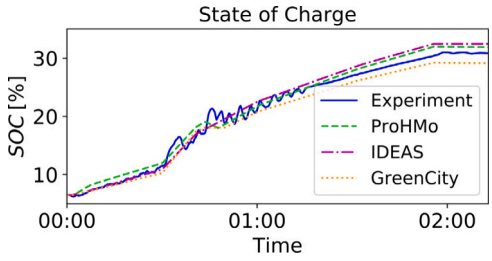

Fig. 10. Comparison of experimental measurements and simulation results of the TES SOC.

4.4. Validation results

4.4.1. Validation of input and output power

The top graphs in Fig. 9 present the electric and heat power of the ASHP. During steady-state operations from 0:10 to 0:35 and 1:00 to 2:00, the ProHMo and IDEAS models exhibit identical power behavior. In contrast, the GreenCity model shows a lower heat generation during part-load conditions, as it does not account for varying part-load efficiencies.

We can further see that both the IDEAS and GreenCity models fail to replicate the dynamic behavior during the start-up phase from 0:00 to 0:10. This behavior is mainly influenced by the ASHP's internal control and is difficult to anticipate without experimental testing. Moreover, the IDEAS model continues to generate heat throughout the ASHP's deicing process from 0:45 to 0:50.

4.4.2. Temperature and state of charge

These discrepancies in the IDEAS and GreenCity models result in less precisely replicating the temperature curve (bottom graph in Fig. 9). The IDEAS model overestimates the temperature by heating up the TES during deicing, whereas the GreenCity model underestimates temperatures, producing less heat during part-load operations. The ProHMo model, on the other hand, shows a more accurate simulation of the temperature behavior. Similar behavior can be seen when analyzing the SOC of the TES in Fig. 10.

Between 0:50 and 1:10, all models exhibit deviations in temperature behavior. This can be explained by the behavior of the layer temperatures of the TES illustrated in the bottom graph in Fig. 8. These fluctuations are caused by internal flows and cannot be replicated in the one-dimensional TES model. However, such fluctuations are rare and short-term events.

4.4.3. Validation metrics

The performance of the ProHMo, IDEAS, and GreenCity simulation models is evaluated using the Coefficient of Variation of the Root Mean Square Error (cv(RMSE)) and Normalized Mean Bias Error (NMBE) between experimental measurements and simulation results. These metrics are chosen for their capacity to standardize comparisons across units and their ability to quantify the direction and extent of model biases. The coefficients are calculated in equation (1) and (2).

$$cv(RMSE) = \frac{1}{\bar{Y}} \cdot \sqrt{\frac{\sum_{i=1}^{n}(Y_i - \hat{Y}_i)^2}{n}} \cdot 100 \tag{1}$$

$$NMBE = \frac{\sum_{i=1}^{n}(Y_i - \hat{Y}_i)}{\sum_{i=1}^{n} Y_i} \cdot 100 \tag{2}$$

The evaluation encompasses four primary parameters in two temperature conditions: cold and mild. The results are detailed in Table 5. The ProHMo model demonstrates moderate cv(RMSE) values for electric and thermal power, suggesting an acceptable agreement with experimental data, particularly in cold temperatures. Notably, it maintains a consistently low cv(RMSE) for output temperature and SOC, implying a high accuracy level. Despite this, the NMBE indicates a tendency of ProHMo to underestimate electric power. This occurs for all models when auxiliary heating is active, as observed in Fig. 9, and is likely due to manufacturing tolerances of the electric heating rod.

Meng et al. [46] and Manfren et al. [47] use NMBE and cv(RMSE) thresholds of 10% and 30%, respectively, for hourly building energy data as per the ASHRAE Guidelines 14:2014 [48]. Although our data resolution is higher (secondly), the ProHMo model adheres to these ranges for most parameters, affirming its accuracy.

In contrast, the IDEAS model exhibits increased cv(RMSE) values in several parameters, with a pronounced disparity during mild temperature and frequent activation and deactivation of the ASHP. This deviation is primarily due to the model's missing representation of the dynamic behavior.

The GreenCity model shows the highest cv(RMSE) values, suggesting a significant deviation from the measured data, especially for heat power and output temperature under mild temperatures. The main limitation arises from the model's structure, which calculates efficiency and power consumption based only on the return temperature while disregarding the influence of power modulation. This inherent structural limitation constrains the model's calibration capabilities and would require substantial structural alterations to achieve lower errors. This underlines the importance of correctly incorporating part-load behavior.

5. Case study: benchmark of energy management systems

This section shows an example EMS comparison to demonstrate the ability of the ProHMo benchmark framework to train, tune, and evaluate different EMS algorithms. The comparison involves the RB control described in section 3.2, an MPC-based EMS, and two RL-based EMS. The MPC based linear optimization problem can differentiate between high-temperature heat for DHW and low-temperature space heating and relies on load, weather, and price forecasts. The RL-based EMS is based

Table 5
cv(RMSE) and NMBE between experimental measurements and simulation results in percent.

Model	Metric	$P_{el,HP}$		$P_{heat,HP}$		$T_{out,HP}$		SOC_{TES}	
		cold	mild	cold	mild	cold	mild	cold	mild
ProHMo	cv(RMSE)	17.9	27.7	37.1	32.8	8.2	11.4	5.0	3.2
	NMBE	-8.7	5.0	2.9	0.4	0.9	2.2	-2.8	0.6
IDEAS	cv(RMSE)	25.2	52.3	52.4	49.3	13.7	25.8	6.0	1.8
	NMBE	-12.1	-2.8	2.0	7.5	0.5	3.7	-3.2	-2.1
GreenCity	cv(RMSE)	18.7	57.1	48.7	50.8	14.4	43.9	6.1	2.5
	NMBE	9.4	23.4	13.8	6.8	5.4	16.8	4.8	4.4

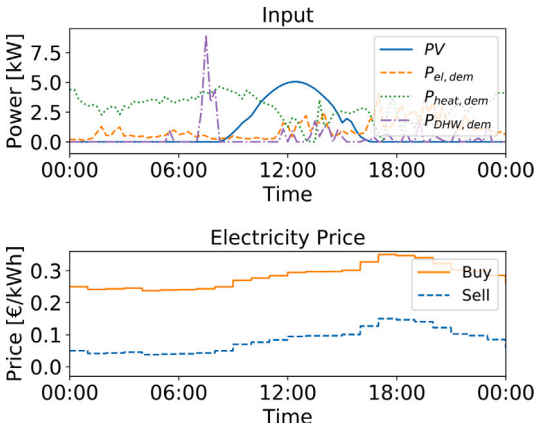

Fig. 11. Time series of demand and PV production (top) and electricity prices (bottom).

```
Simulation time: 127 s
Computation time (EMS): 18 s
Final results:
    Total costs                 636.08 EUR
    Total energy use            1515.44 kWh
    discomfort (heating)        0 K h
    discomfort (cooling)        0 K h
    discomfort (DHW)            0 K l
    HP (number of starts)       358
    HP (operation time)         573.6 h
```

Fig. 12. Screenshot displaying the KPIs of the MPC-based EMS.

on Ludolfinger et al. [12] and does not require forecasts. An additional hybrid approach combines the RB and RL approach, where the RB control ensures comfort requirements, while the RL agent aims at minimizing costs. The different EMS approaches are described in detail in Appendix D.

The comparison is conducted as described in section 3 with the model parameters of Appendix A.1. We employ a variable electricity tariff based on day-ahead prices in Germany, including a levy of 0.20 $€/kWh$ for buying electricity. Fig. 11 shows the inputs and prices for the first day.

5.1. General results

A screenshot of the KPI calculation is presented in Fig. 12 for the MPC-based benchmark simulation conducted in January 2022. Table 6 compares the results of all EMS, where the MPC-based control exhibits the lowest costs and energy consumption. Although the RL-based EMS perform slightly worse than the MPC-based EMS, they are not dependent on the quality of the forecasts, which makes them more robust.

Table 6
Comparison of different EMS.

Algorithm	$C_{op,tot}$	E_{tot}	t_{op}^{ASHP}	n_{starts}^{ASHP}
RB EMS	100%	100%	449.7 h	419
MPC based EMS	93.4%	95.8%	567.0 h	381
RL based EMS	96.4%	98.6%	573.8 h	993
RB+RL based EMS	97.3%	98.1%	492.4 h	460

5.2. Comparison of setpoints

To further compare the different EMS approaches, we analyze their setpoints during the first 24 hours as shown in Fig. 13. During the case study, the backup control was active, which sometimes resulted in the EMS setpoints being overwritten. However, this backup control can also be deactivated, as described in section 3.2.

The RB control frequently activates the HP and occasionally necessitates the use of the auxiliary heater. In contrast, the other control algorithms avoid the auxiliary heater entirely and ramp up heat production when excess PV energy is available. However, as this raises the TES temperature and thus diminishes the COP, not all surplus PV output is channeled into heat generation — a behavior that would be difficult to implement in a standalone RB control.

The MPC-based EMS and the hybrid EMS enhance the efficiency of the ASHP by modulating the setpoint. The MPC-based EMS uses this to reduce the number of starts and prolong the operation. This approach ensures smoother operation and mitigates stress, minimizes start-up losses, and benefits from the increased COP at low modulation.

Both the MPC and RL-based systems demonstrate precision in controlling the ASHP, requiring only minimal safeguard interaction of the RB control. This precision is crucial for the MPC-based system, given the 24-hour interval that we assumed for generating new setpoints. An unexpected activation of the ASHP elevates the TES temperatures, subsequently decreasing the COP of the ASHP.

5.3. State of charge

Comparing the SOC of the TES in Fig. 14 shows that the RB control maintains the TES at its lowest temperatures. It activates the ASHP only when essential due to too low TES temperatures. In contrast, the alternative EMS strategies result in a heightened SOC. This elevation is typically desirable to capitalize on periods of surplus PV power or low electricity rates. Yet, this might also arise from model inaccuracies that over- or underestimate power generation. Careful tuning of the controllers with the help of the proposed benchmark model can mitigate such discrepancies.

6. Discussion

The ProHMo library provides an environment for software-agnostic benchmarking of EMS with its open-access FMUs of building energy systems. The main focus of the framework is on the thermal systems, with particular attention to heat generator and TES models, which have been experimentally validated in this paper. Electric components, including PV and BAT systems, are based on the detailed models of the

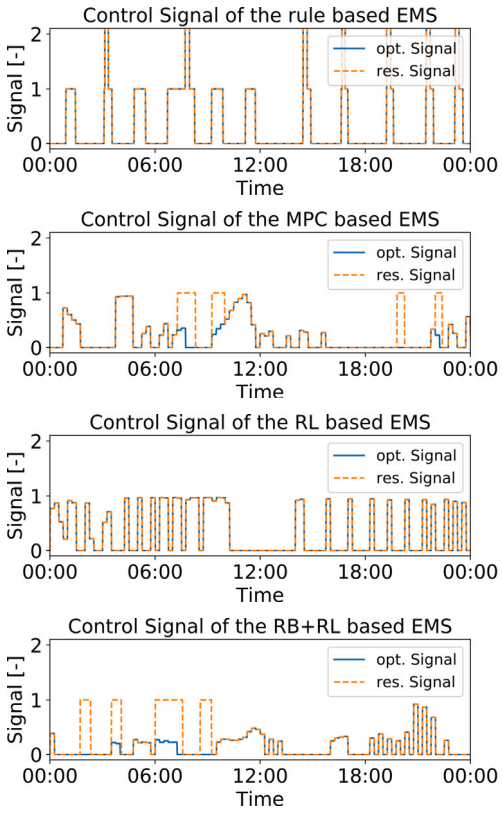

Fig. 13. Control setpoints of the different EMS. The setpoints of the ASHP (res. Signal) are the same as the setpoints from the EMS (opt. Signal), except if the backup control overwrites it.

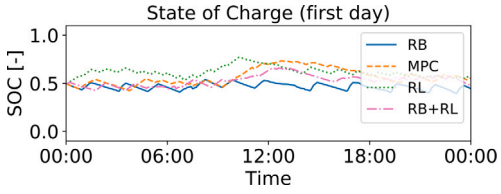

Fig. 14. SOC of the TES for the different control strategies.

commercial GreenCity library. As the main focus of the framework is on thermal systems, we did not validate the electric components. The FMUs include parameters that allow users to customize component sizes to their specific needs. Furthermore, integrating a code template serves to streamline benchmarking, enhancing user accessibility. Although the ProHMo library exhibits numerous strengths, it also faces certain limitations due to its design.

Black box nature of the benchmark framework - Its foundation on the commercial GreenCity library and the 'black box' nature of FMUs limits the flexibility to analyze and alter component and building energy system models. This also restricts transparency, as many users cannot open the model to check certain behaviors or the arrangement of actuators and sensors. We export all relevant model parameters and internal measurements to mitigate these limitations. The position and names of components, actuators and sensors can be checked in the CoSES documentation, e.g., for the TES [49]. These measures enhance both transparency and control.

To improve the scalability and generalizability of the ProHMo framework, users can modify relevant parameters during preprocessing. This includes adjusting building parameters such as size, insulation, or occupancy, which updates all corresponding building parameters. Additionally, users can provide customized weather data to simulate diverse climates and geographical locations. However, modifications to the components of the heating system, particularly the heat generator, may result in inaccuracies since these models are based on commercial hardware of specific sizes, as discussed in the next point.

Specific commercial hardware - Another limitation concerning scalability arises from the representation of specific commercial hardware installed in the CoSES laboratory. These models might not fully capture the operational behaviors of similar products from different manufacturers. While users can vary the size of HVAC equipment by applying scaling factors, this should be done only when absolutely necessary. Scaling these components by large factors is likely to result in unrealistic behavior, as components of different sizes often have different dynamic behavior. Nonetheless, such specificity is essential for realistically modeling systems incorporating commercial hardware. Moreover, the models demonstrate an approach that can be followed to design models of commercial components accurately. Using experimental data, we highlight the benefits of these tailored models.

Unidirectional, pressure independent flow - The ProHMo library deliberately simplifies certain heating system aspects to improve computational efficiency and model clarity. It does not simulate the spatial distances between components or pressure dynamics within the hydraulic network. This simplification is based on the observation that these factors have a minimal effect on the system's functionality. Heating systems generally have unidirectional flows and their pumps can maintain prescribed flow rates. The validity of this modeling approach has been confirmed in the experimental validation.

Perfect foresight during case study - The code template and the case study showcased in this paper employ perfect forecasts for prices, weather, and energy consumption. While price information is likely to be accurately known to users beforehand, weather and energy consumption forecasts are typically subject to some degree of error. While this paper does not address the impact of such prediction errors, future work could explore this aspect. One possibility is to employ different forecasting methods or use historical forecasts like those presented by Yang et al. [50].

Consumption model with three zones - The consumption models abstract the building into three thermal zones to optimize computational efficiency. While this simplification speeds up the simulation process, it does not portray the intricacies of individual room heating behaviors. Consequently, EMS relying on room-specific thermostat regulation may require further adaptation or replacement of the building model to achieve accurate demand-side management simulation. Furthermore, if researchers aim to design specific EMS for more complex building layouts, they will need to create individual models of those buildings.

7. Conclusion

The diversity in analyzing and validating EMS for building energy systems strategies introduces challenges in comparing different EMS. Therefore, this paper presents the ProHMo benchmark framework designed to evaluate EMS. The framework accurately represents building energy systems and their commercial components. Additionally, a code template is provided to facilitate the benchmarking test. This template manages the interaction between the EMS and the software-agnostic, open-access FMU of the building energy system. It handles postprocessing tasks, encompassing basic KPI calculations.

While most frameworks rely on generic models, these often fall short in accurately replicating the dynamic behavior of commercial components. However, this dynamic behavior should not be neglected when evaluating EMS. The ProHMo library showcases that precise representation of commercial hardware necessitates customized models and exemplifies the process of providing these models. This realistic setup includes a backup control system to prevent user discomfort arising from incorrect EMS setpoints. Experimental validation of the building energy system components verified the correct behavior of their models and the advantage compared to models of other simulation libraries.

The ProHMo framework is designed to enable the comparison of different EMS algorithms within real-world data and scenarios. By incorporating models of commercial hardware, real-world weather data, and price information alongside accurate building energy models, the framework provides a comprehensive platform for conducting detailed and realistic assessments. While the presented case study illustrates how the ProHMo framework can effectively compare EMS algorithms, its utility extends beyond this initial demonstration.

Future research endeavors could focus on more detailed case studies utilizing the ProHMo framework with real-world data and scenarios. Beyond the comparative analysis of EMS approaches, investigations could explore nuanced practical implications. These could encompass assessments of forecast accuracy, the generalizability of EMS algorithms across diverse building energy systems, susceptibility to errors, management of data gaps, and the integration of subordinate control algorithms between new setpoints from the EMS.

The models of the ProHMo benchmarking framework are closely aligned with the behavior of the commercial equipment used in the CoSES laboratory. This consistency facilitates testing promising systems in the laboratory using commercial hardware. Conducting these experimental tests can offer several additional insights. It validates EMS performance in real-world conditions in a controlled environment, ensuring that theoretical models translate effectively into practical applications. Observing the interactions between various components in a live setting can reveal intricacies and dependencies not apparent in simulations. Furthermore, such tests can uncover unforeseen issues or areas for improvement in EMS algorithms and lead to more robust and efficient systems. The close alignment between the ProHMo framework and the commercial hardware in the CoSES laboratory can help bridge the gap between research and practical implementation.

CRediT authorship contribution statement

Daniel Zinsmeister: Writing – review & editing, Writing – original draft, Visualization, Validation, Software, Methodology, Investigation, Formal analysis, Data curation, Conceptualization. **Ulrich Ludolfinger:** Writing – review & editing, Software. **Vedran S. Perić:** Writing – review & editing, Supervision. **Christoph Goebel:** Writing – review & editing, Supervision, Resources, Project administration, Funding acquisition.

Declaration of competing interest

The authors declare that they have no known competing financial interests or personal relationships that could have appeared to influence the work reported in this paper.

Data availability

The data is published in GitLab, the link is included in the paper

Declaration of generative AI and AI-assisted technologies in the writing process

During the preparation of this work the authors used ChatGPT in order to check and improve the comprehensibility of the paper. After using this tool/service, the authors reviewed and edited the content as needed and take full responsibility for the content of the publication.

Acknowledgements

This project was funded by the Federal Ministry for Economic Affairs and Climate Action, Germany (FKZ: 03EN3032). The work of Vedran S. Perić was supported by Deutsche Forschungsgemeinschaft (DFG), Germany, through “Optimal Operation of Integrated Low-Temperature Birdirectional Heat and Electric Grids (IntElHeat)” under project number 450821044. The construction of the CoSES laboratory was supported by Deutsche Forschungsgemeinschaft (DFG) through the project “Flexible reconfigurable microgrid laboratory” under project number 350746631.

Appendix A. Model properties

A.1. Building energy system parameters

The simulation model shown in Fig. 3 has the following default parameters, which can be adapted if desired:

- cooling: deactivated
- building size: 300 m^2
- number of inhabitants: 6
- yearly electricity consumption: 7000 kWh
- set room temperature for heating: 21 $°C$
- night-time reduction: deactivated
- TES volume: 785 l
- nominal heating power of the ASHP at A2/W35: 5.75 kW
- nominal COP at A2/W35: 5.92
- heating power of the auxiliary heater: 9 kW
- ST: deactivated
- peak power PV: 20 kW
- BAT: deactivated
- BAT control mode: BAT power mode
  User can choose between providing a direct power setpoint (‘BAT power mode’) or providing a setpoint for the power at the grid connection point (‘grid power mode’). A low-level control charges or discharges the BAT during ‘grid power mode’ to keep the set power at the grid connection point, while the controller does not react to load fluctuations between timesteps in ‘BAT power mode’.

A.2. Setpoints

The setpoints for the building energy system include:

- reference room temperature during heating [$°C$]
- reference room temperature during cooling [$°C$]
- HP mode (0 = heating, 1 = cooling)
- HP modulation [%]
- HP auxiliary heater modulation [%]
- 3WV connecting HP and TES [%]
  (time connected to the bottom segment: $x \cdot dt$, time connected to the top segment: $(1-x) \cdot dt$)
- Power for the BAT control [kW]
  (> 0: charging / drawing, < 0: discharging / feeding in; depending on the BAT control mode)

Appendix B. Discomfort metrics

The calculation of the discomfort metrics is shown in equations (B.1), (B.2), and (B.3). During the day (from 06:00 to 23:00) the room temperature is set at a minimum of 20 $°C$, dropping to 17 $°C$ at night. The upper limit for room temperature stands at 24 $°C$. The tap’s DHW temperature must not fall below 45 $°C$ during active flow.

$$dc_{heat} = \sum_{t=t_0}^{t_{end}} max(T_t^{set,min} - T_t^{room}, 0) \cdot \Delta t \tag{B.1}$$

$$dc_{cool} = \sum_{t=t_0}^{t_{end}} max(T_t^{room} - T_t^{set,max}, 0) \cdot \Delta t \tag{B.2}$$

$$dc_{DHW} = \sum_{t=t_0}^{t_{end}} max(T_t^{DHW} - T_t^{set,max}, 0) \cdot \dot{V}_t^{DHW} \cdot \Delta t \tag{B.3}$$

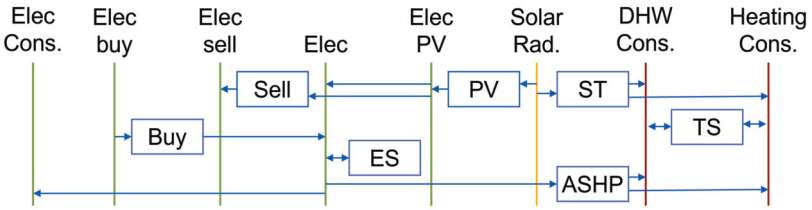

Fig. D.15. Structure of the LP models. The commodities (e.g., 'Elec') can be converted through processes (e.g., 'PV').

Appendix C. Sensors

The following sensors are used for the experimental validation in the CoSES laboratory:

- Temperature measurement:
  4-wire PT100 resistance sensors of quality class A with a tolerance of $\pm(0.15\ K + 0.002 \cdot T)$ [51]
- Water flow measurement:
  Electromagnetic flowmeter 'Proline Promag E 100' with a measurement diameter of 15 mm and a tolerance of $\pm 0.5\% \pm 1\ mm/s$ [52].
- Voltage measurement:
  LEM CV 3-1000 with an accuracy of 0.2% [53].
- Current measurement:
  LEM LF210-S/SP3 with an accuracy of 0.2% [54].

Appendix D. Energy management system descriptions

The code of the EMSs and its integration of the ProHMo benchmark framework are published for both EMS approaches: MPC-based EMS with the included ProHMo template[3] and the RL-based EMS using the Gymnasium API standard.[4]

D.1. Model predictive control-based energy management system

The implemented EMS minimizes the operational cost of the system following the methodology presented in [55] and [56]. The optimization employs a rolling horizon strategy with a 48-hour prediction horizon, generating setpoints in 15-minute intervals. The setpoints for the next 24 hours are sent to the simulation model as shown in Fig. 2. Every 24 hours, the EMS gets the current state of the simulation model and initiates a fresh optimization.

The efficiency of ASHP depends strongly on the heat generation temperature. Furthermore, simulation and experimental results of the TES indicate a distinct separation between the higher temperature upper section and the medium temperature lower section. Therefore, this stratification is incorporated into the optimization model by differentiating between higher temperature heat for DHW and lower temperature for space heating and assuming two separate TESs for heating and DHW.

The structure of the Linear Programming (LP) model is depicted in Fig. D.15. It involves multiple commodities that are consumed: electricity ('Elec Cons.'), DHW ('DHW Cons.'), and heating ('Heating Cons.'). Processes such as an ASHP are used to switch between commodities. Different COPs at different temperatures are accounted for by distinguishing between heating at $40\,°C$ and DHW at $60\,°C$. The model includes electric and thermal storage ('ES' and 'TES'), where the commodity can be stored for later use. It also covers buying and selling electricity at different prices, for which the commodities 'Elec buy' and 'Elec sell' are required. Additionally, the intermediate commodities 'Elec' and 'Elec PV' are used to directly use or sell the electricity generated by a PV plant. Solar radiation ('Solar Rad.') is utilized by the processes 'PV' and 'ST' to generate electricity and heat.

Equations (D.1.1) to (D.1.9) show the structure of the mathematical model. The objective is to minimize the cost of electricity (equation (D.1.1)) based on the amount ($\rho_t^{el,buy/sell}$) and price ($p_t^{el,buy/sell}$) at a given time-step t (equation (D.1.2)). Equation (D.1.3) ensures that all commodity flows are balanced at each time-step, e.g., that the amount of DHW produced by the ASHP or extracted from the TES is equal to the amount consumed or stored in the TES. Commodities for solar radiation c_{sol} and demand are implemented as time series (f_t^c, equation (D.1.4)). Processes are described by their capacity limits (equation (D.1.5)) and efficiency between the inlet and outlet commodities (equation (D.1.6)). Storages are described by equations (D.1.7) to (D.1.9). The energy content of the storage ($E_t^{c,s}$) depends on the content of the previous time-step, losses through discharge ($d_t^{c,s}$), and charging and discharging power with its efficiency (equation (D.1.7)). The energy of the storage must be between 0 and its maximum capacity (equation (D.1.8)) and equal or greater at the end than at the beginning to prevent windfall profits (equation (D.1.9)).

$$\text{minimize} \sum_{t=t_0}^{t_{end}} (C_t^{el,buy} - C_t^{el,sell}) \tag{D.1.1}$$

$$\text{subject to } C_t^{el,buy/sell} = p_t^{el,buy/sell} \cdot \rho_t^{el,buy/sell} \tag{D.1.2}$$

$$\sum \rho_t^{c,p,out} + \sum \rho_t^{c,s,out} + \rho_t^{c,buy} = \tag{D.1.3}$$
$$= \sum \rho_t^{c,p,in} + \sum \rho_t^{c,s,in} + \rho_t^{c,sell} + \rho_t^{c,dem}$$

$$\rho_t^c = f_t^c \tag{D.1.4}$$

$$0 \le \rho_t^{c,p,in} \le \rho^{c,p,max} \tag{D.1.5}$$

$$\rho_t^{c,p,out} = \eta_t^{c,p} \cdot \rho_t^{c,p,in} \tag{D.1.6}$$

$$E_t^{c,s} = E_{t-1}^{c,s} \cdot (1 - d_t^{c,s} \cdot \Delta t) + \tag{D.1.7}$$
$$+ (\eta^{c,s,in} \cdot \rho_t^{c,s,in} - \eta^{c,s,out} \cdot \rho_t^{c,s,out}) \cdot \Delta T$$

$$0 \le E_t^{c,s} \le E^{c,s,max} \tag{D.1.8}$$

$$E_{t_0}^{c,s} \le E_{t_{end}}^{c,s} \tag{D.1.9}$$

Modeling the TES in LP frameworks is challenging because the model does not replicate the temperature stratification. To mitigate this, the relationship between the TES's energy content and temperature is captured in our LP formulation by equation (D.2), where the selection of the reference temperature T^{ref} is critical. A T_{ref} set too low may lead the TES model to overestimate the available energy, potentially causing the outlet temperatures to fall short of heating requirements. Conversely, a T_{ref} set too high could result in maintaining unnecessarily high TES temperatures, leading to inefficiency. Additionally, the definition of efficiency for the heat generation processes, such as for ASHP, is complicated by its dependence on the TES temperature, as noted in equation (D.1.5). To keep the problem linear, this efficiency parameter must remain constant, although it is variable in practice. Users are advised to estimate these parameters based on model information and then refine them based on initial simulation outcomes as done in the case study.

$$E_t^{TES} = m^{TES} \cdot c_p \cdot (T_t^{act} - T^{ref}) \tag{D.2}$$

[3] https://gitlab.lrz.de/energy-management-technologies-public/models-of-prohmo-benchmark-paper.
[4] https://github.com/ULudo/DRL-Building-Energy-Ctr.

D.2. Reinforcement learning based energy management system

The RL-based EMSs in this paper are based on the approach presented by Ludolfinger et al. [12]. The RL problem is described as a partially observable Markov decision process due to the impracticality of fully observing the building energy state. A model-free soft actor-critic algorithm is employed to address this partial observability, which incorporates a recurrent policy featuring two consecutive long-short term memory layers. Therefore, both approaches are independent of forecasts, which increases their practicality.

The reward function is designed to assign rewards to each state. The first algorithm earns rewards when the outlet temperatures for the DHW and heating system exceed specific setpoints (equation (D.3.1)). Its secondary objective involves minimizing electricity costs (equation (D.3.2)). To deter the RL agent from shutting down the ASHP during high electricity prices, the total reward is always non-negative (equation (D.3.3)).

$$r_t^{temp} = \begin{cases} R^{\max} & \text{if } T_t^{heating} \geq T^{min,heating} \text{ and } T_t^{DHW} \geq T^{min,DHW} \\ 0 & \text{otherwise.} \end{cases} \tag{D.3.1}$$

$$r_t^{elec} = C_t^{el,sell} - C_t^{el,buy} \tag{D.3.2}$$

$$r_t = \max(r_t^{temp} - r_t^{el}, 0) \tag{D.3.3}$$

The second algorithm combines both RB and RL-based controllers. The RB-controller ensures that thermal constraints are upheld. This streamlines the RL algorithm's reward function which focuses only on reducing electricity costs (equation (D.3.1)).

Both algorithms are trained in a Python environment adhering to the Gymnasium API standard, incorporating the ProHMo FMU. The training process spans 100k steps, with data from January 2021. The algorithms use an observation history spanning the preceding 6 hours, recorded at 15-minute intervals, and produce new setpoints every 15 minutes.

References

[1] IEA, Net zero by 2050: a roadmap for the global energy sector, https://www.iea.org/reports/net-zero-by-2050, 2021.

[2] I. Jokinen, A. Lund, J. Hirvonen, J. Jokisalo, R. Kosonen, M. Lehtonen, Coupling of the electricity and district heat generation sectors with building stock energy retrofits as a measure to reduce carbon emissions, Energy Convers. Manag. 269 (2022) 115961, https://doi.org/10.1016/j.enconman.2022.115961.

[3] H. Li, Z. Wang, T. Hong, M.A. Piette, Energy flexibility of residential buildings: a systematic review of characterization and quantification methods and applications, Adv. Appl. Energy 3 (2021) 100054, https://doi.org/10.1016/j.adapen.2021.100054.

[4] D. Fischer, J. Bernhardt, H. Madani, C. Wittwer, Comparison of control approaches for variable speed air source heat pumps considering time variable electricity prices and pv, Appl. Energy 204 (2017) 93–105, https://doi.org/10.1016/j.apenergy.2017.06.110, https://www.sciencedirect.com/science/article/pii/S0306261917308607.

[5] J. Gasser, H. Cai, S. Karagiannopoulos, P. Heer, G. Hug, Predictive energy management of residential buildings while self-reporting flexibility envelope, Appl. Energy 288 (2021) 116653, https://doi.org/10.1016/j.apenergy.2021.116653, https://www.sciencedirect.com/science/article/pii/S0306261921001847.

[6] E. Zanetti, M. Aprile, D. Kum, R. Scoccia, M. Motta, Energy saving potentials of a photovoltaic assisted heat pump for hybrid building heating system via optimal control, J. Build. Eng. 27 (2020) 100854, https://doi.org/10.1016/j.jobe.2019.100854.

[7] L. Langer, T. Volling, An optimal home energy management system for modulating heat pumps and photovoltaic systems, Appl. Energy 278 (2020) 115661, https://doi.org/10.1016/j.apenergy.2020.115661, https://www.sciencedirect.com/science/article/pii/S0306261920311570.

[8] E. Zanetti, D. Kim, D. Blum, R. Scoccia, M. Aprile, Performance comparison of quadratic, nonlinear, and mixed integer nonlinear mpc formulations and solvers on an air source heat pump hydronic floor heating system, J. Build. Perform. Simul. 16 (2) (2023) 144–162, https://doi.org/10.1080/19401493.2022.2120631.

[9] T. Peirelinck, F. Ruelens, G. Decnoninck, Using reinforcement learning for optimizing heat pump control in a building model in modelica, in: 2018 IEEE International Energy Conference (ENERGYCON), IEEE, 2018, pp. 1–6.

[10] P. Lissa, C. Deane, M. Schukat, F. Seri, M. Keane, E. Barrett, Deep reinforcement learning for home energy management system control, Energy AI 3 (2021) 100043, https://doi.org/10.1016/j.egyai.2020.100043, https://www.sciencedirect.com/science/article/pii/S2666546820300434.

[11] L. Langer, T. Volling, A reinforcement learning approach to home energy management for modulating heat pumps and photovoltaic systems, Appl. Energy 327 (2022) 120020, https://doi.org/10.1016/j.apenergy.2022.120020, https://www.sciencedirect.com/science/article/pii/S0306261922012776.

[12] U. Ludolfinger, D. Zinsmeister, V.S. Perić, T. Hamacher, S. Hauke, M. Martens, Recurrent soft actor critic reinforcement learning for demand response problems, in: 2023 IEEE Belgrade PowerTech, IEEE, 2023, pp. 1–6.

[13] D. Blum, J. Arroyo, S. Huang, J. Drgoňa, F. Jorissen, H.T. Walnum, Y. Chen, K. Benne, D. Vrabie, M. Wetter, L. Helsen, Building optimization testing framework (boptest) for simulation-based benchmarking of control strategies in buildings, J. Build. Perform. Simul. 14 (5) (2021) 586–610, https://doi.org/10.1080/19401493.2021.1986574.

[14] J. Drgoňa, J. Arroyo, I. Cupeiro Figueroa, D. Blum, K. Arendt, D. Kim, E.P. Ollé, J. Oravec, M. Wetter, D.L. Vrabie, L. Helsen, All you need to know about model predictive control for buildings, Annu. Rev. Control 50 (2020) 190–232, https://doi.org/10.1016/j.arcontrol.2020.09.001.

[15] V.S. Peric, T. Hamacher, A. Mohapatra, F. Christiange, D. Zinsmeister, P. Tzscheutschler, U. Wagner, C. Aigner, R. Witzmann, Coses laboratory for combined energy systems at TU Munich, in: 2020 IEEE Power & Energy Society General Meeting (PESGM), IEEE, 2020, pp. 1–5.

[16] D. Zinsmeister, T. Lickleder, S. Adldinger, F. Christange, P. Tzscheutschler, T. Hamacher, V.S. Perić, A prosumer-based sector-coupled district heating and cooling laboratory architecture, Smart Energy 9 (2023) 100095, https://doi.org/10.1016/j.segy.2023.100095.

[17] Modelica Association, Modelica language (18.05.2023), https://modelica.org/modelicalanguage.html.

[18] D.B. Crawley, L.K. Lawrie, C.O. Pedersen, F.C. Winkelmann, Energy plus: energy simulation program, ASHRAE J. 42 (4) (2000) 49–56.

[19] Trnsys18 (2023), https://trnsys.de/en/trnsys18.

[20] Functional mock-up interface, https://fmi-standard.org/, 2023.

[21] G. Schweiger, C. Gomes, G. Engel, I. Hafner, J. Schoeggl, A. Posch, T. Nouidui, An empirical survey on co-simulation: promising standards, challenges and research needs, Simul. Model. Pract. Theory 95 (2019) 148–163, https://doi.org/10.1016/j.simpat.2019.05.001.

[22] M. Wetter, C. van Treeck, L. Helsen, A. Maccarini, D. Saelens, D. Robinson, G. Schweiger, Ibpsa project 1: bim/gis and modelica framework for building and community energy system design and operation – ongoing developments, lessons learned and challenges, IOP Conf. Ser. Earth Environ. Sci. 323 (1) (2019) 012114, https://doi.org/10.1088/1755-1315/323/1/012114.

[23] M. Wetter, W. Zuo, T.S. Nouidui, X. Pang, Modelica buildings library, J. Build. Perform. Simul. 7 (4) (2014) 253–270, https://doi.org/10.1080/19401493.2013.765506.

[24] D. Müller, T. Lauster, A. Constantin, M. Fuchs, P. Remmen, Aixlib – an open-source modelica library within the iea-ebc annex 60 framework, BauSIM 2016 (2016).

[25] C. Nytsch-Geusen, J. Huber, M. Ljubijankic, J. Rädler, Modelica buildingsystems – eine modellbibliothek zur simulation komplexer energietechnischer gebäudesysteme, Bauphysik 35 (1) (2013) 21–29, https://doi.org/10.1002/bapi.201310045.

[26] F. Jorissen, G. Reynders, R. Baetens, D. Picard, D. Saelens, L. Helsen, Implementation and verification of the ideas building energy simulation library, J. Build. Perform. Simul. 11 (6) (2018) 669–688, https://doi.org/10.1080/19401493.2018.1428361.

[27] R. Unger, T. Schwan, B. Mikoleit, B. Bäker, C. Kehrer, T. Rodemann, Green building - modelling renewable building energy systems and electric mobility concepts using modelica, in: Proceedings of the 9th International MODELICA Conference, 2012, pp. 897–906.

[28] Green city für simulationx, https://www.ea-energie.de/de/projects/green-city-fuer-simulationx/, 2023.

[29] M.S. Roudsari, M. Pak, Ladybug: a parametric environmental plugin for grasshopper to help designers create an environmentally-conscious design, in: Proceedings of the 13th Conference of International Building Performance Simulation Association, 2013.

[30] A. Priarone, F. Silenzi, M. Fossa, Modelling heat pumps with variable eer and cop in energyplus: a case study applied to ground source and heat recovery heat pump systems, Energies 13 (4) (2020) 794, https://doi.org/10.3390/en13040794.

[31] E. Balke, G. Nellis, S. Klein, H. Skye, V. Payne, T. Ullah, Detailed energy model of the nist net-zero energy residential test facility: development, modification, and validation, Sci. Technol. Built Environ. (2018), https://doi.org/10.1080/23744731.2017.1381828.

[32] P. Scharnhorst, B. Schubnel, C. Fernández Bandera, J. Salom, P. Taddeo, M. Boegli, T. Gorecki, Y. Stauffer, A. Peppas, C. Politi, Energym: a building model library for controller benchmarking, Appl. Sci. 11 (8) (2021) 3518, https://doi.org/10.3390/app11083518.

[33] J. Jiménez-Raboso, A. Campoy-Nieves, A. Manjavacas-Lucas, J. Gómez-Romero, M. Molina-Solana, Sinergym: a building simulation and control framework for training reinforcement learning agents, in: X. Jiang, O. Gnawali, Z. Nagy (Eds.), Proceedings of the 8th ACM International Conference on Systems for Energy-Efficient Buildings, Cities, and Transportation, ACM, New York, NY, USA, 2021, pp. 319–323.

[34] F. Pallonetto, E. Mangina, F. Milano, D.P. Finn, Simapi, a smartgrid co-simulation software platform for benchmarking building control algorithms, SoftwareX 9 (2019) 271–281, https://doi.org/10.1016/j.softx.2019.03.003.

[35] S. Huang, R. Lutes, C.A. Faulkner, D.L. Vrabie, S. Katipamula, W. Zuo, An open-source framework for simulation-based testing of buildings control strategies, J.

Build. Perform. Simul. 16 (6) (2023) 631–643, https://doi.org/10.1080/19401493.2023.2191220.
[36] S. Katipamula, J. Haack, G. Hernandez, B. Akyol, J. Hagerman, Volttron: an open-source software platform of the future, IEEE Electrif. Mag. 4 (4) (2016) 15–22, https://doi.org/10.1109/MELE.2016.2614178.
[37] F. Omar, S.T. Bushby, R.D. Williams, Assessing the performance of residential energy management control algorithms: multi-criteria decision making using the analytical hierarchy process, Energy Build. 199 (2019) 537–546, https://doi.org/10.1016/j.enbuild.2019.07.033.
[38] D. Zinsmeister, V. Perić, Implementation of a digital twin of the coses district heating prosumer laboratory, Energy 2004 (2022) 2965.
[39] U. Jordan, K. Vajen, Influence of the dhw load profile on the fractional energy savings, Sol. Energy 69 (2001) 197–208, https://doi.org/10.1016/S0038-092X(00)00154-7.
[40] T. Loga, J. Knissel, N. Diefenbach, R. Born, Development of a simplified data collection method for the assessment of the energy performance of residential buildings, Tech. rep., Institute of Living and Environment (IWU), Darmstadt, 2004.
[41] S. Paardekooper, R. Lund, B. Mathiesen, M. Chang, U. Petersen, L. Grundahl, A. David, J. Dahlbæk, I. Kapetanakis, H. Lund, N. Bertelsen, K. Hansen, D. Drysdale, U. Persson, Heat Roadmap Europe 4: Quantifying the Impact of Low-Carbon Heating and Cooling Roadmaps, Aalborg Universitetsforlag, 2018.
[42] IEA, The future of heat pumps, https://www.iea.org/reports/the-future-of-heat-pumps, 2022.
[43] C. Finck, R. Li, R. Kramer, W. Zeiler, Quantifying demand flexibility of power-to-heat and thermal energy storage in the control of building heating systems, Appl. Energy 209 (2018) 409–425, https://doi.org/10.1016/j.apenergy.2017.11.036, https://www.sciencedirect.com/science/article/pii/S0306261917316112.
[44] P. Fitzpatrick, F. D'Ettorre, M. De Rosa, M. Yadack, U. Eicker, D.P. Finn, Influence of electricity prices on energy flexibility of integrated hybrid heat pump and thermal storage systems in a residential building, Energy Build. 223 (2020) 110142, https://doi.org/10.1016/j.enbuild.2020.110142, https://www.sciencedirect.com/science/article/pii/S0378778819335285.
[45] D. Zinsmeister, Prohmo_experimentalvalidation, https://syncandshare.lrz.de/getlink/fiTv8nL5mN7uPRjAtoSBWj/, 2024.
[46] Q. Meng, M. Mourshed, Degree-day based non-domestic building energy analytics and modelling should use building and type specific base temperatures, Energy Build. 155 (2017) 260–268, https://doi.org/10.1016/j.enbuild.2017.09.034.
[47] M. Manfren, P.A.B. James, V. Aragon, L. Tronchin, Lean and interpretable digital twins for building energy monitoring – a case study with smart thermostatic radiator valves and gas absorption heat pumps, Energy AI 14 (2023) 100304, https://doi.org/10.1016/j.egyai.2023.100304.
[48] ASHRAE, American Society of Heating, Refrigerating and Air-Conditioning Engineers, Measurement of energy, demand, and water savings (guideline 14-2014), 2014.
[49] D. Zinsmeister, Coses laboratory documentation - ts2 - hardware, https://collab.dvb.bayern/display/TUMcoseslab/TS2+-+Hardware, 2024.
[50] D. Yang, W. Wang, T. Hong, A historical weather forecast dataset from the European centre for medium-range weather forecasts (ecmwf) for energy forecasting, Sol. Energy 232 (2022) 263–274, https://doi.org/10.1016/j.solener.2021.12.011.
[51] DKE Deutsche Kommission Elektrotechnik Elektronik Informationstechnik in DIN und VDE, Industrielle platin–widerstandsthermometer und platin–temperatursensoren, 2019.
[52] Endress + Hauser, Technical information proline promag e 100 (1.10.2021), https://portal.endress.com/dla/5000883/5389/000/02/TI01159DEN_0317.pdf.
[53] LEM International SA, Cv3, https://www.lem.com/en/cv-31000, 2023.
[54] LEM International SA, Lem lf210-s, https://www.lem.com/en/lf-210ssp3, 2023.
[55] D. Atabay, An open-source model for optimal design and operation of industrial energy systems, Energy 121 (2017) 803–821, https://doi.org/10.1016/j.energy.2017.01.030.
[56] Johannes Dorfner, Konrad Schönleber, Magdalena Dorfner, sonercandas, froehlie, smuellr, dogauzrek, WYAUDI, Leonhard-B, lodersky, yunusozsahin, adeeljsid, Thomas Zipperle, Simon Herzog, kais siala, Okan Akca, tum-ens/urbs: urbs v1.0.1, https://doi.org/10.5281/zenodo.594200, 2019.

4.3 CoSES as research infrastructure

The experiment and simulation infrastructure of CoSES was applied in various studies and projects. Phenomena such as pump-hunting and pump-blocking were confirmed experimentally, highlighting the nuanced complexities of decentralized energy feed-in [29]. The effectiveness of the weighted PID control strategy [131] in tackling these issues will be further validated using the laboratory's commercial components.

The laboratory also validated the MEMAP project's communication and control model, confirming its practicality with real devices [30, 148]. The experiments showed that the MPC-based control, while accurately predicting the TES state of charge, failed to provide the temperature at a sufficiently high level if the stratification of the TES is bad. Similar challenges were observed in controlling HPs [29]. This highlights the need for a backup control mechanism to compensate for control inaccuracies and ensure that users' comfort requirements are always satisfied. An example of such a backup control is implemented in the ProHMo benchmark tool [149].

A novel hydraulic design for 5GDHC networks was explored, comparing two different control strategies: fixed grid temperature control versus volume flow-based control with free-floating grid temperatures [141]. Experimental findings suggest that while the latter can reduce the electrical consumption of BHPs, a fixed temperature control offers superior control across the network, ensuring consistent temperatures for all prosumers.

The comprehensive component characterization within the laboratory provided data for the detailed simulation models of the ProHMo framework, yielding highly accurate building energy system models [149, 150]. The TES measurements were further pivotal in highlighting the benefits of two novel modeling methodologies and experimentally demonstrated the higher accuracy of these approaches [95, 151]. Moreover, a data-driven model of the ASHP was trained with laboratory measurements to replicate its dynamics in detail and inverted to derive an adaptive open-loop controller. This controller enables faster control of the ASHP's power setpoints compared to a PID controller [152].

The ProHMo simulation environment was utilized in the training and evaluation of a RL-based EMSs [153, 154]. It will be used in future publications to generate harmonized consumption profiles for electricity and heat. The profiles are correlated with the occupancy profiles derived from electrical usage patterns. A data-driven model will be trained with the same models to replicate the dynamic behavior of various buildings. The objective is to develop a universally applicable RL agent that accurately represents the room temperature dynamics without requiring training for each new building.

Chapter 5

Control strategy design

A dominant approach in EMSs is the application of MPC-based optimization algorithms to reduce energy costs and improve operational processes. MPC is a sophisticated control strategy that employs mathematical models to forecast a system's future behavior. Using optimization algorithms, MPC determines control inputs that optimize future outcomes based on specified criteria. For MPC to be effective in real-world applications of EMSs, there is often a reliance on simplified models to maintain computational efficiency and practical applicability.

Implementing MPC models for thermal components is challenging due to the dependence of thermal performance on flow rate and temperature differences. Most MPC-based EMSs employ linear models and assume a fixed temperature difference for power calculations. The energy content of a TES (Q_{TES}) is calculated based on its average storage temperature (T_{avg}), as shown in Equation 5.1, where volume (V_{TES}), density (ρ), and specific heat capacity (c_p) are constants.

$$Q_{TES} = V_{TES} \cdot \rho \cdot c_p \cdot (T_{avg} - T_{ref}) \tag{5.1}$$

Such assumptions introduce complications as they do not account for the temperature distribution within the TES. However, this temperature distribution is pivotal as a well-stratified TES can deliver more heat at elevated temperatures than a mixed TES with identical heat content and is thus more efficient [92]. Figure 5.1 illustrates this with two TESs with equivalent heat content. The stratified TES (a) provides heat at 60 $°C$ for DHW, while the mixed TES (b) only offers heat at 40 $°C$, generally considered too low due to legionella problems. Moreover, stratification in a TES can enhance efficiency, especially when managing varying heating requirements, such as space heating systems with lower supply temperatures than DHW. In this case, the heating system can be connected to the TES at a lower height, as illustrated in Figure 5.1.

Another challenge centers on defining the reference temperature (T_{ref}). When set too low, the TES model might inaccurately indicate available energy, even if outlet temperatures are too low. This would result in insufficient room or feed-in temperatures, as shown in [29]. On the other hand, if T_{ref} is set too high, the TES outlet temperature in a stratified TES could be high enough even when the energy content of the TES is still negative. Given that most optimization models prevent negative energy storage content, the TES is heated too much. This overheating reduces the efficiency of the heat generator and increases heat losses in the TES.

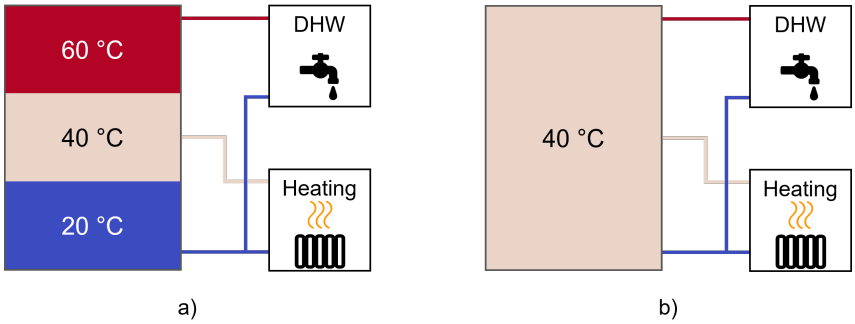

Figure 5.1: Temperature stratification within a TES: a) Stratified TES with different temperature layers; b) Mixed TES with consistent temperature throughout.

To overcome this difficulty, the following paper presents an MPC formulation for a TES, described as quadratic or simpler functions. The functions include the volume flow into the TES and between its layers, and the associated temperatures. Employing quadratic or simpler functions ensures the model remains computationally efficient while delivering accurate results.

Stratified Thermal Energy Storage Model with Constant Layer Volume for Predictive Control - Formulation, Comparison, and Empirical Validation

Authors Daniel Zinsmeister, Peter Tzscheutschler, Vedran S. Perić, Christoph Goebel

Publication medium Renewable Energy, Volume 219

Digital object identifier https://doi.org/10.1016/j .renene.2023.119511

Author contributions

Daniel Zinsmeister:	Conceptualization, Visualization, Writing – original draft, review & editing.
Peter Tzscheutschler:	Conceptualization, Writing - review, Supervision, Project administration, Funding acquisition.
Vedran S. Perić:	Conceptualization, Writing - review, Supervision, Project administration, Funding acquisition.
Christoph Goebel:	Conceptualization, Writing - review, Supervision, Project administration, Funding acquisition.

Renewable Energy 219 (2023) 119511

Contents lists available at ScienceDirect

Renewable Energy

journal homepage: www.elsevier.com/locate/renene

Stratified thermal energy storage model with constant layer volume for predictive control — Formulation, comparison, and empirical validation

Daniel Zinsmeister *, Peter Tzscheutschler, Vedran S. Perić, Christoph Goebel

Technical University of Munich, Arcisstrasse 21, Munich, 80333, Bavaria, Germany

ARTICLE INFO

Keywords:
Thermal energy storage
Model predictive control
Optimization
Energy management system
Experimental validation

ABSTRACT

Recent developments in heating systems have witnessed a significant increase of heat pumps with a highly temperature-dependent efficiency. Optimal real-time operation of these heating systems with predictive control requires a thorough understanding and modeling of the internal temperature distribution of the associated thermal energy storage. At the same time, the thermal energy storage models need to be sufficiently simple to ensure computational tractability in real-time predictive control. Therefore, this article presents a stratified thermal energy storage model with constant layer volume and variable temperature suitable for real-time predictive control. The model employs a novel formulation with quadratic or simpler constraints which enable high accuracy at low computation burden. The proposed model is validated experimentally and compared with other models available in literature. The results show that the proposed stratified thermal energy storage model represents the real-world behavior of a thermal energy storage with great accuracy, while reducing the required computational burden as compared to other models for real-time operation and control. A case study further demonstrates that the increased accuracy of the proposed new model leads to cost and energy savings for the operator.

1. Introduction

Heat Pumps (HP)s are a key technology to decarbonize the heating sector due to their high efficiency [1,2]. However, they represent additional electrical loads, and their massive deployment can impose operational challenges for the power grid. Concurrently, HPs in combination with Thermal Energy Storages (TES)s can provide flexibility to the power grid, which is key to integrating intermittent renewable energy sources into the power grid [3].

To leverage this potential, optimal real-time operation with Energy Management Systems (EMS)s can play a central role to intelligently integrate HPs into future energy systems [4]. In this context, Model Predictive Control (MPC)-based EMSs are a dominant trend in the relevant literature [3,5]. This approach calculates optimal control signals for energy resources based on mathematical models of the system and predicted exogenous variables [6]. Hermansen et al. [7] showed that MPC-based EMSs with a good description of the TES provide better results for complex heating systems than rule-based control strategies.

Real-time optimization requires a good compromise between model accuracy and computational effort [3,8]. When modeling heating systems with HPs, the temperature profile in TESs is important as it has a high influence on the efficiency of the overall system. It can be maximized if the TES is well stratified, which means that there is ideally a layer of hot water at the top and a layer of cold water at the bottom [9]. In addition, stratified TESs can be divided into several temperature zones for simultaneous applications that require different temperatures.

Tarragona et al. [5] provide a detailed overview of EMSs with TESs. The implemented TES models range from mixed TES models that neglect the temperature profile as done by D'Ettorre et al. [10] to models that reproduce them in detail. A common method of modeling stratification is through a composite system of several TESs with different temperature ranges [11–15]. However, this approach does not consider any exchange between the different temperature layers, which is important for representing the water flow within the TES and the resulting change in stratification.

Muschick et al. [16] proposed an accurate stratified TES model, which considers layers with constant temperatures and varying volumes. The temperature layers are arranged in monotonically ascending order, with the lowest layer representing the lowest temperature. When heat is supplied to or extracted from the TES, the volume of the layer with the corresponding temperature increases or decreases accordingly. An integer term in the resulting model indicates, from which layer water can be extracted. However, Muschick et al. only modeled convective heat exchange, while conductive heat exchanges, such as

* Corresponding author.
E-mail address: d.zinsmeister@tum.de (D. Zinsmeister).

https://doi.org/10.1016/j.renene.2023.119511
Received 1 August 2023; Received in revised form 29 September 2023; Accepted 24 October 2023
Available online 27 October 2023
0960-1481/

Nomenclature

Constants

Δt	Time step size [s];
ρ	Density [kg/dm^3];
A	Area [m^2];
c_p	Specific heat capacity [kJ/kg K];
h	Height [m];
U	Thermal transmittance [W/m^2 K];
V	Volume [m^3];

Subscripts

amb	Ambient;
b	Bigger;
$buoy$	Buoyancy;
$cond$	Conductive;
$conn$	Connection wild card: p (port) or hx (heat exchanger);
$conv$	Convective;
cum	Cumulative;
d	Demand;
eh	Electric heater;
g	Generation;
hx	Heat exchanger;
in/out	Flow direction: in or out;
ins	Insulation;
l	Layer index;
$loss$	Losses;
p	Port;
ref	Reference;
ret	Return;
s	Smaller;
sto	Storage;
sup	Supply;
t	Time index;
x	Process wild card: g (generation) or d (demand);

Variables

δ	Boolean variable [–];
η	Efficiency [–];
C	Costs [pu];
dQ	Heat energy change per time step [kWh];
dT	Temperature change per time step [°C];
Q	Heat energy [kWh];
T	Temperature [°C];

heat exchangers or electric heating rods, as well as buoyancy effects are neglected. The integer terms further result in a high computation burden for real-time control.

Schütz et al. [17] and Rastegarpour et al. [18] use a different approach by discretizing the TES into multiple layers with fixed volume and varying temperatures. However, they linearize their models by considering the temperature of the TES only for discharging, while charging is modeled solely based on the input power. This simplification neglects temperature-dependent efficiencies and the influence of changing volume flow from the heat source.

To address these challenges, this paper proposes a stratified TES model with fixed volume and varying temperatures that considers varying volume flows and inlet temperatures. The proposed model is formulated with quadratic and simpler constraints, which ensures lower computation burden compared to the integer-based stratified TES model of Muschick et al. [16]. It is available as an open access repository.[1] An Excel mask further simplifies the parametrization of the model.

Furthermore, to the best of the authors' knowledge, there have been no attempts to experimentally validate TES models for predictive control, despite numerous modeling approaches in the literature [11–18]. We therefore validate and compare the model using experimental data from the Center for Combined Smart Energy (CoSES) laboratory [19].

The remainder of the paper is structured as follows: First, some basic information on modeling TES is provided in Section 2. We then present the predictive control model of the stratified TES (Section 3). The model is validated in Section 4 and used in a case study, where it is integrated into an EMS that applies optimization to minimize operational costs to show the applicability of the model and compare it with other TES models (Section 5). Section 6 discusses the possibilities and limitations before the conclusion is drawn in Section 7.

2. Thermal energy storage models

The energy content of a TES is described by its volume and the temperature difference to the reference temperature (T^{ref}):

$$Q = \rho \cdot V \cdot c_p \cdot \int_V (T(x,y,z) - T^{ref}) dV \tag{1}$$

There are various approaches to model TESs. These methods range from solving the space integral by diving the TES into small finite space elements, to simple approaches that assume constant temperature in the whole volume of the TES, resulting in a so-called mixed TES model.

However, most common approaches in modeling TES for energy systems assume constant temperature along the horizontal plane, which results in one dimensional (1D) TES models. These models discretize the integral over the vertical axis and divide the TES in several layers.

The layers are discretized to have either Constant Layer Volume (CLV) and variable layer temperature, or Constant Layer Temperature (CLT) and variable layer volume. The energy change of CLV models is described by its temperature change (see Eq. (2)), while the energy change of CLT models is the change of the corresponding layer volume (see Eq. (3)).

$$dQ_l = \rho \cdot V_l \cdot c_p \cdot (dT_l - T^{ref}) \tag{2}$$

$$dQ_l = \rho \cdot dV_l \cdot c_p \cdot (T_l - T^{ref}) \tag{3}$$

The energy content of each layer changes due to:

- Convective heat exchange: Heat exchange via volume flows, which occurs from/to the outside through ports or within the TES.
- Conductive heat exchange: TES can exchange heat conductively using internal heat exchanger or electric heaters. Temperature zones within a stratified TES also exchange heat via conduction.
- Buoyancy: Buoyancy in TES is an undesired effect that occurs when a heavier cold water layer is formed above a layer of lighter hot water. Due to the higher density of the colder water, it sinks, leading to an undesired mixing of the TES. It can be avoided with several measures:
  - Optimizing the heating system to prevent too high return temperatures.
  - Using multiple inflow ports at different heights. By switching between ports, the inflow temperature can be close to the respective layer temperature.
  - Using stratification lances.

[1] https://gitlab.lrz.de/energy-management-technologies-public/strats-e.

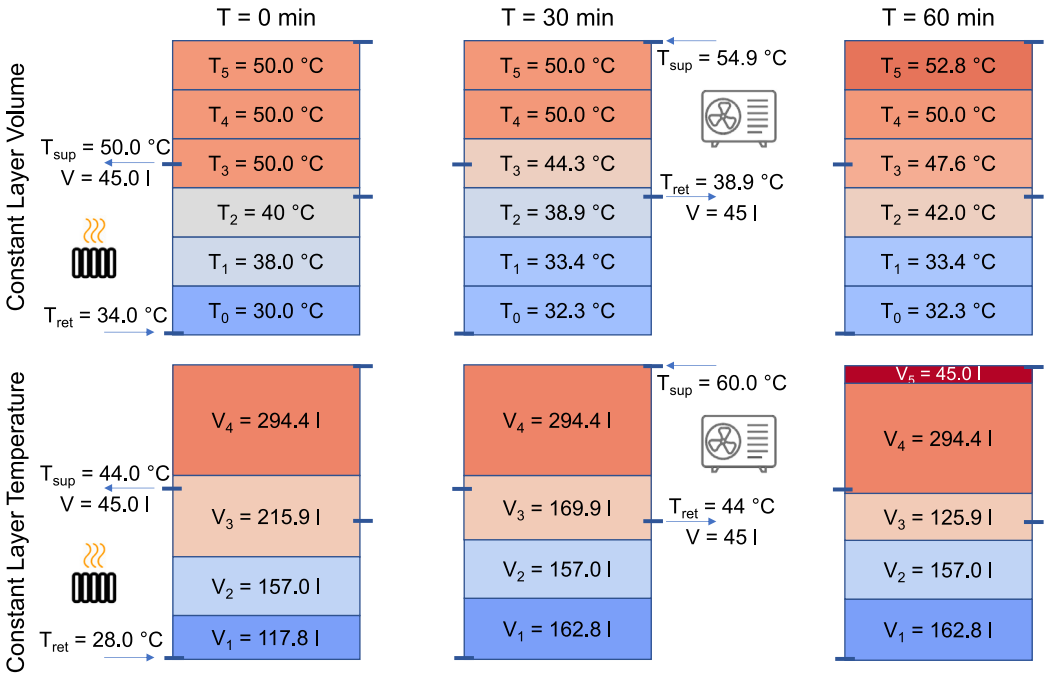

Fig. 1. Behavior of 1D TES models: CLV (top) and CLT (bottom). The temperature distribution changes over time. In the first time step, the TES is discharged through the ports on the left side, after that, the TES is charged through the ports at the right side. Charging and discharging is carried out with 45 *l* at a temperature difference of 16 K.

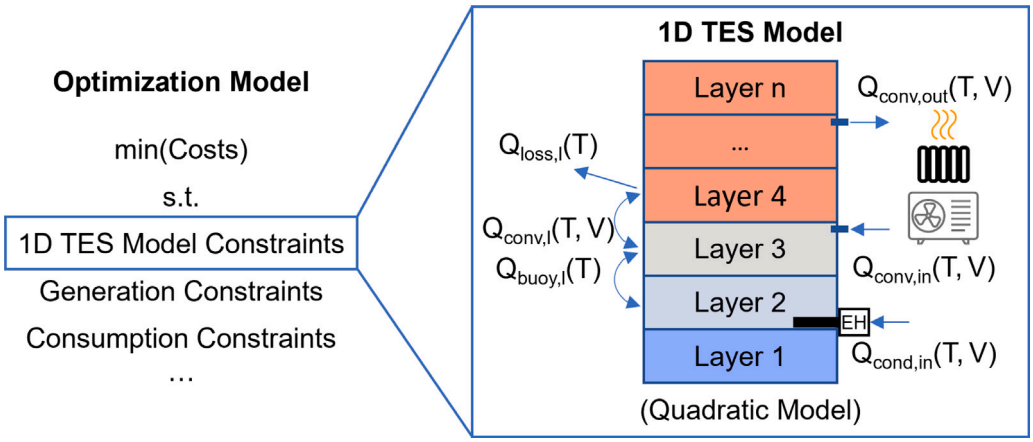

Fig. 2. Methodology of the presented MPC approach.

- Heat losses: Heat losses to the environment occur through the surface of the TES. They depend on the thermal transmittance of the insulation and the total area.

CLV models have been shown to adequately describe the behavior of TESs and are mostly used in commercial simulation software such as TRNSYS [20], Apros [21] or Green City [22,23]. However, the thermocline, the boundary between warm and cold layers, is not perfectly represented [24,25]. CLT models, as used by Kleinbach et al. [26], can model this effect better, but have difficulties in modeling buoyancy. Due to the ordered temperature layer in these models, upward or downward flows caused by buoyancy cannot be represented. De la Cruz-Loredo et al. [24] combined both approaches by using a flat thermocline barrier that moves with inflows and outflows to better represent the thermocline in a 1D TES system.

Fig. 1 shows an example of the charging and discharging behavior of CLV and CLT models. CLV ports are always connected to the same layer and the outlet temperature depends on the temperature of that layer, while for CLT the ports are connected to different layers over time and layers can also be completely depleted.

We show in Section 3 and Appendix A how CLV and CLT can be formulated to integrate them optimization-based EMS.

3. Stratified thermal energy storage model with constant layer volume

We formulate in this section a 1D TES model with CLV for predictive control. Our modeling approach is similar to the 1D simulation models discussed in Section 2. However, these simulation models use differential equations, which are solved step by step. While effective for simulations, these models are not suitable for real-time optimization, due to their computational complexity. To solve all equations of the model simultaneously during optimization, the model must be simplified. The novelty of our approach is that the TES model is represented only with linear and quadratic constraints. By doing so, we can reduce the computational burden while preserving crucial information about the stratification in the TES. Fig. 2 shows the 1D TES model approach and its integration in a MPC based EMS.

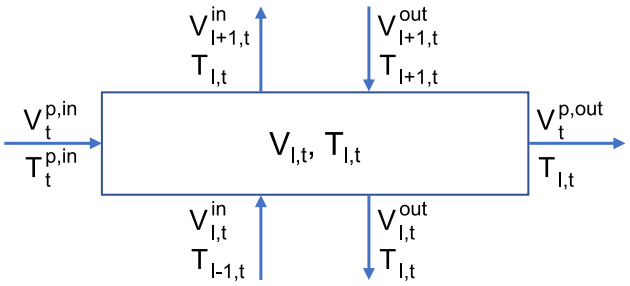

Fig. 3. Convective inflow and outflow of the layers.

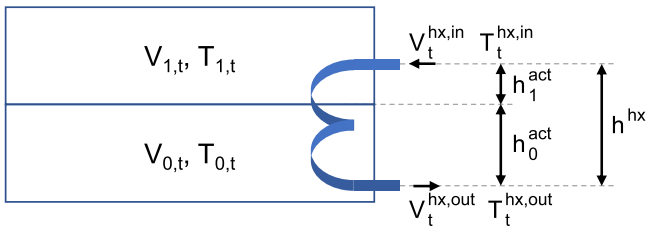

Fig. 4. Conductive inflow and outflow of the layers.

The temperature of each layer l is discretized over each time step t. It depends on the temperature of the last time step and temperature changes due to convection ($dT^{conv}_{l,t}$, see Section 3.1), conduction ($dT^{cond}_{l,t}$, see Section 3.2), buoyancy ($dT^{buoy}_{l,t}$, see Section 3.3) and heat losses ($dT^{loss}_{l,t}$, see Section 3.4):

$$T_{l,t} = T_{l,t-1} + dT^{conv}_{l,t} + dT^{cond}_{l,t} + dT^{buoy}_{l,t} - dT^{loss}_{l,t} \tag{4}$$

3.1. Convective heat exchange

Convective heat exchange in this system is primarily determined by two factors: volume exchange and the temperature difference between the layer and its inflows and outflows. In 1D TES models, the outflows ($V^{out}_{l,t}$) have the same temperature as the layer from which they originate, which means that they do not affect the total energy content of the layer. As a result, the energy change of a layer is exclusively influenced by its inflows (V^{in}, T^{in}):

$$dQ^{conv}_{l,t} = \rho \cdot c_p \cdot V^{in}_t \cdot (T^{in}_t - T_{l,t-1}) \tag{5}$$

Fig. 3 illustrates all inflows and outflows of a layer. In- and outflows can be simultaneous through the ports connected to the layer ($V^{p,in/out}_t$), or the upper ($V^{in/out}_{l+1,t}$) and lower layer ($V^{in/out}_{l,t}$). As the layer volume does not change over time, inflows and outflows must be balanced:

$$\sum V^{p,in}_t + \sum V^{p,out}_t + V^{in}_{l-1,t} + V^{out}_{l-1,t} + V^{in}_{l+1,t} + V^{out}_{l+1,t} = 0 \tag{6}$$

Since the temperature change is solely influenced by inflows within the system, it becomes necessary to decompose the convective volume flow between the layers ($V^{in/out}_{l,t}$, not through the ports) into its positive inflow ($V^{in}_{l,t}$) and negative outflow ($V^{out}_{l,t}$) components (Eq. (7)). To incorporate this as MPC constraints, two equations are employed, where Eq. (8) decomposes inflow and outflow. Since normal TES have no problems with circular flow, where water flows up one side of the layer and down the other, Eq. (9) ensures that either internal upward or downward flow is zero. However, these constraints do not affect simultaneous charging and discharging through the port, which is modeled in Eq. (6).

$$V^{in}_{l,t} = \begin{cases} V^{in/out}_{l,t} & \text{if } V^{in/out}_{l,t} > 0 \\ 0 & \text{otherwise} \end{cases} \tag{7}$$

$$V^{in/out}_{l,t} = V^{in}_{l,t} - V^{out}_{l,t} \tag{8}$$

$$V^{in}_{l,t} \cdot V^{out}_{l,t} = 0 \tag{9}$$

$$V^{in}_{l,t}, V^{out}_{l,t} \in \mathbb{R}^+_0$$

The resulting temperature change of the layer is determined by Eq. (10), which is based on the energy change of the layer (see Eq. (5)). Since it involves dividing the volume flow per time step by the layer volume, the volume flow must not exceed the layer volume to obtain meaningful results. While an additional constraint that prevents this could potentially lead to falsified results and an infeasible model, this limitation can be checked in pre/postprocessing.

$$dT^{conv}_{l,t} = \frac{dQ^{conv}_{l,t}}{V_l} = \frac{V^{p,in}_t}{V_l} \cdot (T^{p,in}_t - T_{l,t-1}) + \frac{V^{out}_{l+1,t}}{V_l} \cdot (T_{l+1,t-1} - T_{l,t-1}) + \frac{V^{in}_{l,t}}{V_l} \cdot (T_{l-1,t-1} - T_{l,t-1}) \tag{10}$$

The outlet temperature of the port corresponds to the layer temperature of the last time step:

$$T^{p,out}_t = T_{l,t-1} \tag{11}$$

3.2. Conductive heat exchange

Conductive heat elements, such as heat exchangers or electric heaters, change the temperature directly without any mass transfer. Fig. 4 shows an example of a heat exchanger, connected to layer 0 and 1.

The total heat transferred by the heat exchanger is calculated using Eq. (12). The resulting temperature change of the layer is determined by Eq. (13). When a heat exchanger affects multiple layers, we simplify the calculation by considering the heat transfer into each layer as a function of its relative height share (h^{act}_l / h^{hx}).

$$dQ^{cond}_t = V^{cond}_t \cdot \rho \cdot c_p \cdot (T^{hx,in}_t - T^{hx,out}_t) \tag{12}$$

$$dT^{cond}_{l,t} = \frac{dQ^{cond}_t}{\rho \cdot c_p \cdot V_l} \cdot \frac{h^{act}_l}{h^{hx}} \tag{13}$$

The outlet temperature from the heat exchanger is higher/lower than the temperature in the TES during charging/discharging. This temperature difference is a nonlinear function that depends on several factors such as the volume flow, the inlet temperature, and the storage tank temperature. To linearize this behavior, we assume a constant temperature difference between the average temperature of the layers in contact with the heat exchanger (ΔT^{hx}, Eq. (14)). This assumption is acceptable when the time step size is small enough. The offset is positive when heat is fed into the storage and negative when heat is extracted.

$$T^{hx,out}_t = \Delta T^{hx} + \sum_{l=l^{hx,out}}^{l^{hx,in}} T_{l,t-1} \tag{14}$$

3.3. Buoyancy

Buoyancy occurs due to the temperature-dependent density of water when there is a positive temperature difference between the upper and lower layers ($\Delta T^{buoy,pos}_{l,t}$). The temperature change caused by buoyancy is calculated in Eq. (15) based on the buoyant heat inflow and outflow ($dQ^{buoy}_{l,t}$).

$$dT^{buoy}_{l,t} = \frac{dQ^{buoy}_{l-1,t} - dQ^{buoy}_{l,t}}{\rho \cdot c_p \cdot V_l} \tag{15}$$

The buoyant heat flow ($dQ^{buoy}_{l,t}$) is a nonlinear function, based on the positive temperature difference between the layers ($\Delta T^{buoy,pos}_{l,t}$). Eq. (16)

shows the linearized equation using a buoyancy constant ($const^{buoy}$). Experiments in the CoSES laboratory showed that the buoyancy constant is 0.9 kW/K for the exemplary storage.

$$dQ_{l,t}^{buoy} = \Delta T_{l,t}^{buoy,pos} \cdot const^{buoy} \cdot \Delta t \tag{16}$$

To formulate the positive temperature difference (Eq. (17)) as a constraint, the temperature difference between layers (Eq. (18)) is decomposed into its positive and negative components ($\Delta T_{l,t}^{buoy,pos}$, $\Delta T_{l,t}^{buoy,neg}$, see Eqs. (19) and (20)) similar to the volumetric flow in Section 3.1.

$$\Delta T_{l,t}^{buoy,pos} = \begin{cases} \Delta T_{l,t}^{buoy} & \text{if } \Delta T_{l,t}^{buoy} > 0 \\ 0 & \text{otherwise} \end{cases} \tag{17}$$

$$\Delta T_{l,t}^{buoy} = T_{l,t-1} - T_{l+1,t-1} \tag{18}$$

$$\Delta T_{l,t}^{buoy} = \Delta T_{l,t}^{buoy,pos} - \Delta T_{l,t}^{buoy,neg} \tag{19}$$

$$\Delta T_{l,t}^{buoy,pos} \cdot \Delta T_{l,t}^{buoy,neg} = 0 \tag{20}$$

$$\Delta T_{l,t}^{buoy,pos/neg} \in \mathbb{R}_0^+$$

3.4. Losses

Losses depend on the thermal transmittance (U), the surface of the TES insulation (A^{ins}) and the ambient temperature (T^{amb}). The temperature change caused by losses is calculated as:

$$dT_{l,t}^{loss} = \frac{Q_{l,t}^{loss}}{\rho \cdot c_p \cdot V_l} = \frac{U \cdot A^{ins} \cdot (T_{l,t-1} - T^{amb}) \cdot \Delta t}{\rho \cdot c_p \cdot V_l} \tag{21}$$

3.5. Integration into energy management systems

In Section 5, we compare different EMS models in a case study. We therefore introduce an optimization model that minimizes costs using the CLV model, which has a similar structure to the optimization model of *ficus* [27] and *urbs* [28]. The objective function in Eq. (22a) minimizes the operation costs C^{op} associated with heat generation Q from all heat generators g within the time horizon $t \in [0 : t^{end}]$.

$$\text{minimize} \quad \sum_{t=0}^{t^{end}} \sum_{g} C^{op}(Q_t^g) \tag{22a}$$

$$\text{subject to } 0 \le Q_t^g \le Q^{g,max} \tag{22b}$$

$$Q_t^d = Q_t^{d,fc} \tag{22c}$$

$$Q_t^x \cdot \eta(T_t^x) = \sum_{t}^{t} V_t^{conn_x} \cdot \rho \cdot c_p \cdot \Delta T^x \tag{22d}$$

$$T_t^{conn_g,in} \cdot V_t^{conn_g} \le T^{g,max} \cdot V_t^{conn_g} \tag{22e}$$

$$T_t^{conn_d,out} \cdot V_t^{conn_d} \ge T^{d,min} \cdot V_t^{conn_d} \tag{22f}$$

$$T_t^{conn_x,in} = T_t^{conn_x,out} \pm \Delta T^x \tag{22g}$$

$$T_{l,t} = T_{l,t-1} + dT_{l,t}^{conv} + dT_{l,t}^{cond} + dT_{l,t}^{buoy} - dT_{l,t}^{loss} \tag{22h}$$

$$\text{with} \quad Q_t^x, V_t^{conn_x} \in \mathbb{R}_0^+ \tag{22i}$$

The capacities of the heat generators are limited in Eq. (22b) to account for the maximum capacity of the modeled generators. Eq. (22c) models the heat demand (Q_t^d) based on the forecasted demand ($Q_t^{d,fc}$).

The volume flow through the processes ($V_t^{conn_x}$, where x represents heat generator or demand) is determined by several factors, as described in Eq. (22d). These factors include the heat input/output of the process (Q_t^x), its efficiency ($\eta(T_t^x)$), and its temperature difference (ΔT^x). If a process is connected to multiple TES connections ($conn$, which represents a port or heat exchanger), the total volume flow is the sum of the individual flows. To avoid a nonlinear problem, the generator and demand models are linearized by assuming a constant temperature difference and a linear temperature dependence of the efficiency.

The temperatures for heat generation and demand are further restricted by the processes. Eqs. (22e) and (22f) guarantee that these restrictions are satisfied when there is a volume flow through the respective processes.

Lastly, Eqs. (22g) and (22h) link heat generation, heat demand and the CLV storage model, incorporating the temperature dynamics within the TES. This enables to use the stratification of the TES and the resulting temperature distribution in the optimization model, which allows the TES potential to be fully utilized.

Table 1
TES parameters.

Parameter	Value
TES volume (V^{sto})	0.785 m^3
TES height (h^{sto})	1.755 m
Inlet port height ($h^{p,in}$)	1.6 m
Outlet port height ($h^{p,out}$)	0.26 m

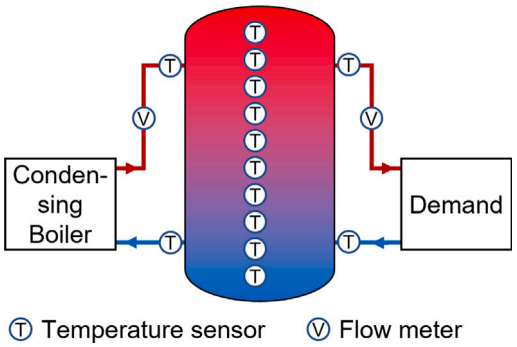

Fig. 5. Schematic diagram of the experiment setup with a condensing boiler, TES and heat demand unit connected by the supply (red) and return (blue) pipe. Temperature sensors and flow meters measure the temperature distribution of the TES and charging/discharging.

4. Validation

The CLV model is validated in this section with experimental data, acquired in the CoSES laboratory [19].

4.1. Experimental setup

The TES is charged and discharged in the CoSES laboratory with a condensing boiler and a heat sink emulator, as described in [29]. We use a Wolf BSP-800 TES with the parameters shown in Table 1.

The TES is charged with a Wolf CBG-2/20 condensing boiler with a nominal power of 20 kW. Its internal control logic aims to maintain a temperature difference between supply and return of 20 K.

The heat demand for discharge is emulated with the aim of replicating the behavior of a real heating system, as described in [19]. Heat can be extracted from the system with a heat exchanger connected to a cooling system. A control valve in the cooling system controls the outlet temperature of the heat exchanger according to the return temperature of the heating system (e.g. 45 °C for radiators or 30 °C for space heating systems). To avoid too high temperatures in the heating system, a commercial device with a mixing valve and pump controls the temperature according to the requirements (e.g. 60 °C for radiators or 40 °C for space heating systems). It further provides the required volume flow.

Fig. 5 shows the schematic representation of the experimental setup. The red lines in the figure represent the warm supply line, the blue lines the cold return line.

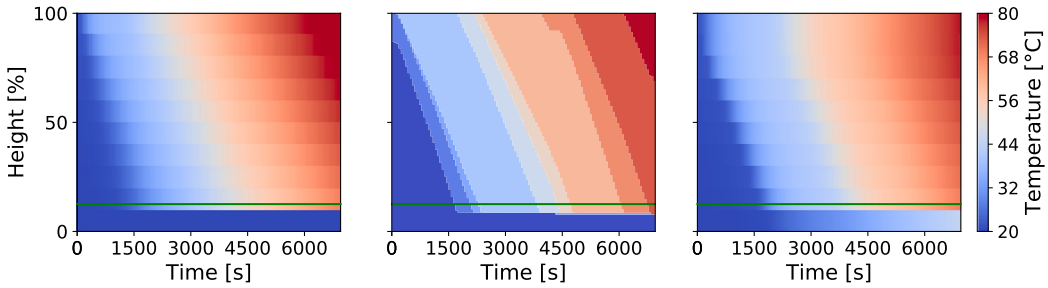

Fig. 6. Heatmaps of the temperature distribution within the TES during the charging experiment for the CLV model (left), CLT model (center) and experiment (right). The green line marks the outlet port height.

Temperature sensors (T) in the supply and return line and volume flow meters (V) measure the charging and discharging rate. Furthermore, 10 temperature sensors are evenly distributed over the surface of the TES between the outside wall and the thermal insulation to measure the temperature distribution. The following sensors are used in the CoSES laboratory:

- Temperature measurement:
  4-wire PT100 resistance sensors of quality class A with a tolerance of $\pm(0.15\,\mathrm{K} + 0.002 \cdot T)$ [30]
- Water flow measurement:
  Electromagnetic flowmeter 'Proline Promag E 100' with a measurement diameter of 15 mm and a tolerance of $\pm 0.5\,\% \pm 1\,\mathrm{mm/s}$ [31].

We perform the following experiments to validate different operation states of the TES models:

- Experiment 1: Convective heat exchange with fixed temperature difference. The TES is charged by a condensing boiler, where the temperature difference between supply and return varies between 22 K and 15 K.
- Experiment 2: Convective heat exchange with fixed inlet temperature. A heat sink with a constant return temperature is used. The return temperature is at 45 °C or 30 °C to represent radiator and space heating.

4.2. Validation results

The behavior of the proposed model is compared to the experimental data and to an extended CLT model from Muschick et al. [16] (see Appendix A). The initial model state and resulting temperatures are calculated as shown in Appendix B. The models are parametrized according to Table 1. Furthermore, the characterization measurements show a buoyancy constant ($const^{buoy}$) of 0.9 kW/K and a thermal transmittance (U) of 0.35 $\mathrm{W/m^2\,K}$.

The layer connected to the inlet and outlet port can be calculated according to Eq. (23) for the CLV model. For the validation with 10 layers, the inlet port was connected to layer 9 and the outlet port was connected to layer 2.

$$l^p = \mathrm{floor}(h^p / h^{sto} \cdot n_l) + 1 \tag{23}$$

Fig. 6 shows the comparison of the temperature distribution within the TES for experiment 1 in a heatmap plotting the temperature at different heights against the experiment time. Both models show similar temperature behavior, the hot water flowing into the upper part of the TES heats it from top to bottom over time. The heating occurs in 'waves' with a temperature difference of 20 K caused by the internal control of the condensing boiler. The behavior within the TES is modeled well by both models, except for the dead volume at the bottom, similar to the results of De la Cruz-Loredo et al. [24]. They explain this effect by a possible deformation of the water stream at the cold outlet, which generates an unexpected and unwanted mixing that cannot be captured by 1D TES models. Due to its structure with fixed temperature layers, the temperature distribution of the CLT is more homogeneous than the CLV.

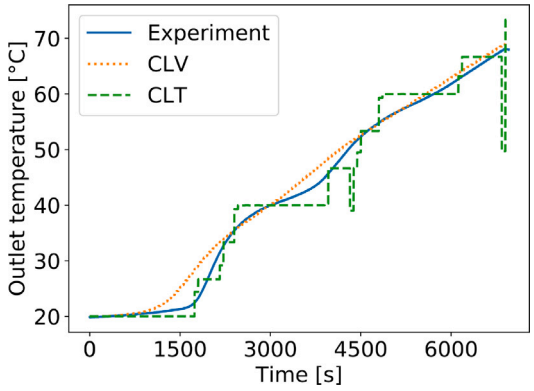

Fig. 7. Storage outlet temperature of the condensing boiler experiment and different model types.

The outlet temperature of the TES is illustrated in Fig. 7. The figure demonstrates that the CLV model adequately represents the temperature behavior but encounters difficulties in reproducing rapid temperature changes. This limitation is attributed to the CLV model's imperfect representation of the thermocline within the TES, which leads to blurred temperature transitions between the hot and cold layers. The CLT model performs better in capturing these fast changes, yet it falls short in representing the overall temperature behavior due to its discrete layer temperatures.

Table 2 provides a quantitative comparison of the models based on the Root Mean Squared Error (RMSE) of the temperatures within the TES, its outlet temperature and the State of Charge (SOC). As seen in Fig. 6, layer 1 significantly deviates from the experimental measurements due to the aforementioned disturbances caused by the deformation of the water stream in the dead volume, resulting in a high error. This discrepancy leads to a slight overestimation of the outlet temperature and a too high temperature in layer 10. Since these layers are not located in the active area of the inlet and outlet ports, they do not affect the validity of the model, whose main objective is to accurately model the outlet temperature to the connected heat generators and the heat demand. For layers 2 to 9 and the outlet temperature, the error is small, with the CLV model outperforming the CLT model, and both models exhibiting comparable accuracy to the 12-node simulation model used as benchmark by De la Cruz-Loredo et al. [24]. For completeness, the SOC was also analyzed. However, since the charging power is identical, any deviations are due to discretization errors and inaccurately modeled losses. The low RMSE indicates that these discrepancies can be ignored.

Table 2
Validation results: RMSE of the layer temperatures within the TES (T_{layer}), the outlet temperature (T_{out}) and the SOC.

Model	RMSE T_{layer} [K]										RMSE T_{out} [K]	RMSE SOC [%]
	1	2	3	4	5	6	7	8	9	10		
CLV	13.34	1.33	1.15	1.13	1.17	1.48	1.70	2.04	2.90	4.56	1.87	0.19
CLT	8.55	1.95	1.99	1.96	1.95	2.04	2.15	2.33	2.59	4.36	2.86	0.39

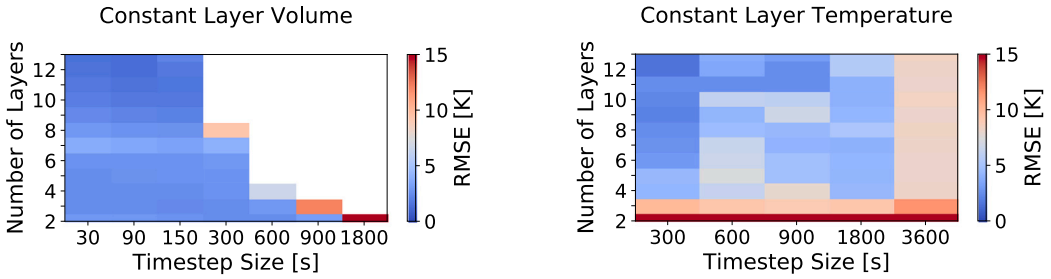

(a) (b)

Fig. 8. Convective heat exchange with constant temperature difference: RMSE plotted against the number of layers and time step size for (a) CLV and (b) CLT.

4.3. Model parameter tuning

After validating the 1D TES models, we want to analyze the influence of the time step size and the layer numbers on the accuracy and computation time. To compare them in their use case scenario, they are integrated into an optimization model, where the charging/discharging power and the temperature difference or return temperature is specified as time series, according to the measurements of the experiment. The models are implemented in Pyomo [32,33] and solved with gurobi [34]. The analysis is run on a laptop with an AMD Ryzen™ 5 5500U with 6 cores @ 2.10 GHz, 16 GB RAM.

As the outlet temperature of the TES is a good metric of the system accuracy, the models are compared based on the RMSE of the outlet temperature. A mixed TES model is used as a minimum benchmark, as it is often used in optimization problems.

4.3.1. Experiment 1: Convective heat exchange with fixed temperature difference

Fig. 8 shows the accuracy of the models for experiment 1, plotted against the time step size and the number of layers.

The white area in Fig. 8(a) shows model configurations, where the volume flow into the TES per time step exceeds the maximum volume of the layers. As mentioned in Section 3.1, this leads to model inaccuracies and/or the model becoming infeasible. To prevent this, the time step size must be small enough and/or the number of layers low enough. We can further see that the time step size has a minor influence on the RMSE.

In contrast, CLT models do not have restrictions to obtain a feasible model. We can see that a good solution can already be found with a time step size of 1800 s if the number of layers is sufficiently high (Fig. 8(b)).

Fig. 9 compares the effects of different number of layers. Therefore, time step sizes of 90 and 300 s for the CLV, and 300 and 900 s for the CLT are chosen.

We can see that the accuracy of CLV models depends not only on the number of layers but also on how the layers are distributed. It is important to select the number of layers so that the location of the ports is optimal. For example, the model with 7 layers performs worse than the model with 6 layers, despite having more layers. This can be explained with Fig. 10, where the position of the outlet port is shown. The 7-layer configuration suffers from having the outlet port of the TES positioned close to the bottom, which reduces the model accuracy for charging operations. This can be explained by the deformation

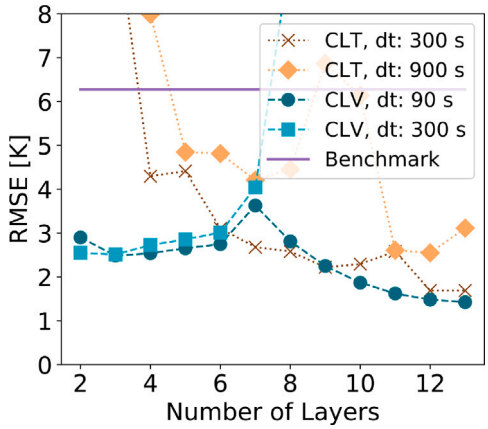

Fig. 9. Influence of the number of layers and time step size (dt) on the accuracy of convective heat exchange with constant temperature.

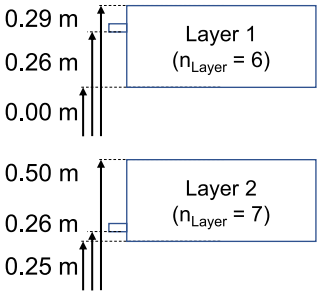

Fig. 10. Position of the outlet port for convective heat exchange.

of the water stream, similar to the inaccurate modeling of the dead volume in Section 4.2. This disturbance mixes the water layer below the port. If the connection is not to close to the bottom of a layer, the deformation of the water flow does not affect multiple layers, improving the accuracy of the model. A variable layer size can enable this already with a smaller number of layers but must be adapted for each storage integration.

Furthermore, the CLT model with a time step size of 900 s only improves slightly after a minimum number of 4 layers, corresponding to a temperature difference of 20 K. This temperature difference is

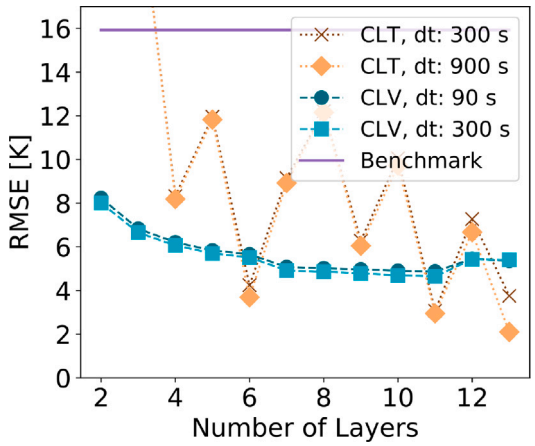

Fig. 11. Convective heat exchange with constant storage inlet temperature: influence of the number of layers on the accuracy.

significantly higher than the average temperature difference of the processes of 15 K. This allows a selection of fewer layers than the minimum temperature difference indicates for decent results, leading to less integer variables and consequently decreasing the computation time.

4.3.2. Experiment 2: Convective heat exchange with fixed inlet temperature

CLV models cannot account for constant inlet temperatures and varying temperature differences because they are modeled with a constant temperature difference to prevent nonlinearities (see Eq. (22d)). Fig. 11 shows that the accuracy of the CLV model for the experiment with constant inlet temperature behaves different to Section 4.3.1 and only changes slightly with varying time step size or layer numbers. Although the RMSE is higher compared to the results in Section 4.3.1, it remains satisfactory. This observation confirms the validity of the simplification made in Section 3.5.

We can further see that the accuracy of the CLT model depends strongly on the number of layers, but only weakly on the time step size. The number of layers should be so that the layer temperature is close to the expected inlet and outlet temperatures of the process.

4.3.3. Computation time for model integration

Fig. 12 shows the computation time for the convective heat exchange with fixed temperature difference (a) and fixed inlet temperature (b). Both graphs show a similar behavior for the models. With a small number of layers, the computational effort for the CLT models is lower, but it increases strongly with increasing layer number or smaller time step size. This indicates, that the proposed new CLV model scales better.

5. Case study

In the previous section we validated the TES models with experimental data to show the accuracy of the TES models. In this section we conduct a case study with EMS to demonstrate the applicability of the models and their energy and cost saving potential. The results are benchmarked against an EMS with a mixed TES model.

We consider a HP, connected to a TES that decouples heat generation and demand as shown in Fig. 13. Domestic Hot Water (DHW) is provided by the top half of the TES and the space heating system is connected to the bottom. A three-way valve can switch the heat generation from the HP to charge the top or bottom of the TES. The TES parameters are the same as in the validation (Section 4), the height of the ports are according to Table 3.

Table 3
Port height for the case study.

p_1	0.26 m
p_2	0.63 m
p_3	1.03 m
p_4	1.70 m

Table 4
Results of the case study: Costs and energy consumption of the different model types.

	Mixed TES	CLV 5 layers	CLT 5 layers
Costs	100%	80%	76%
Energy consumption	100%	83%	82%

The implementation of the EMS is based on Section 3.5 and Appendix A.5 and published with the TES models on gitlab. The CLV optimization problem is solved using NEOS [35] and the conopt solver and the mixed TES and CLT models were solved with gurobi [34].

The heating system must always provide heat at the required temperature, even if the EMS controls the system poorly. To guarantee this, a rule-based low-level control operates in the background. This control automatically overrides the EMS setpoints if temperatures fall below predefined minimum limits due to model inaccuracies. The low-level control has the following parameters:

- HP: switched on at 100 % modulation, when $T_{Storage,top} < 50\,°C$ or $T_{Storage,middle} < 40\,°C$
- Three-way valve:
  DHW is produced at higher priority.

The optimization is conducted over 12 h. The time step size is 300 s, both TES models have 5 layers. The electricity price and demand are time dependent and can be seen in Fig. 14 (top).

We use a simulation model based on the experimentally validated CoSES ProHMo library [25] to evaluate the different EMS. To ensure consistent and comparable results, any difference in energy content before and after the simulation is adjusted using the average electricity costs (1.32 pu) and an average Coefficient of Performance (COP) of 4.

The results are presented in Table 4, where energy costs and total electricity consumption are normalized using the values of the mixed TES model. The study shows that the stratified TES models result in a cost reduction of 20 % and 26 % for the CLV and CLT model respectively. Although the CLT model shows lower accuracy in Section 4, it has higher cost savings, which indicates that the CLV generator model should be further improved.

Fig. 14 analyzes the setpoints and electric power demand of the HP in detail. It shows that in contrast to the CLV model, the low-level control overwrites the input signals of the mixed TES model more frequently (e.g. around 1:00, 2:45, 7:30). This leads to higher costs and reduced reliability of the scheduled plan, as heat must be generated off-schedule at times when prices are high. It further leads to the problem that the actual energy content of the TES deviates from the predicted energy content of the optimization.

Another advantage of the CLV model is that it represents the temperature-dependent efficiency better, while the mixed TES model underestimates the temperature influence. This results in the mixed TES EMS scheduling a high heat generation during a period of low electricity costs (3:00 to 6:00). However, the decrease in COP due to the high return temperature cancels the savings from lower electricity prices. The bottom plot of Fig. 14 shows that the COP of the mixed TES model is consistently lower than that of the CLV model during the period of low electricity costs.

6. Discussion

This section explores the advantages and disadvantages of the CLV model compared to other TES models. Both 1D TES models offer

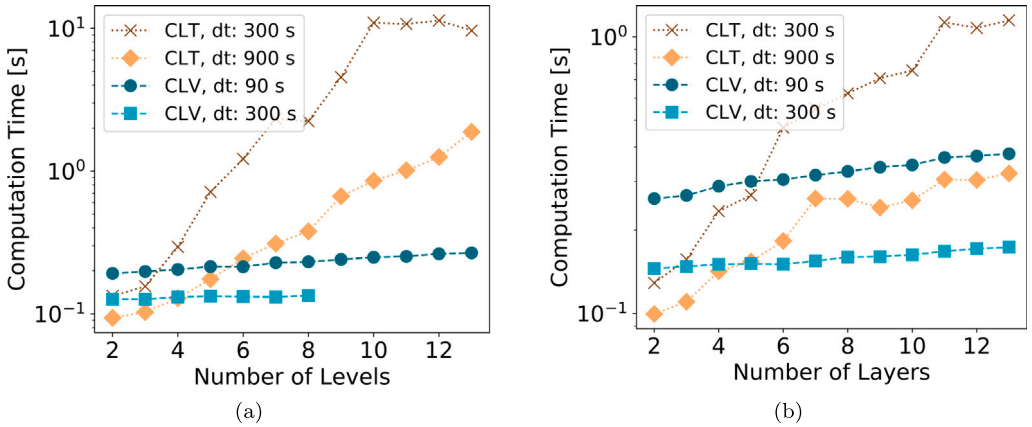

Fig. 12. Influence of the number of layers on the computation time of the convective heat exchange with constant temperature difference (a) and constant inlet temperature (b).

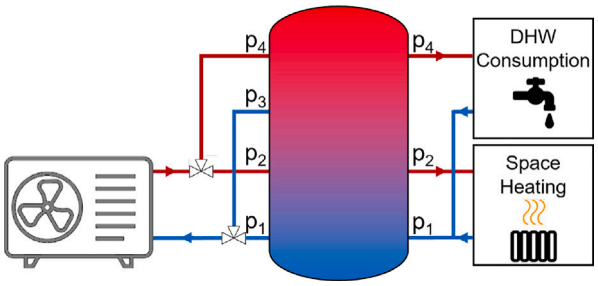

Fig. 13. Energy system of a residential building.

a precise representation of internal TES behavior compared to commonly used mixed TES models. The proposed CLV TES model exhibits slightly higher accuracy compared to the CLT model with a lower computational burden. This suggests that the CLV model scales better.

The increased accuracy of the 1D TES models leads to notable cost and energy reductions, as demonstrated in the case study. The closer alignment of the actual system behavior with reality further reduces the need for low-level control interventions, thereby additionally enhancing operation planning. Despite the slightly lower accuracy in the validation, the CLT model exhibits slightly higher cost savings. This indicates that the heat generator and consumer models of the optimization problem with the CLV model hold potential for improvement, but these models were not the subject of this publication.

However, the more detailed 1D TES models come with an increased computational burden due to the inclusion of the internal TES behavior. There are workarounds that might mitigate this limitation: Users could employ a variable layer size for CLV models and intelligently dimension the height of each layer based on their connection positions. As shown in the experimental validation, the position of the outlet port within the layer has an influence on the accuracy (see Fig. 10). Intelligent dimensioning of the different layers allows the outlet ports within the layer to be optimally positioned for the respective use case. This might lead to similar or higher accuracy with fewer layers, reducing the computational burden. Another potential workaround is to implement a rolling horizon optimization, with varying model accuracy as proposed by Muschick et al. [16]. For the control horizon, a high accuracy is required, but afterwards fewer layers or bigger time step sizes in later steps might be sufficient.

Furthermore, the increased complexity of the TES model poses challenges in its implementation, making it more difficult for users to adopt. To promote accessibility and facilitate the utilization of the proposed TES models, the models and their implementation in optimization problems is available in the open access repositories. This allows users to integrate the TES models into their own optimization models or explore different modeling examples.

7. Conclusion and outlook

In this article, we have proposed and validated a novel approach for modeling stratified TES systems in predictive control. The model is used in a case study as part of an EMS that applies optimization to minimize operational costs. Another application, as suggested by Muschick et al. [16], can be in capacity expansion planning, where a lack of temperature information and the resulting incorrectly applied control strategies can lead to incorrect sizing.

By formulating the TES model with multiple layers of constant volume and changing temperature (CLV), our approach accurately represents essential physical phenomena, including the temperature distribution within the TES, losses to the environment, and charging/discharging dynamics. Furthermore, to ensure low computation burden, all constraints of the model are formulated as quadratic or simpler constraints.

The experimental validation of the CLV model has yielded promising results, showcasing high accuracy, and justifying the simplifications made in the model. The model demonstrates comparable accuracy to 1D simulation models from commercial software. Through a parameter analysis, we have shown that a larger time step size and/or a smaller number of layers still leads to acceptable results at a lower computational burden. This allows the parametrization of the model depending on the application requirements and available computing power.

A case study has demonstrated that detailed modeling of the storage stratification is advantageous in applications where precise temperature information has a high impact, such as HPs, or systems extracting heat at multiple temperature levels. In such contexts, EMSs based on simple mixed TES models often fail to provide accurate setpoints, requiring rule-based low-level controllers to intervene more frequently to ensure user comfort. Combined with a worse representation of the temperature-dependent efficiency, this leads to higher overall costs.

To fully leverage the strengths of the CLV TES model, future work can focus on improving heat generator models that represent the influence of varying inlet temperature and power modulation on their efficiency. This is especially advantageous for heat generators with a strong temperature and power modulation influence such as HPs, or to optimize the interaction of multiple heat generators with different temperature-dependencies.

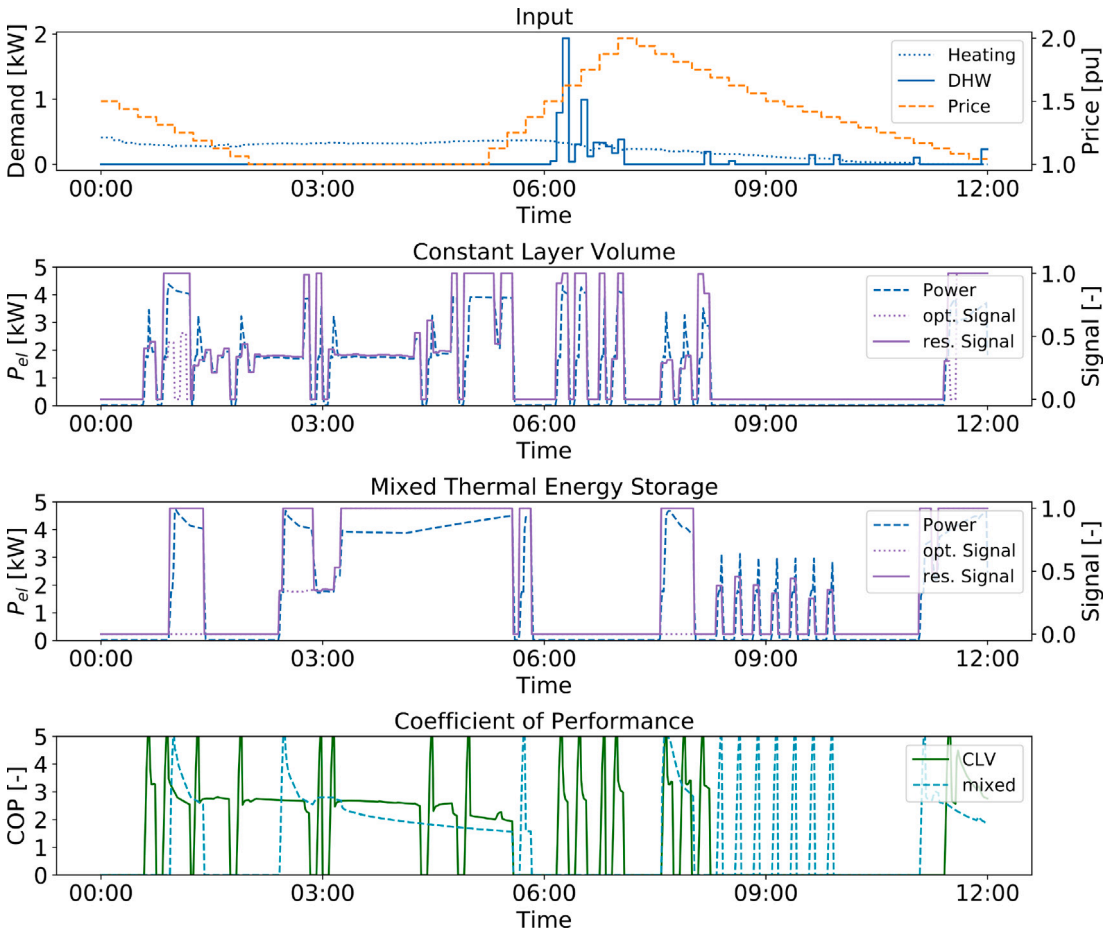

Fig. 14. Time series of demand and electricity price (top), control setpoints and electricity consumption of the CLV and mixed TES model and COP of both models (bottom). The setpoints of the HP (res. Signal) are the same as the setpoints from the optimization (opt. Signal), except if the low-level control overwrites it due to too low storage temperatures.

CRediT authorship contribution statement

Daniel Zinsmeister: Conceptualization, Visualization, Writing – original draft, Editing. **Peter Tzscheutschler:** Conceptualization, Writing – review, Supervision, Project administration, Funding acquisition. **Vedran S. Perić:** Conceptualization, Writing – review, Supervision, Project administration, Funding acquisition. **Christoph Goebel:** Conceptualization, Writing – review, Supervision, Project administration, Funding acquisition.

Declaration of competing interest

The authors declare that they have no known competing financial interests or personal relationships that could have appeared to influence the work reported in this paper.

Data availability

Data will be made available on request.

Declaration of Generative AI and AI-assisted technologies in the writing process

During the preparation of this work the authors used ChatGPT in order to check and improve the comprehensibility of the paper. After using this tool/service, the authors reviewed and edited the content as needed and take full responsibility for the content of the publication.

Acknowledgments

This project was funded by the Federal Ministry for Economic Affairs and Climate Action, Germany (FKZ: 03EN3032A). The work of Vedran S. Perić was supported by Deutsche Forschungsgemeinschaft (DFG), Germany through "Optimal Operation of Integrated Low-Temperature Bidirectional Heat and Electric Grids (IntElHeat)" under project number 450821044. The construction of the CoSES laboratory was supported by Deutsche Forschungsgemeinschaft (DFG), Germany through the project "Flexible reconfigurable microgrid laboratory" under project number 350746631.

Appendix A. Stratified thermal energy storage model with constant layer temperature

The formulation of the CLT model with layers of fixed temperature and varying content is described in this appendix, which extends the model of Muschick et al. [16]. Fig. A.15 shows an example of the layering within the TES.

The volume of each layer depends on the volume of the last time step and can change due to convection ($dV_{l,t}^{conv}$, see Appendix A.2), conduction ($dV_{l,t}^{cond}$ see Appendix A.3) and heat losses ($dV_{l,t}^{loss}$ see Appendix A.4):

$$V_{l,t} = V_{l,t-1} + dV_{l,t}^{conv} + dV_{l,t}^{cond} + dV_{l,t}^{loss} \tag{A.1}$$

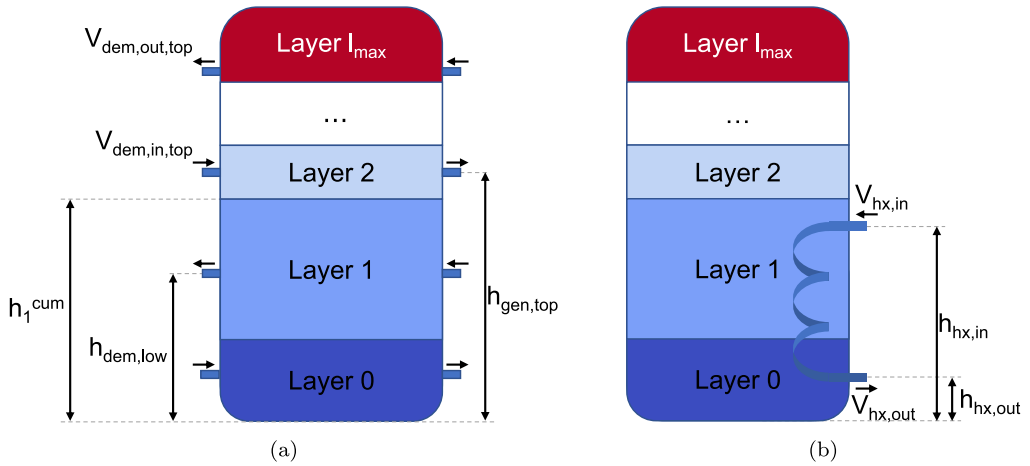

Fig. A.15. Example of the layering of a CLT. Figure (a) shows the ports of the TES with the flow direction and the height of the lower outlet port of the demand side (e.g. for heating) and the upper outlet port of the heat generator. Figure (b) shows the heat exchanger and its inlet- and outlet height, which affects in this example layer 0 and 1.

A.1. Active connection

Muschick et al. [16] show that if water can be drawn from all layers, this leads to unrealistic results. Therefore, they introduced an additional binary term (δ) to ensure that water is only drawn from layers within reach of the connection.

To define active layers, the cumulative height of the layers h_l^{cum} (see h_1^{cum} in Fig. A.15(a)) is calculated:

$$h_{l,t}^{cum} = \frac{1}{V^{sto}} \cdot \sum_{i=0}^{l} V_{i,t} \tag{A.2}$$

Layer l is active, when the height of the outlet connection (h^x) is smaller than the cumulative height of layer l ($h_{l,t}^{cum}$, see Eq. (A.3)) and is bigger than the cumulative height of layer $l-1$ ($h_{l-1,t}^{cum}$, see Eq. (A.4)). In the example in Fig. A.15(a), layer 1 is active, since $h^{dem,low} < h_1^{cum}$ and $h^{dem,low} > h_0^{cum}$.

$$\delta_{l,t}^{p,s} = \begin{cases} 1 & \text{if } h^p \le h_{l,t}^{cum} \\ 0 & \text{otherwise} \end{cases} \tag{A.3}$$

$$\delta_{l,t}^{p,b} = \begin{cases} 1 & \text{if } h^p \ge h_{l-1,t}^{cum} \\ 0 & \text{otherwise} \end{cases} \tag{A.4}$$

To use these constraints in a Mixed Integer Linear Programming (MILP) optimization, we formulate them as follows, where Eq. (A.5) to (A.8) are the MILP formulation of Eqs. (A.3) and (A.4) respectively. We use a variable M, which must be set carefully. If M is too low, it could result in both auxiliary variables y^1, or y^2 not being set to zero, too high a value could result in a loss of precision and numerical instabilities.

$$h_{l,t}^{cum} - y_{l,t}^{1,p,s} + y_{l,t}^{2,p,s} = h^p \tag{A.5}$$

$$h_{l,t}^{cum} + y_{l,t}^{1,p,b} - y_{l,t}^{2,p,b} = h^p \tag{A.6}$$

$$y_{l,t}^{1,p,\{s,b\}} \le \delta_{l,t}^{p,\{s,b\}} \cdot M \tag{A.7}$$

$$y_{l,t}^{2,p,\{s,b\}} \le (1 - \delta_{l,t}^{p,\{s,b\}}) \cdot M \tag{A.8}$$

with $\delta \in [0,1],\ y^1, y^2 \in \mathbb{R}_0^+$

Due to the time discretization, it can happen that the active temperature layer is completely depleted within one time step, which would stop heat extraction from the TES. To prevent this model inaccuracy, Muschick et al. [16] considered the current and last time step to define active layers as done in Eqs. (A.9) and (A.11). The implemented MILP formulation of the 'and' and 'or' statement can be found in Eqs. (A.10) and (A.12).

$$\delta_{l,t}^{p} = \delta_{l,t}^{p,s\ comb} \text{ and } \delta_{l,t}^{p,b\ comb} \tag{A.9}$$

$$0 \le -2 \cdot \delta_{l,t}^{p} + \delta_{l,t}^{p,s\ comb} + \delta_{l,t}^{p,b\ comb} \le 1 \tag{A.10}$$

$$\delta_{l,t}^{p,\{s,b\}\ comb} = \delta_{l,t}^{p,\{s,b\}} \text{ or } \delta_{l,t-1}^{p,\{s,b\}} \tag{A.11}$$

$$0 \le 2 \cdot \delta_{l,t}^{p,\{s,b\}\ comb} - \delta_{l,t}^{p,\{s,b\}} - \delta_{l,t-1}^{p,\{s,b\}} \le 1 \tag{A.12}$$

A.2. Convective heat exchange

CLT models consider convective heat exchange only through the ports and not between layers. The convective heat exchange between layers is considered indirectly by moving the position of the layer up or down. Muschick et al. [16] assumed the inlet to be at the correct temperature layer or through stratification lances to prevent buoyancy and thus simplify the problem.

The change of the layer volume due to convection is defined as:

$$dV_{l,t}^{conv} = V_{l,t}^{p,in} - V_{l,t}^{p,out} \tag{A.13}$$

A.3. Conductive heat exchange

Muschick et al. [16] modeled axial heat conduction between layers, but neglected conductive heat exchange. Conductive heat exchange cannot be included directly in CLTs, since conductive heat sources exchange thermal energy without any mass flow and can affect multiple layers at the same time.

Experiments in the CoSES laboratory [29] showed that axial heat conduction has little effect. Since it requires several additional binary variables to formulate them, they are neglected in this paper.

To model conductive heat exchange, we extend the model proposed by Muschick et al. [16] by employing the following simplification: When the TES is being charged, the bottom-most layer, which is in direct contact with the conductive heat source, is heated and transitions to a higher layer. The temperature of the lowest layer determines the outlet temperature of the heat exchanger. For discharging, the same applies vice versa. The inlet and outlet connections are determined as described in Appendix A.1.

Fig. A.15(b) shows an example of a heat exchanger, integrated in a TES. The change of the layer volume due to conductive heat sources is defined by Eqs. (A.14) and (A.15).

$$dV_{l,t}^{cond} = V_{l-1,t}^{hx} - V_{l,t}^{hx} \tag{A.14}$$

$$V_{l,t}^{hx} = \frac{Q_t^{g_{hx}} \cdot \eta(g_{hx}, l)}{\rho \cdot c_p \cdot \Delta T} \tag{A.15}$$

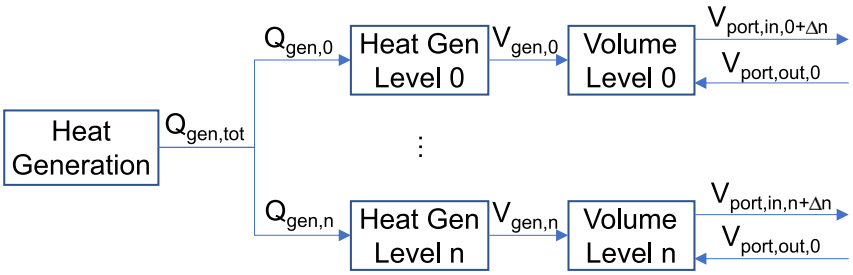

Fig. A.16. Structure of the EMS for the CLT. Heat is discretized into several layers with different temperatures and efficiencies.

A.4. Losses

Losses in the CLT decrease the content of the layer. To keep the mass balance, this means that the lower layer increases by the same amount. The change of volume caused by losses can be calculated as:

$$dV_{l,t}^{loss} = V_{l+1,t-1} \cdot (1-(1-d_{l+1})^{\Delta t}) - V_{l,t-1} \cdot (1-(1-d_l)^{\Delta t}) \tag{A.16}$$

In this equation, the losses are not calculated as a function of the insulation, but by the hourly discharge rate d_l, which is calculated based on measurements from the CoSES laboratory [29].

A.5. Integration into energy management systems

To integrate the TES model into an EMS, heat must be split into discrete layers as shown in Fig. A.16. The advantage of this approach compared to the CLV is that the efficiency for each temperature layer is calculated in advance, which allows to model nonlinear efficiency behavior.

Similar to Section 3.5, we provide an example for an optimization based EMS that minimizes the operation costs C^{op} associated with heat generation Q from all heat generators g within the time horizon $t \in [0 : t^{end}]$ (Eq. (A.17a)).

The capacities of the heat generators are constrained by Eq. (22b) to account for their minimum and maximum capacity, where on/off behavior can be modeled using an additional integer variable δ_t^g. Eq. (A.17c) models the total heat demand ($Q_t^{d,tot}$) based on the forecasted demand ($Q_t^{d,fc}$). To calculate the total heat of different processes (denoted as x for heat generator or demand) Eq. (A.17d) sums up the heat across all layers, as shown in Fig. A.16. In this equation, $l_{x,max}$ and $l_{x,min}$ impose temperature constraints on both heat generation and demand. The binary variable $\delta_{l,t}^x$ in Eq. (A.17e) ensures that only active processes can exchange heat (see Appendix A.1).

$$\text{minimize} \quad \sum_{t=0}^{t^{end}} \sum_{g} C^{op}(Q_t^{g,tot}) \tag{A.17a}$$

$$\text{subject to} \quad \delta_t^g \cdot Q^{g_x,max} \le Q_t^{g,tot} \le \delta_t^g \cdot Q^{g_x,max} \tag{A.17b}$$

$$Q_t^{d,tot} = Q_t^{d,fc} \tag{A.17c}$$

$$Q_t^{x,tot} = \sum_{l=l_{x,min}}^{l_{x,max}} Q_{l,t}^x \tag{A.17d}$$

$$Q_{l,t}^x \le \delta_{l,t}^x \cdot Q^{x,max} \tag{A.17e}$$

$$Q_{l,t}^x \cdot \eta(T_t^x) = V_{l,t}^{conn_x,out} \cdot \rho \cdot c_p \cdot \Delta T^x \tag{A.17f}$$

$$\Delta T^x = \Delta^x \cdot \Delta T_l \tag{A.17g}$$

$$\Delta T^x = (l - l^{x,conn,in}) \cdot \Delta T_l \tag{A.17h}$$

$$V_{l,t}^{conn_x,\Delta T,in} = V_{l,t}^{conn_x,out} + \Delta l^x \tag{A.17i}$$

$$V_{l,t}^{conn_x,T,in} = \sum_{l=l_{x,min}}^{l_{x,max}} V_{l,t}^{conn_x,out} \tag{A.17j}$$

$$V_{l,t} = V_{l,t-1} + dV_{l,t}^{conv} + dV_{l,t}^{cond} + dV_{l,t}^{loss} \tag{A.17k}$$

$$\text{with} \quad Q_{l,t}^x, V_t^x \in \mathbb{R}_0^+ \tag{A.17l}$$

The volume flow through the processes ($V_t^{conn_x,out}$) is influenced by various factors, as described in Eq. (A.17f) and formulated the same way as in Section 3.5. In contrast to the CLV model, the temperature difference can either be constant (Eq. (A.17g)) or a fixed storage inlet temperature (Eq. (A.17h)). If the temperature difference is constant, the difference between the outlet layer and the inlet layer is constant (Eq. (A.17i)). Otherwise, the return flow has a fixed temperature, and the flow of the corresponding layer is equal to the sum of the outlet flows from all layers (Eq. (A.17j)).

Lastly, Eq. (A.17j) links heat generation, heat demand and the CLT model, reproducing the temperature dynamics within the TES.

Appendix B. Conversion between experimental measurements and model predictive control

To initialize the content or temperature of each layer, we assume that each temperature sensor i covers the same volume of the TES. The number of temperature sensors n_{sens} for the validation is 10.

B.1. Constant layer volume models

Initial temperature

The conversion from measured temperatures T_i to the layer temperature T_l is described in Eqs. (B.1) and (B.2), with $A = \frac{l}{l_{max}} - \frac{l-1}{l_{max}}$ as the layer size of the model and $S = \frac{i}{n_{sens}} - \frac{i-1}{n_{sens}}$ as the layer size of the sensor.

$$T_{n,i} = \begin{cases} \frac{1}{l_{max}} \cdot T_i & \text{if } A \text{ in } S \\ \frac{1}{n_{sens}} \cdot T_i & \text{if } S \text{ in } A \\ |\frac{i}{n_{sens}} - \frac{l}{l_{max}}| \cdot T_i & \text{if } A \text{ part of } S \\ 0 & \text{otherwise} \end{cases} \tag{B.1}$$

$$T_l = l_{max} \cdot \sum_{i=1}^{n_{sens}} T_{l,i} \tag{B.2}$$

B.2. Constant layer temperature models

Initial temperature

The conversion from measured temperatures T_i to the layer content V_l, is calculated according to Eqs. (B.3) and (B.4):

- All temperatures below the temperature of the lowest layer are added to the lowest layer (Eq. (B.3) line 1).
- All temperatures above the temperature of the highest layer are added to the highest layer (Eq. (B.3) line 2).
- Temperatures between the temperatures of two layers are divided between the two layers (Eq. (B.3) line 3 and 4).

$$V_{l,i} = \begin{cases} 1/n_{sens} & \text{if } l = 0 \text{ and } T_l \geq T_i \\ 1/n_{sens} & \text{if } l = l_{max} \text{ and } T_l < T_i \\ (1 - (T_i - T_l)/\Delta T)/n_{sens} & \text{if } T_l < T_i < T_l + \Delta T \\ (T_i - T_{l-1})/(\Delta T \cdot n_{sens}) & \text{if } T_{l-1} < T_i < T_{l-1} + \Delta T \\ 0 & \text{otherwise} \end{cases} \tag{B.3}$$

$$V_l = \sum_{i=1}^{n_{sens}} V_{l,i} \tag{B.4}$$

Outlet temperature

The outlet flow of the CLT is a mix of the temperature layers from which water was drawn. The resulting temperature can be calculated as follows:

$$T_{out} = \sum_{i=1}^{l_{max}} \frac{T_i \cdot V_{out,i}}{V_{sto}} \tag{B.5}$$

Layer Temperature

The layer temperature can be calculated as a function of the height of the sensor (h_n) and of the layer volume (h_l) as follows:

$$T_{n,l} = \begin{cases} T_l & \text{if } h_l \leq h_n \text{ and } h_{n+1} \leq h_{l+1} \\ (h_l - h_n) \cdot T_l & \text{if } h_l \leq h_n \leq h_{l+1} \\ (h_{l+1} - h_l) \cdot T_l & \text{if } h_n \leq h_l \text{ and } h_{l+1} \leq h_{n+1} \\ (h_{n+1} - h_l) \cdot T_l & \text{if } h_n \leq h_l \leq h_{n+1} \\ 0 & \text{otherwise} \end{cases} \tag{B.6}$$

$$T_n = \sum_{l=1}^{l_{max}} \frac{T_{n,l} \cdot n_{max}}{V_{sto}} \tag{B.7}$$

References

[1] IEA, The Future of Heat Pumps, IEA, Paris, 2022, URL https://www.iea.org/reports/the-future-of-heat-pumps.

[2] S. Paardekooper, R.S. Lund, B.V. Mathiesen, M. Chang, U.R. Petersen, L. Grundahl, A. David, J. Dahlbæk, I.A. Kapetanakis, H. Lund, N. Bertelsen, K. Hansen, D.W. Drysdale, U. Persson, Heat roadmap europe 4: Quantifying the impact of low-carbon heating and cooling roadmaps, 2018.

[3] T.Q. Péan, J. Salom, R. Costa-Castelló, Review of control strategies for improving the energy flexibility provided by heat pump systems in buildings, J. Process Control 74 (2019) 35–49, http://dx.doi.org/10.1016/j.jprocont.2018.03.006.

[4] S. Candas, B. Reveron Baecker, A. Mohapatra, T. Hamacher, Optimization-based framework for low-voltage grid reinforcement assessment under various levels of flexibility and coordination, Appl. Energy 343 (2023) 121147, http://dx.doi.org/10.1016/j.apenergy.2023.121147, URL https://www.sciencedirect.com/science/article/pii/S0306261923005111.

[5] J. Tarragona, A.L. Pisello, C. Fernández, A. de Gracia, L.F. Cabeza, Systematic review on model predictive control strategies applied to active thermal energy storage systems, Renew. Sustain. Energy Rev. 149 (2021) 111385, http://dx.doi.org/10.1016/j.rser.2021.111385.

[6] R. Palma-Behnke, C. Benavides, F. Lanas, B. Severino, L. Reyes, J. Llanos, D. Saez, A microgrid energy management system based on the rolling horizon strategy, IEEE Trans. Smart Grid 4 (2) (2013) 996–1006, http://dx.doi.org/10.1109/TSG.2012.2231440.

[7] R. Hermansen, K. Smith, J.E. Thorsen, J. Wang, Y. Zong, Model predictive control for a heat booster substation in ultra low temperature district heating systems, Energy 238 (2022) 121631, http://dx.doi.org/10.1016/j.energy.2021.121631.

[8] R. Renaldi, A. Kiprakis, D. Friedrich, An optimisation framework for thermal energy storage integration in a residential heat pump heating system, Appl. Energy 186 (2017) 520–529, http://dx.doi.org/10.1016/j.apenergy.2016.02.067, URL https://www.sciencedirect.com/science/article/pii/S0306261916302045.

[9] Y.M. Han, R.Z. Wang, Y.J. Dai, Thermal stratification within the water tank, Renew. Sustain. Energy Rev. 13 (5) (2009) 1014–1026, http://dx.doi.org/10.1016/j.rser.2008.03.001.

[10] F. D'Ettorre, P. Conti, E. Schito, D. Testi, Model predictive control of a hybrid heat pump system and impact of the prediction horizon on cost-saving potential and optimal storage capacity, Appl. Therm. Eng. 148 (2019) 524–535, http://dx.doi.org/10.1016/j.applthermaleng.2018.11.063.

[11] S. Fazlollahi, G. Becker, F. Maréchal, Multi-objectives, multi-period optimization of district energy systems: II—Daily thermal storage, Comput. Chem. Eng. 71 (2014) 648–662, http://dx.doi.org/10.1016/j.compchemeng.2013.10.016.

[12] L. Moretti, G. Manzolini, E. Martelli, MILP and MINLP models for the optimal scheduling of multi-energy systems accounting for delivery temperature of units, topology and non-isothermal mixing, Appl. Therm. Eng. 184 (2021) 116161, http://dx.doi.org/10.1016/j.applthermaleng.2020.116161.

[13] D. Patteeuw, L. Helsen, Combined design and control optimization of residential heating systems in a smart-grid context, Energy Build. 133 (2016) 640–657, http://dx.doi.org/10.1016/j.enbuild.2016.09.030.

[14] D. Steen, M. Stadler, G. Cardoso, M. Groissböck, N. DeForest, C. Marnay, Modeling of thermal storage systems in MILP distributed energy resource models, Appl. Energy 137 (2015) 782–792, http://dx.doi.org/10.1016/j.apenergy.2014.07.036.

[15] T. Terlouw, T. AlSkaif, C. Bauer, W. van Sark, Optimal energy management in all-electric residential energy systems with heat and electricity storage, Appl. Energy 254 (2019) 113580, http://dx.doi.org/10.1016/j.apenergy.2019.113580.

[16] D. Muschick, S. Zlabinger, A. Moser, K. Lichtenegger, M. Gölles, A multi-layer model of stratified thermal storage for MILP-based energy management systems, Appl. Energy 314 (2022) 118890, http://dx.doi.org/10.1016/j.apenergy.2022.118890.

[17] T. Schütz, R. Streblow, D. Müller, A comparison of thermal energy storage models for building energy system optimization, Energy Build. 93 (2015) 23–31, http://dx.doi.org/10.1016/j.enbuild.2015.02.031.

[18] S. Rastegarpour, M. Ghaemi, L. Ferrarini, A predictive control strategy for energy management in buildings with radiant floors and thermal storage, in: 2018 SICE International Symposium on Control Systems (SICE ISCS), IEEE, 2018, pp. 67–73, http://dx.doi.org/10.23919/SICEISCS.2018.8330158.

[19] D. Zinsmeister, T. Licklederer, S. Adldinger, F. Christange, P. Tzscheutschler, T. Hamacher, V.S. Perić, A prosumer-based sector-coupled district heating and cooling laboratory architecture, Smart Energy 9 (2023) 100095, http://dx.doi.org/10.1016/j.segy.2023.100095.

[20] Trnsys18, 2023, URL https://trnsys.de/en/trnsys18.

[21] Apros® dynamic process simulation software, 2023, URL https://www.vttresearch.com/en/ourservices/aprosr-dynamic-process-simulation-software.

[22] R. Unger, T. Schwan, B. Mikoleit, B. Bäker, C. Kehrer, T. Rodemann, Green Building - Modelling renewable building energy systems and electric mobility concepts using Modelica, in: Proceedings of the 9th International MODELICA Conference, 2012, pp. 897–906, http://dx.doi.org/10.3384/ecp12076897.

[23] Thermaly stratified heat storage, 2023, URL http://doc.simulationx.com/4.0/1033/Default.htm#Libraries/GreenCity/GreenBuilding/HeatStorage/HeatStorageStratified.htm.

[24] I. de La Cruz-Loredo, D. Zinsmeister, T. Licklederer, C.E. Ugalde-Loo, D.A. Morales, H. Bastida, V.S. Perić, A. Saleem, Experimental validation of a hybrid 1-D multi-node model of a hot water thermal energy storage tank, Appl. Energy 332 (2023) 120556, http://dx.doi.org/10.1016/j.apenergy.2022.120556.

[25] D. Zinsmeister, V. Perić, Implementation of a digital twin of the CoSES district heating prosumer laboratory, Energy Proc. (2022) http://dx.doi.org/10.46855/energy-proceedings-10153.

[26] E.M. Kleinbach, W.A. Beckman, S.A. Klein, Performance study of one-dimensional models for stratified thermal storage tanks, Sol. Energy 50 (2) (1993) 155–166, http://dx.doi.org/10.1016/0038-092X(93)90087-5.

[27] D. Atabay, An open-source model for optimal design and operation of industrial energy systems, Energy 121 (2017) 803–821, http://dx.doi.org/10.1016/j.energy.2017.01.030.

[28] J. Dorfner, K. Schönleber, M. Dorfner, sonercandas, froehlie, smuellr, dogauzrek, WYAUDI, Leonhard-B, lodersky, yunusozsahin, adeeljsid, T. Zipperle, S. Herzog, kais siala, O. Akca, tum-ens/urbs: urbs v1.0.1, 2019, http://dx.doi.org/10.5281/zenodo.594200.

[29] D. Zinsmeister, T. Licklederer, Characterization of a thermal storage at the CoSES laboratory, 2022, http://dx.doi.org/10.13140/RG.2.2.13461.19687.

[30] DKE Deutsche Kommission Elektrotechnik Elektronik Informationstechnik in DIN und VDE, Industrielle platin-widerstandsthermometer und platin-temperatursensoren, 2018.

[31] Endress + Hauser, Technical information proline promag e 100, 2021, URL https://portal.endress.com/dla/5000883/5389/000/02/TI01159DEN_0317.pdf.

[32] M.L. Bynum, G.A. Hackebeil, W.E. Hart, C.D. Laird, B.L. Nicholson, J.D. Siirola, J.-P. Watson, D.L. Woodruff, Pyomo-Optimization Modeling in Python, Vol. 67, third ed., Springer Science & Business Media, 2021.

[33] W.E. Hart, J.-P. Watson, D.L. Woodruff, Pyomo: modeling and solving mathematical programs in Python, Math. Program. Comput. 3 (3) (2011) 219–260.

[34] L.L. Gurobi Optimization, Gurobi optimizer reference manual, 2023, URL https://www.gurobi.com.

[35] J. Czyzyk, M.P. Mesnier, J.J. Moré, The NEOS server, IEEE J. Comput. Sci. Eng. 5 (3) (1998) 68—-75.

Chapter 6

Conclusion and future research

This dissertation outlines the CoSES simulation and experimental environment, focusing on integrating prosumers into DHC grids. While prosumers can significantly enhance the efficiency and operational economy of DHC grids, their integration poses various challenges.

The first publication in this dissertation describes the optimal configuration of components within DH prosumers. Based on these findings, an experimental and simulation framework is designed to investigate individual building energy systems and prosumers in DHC grids. This framework is applied in the design and evaluation of a novel MPC-based EMS approach, which accurately replicates TES behavior. Based on these findings, the RQs formulated in Section 1.1 are answered.

6.1 Conclusion

RQ 1 asks for the optimal arrangement of components in DH prosumers. This includes considering the unique properties of different heat generators - combustion-based, HPs, and ST systems - and their primary operational modes - feeding into or drawing from the grid. The study identifies optimal configurations for each generator type to achieve high efficiencies and low grid return temperatures. Combustion-based heat generators benefit from a common connection point of all components, while HPs and ST systems should be connected only to the TES, ideally at multiple heights to effectively reach the required supply temperatures.

RQ 2 addresses the need for a simulative and experimental environment to analyze the integration of prosumers into DHC grids. The CoSES laboratory's versatility and adaptability allow a comprehensive analysis of these prosumers and their integration into a smart energy system. Its modular design is instrumental in providing flexibility for various experiments. The laboratory has been used to characterize equipment, enhance control strategies, and evaluate EMSs, effectively bridging the gap between theoretical simulations and practical applications. Additionally, the ProHMo library features models that accurately replicate the behavior of the commercial hardware within the CoSES laboratory This environment is integral for designing innovative control strategies in both 4GDH and 5GDHC and bridging the research-to-implementation gap. Providing open-access benchmarking models of various building energy systems encourages the development and comparative analysis of new EMSs, furthering advancements in this field.

Experiments in the CoSES laboratory have highlighted the necessity of improved control sys-

tems, particularly for buildings equipped with HPs and for prosumers within DH grids (**RQ 3**). A novel stratified TES model for predictive control is formulated to answer this question. Experimental validation shows that this model accurately represents the temperature distribution within the TES. The formulation with quadratic or simpler constraints ensures low computational demands, making it suitable for MPC-based EMSs for heating systems. A case study demonstrates the advantages of the proposed approach compared to other MPC-based EMSs.

Together, these contributions advance the comprehension, development, and practical application of prosumer-based DHC systems, their integration into smart energy systems, and the implementation of sophisticated control strategies.

6.2 Future research

The methodologies and insights developed in this thesis establish a solid foundation for future research endeavors. The presented CoSES research infrastructure has already been used for several studies, as shown in Section 4.3. Additionally, the research trends highlighted in Section 2.5 can be thoroughly explored using the simulation and experiment environment developed in this dissertation.

The research environment is particularly well-suited for analyzing prosumers in DHC grids, offering an in-depth assessment of their design and control concepts. Various 5GDHC grid configurations, such as those with a passive balancing unit [141], single-pipe reservoir grids [46, 138], or grids with a pressurized supply line like 4GDH [45], can be compared within the adaptable framework of the CoSES laboratory. Different control approaches for prosumers can be designed and tested using the digital twin. This ranges from high-level EMSs to low-level field controllers, essential for managing the intricate interactions among multiple prosumers and pumps.

In the context of smart energy systems and sector coupling, the CoSES infrastructure can be used to assess the supportive role of buildings or DHC grids for the electric grid. The research environment is optimally suited for developing and conducting realistic evaluations of various EMS approaches applicable to grid and building levels. On the one hand, ProHMo's open-access, software-independent, and user-friendly benchmarking simulation models aid researchers in designing, refining, and comparing different EMS. On the other hand, these systems can undergo practical testing within the laboratory to confirm their effectiveness alongside commercial hardware and to verify their support of the electric grid. The laboratory further enables the validation of control algorithms and the analysis of distributed control with real hardware, similar to the work of Cornejo et al. [155] on the electric grid.

Most laboratories analyzing the optimal design for DHW preparation and the influence of circulation only consider a few designs.By contrast, the CoSES laboratory's flexible configuration allows the analysis of proposed design ideas in one research environment, ensuring comparable results. This is crucial for a fair comparison of various design and control concepts for DHW extraction. Moreover, the laboratory's configuration enables experimental analysis of different cascading grid approaches and their impact on the DH grid. For instance, all heat transfer stations are equipped with two heat exchangers, enabling the study of cascaded grids with three temperature levels in parallel, and DH grid emulators can emulate high- or low-temperature grids to analyze the effects of coupling grids on cascade systems.

The CoSES laboratory can also be instrumental in preparing field tests, which are typically expensive and time-consuming. Should unforeseen events occur during these tests, there are risks of exceeding budgetary or time constraints, which could diminish the quality of the insights of the field test. The laboratory's existing communication systems and accessibility allow fast and reproducible prequalifying of field tests. This prequalification helps anticipate and address potential issues, thus saving costs, preventing errors, and enhancing the value of the results. Similarly, the laboratory can analyze and recreate faults in existing DHC grids. This can help understand the impact of different faults on the grid, train and optimize algorithms for fault detection, and develop solutions for existing faults.

From an educational perspective, the CoSES laboratory is a resource for student learning by providing students with hands-on experience with real hardware through student theses or practical courses. This exposure helps them to grasp the specific requirements and challenges of various technologies, deepen their understanding of theoretical concepts, and familiarize them with practical limitations and challenges. The ProHMo benchmark models can further be used in courses where students learn to design different EMSs.

In summary, this dissertation's experiment and simulation infrastructure opens a wide range of possibilities, extending well beyond the thesis's scope. It is a versatile instrument for advancing research and education in energy systems.

Appendix A

List of publications

A.1 First-authored publications

1. Daniel Zinsmeister, Ulrich Ludolfinger, Vedran S. Perić, and Christoph Goebel. *A benchmarking framework for energy management systems with commercial hardware models.* Energy and Buildings, 2024.
   URL: https://doi.org/10.1016/j .enbuild.2024.114648

2. Daniel Zinsmeister, Peter Tzscheutschler, Vedran S. Perić, and Christoph Goebel. *Stratified Thermal Energy Storage Model with Constant Layer Volume for Predictive Control - Formulation, Comparison, and Empirical Validation.* Renewable Energy, 2023.
   URL: https://doi.org/10.1016/j .renene.2023.119511

3. Daniel Zinsmeister, Thomas Lickleder er, Stefan Adldinger, Franz Christange, Peter Tzscheutschler, Thomas Hamacher, and Vedran S. Perić. *A prosumer-based sector-coupled district heating and cooling laboratory architecture.* Smart Energy, 2023.
   URL: https://doi.org/10.1016/j .segy.2023.100095

4. Daniel Zinsmeister, and Vedran S. Perić. *Implementation of a Digital Twin of the CoSES District Heating Prosumer Laboratory.* Energy Proceedings, 2022.
   URL: https:// doi.org/10.46855/energy-proceedings-10153

5. Daniel Zinsmeister, Thomas Lickleder er, Franz Christange, Peter Tzscheutschler, and Vedran S. Perić. *A comparison of prosumer system configurations in district heating networks.* Energy Reports, 2021.
   URL: https://doi.org/10.1016/j .egyr.2021.08.085

A.2 Co-authored publications

1. Orestis Angelidis, Daniel Zinsmeister, Anastasia Ioannou, Daniel Friedrich, Alan Thomson, Ulrich Ganslmeier, Gioia Falcone. *Development and experimental validation of a hydraulic design and control philosophies for 5th Generation District Heating and Cooling Networks.* Energy, 2024.
   URL: https://doi.org/10.1016/j.energy.2024.132835

2. Saltanat Kuntuarova, Thomas Lickleder, Thanh Huynh, Daniel Zinsmeister, Thomas Hamacher, Vedran Perić. *Design and simulation of district heating networks: A review of modeling approaches and tools.* Energy, 2024.
URL: https://doi.org/10.1016/j.energy.2024.132189

3. Thomas Lickleder, Daniel Zinsmeister, Lorenz Lukas, Fabian Speer, Thomas Hamacher, and Vedran S. Perić. *Control of bidirectional prosumer substations in smart thermal grids: A weighted proportional-integral control approach.* Applied Energy, 2024.
URL: https://doi.org/10.1016/j .apenergy.2023.122239

4. Orestis Angelidis, Daniel Zinsmeister, Anastasia Ioannou, Daniel Friedrich, Alan Thomson, Gioia Falcone. *5th Generation District Heating and Cooling Modelica Models for Prosumer Interaction Analysis.* Modelica Conference, 2023.
URL: https://doi.org/10.3384/ecp204607

5. Ruihao Song, Daniel Zinsmeister, Thomas Hamacher, Haoran Zhao, Vladmir Terzija, and Vedran S. Perić. *Adaptive Control of Practical Heat Pump Systems for Power System Flexibility based on Reinforcement Learning.* Power Con, 2023.
URL: http://dx.doi.org/10.1109/PowerCon58120.2023.10331231

6. Stefan Adldinger, Lothar Behringer, Thomas Lickleder, Daniel Zinsmeister, and Thomas Hamacher. *Temperature flexible operation of district heating with booster heat pumps – Improving efficiency of existing networks.* Cisbat, 2023.
URL: http://dx.doi.org/10.1088/1742-6596/2600/8/082028

7. Ulrich Ludolfinger, Daniel Zinsmeister, Vedran S. Perić, Thomas Hamacher, Sascha Hauke, and Maren Martens. *Recurrent Soft Actor Critic Reinforcement Learning for Demand Response Problem.* IEEE Belgrade PowerTech, 2023.
URL: https://doi.org/10.1109/PowerTech55446.2023.10202844

8. Iván De la Cruz-Loredo, Daniel Zinsmeister, Thomas Lickleder, Carlos E. Ugalde-Loo, Daniel A. Morales, Héctor Bastida, Vedran S. Perić, and Arslan Saleem. *Experimental validation of a hybrid 1-D multi-node model of a hot water thermal energy storage tank.* Applied Energy, 2023.
URL: https://doi.org/10.1016/j .apenergy.2022.120556

9. Fabian Speer, Thomas Lickleder, Daniel Zinsmeister, and Vedran S. Perić. *Dimensioning radial prosumer-based thermal networks.* IEWT, 2023.
URL: https://iewt2023.eeg.tuwien.ac.at/download/contribution/fullpaper/104/104_fullpaper_20230210_224423.pdf

10. Thomas Lickleder, Daniel Zinsmeister, Ilya Elizarov, Vedran S. Perić, and Peter Tzscheutschler. *Characteristics and Challenges in Prosumer-Dominated Thermal Networks.* Journal of Physics: Conference Series, 2021.
URL: https://doi.org/10.1088/1742-6596/2042/1/012039

11. Sai Kiran Samboju, Vivek Teja Tanjavooru, Daniel Zinsmeister, and Vedran S. Perić. *Modeling of combined heat and power generation unit for dynamic analysis of integrated thermal-electric grids.* MSCPES, 2021.
URL: https://doi.org/10.1145/3470481.3472711

12. Vedran S. Perić, Thomas Hamacher, Anurag Mohapatra, Franz Christange, Daniel Zinsmeister, Peter Tzscheutschler, Ulrich Wagner, Christian Aigner, Rolf Witzmann. *CoSES Laboratory for Combined Energy Systems At TU Munich.* IEEE Power & Energy Society General Meeting (PESGM), 2020.
URL: doi:10.1109/pesgm41954.2020.9281442

A.3 Not peer-reviewed publications

1. Daniel Zinsmeister, and Thomas Lickleder. *Characterization of a Thermal Storage at the CoSES laboratory.* Researchgate, 2022.
URL: http://dx.doi.org/10.13140/RG.2.2.13461.19687

2. Daniel Zinsmeister, and Thomas Lickleder. *Characterization of a Combined Heat and Power Unit at the CoSES laboratory.* Researchgate, 2021.
URL: http://dx.doi.org/10.13140/RG.2.2.31035.34089/1

3. Daniel Zinsmeister, Thomas Lickleder, Peter Tzscheutschler, and Vedran S. Perić. *OSkit - Optimized Sector Coupling in Districts through Intelligent Thermal Prosumer Networks.* MSE Kolloquium, 2021.
URL: https://mediatum.ub.tum.de/node?id=1622092

4. Daniel Zinsmeister, Wessam El-Baz, and Peter Tzscheutschler. *Hardware-in-the-Loop Applications for Intelligent Energy Management and Coupled Energy System Analysis.* ESI SimulationX Conference, 2018.

A.4 Open-source repositories

1. Daniel Zinsmeister, Orestis Angelidis. *CoSES ProHMo.*
URL: https://gitlab.lrz.de/energy-management-technologies-public/coses_prohmo

2. Daniel Zinsmeister. *StraTS-E.*
URL: https://gitlab.lrz.de/energy-management-technologies-public/strats-e

Bibliography

[1] IRENA, IEA, and REN21. *Renewable Energy Policies in a Time of Transition: Heating and Cooling*. Ed. by O. IRENA and REN21. 2020. ISBN: 978-92-9260-289-5.

[2] Bundesministerium für Wohnen, Stadtentwicklung und Bauwesen. *Gebäudeenergiegesetz: GEG*. 2023.

[3] Bundesministerium für Wohnen, Stadtentwicklung und Bauwesen. *Entwurf eines Gesetzes für die Wärmeplanung und zur Dekarbonisierung der Wärmenetze*. 2023.

[4] H. Lund, S. Werner, R. Wiltshire, S. Svendsen, J. E. Thorsen, F. Hvelplund, and B. V. Mathiesen. "4th Generation District Heating (4GDH)". In: *Energy* 68 (2014), pp. 1–11. ISSN: 03605442. DOI: 10.1016/j.energy.2014.02.089.

[5] IEA. *The Future of Heat Pumps*. Paris, 2022. URL: https://www.iea.org/reports/the-future-of-heat-pumps.

[6] S. Paardekooper, R. S. Lund, B. V. Mathiesen, M. Chang, U. R. Petersen, L. Grundahl, A. David, J. Dahlbæk, I. A. Kapetanakis, H. Lund, N. Bertelsen, K. Hansen, D. W. Drysdale, and U. Persson. *Heat Roadmap Europe 4: Quantifying the Impact of Low-Carbon Heating and Cooling Roadmaps*. Ed. by Aalborg Universitetsforlag. 2018.

[7] H. Lund, P. A. Østergaard, D. Connolly, and B. V. Mathiesen. "Smart energy and smart energy systems". In: *Energy* 137 (2017), pp. 556–565. ISSN: 03605442. DOI: 10.1016/j.energy.2017.05.123.

[8] B. V. Mathiesen, H. Lund, D. Connolly, H. Wenzel, P. A. Østergaard, B. Möller, S. Nielsen, I. Ridjan, P. Karnøe, K. Sperling, and F. K. Hvelplund. "Smart Energy Systems for coherent 100% renewable energy and transport solutions". In: *Applied Energy* 145 (2015), pp. 139–154. ISSN: 03062619. DOI: 10.1016/j.apenergy.2015.01.075.

[9] S. Oxenaar, R. Lowes, and J. Rosenow. *Warming up to it: Principles for clean, efficient and smart district heating*. Ed. by Regulatory Assistance Project. 2023.

[10] M. Wirtz, L. Kivilip, P. Remmen, and D. Müller. "Quantifying Demand Balancing in Bidirectional Low Temperature Networks". In: *Energy and Buildings* 224 (2020), p. 110245. ISSN: 03787788. DOI: 10.1016/j.enbuild.2020.110245.

[11] P. A. Østergaard and A. N. Andersen. "Booster heat pumps and central heat pumps in district heating". In: *Applied Energy* 184 (2016), pp. 1374–1388. ISSN: 03062619. DOI: 10.1016/j.apenergy.2016.02.144.

[12] O. Angelidis, A. Ioannou, D. Friedrich, A. Thomson, and G. Falcone. "District heating and cooling networks with decentralised energy substations: Opportunities and barriers for holistic energy system decarbonisation". In: *Energy* 269 (2023), p. 126740. ISSN: 03605442. DOI: 10.1016/j.energy.2023.126740.

[13] S. Buffa, M. Cozzini, M. D'Antoni, M. Baratieri, and R. Fedrizzi. "5th generation district heating and cooling systems: A review of existing cases in Europe". In: *Renewable and Sustainable Energy Reviews* 104 (2019), pp. 504–522. ISSN: 13640321. DOI: 10.1016/j.rser.2018.12.059.

[14] K. Gjoka, B. Rismanchi, and R. H. Crawford. "Fifth-generation district heating and cooling systems: A review of recent advancements and implementation barriers". In: *Renewable and Sustainable Energy Reviews* 171 (2023), p. 112997. ISSN: 13640321. DOI: 10.1016/j.rser.2022.112997.

[15] M. Cozzini, M. D'Antoni, S. Buffa, R. Fedrizzi, and F. Bava. *District heating and cooling networks based on decentralized heat pumps: Energy efficiency and reversibility at affordable costs.* Ed. by HPT Mag 36. 2018.

[16] I. Franzén, L. Nedar, and M. Andersson. "Environmental Comparison of Energy Solutions for Heating and Cooling". In: *Sustainability* 11.24 (2019), p. 7051. DOI: 10.3390/su11247051.

[17] K. Gjoka, B. Rismanchi, and R. H. Crawford. "Fifth-generation district heating and cooling: Opportunities and implementation challenges in a mild climate". In: *Energy* 286 (2024), p. 129525. ISSN: 03605442. DOI: 10.1016/j.energy.2023.129525.

[18] O. Gudmundsson, R.-R. Schmidt, A. Dyrelund, and J. E. Thorsen. "Economic comparison of 4GDH and 5GDH systems – Using a case study". In: *Energy* 238 (2022), p. 121613. ISSN: 03605442. DOI: 10.1016/j.energy.2021.121613.

[19] F. Calise, F. L. Cappiello, L. Cimmino, M. Dentice d'Accadia, and M. Vicidomini. "A comparative thermoeconomic analysis of fourth generation and fifth generation district heating and cooling networks". In: *Energy* 284 (2023), p. 128561. ISSN: 03605442. DOI: 10.1016/j.energy.2023.128561.

[20] Y. Zhang, P. Johansson, and A. S. Kalagasidis. "Quantification of overlapping heating and cooling demand for the feasibility assessment of bi-directional systems over Europe". In: *Energy and Buildings* 294 (2023), p. 113244. ISSN: 03787788. DOI: 10.1016/j.enbuild.2023.113244.

[21] H. Lund, P. A. Østergaard, T. B. Nielsen, S. Werner, J. E. Thorsen, O. Gudmundsson, A. Arabkoohsar, and B. V. Mathiesen. "Perspectives on fourth and fifth generation district heating". In: *Energy* 227 (2021), p. 120520. ISSN: 03605442. DOI: 10.1016/j.energy.2021.120520.

[22] H. Lund, P. A. Østergaard, M. Chang, S. Werner, S. Svendsen, P. Sorknæs, J. E. Thorsen, F. Hvelplund, B. O. G. Mortensen, B. V. Mathiesen, C. Bojesen, N. Duic, X. Zhang, and B. Möller. "The status of 4th generation district heating: Research and results". In: *Energy* 164 (2018), pp. 147–159. ISSN: 03605442. DOI: 10.1016/j.energy.2018.08.206.

[23] T. Tereshchenko and N. Nord. "Future Trends in District Heating Development". In: *Current Sustainable/Renewable Energy Reports* 5.2 (2018), pp. 172–180. DOI: 10.1007/s40518-018-0111-y.

[24] M. A. Sayegh, J. Danielewicz, T. Nannou, M. Miniewicz, P. Jadwiszczak, K. Piekarska, and H. Jouhara. "Trends of European research and development in district heating technologies". In: *Renewable and Sustainable Energy Reviews* 68 (2017), pp. 1183–1192. ISSN: 13640321. DOI: 10.1016/j.rser.2016.02.023.

[25] L. Brange, P. Lauenburg, K. Sernhed, and M. Thern. "Bottlenecks in district heating networks and how to eliminate them – A simulation and cost study". In: *Energy* 137 (2017), pp. 607–616. ISSN: 03605442. DOI: 10.1016/j.energy.2017.04.097.

[26] H. Kauko, K. H. Kvalsvik, D. Rohde, N. Nord, and Å. Utne. "Dynamic modeling of local district heating grids with prosumers: A case study for Norway". In: *Energy* 151 (2018), pp. 261–271. ISSN: 03605442. DOI: 10.1016/j.energy.2018.03.033.

[27] L. Brange, J. Englund, and P. Lauenburg. "Prosumers in district heating networks – A Swedish case study". In: *Applied Energy* 164 (2016), pp. 492–500. ISSN: 03062619. DOI: 10.1016/j.apenergy.2015.12.020.

[28] *Einweihung des CoSES-Labors*. 2019. URL: https://www.mep.tum.de/mep/aktuelles/news-single-view/article/einweihung-des-coses-labors/ (visited on 12/12/2023).

[29] D. Zinsmeister, T. Licklederer, S. Adldinger, F. Christange, P. Tzscheutschler, T. Hamacher, and V. S. Perić. "A prosumer-based sector-coupled district heating and cooling laboratory architecture". In: *Smart Energy* 9 (2023), p. 100095. ISSN: 26669552. DOI: 10.1016/j.segy.2023.100095.

[30] T. Licklederer, J. Mayer, D. Bytschkow, V. Ahuir, D. Birkeneder, A. Capone, M. Dagn, E. Holsten, M. Irlbeck, M. Kramer, D. Malinowsky, N. Miedl, R. Nebel, A. Oji, C. Reiser, L. Schumacher, P. Täubrich, C. Wieland, S. D. Agudelo Sanabria, L. Beißwenger, S.-A. Bröcker, J. Burger, I. Elizarov, T. Freiesleben, L. Heidemann, J. Kainz, A. Krüger, A. Thut, M. Duchon, and T. Hamacher. *Abschlussbericht „Multi-Energie Management und Aggregationsplattform (MEMAP)"*. 2022.

[31] D. Zinsmeister, T. Licklederer, F. Christange, P. Tzscheutschler, and V. S. Perić. "A comparison of prosumer system configurations in district heating networks". In: *Energy Reports* 7 (2021), pp. 430–439. ISSN: 23524847. DOI: 10.1016/j.egyr.2021.08.085.

[32] M. Pipiciello, M. Caldera, M. Cozzini, M. A. Ancona, F. Melino, and B. Di Pietra. "Experimental characterization of a prototype of bidirectional substation for district heating with thermal prosumers". In: *Energy* 223 (2021), p. 120036. ISSN: 03605442. DOI: 10.1016/j.energy.2021.120036.

[33] G. E. Dino, P. Catrini, A. Buscemi, A. Piacentino, V. Palomba, and A. Frazzica. "Modeling of a bidirectional substation in a district heating network: Validation, dynamic analysis, and application to a solar prosumer". In: *Energy* 284 (2023), p. 128621. ISSN: 03605442. DOI: 10.1016/j.energy.2023.128621.

[34] T. Rosemann, J. Löser, and K. Rühling. "A New DH Control Algorithm for a Combined Supply and Feed-In Substation and Testing Through Hardware-In-The-Loop". In: *Energy Procedia* 116 (2017), pp. 416–425. ISSN: 18766102. DOI: 10.1016/j.egypro.2017.05.089.

[35] N. Lamaison, R. Bavière, D. Cheze, and C. Paulus. "A Multi-Criteria Analysis of Bidirectional Solar District Heating Substation Architecture". In: *Proceedings of SWC2017 / SHC2017*. Ed. by M. Romero, D. Mugnier, D. Renné, K. Guthrie, and S. Griffiths. Freiburg, Germany: International Solar Energy Society, 2016, pp. 1–11. ISBN: 978-3-9814659-7-6. DOI: 10.18086/swc.2017.10.02.

[36] N. Lamaison, D. Cheze, J.-F. Robin, F. Bruyat, and F. Lefrancois. "Operational Behaviour of a Solar-Fed Bidirectional Substation for 4GDH Networks". In: *Proceedings of the ISES Solar World Congress 2021*. Ed. by D. Renné, E. Weber, C. Hachem-Vermette, and E. Frank. Freiburg, Germany: International Solar Energy Society, 2021, pp. 1–10. ISBN: 978-3-9820408-7-5. DOI: 10.18086/swc.2021.28.03.

[37] C. Paulus and P. Papillon. "Substations for Decentralized Solar District Heating: Design, Performance and Energy Cost". In: *Energy Procedia* 48 (2014), pp. 1076–1085. ISSN: 18766102. DOI: 10.1016/j.egypro.2014.02.122.

[38] Modelica Association. *Modelica Language*. 2023. URL: https://modelica.org/ (visited on 10/26/2023).

[39] M. Abugabbara, S. Javed, H. Bagge, and D. Johansson. "Bibliographic analysis of the recent advancements in modeling and co-simulating the fifth-generation district heating and cooling systems". In: *Energy and Buildings* 224 (2020), p. 110260. ISSN: 03787788. DOI: 10.1016/j.enbuild.2020.110260.

[40] M. Wetter, C. van Treeck, L. Helsen, A. Maccarini, D. Saelens, D. Robinson, and G. Schweiger. "IBPSA Project 1: BIM/GIS and Modelica framework for building and community energy system design and operation – ongoing developments, lessons learned and challenges". In: *IOP Conference Series: Earth and Environmental Science* 323.1 (2019), p. 012114. ISSN: 1755-1307. DOI: 10.1088/1755-1315/323/1/012114.

[41] M. Wetter, W. Zuo, T. S. Nouidui, and X. Pang. "Modelica Buildings library". In: *Journal of Building Performance Simulation* 7.4 (2014), pp. 253–270. ISSN: 1940-1493. DOI: 10.1080/19401493.2013.765506.

[42] D. Müller, T. Lauster, A. Constantin, M. Fuchs, and P. Remmen. "AixLib – An Open-Source Modelica Library within the IEA-EBC Annex 60 Framework". In: (2016).

[43] C. Nytsch-Geusen, J. Huber, M. Ljubijankic, and J. Rädler. "Modelica BuildingSystems – eine Modellbibliothek zur Simulation komplexer energietechnischer Gebäudesysteme". In: *Bauphysik* 35.1 (2013), pp. 21–29. ISSN: 01715445. DOI: 10.1002/bapi.201310045.

[44] F. Jorissen, G. Reynders, R. Baetens, D. Picard, D. Saelens, and L. Helsen. "Implementation and verification of the IDEAS building energy simulation library". In: *Journal of Building Performance Simulation* 11.6 (2018), pp. 669–688. ISSN: 1940-1493. DOI: 10.1080/19401493.2018.1428361.

[45] F. Bünning, M. Wetter, M. Fuchs, and D. Müller. "Bidirectional low temperature district energy systems with agent-based control: Performance comparison and operation optimization". In: *Applied Energy* 209 (2018), pp. 502–515. ISSN: 03062619. DOI: 10.1016/j.apenergy.2017.10.072.

[46] E. Zanetti, D. Blum, and M. Wetter. "Control development and sizing analysis for a 5th generation district heating and cooling network using Modelica". In: *Proceedings of the 15th International Modelica Conference*. Ed. by Modelica Association. 2023.

[47] J. von Rhein, G. P. Henze, N. Long, and Y. Fu. "Development of a topology analysis tool for fifth-generation district heating and cooling networks". In: *Energy Conversion and Management* 196 (2019), pp. 705–716. ISSN: 01968904. DOI: 10.1016/j.enconman.2019.05.066.

[48] K. Hinkelman, J. Wang, W. Zuo, A. Gautier, M. Wetter, C. Fan, and N. Long. "Modelica-based modeling and simulation of district cooling systems: A case study". In: *Applied Energy* 311 (2022), p. 118654. ISSN: 03062619. DOI: 10.1016/j.apenergy.2022.118654.

[49] M. Mans, T. Blacha, P. Remmen, and D. Müller. "Automated model generation and simplification for district heating and cooling networks". In: *Proceedings of the 13th International Modelica Conference, Regensburg, Germany, March 4–6, 2019*. Linköping Electronic Conference Proceedings. Linköing University Electronic Press, 2019, pp. 179–186. DOI: 10.3384/ecp19157179.

[50] T. Blacha, M. Mans, P. Remmen, and D. Müller. "Dynamic Simulation Of Bidirectional Low-Temperature Networks - A Case Study To Facilitate The Integration Of Renewable Energies". In: *Proceedings of Building Simulation 2019: 16th Conference of IBPSA*. Ed. by V. Corrado, E. Fabrizio, A. Gasparella, and F. Patuzzi. Building Simulation Conference proceedings. IBPSA, 2020, pp. 3491–3498. DOI: 10.26868/25222708.2019.210670.

[51] R. Unger, T. Schwan, B. Mikoleit, B. Bäker, C. Kehrer, and T. Rodemann. ""Green Building" - Modelling renewable building energy systems and electric mobility concepts using Modelica". In: *Proceedings of the 9th International Modelica Conference*. Ed. by Modelica Association. 2012, pp. 897–906. DOI: 10.3384/ecp12076897.

[52] EA Systems Dresden GmbH, ed. *Green City für SimulationX*. 2023. URL: https://www.ea-energie.de/de/projects/green-city-fuer-simulationx/ (visited on 10/26/2023).

[53] M. Abugabbara, S. Javed, and D. Johansson. "A simulation model for the design and analysis of district systems with simultaneous heating and cooling demands". In: *Energy* 261 (2022), p. 125245. ISSN: 03605442. DOI: 10.1016/j.energy.2022.125245.

[54] EQUA Simulation AB, ed. *IDA ICE*. 2023. URL: https://www.equa.se/de/ida-ice.

[55] Transsolar Energietechnik GmbH, ed. *Trnsys18*. 2023. URL: https://trnsys.de/en/trnsys18.

[56] N. Vetterli and M. Sulzer. *Dynamic analysis of the low-temperature district network "Suurstoffi" through monitoring*. 2015. DOI: 10.5075/EPFL-CISBAT2015-517-522.

[57] P. Kräuchi, M. Kolb, T. Gautschi, U. .-. Menti, and M. Sulzer. "Modellbildung für thermische Arealvernetzung mit IDA-ICE". In: *Proceedings of BauSim Conference 2014: 5th Conference of IBPSA-Germany and Austria*. Vol. 5. BauSim Conference. Dresden, Germany: IBPSA-Germany and Austria, 2014, pp. 160–165. ISBN: 978-3-00-047160-5. URL: https://publications.ibpsa.org/conference/paper/?id=bausim2014_1130.

[58] P. Kräuchi, T. Schluck, and M. Sulzer. "Modelling of low temperature heating networks with IDA-ICE". In: *Proceedings of International Conference CISBAT 2015*. 2015. DOI: 10.5075/EPFL-CISBAT2015-827-832.

[59] T. Schluck, P. Kräuchi, and M. Sulzer. "Non-linear thermal networks - How can a meshed network improve energy efficiency?" In: *Proceedings of International Conference CISBAT 2015*. 2015.

[60] K. M. Heissler, L. Franke, I. Nemeth, and T. Auer. "Modeling low temperature district heating networks for the utilization of local energy potentials". In: *Bauphysik* 38.6 (2016), pp. 372–377. ISSN: 01715445. DOI: 10.1002/bapi.201610038.

[61] K. M. Heissler. "5th Generation District Heating Networks - Potentials for Reducing CO2-Emissions and Increasing the Share of Renewable Energies in Residential Districts". PhD thesis. Technical University of Munih, 2021.

[62] G. F. Schneider, J. Oppermann, A. Constantin, R. Streblow, and D. Müller. "Hardware-in-the-Loop-Simulation of a Building Energy and Control System to Investigate Circulating Pump Control Using Modelica". In: *Proceedings of the 11th International Modelica Conference, Versailles, France, September 21-23, 2015*. Linköping Electronic Conference Proceedings. Linköping University Electronic Press, 2015, pp. 225–233. DOI: 10.3384/ecp15118225.

[63] K. N. Rhee, M. S. Yeo, and K. W. Kim. "Evaluation of the control performance of hydronic radiant heating systems based on the emulation using hardware-in-the-loop simulation". In: *Building and Environment* 46.10 (2011), pp. 2012–2022. ISSN: 03601323. DOI: 10.1016/j.buildenv.2011.04.012.

[64] W. El-Baz, L. Mayerhofer, P. Tzscheutschler, and U. Wagner. "Hardware in the Loop Real-Time Simulation for Heating Systems: Model Validation and Dynamics Analysis". In: *Energies* 11.11 (2018), p. 3159. DOI: 10.3390/en11113159.

[65] W. El-Baz, P. Tzscheutschler, and U. Wagner. "Experimental Study and Modeling of Ground-Source Heat Pumps with Combi-Storage in Buildings". In: *Energies* 11.5 (2018), p. 1174. DOI: 10.3390/en11051174.

[66] F. Ceglia, E. Marrasso, C. Roselli, M. Sasso, and P. Tzscheutschler. "Exergetic and exergoeconomic analysis of an experimental ground source heat pump system coupled with a thermal storage based on Hardware in Loop". In: *Applied Thermal Engineering* 212 (2022), p. 118559. ISSN: 13594311. DOI: 10.1016/j.applthermaleng.2022.118559.

[67] A. La Tejeda De Cruz, P. Riviere, D. Marchio, O. Cauret, and A. Milu. "Hardware in the loop test bench using Modelica: A platform to test and improve the control of heating systems". In: *Applied Energy* 188 (2017), pp. 107–120. ISSN: 03062619. DOI: 10.1016/j.apenergy.2016.11.092.

[68] A. Vannahme, M. Ehrenwirth, and T. Schrag. "Enhancement of a District Heating Substation as Part of a Low-Investment Optimization Strategy for District Heating Systems". In: *Resources* 10.5 (2021), p. 53. ISSN: 2079-9276. DOI: 10.3390/resources10050053. URL: https://www.mdpi.com/2079-9276/10/5/53.

[69] "Experimental Study of District Heating Substations in a Hardware-in-the-Loop Test Rig". In: *Resources* 12.4 (2023), p. 43. ISSN: 2079-9276. DOI: 10.3390/resources12040043. URL: https://www.mdpi.com/2079-9276/12/4/43.

[70] K. Schäfer and T. Schmidt. "Experimental Plant for Analyzing the Technical Feasibility of Decentralized Solar Heat Feed-In". In: *Proceedings of EuroSun 2018*. Ed. by A. Häberle. Freiburg, Germany: International Solar Energy Society, 2018, pp. 1–9. ISBN: 978-3-9820408-0-6. DOI: 10.18086/eurosun2018.05.04.

[71] M. Heymann, T. Rosemann, K. Rühling, and B. Hafner. "Concept, construction and measurement results of a decentralized feed-in substation". In: *5th International Solar District Heating Conference*. 2018.

[72] J. Chung, S. Sukumaran, A. Hlebnikov, and A. Volkova. "Design and Development of a Conceptual Solar Energy Laboratory for District Heating Applications". In: *Solar* 3.3 (2023), pp. 504–521. DOI: 10.3390/solar3030028.

[73] E. Widl, A. Sporr, M. Mairhofer, T. Natiesta, N. Marx, and R.-R. Schmidt. "Prototype of an open testbed for the lab validation of smart applications of district heating substations". In: *2022 10th Workshop on Modelling and Simulation of Cyber-Physical Energy Systems (MSCPES)*. IEEE, 2022, pp. 1–6. ISBN: 978-1-6654-6865-7. DOI: 10.1109/MSCPES55116.2022.9770173.

[74] E. Widl, A. Sporr, R.-R. Schmidt, T. Natiesta, and N. Marx. "DigitalEnergyTestbed: An Open Testbed Prototype for Integrated Energy Systems". In: *2023 Open Source Modelling and Simulation of Energy Systems (OSMSES)*. IEEE, 2023, pp. 1–7. DOI: 10.1109/OSMSES58477.2023.10089634.

[75] Austrian Institute of Technology GmbH, ed. *Welcome to the AIT Lablink documentation!* 2023. URL: https://ait-lablink.readthedocs.io/en/latest/ (visited on 10/27/2023).

[76] Eurac Research, ed. *Energy Exchange Lab*. 2023. URL: https://www.eurac.edu/en/institutes-centers/institute-for-renewable-energy/pages/energy-exchange-lab.

[77] S. Buffa, A. Soppelsa, M. Pipiciello, G. Henze, and R. Fedrizzi. "Fifth-Generation District Heating and Cooling Substations: Demand Response with Artificial Neural Network-Based Model Predictive Control". In: *Energies* 13.17 (2020), p. 4339. DOI: 10.3390/en13174339.

[78] A. Kallert, D. Lottis, M. Shan, and D. Schmidt. "New experimental facility for innovative district heating systems—District LAB". In: *Energy Reports* 7 (2021), pp. 62–69. ISSN: 23524847. DOI: 10.1016/j.egyr.2021.09.039.

[79] T. Sommer, S. Mennel, and M. Sulzer. "Lowering the pressure in district heating and cooling networks by alternating the connection of the expansion vessel". In: *Energy* 172 (2019), pp. 991–996. ISSN: 03605442. DOI: 10.1016/j.energy.2019.02.010.

[80] T. Q. Péan, J. Salom, and R. Costa-Castelló. "Review of control strategies for improving the energy flexibility provided by heat pump systems in buildings". In: *Journal of Process Control* 74 (2019), pp. 35–49. ISSN: 09591524. DOI: 10.1016/j.jprocont.2018.03.006.

[81] R. Renaldi, A. Kiprakis, and D. Friedrich. "An optimisation framework for thermal energy storage integration in a residential heat pump heating system". In: *Applied Energy* 186 (2017), pp. 520–529. ISSN: 03062619. DOI: 10.1016/j.apenergy.2016.02.067.

[82] A. Vandermeulen, B. van der Heijde, and L. Helsen. "Controlling district heating and cooling networks to unlock flexibility: A review". In: *Energy* 151 (2018), pp. 103–115. ISSN: 03605442. DOI: 10.1016/j.energy.2018.03.034.

[83] L. Merkert, A. Haime, and S. Hohmann. "Optimal Scheduling of Combined Heat and Power Generation Units Using the Thermal Inertia of the Connected District Heating Grid as Energy Storage". In: *Energies* 12.2 (2019), p. 266. DOI: 10.3390/en12020266.

[84] M. Wirtz, L. Neumaier, P. Remmen, and D. Müller. "Temperature control in 5th generation district heating and cooling networks: An MILP-based operation optimization". In: *Applied Energy* 288 (2021), p. 116608. ISSN: 03062619. DOI: 10.1016/j.apenergy.2021.116608.

[85] R. Khir and M. Haouari. "Optimization models for a single-plant District Cooling System". In: *European Journal of Operational Research* 247.2 (2015), pp. 648–658. ISSN: 03772217. DOI: 10.1016/j.ejor.2015.05.083.

[86] W. Gu, J. Wang, S. Lu, Z. Luo, and C. Wu. "Optimal operation for integrated energy system considering thermal inertia of district heating network and buildings". In: *Applied Energy* 199 (2017), pp. 234–246. ISSN: 03062619. DOI: 10.1016/j.apenergy.2017.05.004.

[87] Z. Li, W. Wu, M. Shahidehpour, J. Wang, and B. Zhang. "Combined Heat and Power Dispatch Considering Pipeline Energy Storage of District Heating Network". In: *IEEE Transactions on Sustainable Energy* 7.1 (2016), pp. 12–22. ISSN: 1949-3029. DOI: 10.1109/TSTE.2015.2467383.

[88] Z. Chiam, A. Easwaran, D. Mouquet, S. Fazlollahi, and J. V. Millás. "A hierarchical framework for holistic optimization of the operations of district cooling systems". In: *Applied Energy* 239 (2019), pp. 23–40. ISSN: 03062619. DOI: 10.1016/j.apenergy.2019.01.134.

[89] M. Mohammadi, Y. Noorollahi, B. Mohammadi-Ivatloo, and H. Yousefi. "Energy hub: From a model to a concept – A review". In: *Renewable and Sustainable Energy Reviews* 80 (2017), pp. 1512–1527. ISSN: 13640321. DOI: 10.1016/j.rser.2017.07.030.

[90] M. Mohammadi, Y. Noorollahi, B. Mohammadi-Ivatloo, M. Hosseinzadeh, H. Yousefi, and S. T. Khorasani. "Optimal management of energy hubs and smart energy hubs – A review". In: *Renewable and Sustainable Energy Reviews* 89 (2018), pp. 33–50. ISSN: 13640321. DOI: 10.1016/j.rser.2018.02.035.

[91] S. Boesten, W. Ivens, S. C. Dekker, and H. Eijdems. "5th generation district heating and cooling systems as a solution for renewable urban thermal energy supply". In: *Advances in Geosciences* 49 (2019), pp. 129–136. DOI: 10.5194/adgeo-49-129-2019.

[92] Y. M. Han, R. Z. Wang, and Y. J. Dai. "Thermal stratification within the water tank". In: *Renewable and Sustainable Energy Reviews* 13.5 (2009), pp. 1014–1026. ISSN: 13640321. DOI: 10.1016/j.rser.2008.03.001.

[93] R. Hermansen, K. Smith, J. E. Thorsen, J. Wang, and Y. Zong. "Model predictive control for a heat booster substation in ultra low temperature district heating systems". In: *Energy* 238 (2022), p. 121631. ISSN: 03605442. DOI: 10.1016/j.energy.2021.121631.

[94] J. Tarragona, A. L. Pisello, C. Fernández, A. de Gracia, and L. F. Cabeza. "Systematic review on model predictive control strategies applied to active thermal energy storage systems". In: *Renewable and Sustainable Energy Reviews* 149 (2021), p. 111385. ISSN: 13640321. DOI: 10.1016/j.rser.2021.111385.

[95] D. Zinsmeister, P. Tzscheutschler, V. S. Perić, and C. Goebel. "Stratified thermal energy storage model with constant layer volume for predictive control — Formulation, comparison, and empirical validation". In: *Renewable Energy* 219 (2023), p. 119511. ISSN: 09601481. DOI: 10.1016/j.renene.2023.119511.

[96] S. Fazlollahi, G. Becker, and F. Maréchal. "Multi-objectives, multi-period optimization of district energy systems: II—Daily thermal storage". In: *Computers & Chemical Engineering* 71 (2014), pp. 648–662. ISSN: 00981354. DOI: 10.1016/j.compchemeng.2013.10.016.

[97] L. Moretti, G. Manzolini, and E. Martelli. "MILP and MINLP models for the optimal scheduling of multi-energy systems accounting for delivery temperature of units, topology and non-isothermal mixing". In: *Applied Thermal Engineering* 184 (2021), p. 116161. ISSN: 13594311. DOI: 10.1016/j.applthermaleng.2020.116161.

[98] D. Patteeuw and L. Helsen. "Combined design and control optimization of residential heating systems in a smart-grid context". In: *Energy and Buildings* 133 (2016), pp. 640–657. ISSN: 03787788. DOI: 10.1016/j.enbuild.2016.09.030.

[99] D. Steen, M. Stadler, G. Cardoso, M. Groissböck, N. DeForest, and C. Marnay. "Modeling of thermal storage systems in MILP distributed energy resource models". In: *Applied Energy* 137 (2015), pp. 782–792. ISSN: 03062619. DOI: 10.1016/j.apenergy.2014.07.036.

[100] T. Terlouw, T. AlSkaif, C. Bauer, and W. van Sark. "Optimal energy management in all-electric residential energy systems with heat and electricity storage". In: *Applied Energy* 254 (2019), p. 113580. ISSN: 03062619. DOI: 10.1016/j.apenergy.2019.113580.

[101] R. Delubac, M. Sadr, S. Sochard, S. Serra, and J.-M. Reneaume. "Optimized Operation and Sizing of Solar District Heating Networks with Small Daily Storage". In: *Energies* 16.3 (2023), p. 1335. DOI: 10.3390/en16031335.

[102] T. Schütz, R. Streblow, and D. Müller. "A comparison of thermal energy storage models for building energy system optimization". In: *Energy and Buildings* 93 (2015), pp. 23–31. ISSN: 03787788. DOI: 10.1016/j.enbuild.2015.02.031.

[103] S. Rastegarpour, M. Ghaemi, and L. Ferrarini. "A predictive control strategy for energy management in buildings with radiant floors and thermal storage". In: *2018 SICE International Symposium on Control Systems (SICE ISCS)*. IEEE, 2018, pp. 67–73. ISBN: 978-4-9077-6458-6. DOI: 10.23919/SICEISCS.2018.8330158.

[104] D. Muschick, S. Zlabinger, A. Moser, K. Lichtenegger, and M. Gölles. "A multi-layer model of stratified thermal storage for MILP-based energy management systems". In: *Applied Energy* 314 (2022), p. 118890. ISSN: 03062619. DOI: 10.1016/j.apenergy.2022.118890.

[105] M. A. Hassan, S. Serra, S. Sochard, H. Viot, F. Marias, and J.-M. Reneaume. "Optimal scheduling of energy storage in district heating networks using nonlinear programming". In: *Energy Conversion and Management* 295 (2023), p. 117652. ISSN: 01968904. DOI: 10.1016/j.enconman.2023.117652.

[106] T. Capper, A. Gorbatcheva, M. A. Mustafa, M. Bahloul, J. M. Schwidtal, R. Chitchyan, M. Andoni, V. Robu, M. Montakhabi, I. J. Scott, C. Francis, T. Mbavarira, J. M. Espana, and L. Kiesling. "Peer-to-peer, community self-consumption, and transactive energy: A systematic literature review of local energy market models". In: *Renewable and Sustainable Energy Reviews* 162 (2022), p. 112403. ISSN: 13640321. DOI: 10.1016/j.rser.2022.112403.

[107] L. Frölke, T. Sousa, and P. Pinson. "A network-aware market mechanism for decentralized district heating systems". In: *Applied Energy* 306 (2022), p. 117956. ISSN: 03062619. DOI: 10.1016/j.apenergy.2021.117956.

[108] L. Mitridati, J. Kazempour, and P. Pinson. "Heat and electricity market coordination: A scalable complementarity approach". In: *European Journal of Operational Research* 283.3 (2020), pp. 1107–1123. ISSN: 03772217. DOI: 10.1016/j.ejor.2019.11.072.

[109] L. Mitridati, J. Kazempour, and P. Pinson. "Design and game-Theoretic analysis of community-Based market mechanisms in heat and electricity systems". In: *Omega* 99 (2021), p. 102177. ISSN: 03050483. DOI: 10.1016/j.omega.2019.102177.

[110] V. Stennikov and A. Penkovskii. "The pricing methods on the monopoly district heating market". In: *Energy Reports* 6 (2020), pp. 187–193. ISSN: 23524847. DOI: 10.1016/j.egyr.2019.11.061.

[111] C. Sun, Y. Liu, Y. Li, S. Lin, H. B. Gooi, and J. Zhu. "Network-aware P2P multi-energy trading in decentralized electric-heat systems". In: *Applied Energy* 345 (2023), p. 121298. ISSN: 03062619. DOI: 10.1016/j.apenergy.2023.121298.

[112] H. Qiu, A. Vinod, S. Lu, H. B. Gooi, G. Pan, S. Zhang, and V. Veerasamy. "Decentralized mixed-integer optimization for robust integrated electricity and heat scheduling". In: *Applied Energy* 350 (2023), p. 121693. ISSN: 03062619. DOI: 10.1016/j.apenergy.2023.121693.

[113] V. Kaisermayer, D. Muschick, M. Horn, and M. Gölles. "Operation of coupled multi-owner district heating networks via distributed optimization". In: *Energy Reports* 7 (2021), pp. 273–281. ISSN: 23524847. DOI: 10.1016/j.egyr.2021.08.145.

[114] M. Capone, E. Guelpa, and V. Verda. "Potential for supply temperature reduction of existing district heating substations". In: *Energy* 285 (2023), p. 128597. ISSN: 03605442. DOI: 10.1016/j.energy.2023.128597.

[115] D. S. Østergaard and S. Svendsen. "Replacing critical radiators to increase the potential to use low-temperature district heating – A case study of 4 Danish single-family houses from the 1930s". In: *Energy* 110 (2016), pp. 75–84. ISSN: 03605442. DOI: 10.1016/j.energy.2016.03.140.

[116] W. Bergstraesser, A. Hinz, H. Braas, J. Orozaliev, and K. Vajen. "Lessons learned from excess flow analyses for various district heating systems". In: *Smart Energy* 1 (2021), p. 100005. ISSN: 26669552. DOI: 10.1016/j.segy.2021.100005.

[117] D. Basciotti, M. Köfinger, C. Marguerite, O. Terreros, G. Agugiaro, and R.-R. Schmidt. "Methodology for the assessment of temperature reduction potentials in district heating networks by demand side measures and cascading solutions". In: *12th REHVA world congress CLIMA*. 2016.

[118] DVGW Deutscher Verein des Gas- und Wasserfaches e. V. *Trinkwassererwärmungs- und Trinkwasserleitungsanlagen: Technische Maßnahmen zur Verminderung des - Planung, Errichtung, Betrieb und Sanierung von Trinkwasser-Installationen*. 2004.

[119] X. Yang, H. Li, and S. Svendsen. "Decentralized substations for low-temperature district heating with no Legionella risk, and low return temperatures". In: *Energy* 110 (2016), pp. 65–74. ISSN: 03605442. DOI: 10.1016/j.energy.2015.12.073.

[120] T. Huang, X. Yang, and S. Svendsen. "Multi-mode control method for the existing domestic hot water storage tanks with district heating supply". In: *Energy* 191 (2020), p. 116517. ISSN: 03605442. DOI: 10.1016/j.energy.2019.116517.

[121] Q. Yang, R. Salenbien, E. Motoasca, K. Smith, and M. Tunzi. "Development and test: Future-proof substation designs for the low-temperature operation of domestic hot water systems with a circulation loop". In: *Energy and Buildings* 298 (2023), p. 113490. ISSN: 03787788. DOI: 10.1016/j.enbuild.2023.113490.

[122] X. Yang and S. Svendsen. "Achieving low return temperature for domestic hot water preparation by ultra-low-temperature district heating". In: *Energy Procedia* 116 (2017), pp. 426–437. ISSN: 18766102. DOI: 10.1016/j.egypro.2017.05.090.

[123] J. C. Flores, B. Lacarrière, J. Chiu, and V. Martin. "Assessing the techno-economic impact of low-temperature subnets in conventional district heating networks". In: *Energy Procedia* 116 (2017), pp. 260–272. ISSN: 18766102. DOI: 10.1016/j.egypro.2017.05.073.

[124] M. Imran, M. Usman, Y. H. Im, and B. S. Park. "The feasibility analysis for the concept of low temperature district heating network with cascade utilization of heat between networks". In: *Energy Procedia* 116 (2017), pp. 4–12. ISSN: 18766102. DOI: 10.1016/j.egypro.2017.05.050.

[125] M. Köfinger, D. Basciotti, and R.-R. Schmidt. "Reduction of return temperatures in urban district heating systems by the implementation of energy-cascades". In: *Energy Procedia* 116 (2017), pp. 438–451. ISSN: 18766102. DOI: 10.1016/j.egypro.2017.05.091.

[126] A. Volkova, I. Krupenski, A. Ledvanov, A. Hlebnikov, K. Lepiksaar, E. Latõšov, and V. Mašatin. "Energy cascade connection of a low-temperature district heating network to the return line of a high-temperature district heating network". In: *Energy* 198 (2020), p. 117304. ISSN: 03605442. DOI: 10.1016/j.energy.2020.117304.

[127] A. Volkova, S. Reuter, S. Puschnigg, H. Kauko, R.-R. Schmidt, B. Leitner, and S. Moser. "Cascade sub-low temperature district heating networks in existing district heating systems". In: *Smart Energy* 5 (2022), p. 100064. ISSN: 26669552. DOI: 10.1016/j.segy.2022.100064.

[128] T. van Oevelen, D. Vanhoudt, and R. Salenbien. "Evaluation of the return temperature reduction potential of optimized substation control". In: *Energy Procedia* 149 (2018), pp. 206–215. ISSN: 18766102. DOI: 10.1016/j.egypro.2018.08.185.

[129] J. Gustafsson, J. Delsing, and J. van Deventer. "Improved district heating substation efficiency with a new control strategy". In: *Applied Energy* 87.6 (2010), pp. 1996–2004. ISSN: 03062619. DOI: 10.1016/j.apenergy.2009.12.015.

[130] T. van Oevelen, T. Neven, A. Brès, R.-R. Schmidt, and D. Vanhoudt. "Testing and evaluation of a smart controller for reducing peak loads and return temperatures in district heating networks". In: *Smart Energy* 10 (2023), p. 100105. ISSN: 26669552. DOI: 10.1016/j.segy.2023.100105.

[131] T. Lickleder, D. Zinsmeister, L. Lukas, F. Speer, T. Hamacher, and V. S. Perić. "Control of bidirectional prosumer substations in smart thermal grids: A weighted proportional-integral control approach". In: *Applied Energy* 354 (2024), p. 122239. ISSN: 03062619. DOI: 10.1016/j.apenergy.2023.122239.

[132] A. Tahiri, K. M. Smith, J. E. Thorsen, C. A. Hviid, and S. Svendsen. "Staged control of domestic hot water storage tanks to support district heating efficiency". In: *Energy* 263 (2023), p. 125493. ISSN: 03605442. DOI: 10.1016/j.energy.2022.125493.

[133] L. Brand, A. Calvén, J. Englund, H. Landersjö, and P. Lauenburg. "Smart district heating networks – A simulation study of prosumers' impact on technical parameters in distribution networks". In: *Applied Energy* 129 (2014), pp. 39–48. ISSN: 03062619. DOI: 10.1016/j.apenergy.2014.04.079.

[134] G. Lennermo, P. Lauenburg, and L. Brand. "Decentralised heat supply in district heating systems: Implications of varying differential pressure". In: *The 14th International Symposium on District Heating and Cooling*. 2014.

[135] T. Lickleder. "Technical Implementation and Operation of Prosumer-Based Smart District Heating". Promotion. 2024.

[136] G. Lennermo, P. Lauenburg, and S. Werner. "Control of decentralised solar district heating". In: *Solar Energy* 179 (2019), pp. 307–315. ISSN: 0038092X. DOI: 10.1016/j.solener.2018.12.080.

[137] I. Elizarov. "Analysis, modelling and control strategy development for prosumer-based heat networks". Master thesis. Munich: Technical University of Munich, 2020.

[138] T. Sommer, M. Sulzer, M. Wetter, A. Sotnikov, S. Mennel, and C. Stettler. "The reservoir network: A new network topology for district heating and cooling". In: *Energy* 199 (2020), p. 117418. ISSN: 03605442. DOI: 10.1016/j.energy.2020.117418.

[139] M. Wetter and J. Hu. *Quayside Energy Systems Analysis*. Ed. by Lawrence Berkeley National Laboratory. 2019. URL: https://buildings.lbl.gov/publications/quayside-energy-systems-analysis.

[140] D. Lottis and A. Kallert. "Simulative comparison of concepts for simultaneous control of heat flow and outlet temperature of heat exchangers for highly flexible use in the test facility "District LAB"". In: *Energy Informatics* 5.S1 (2022). DOI: 10.1186/s42162-022-00202-x.

[141] O. Angelidis, D. Zinsmeister, A. Ioannou, D. Friedrich, A. Thomson, U. Ganslmeier, and G. Falcone. "Development and experimental validation of a hydraulic design and control philosophies for 5th Generation District Heating and Cooling Networks". In: *Energy* (2024), p. 132835. DOI: https://doi.org/10.1016/j.energy.2024.132835.

[142] J. Siegenthaler. *Different ways to pipe a thermal storage tank: Four-pipe vs. two-pipe.* URL: https://www.pmengineer.com/articles/92398-different-ways-to-pipe-a-thermal-storage-tank (visited on 10/04/2023).

[143] T. Rinneberg. *Pufferspeicher für Wärmepumpen: Vor- und Nachteile.* URL: https://energiewende.eu/pufferspeicher-fuer-waermepumpen-vor-und-nachteile/ (visited on 10/04/2023).

[144] A. Mohapatra, T. Hamacher, and V. S. Peric. "PHIL Infrastructure in CoSES Microgrid Laboratory". In: *2022 IEEE PES Innovative Smart Grid Technologies Conference Europe (ISGT-Europe)*. IEEE, 2022, pp. 1–6. ISBN: 978-1-6654-8032-1. DOI: 10.1109/ISGT-Europe54678.2022.9960295.

[145] Daniel Zinsmeister and Thomas Licklederer. *Characterization of a Combined Heat and Power Unit at the CoSES laboratory.* 2021. DOI: 10.13140/RG.2.2.31035.34089/1.

[146] Daniel Zinsmeister and Thomas Licklederer. *Characterization of a Thermal Storage at the CoSES laboratory.* 2022. DOI: 10.13140/RG.2.2.13461.19687.

[147] I. Elizarov and T. Licklederer. "ProsNet – a Modelica library for prosumer-based heat networks: description and validation". In: *Journal of Physics: Conference Series* 2042.1 (2021), p. 012031. ISSN: 1742-6588. DOI: 10.1088/1742-6596/2042/1/012031.

[148] T. Licklederer, J. Mayer, D. Bytschkow, M. Kramer, A. Capone, J. Burger, and M. Duchon. "A Digital Platform for Smart Multi-Energy Management in Districts: Conceptualization, Modeling, Software Implementation and Laboratory Validation". In: *manuscript submitted to 'Energy Conversion and Management' on 03/08/2023* (2024).

[149] D. Zinsmeister, U. Ludolfinger, V. S. Peric, and C. Goebel. "A benchmarking framework for energy management systems with commercial hardware models". In: *Energy and Buildings* 321 (2024), p. 114648. ISSN: 0378-7788. DOI: https://doi.org/10.1016/j.enbuild.2024.114648.

[150] D. Zinsmeister and V. S. Perić. *Implementation of a Digital Twin of the CoSES District Heating Prosumer Laboratory.* 2022. DOI: 10.46855/energy-proceedings-10153.

[151] I. de La Cruz-Loredo, D. Zinsmeister, T. Licklederer, C. E. Ugalde-Loo, D. A. Morales, H. Bastida, V. S. Perić, and A. Saleem. "Experimental validation of a hybrid 1-D multi-node model of a hot water thermal energy storage tank". In: *Applied Energy* 332 (2023), p. 120556. ISSN: 03062619. DOI: 10.1016/j.apenergy.2022.120556.

[152] R. Song, D. Zinsmeister, T. Hamacher, H. Zhao, V. Terzija, and V. S. Perić. "Adaptive Control of Practical Heat Pump Systems for Power System Flexibility based on Reinforcement Learning". In: 2023. DOI: 10.1109/PowerCon58120.2023.10331231.

[153] U. Ludolfinger, D. Zinsmeister, V. S. Perić, T. Hamacher, S. Hauke, and M. Martens. "Recurrent Soft Actor Critic Reinforcement Learning for Demand Response Problems". In: *2023 IEEE Belgrade PowerTech*. IEEE, 2023, pp. 1–6. ISBN: 978-1-6654-8778-8. DOI: 10.1109/PowerTech55446.2023.10202844.

[154] U. Ludolfinger, V. S. Peric, T. Hamacher, S. Hauke, and M. Martens. "Transformer Model Based Soft Actor-Critic Learning for HEMS". In: *2023 International Conference on Power System Technology (PowerCon)*. 2023. DOI: 10.1109/PowerCon58120.2023.10331287.

[155] M. Cornejo, A. Mohapatra, S. Candas, and V. S. Peric. "PHIL implementation of a decentralized online OPF for active distribution grids". In: *2022 IEEE Power & Energy Society General Meeting (PESGM)*. IEEE, 2022, pp. 1–5. ISBN: 978-1-6654-0823-3. DOI: 10.1109/PESGM48719.2022.9916705.